Role of the defensin-like protein gene family in plant reproductive isolation and disease resistance in *Arabidopsis thaliana*

DISSERTATION ZUR ERLANGUNG DES DOKTORGRADES DER NATURWISSENSCHAFTEN (DR. RER. NAT.) DER FAKULTÄT FÜR BIOLOGIE UND VORKLINISCHE MEDIZIN

DER UNIVERSITÄT REGENSBURG

Vorgelegt von

Ajay John Arputharaj

aus

Dubai, U.A.E

im Januar 2017

Das Promotionsgesuch wurde eingereicht am: 7.1.2017

Die Arbeit wurde angeleitet von: Dr. Mariana Mondragón-Palomino

Unterschrift:

(Ajay John Arputharaj)

To the Glory of Jesus Christ

Table of Contents

List of Figures

List of Tables

Abbreviations

Abbreviations used in figures are explained in the respective caption.

bp	Base pairs
CCG	Central cell guidance
cDNA	Complementary DNA
CDS	Coding sequence
CNRQs	Calibrated normalized relative quantities
CLSM	Confocal Laser Scanning Microscopy
cm	Centimeter(s)
COL-0	Columbia-0
CRP	Cysteine-rich peptides
CSα/β	Cysteine-stabilized α/β motif
DAE	Day after emasculation
DAI	Day after infection
DAT	Day after mock treatment
DEG	Differentially expressed genes
DEFL	Defensins and defensin-like proteins
DNA	Deoxyribonucleic Acid
DON	Deoxynivalenol
eGFP	enhanced Green fluorescent signal
ER	Endoplasmic reticulum
ETI	Effector-triggered immunity
ETS	Effector-triggered susceptibility
FER	Feronia
FHB	Fusarium head blight
g	Gramm
GOI	Gene of interest
HAP	Hours after pollination
hr	Hour
JA/ET	Jasmonic acid mediated Ethylene signalling
Kg	Kilogram
L	Liter(s)
LCR	Low-molecular-weight Cysteine-Rich Protein
LYK	Lysin motif receptor kinase
M	Molar
MAP	Mitogen activated protein
MAPK	MAP kinase
MAPKK	MAP kinase kinase
mg	milligram
min	minutes
mL	milliLiter
mM	milliMolar
MS	Murashige & Skoog
MW	Molecular Weight
NB-LRR	Nucleotide-Binding Leucine-Rich Repeat
NIV	Nivalenol
NLS	Nuclear Localization Signal
NP	Non-Pollinated pistil
NTC	Non-Template Control
PAMPs	Pathogen-Associated Molecular Patterns
PBS	Phosphate Buffered Saline

PCD	Programmed Cell Death
PCR	Polymerase Chain Reaction
PDA	Potato Dextrose Agar
PDF	Plant Defensins Family
PG	Pollen Grain
PGM	Pollen Germination Medium
PRR	Pathogen Recognition Receptors
PrsS	*Papaver rhoeas* stigma S-determinant
PrpS	*Papaver rhoeas* pollen S-determinant
PTG	Pollen Tube Germination
PTI	PAMP-Triggered Immunity
RFP	Red Fluorescent Protein
RNA	Ribonucleic Acid
RNAi	RNA interference
qPCR	Quantitative real time Polymerase Chain Reaction
ROS	Reactive Oxygen Species
SA	Salicylic Acid
SCA	Stigma/style Cysteine-rich Adhesin
SCR	S-locus Cysteine-Rich
SE	Synergid Endosperm
SLR	S Locus-Related glycoprotein
SI	Self-Incompatibility
SP11	S-locus Protein 11
SRK	S-locus Receptor Kinase
T-DNA	Transfer-DNA
VPE	Vacuolar Processing Enzyme
v/v	Volume/volume
WGA-TMR	Wheat Germ Agglutinin-TetraMethylRhodamine
WT	Wild type
w/v	weight /volume
µg	Microgram(s)
µL	Microliter(s)
µm	Micrometer(s)
µM	Micromolar

1. Summary

In contrast to animals and lower plants, male gametes of angiosperms are immobile and require transportation via the pollen tube cell to reach the female gametophyte, and together complete double fertilization. The path of the pollen tube towards the female gametes is guided by different types of signalling molecules, among them are defensin and defensin-like (DEFL) cysteine-rich peptides. Although *A. thaliana* has more than 300 genes encoding DEFLs, several of which are involved in plant immunity and cell-to-cell communication during fertilization, the roles of most members of this family are unknown.

The main aim of this project was to systematically identify DEFL genes expressed in *A. thaliana* during double fertilization particularly during pollen-tube guidance as well as in response to fungal infection. This was accomplished by analysis of *A. thaliana* transcriptomes of pistils selfed, treated with *A. lyrata* or *A. halleri* pollen or infected with *F. graminearum.* Candidate DEFLs exclusively expressed in pistils were selected to carry out a detailed characterization of their expression *in planta*. The second objective of this project was to gain insight into the molecular basis of *Arabidopsis-Fusarium* interaction based on the expression patterns of DEFLs. *A. thaliana* is an appropriate translational model for investigating how DEFLs counteract *F. graminearum* infection because the immune response of *A. thaliana* is very well documented.

Analysis of pistil transcriptome data showed that a total of 72 DEFL genes were differentially expressed in *A. thaliana* pistils. Detailed studies of eGFP localization of 25 DEFL candidate genes, showed 11 of them were expressed before pollination in specific cells of the mature female gametophyte, while four candidates were expressed in mature pollen grains, but not in growing pollen tubes. Post-fertilization, most genes expressed in the central cell of the ovule were expressed in the developing seed endosperm. Key results hinting at the possibility of DEFL involvement in different biological processes are the expression in roots of several candidates detected in the gametophytes and the upregulation of LURE1.1 in infected pistils, suggesting this known pollen tube attractant might also participate in the immune response. Further statistical analysis of candidate DEFL gene expression data, showed there is a high correlation between the transcription of those expressed in the central cell of the embryo sac and the ones expressed in the synergids, suggesting co-regulated DEFLs play a role in guidance of the pollen tube before fertilization and during polytubey block after fertilization.

Analysis of the infected pistil transcriptome and the literature suggests specific DEFL genes may be part of the first line of defence to *F. graminearum* via PAMP-triggered immunity (PTI). Some of these DEFL genes are regulated as secondary messengers of ROS production and also in the downstream process of MAPK signalling cascade. Furthermore, the patterns of differential expression of five DEFL genes (PDF1.2a-c, PDF1.4, PDF1.3), hint they are possibly regulated by the JA/ET defence signalling pathway during the necrotrophic phase of *Fusarium* infection.

In this context, the detrimental influence of *F. graminearum* infection in reproduction was investigated through analysis of seed development and seed set. This work suggests unfertilized ovules are more prone to *Fusarium* infection and its necrotrophic phase has a major detrimental influence in seed development. Furthermore, the reduction in seed set observed during *Fusarium* infection was caused by programmed cell death (PCD) of unfertilized ovules as documented by observation of ovule micromorphology in marker line AtCEP1-eGFP and analysis of RNAseq data. Specifically, the upregulation of genes encoding proteases involved in PCD in the infected pistil transcriptome suggests a mechanism where necrotrophic *Fusarium* obtains nutrients by manipulating the immune response of its host.

Our findings suggest that DEFL genes which are specifically expressed in reproductive tissues might play a role in defence and some of them, like LURE1.1 also possess dual function in reproduction. We hypothesize that DEFL genes initially had a role in protecting reproductive tissues and later on some of them acquired additional roles in cell-to-cell communication during pollination. The results of this study are relevant to understand the similarities between the processes of double fertilization and the immune response, identify interesting candidate genes to address the molecular basis of reproductive isolation and to develop strategies to counteract *Fusarium* head blight, a major crop disease affecting yield and jeopardizing food and feed safety worldwide.

2. Zusammenfassung

Im Gegensatz zu Tieren und niederen Pflanzen sind männliche Gameten von Angiospermen unbeweglich und erfordern einen aktiven Transport zu den weiblichen Gameten über die Pollenschlauchzelle.Der Weg des Pollenschlauchs zu den weiblichen Gameten wird von verschiedenen Arten von Signalmolekülen geleitet; Darunter kommt defensinähnliche (DEFL) cysteinreiche Peptiden eine besondere Bedeutung zu. *A. thaliana* hat mehr als 300 DEFL-Gene, die sowohl an der Pflanzenimmunität als auch an der Zell-Zell-Kommunikation beteiligt sind, jedoch sind die Rollen der meisten DEFL-Gene in *A. thaliana* weitgehend unbekannt.

In diesem Projekt wurde die Analyse von mehreren Pistil-Transkriptomen zur systematischen Identifizierung von DEFL-Gene herangezogen. Zu diesem Zweck wurde *A. thaliana* mit sich selbst, gekreuzt und mit den nahestehenden Arten *A. lyrata* und *A. halleri*. Um die DEFL Gene zu identifizieren, die während der Abwehrreaktion exprimiert wurden, wurden Infektionsstudien mit F. graminearum durchgeführt. Kandidaten DEFLs, die ausschließlich in Pistillen exprimiert wurden, wurden ausgewählt, um eine detaillierte Charakterisierung ihrer Expression in der Pflanze einschließlich Stempel und Wurzeln durchzuführen. Diese Informationen wurden verwendet, um ihre möglichen Rolle bei der Befruchtung und Infektion zu untersuchen.

Ein Ziel dieses Projekts war es, einen Einblick in die molekulare Basis der *Arabidopsis-Fusarium*-Wechselwirkung zu gewinnen, basierend auf den Expressionsmustern der DEFLs.Die Ergebnisse dieser Analyse sind relevant für die Entwicklung von Strategien zur Bekämpfung der Fusarium-Kopffäule, einer großen Erntekrankheit, die den Ertrag beeinträchtigt und die Nahrungsmittel- und Futtermittelsicherheit weltweit gefährdet.

Die Transkriptomdaten zeigten, dass insgesamt 72 DEFL Gene differentiell exprimiert wurden. Unter diesen wurde LURE1.1, von infiziertem Pistil differentiell exprimiert, was nahelegt, dass dieses Peptid mehrere Funktionen haben könnte. Detaillierte GFP-Lokalisierungsstudien in 25 Kandidaten zeigten, dass 11 DEFL-Gene vor der Bestäubung in spezifischen Zellen des reifen weiblichen Gametophyten exprimiert wurden, wohingegen vier DEFL-Gene in reifen Pollenkörnern Expression zeigten. Zusätzlich konnte gezeigt werden, dass 6 von 15 DEFLs auch in Wurzeln exprimierten.

Eine weitere statistische Analyse der Kandidaten-DEFL-Genexpressionsdaten zeigte eine hohe Korrelation zwischen der Transkription der ausgeprägten zentralen Zelle und jenen, die in den Synergiden exprimiert wurden, was darauf hindeutet, dass co-regulierte DEFLs eine

Rolle bei der Handhabung des Pollen-Röhrchens vor der Befruchtung und während der Zeit spielen Polytubey-Block nach der BefruchtungDer Einfluss der F. graminearum-Infektion bei der Reproduktion wurde durch Analyse des Samenkörner je Schote dokumentiert. Hierbei zeigte sich, dass die nekrotrophische Phase von F. graminearum einen großen Einfluss auf die Samenentwicklung hat und dass die unbefruchtete Eizelle anfälliger für eine Fusariuminfektion war, als die umliegenden Zellen. Die Wirkung der Fusarieninfektion auf die unbefruchtete Eizelle wurde auch durch die Entwicklungsstudien unterstützt. Die unbefruchtete Eizelle unterzog PCD während der *F. graminearum*-Infektion, die durch die PCD-Markerlinie AtCEP1: eGFP beobachtet wurde. Dies wurde durch die Hochregulation der Endopeptidase CEP1 und des α-Vakuol-Verarbeitungsenzyms (αVPE) in den Transkriptomdaten des infizierten Pistils unterstützt. Somit erscheint es naheliegend, dass F. graminearum Toxine die Eizelle manipulieren, um VPE und andere Proteasen zu produzieren, welche PCD nach sich ziehen, um Nährstoffe während der nekrotrophischen Phase zu erhalten.

Schließlich kann die Analyse des infizierten Pistil-Transkriptoms und der Literaturanalyse zu dem Ergebnis, dass spezifische DEFL-Gene Teil der ersten Verteidigungslinie zu F. graminearum über PAMP-getriggerte Immunität (PTI) sein können. Einige dieser DEFL-Gene werden als sekundäre Botenstoffe der ROS-Produktion und auch im nachgeschalteten Prozess der MAPK-Signalkaskade reguliert. Darüber hinaus deuten die Muster der differentiellen Expression von fünf DEFL-Genen (PDF1.2a-c, PDF1.4, PDF1.3) darauf hin, dass sie möglicherweise durch den JA / ET-Abwehr-Signalweg während der nekrotrophischen Phase der Fusarium-Infektion reguliert werden.

A. thaliana verwendet DEFLs als einen der Abwehrmechanismen gegen F. graminearum, die in die nährstoffreichen Gewebe der Stempel eindringen. Zusammenfassend bestätigen diese Ergebnisse die Rolle der DEFLs bei der Pflanzenimmunität im *Arabidopsis* Pistil.

Die gezeigten Ergebnisse deuten darauf hin, dass DEFL-Gene, die spezifisch im Fortpflanzungsgewebe exprimiert werden, eine Rolle bei der Verteidigung spielen können.

3. Introduction

3.1 Double fertilization

Double fertilization is the defining feature of angiosperms and was discovered by Nawaschin in 1898 (Nawaschin 1898). Double fertilization involves fusion of two sperm cells with the egg and central cell to form both embryo and endosperm respectively (Berger et al. 2008). The embryo gives rise to the next plant generation which is nourished by the endosperm during its development (Bleckmann et al. 2014). Signalling events during pollen-pistil interactions are highly orchestrated, which enables plant species to avoid inbreeding and encourages outcrossing. The amount and total mass of seed produced by a given species are closely linked to successful reproduction, and thus we can consider double fertilization as one of the important agronomical traits. Our daily nutrition is highly dependent either directly or indirectly on reproductive success of flowering plants.

In angiosperms such as *Arabidopsis thaliana* (*A. thaliana*), immotile sperm cells are transported by the pollen tube through the transmitting tract towards the female gametophytic cells (Dresselhaus et al. 2013). The female gametophyte (embryo sac) consists of seven cells and four cell types: three antipodal cells, two synergid cells, an egg cell and a central cell (Sundaresan et al. 2010).

Sexual reproduction in *A. thaliana* requires a great deal of coordination between gametic cells of male and female reproductive organs. There is an active crosstalk between the pollen tube and pistil during double fertilization (Dresselhaus et al. 2013). The pollen grains released by the anthers are attached to the papilla cells of the stigma by physical adhesion (Dresselhaus et al. 2013). This adhesion is called pollen capture and the sporopollenin which makes up the exine of the pollen coat plays an important role in that this step takes place in a species-preferential manner (Swanson et al. 2004). The following stage is the pollen-stigma cross-linking where proteins, lipids, and carbohydrates of the stigma and pollen membrane interact for the first time (Swanson et al. 2004). Subsequently, pollen hydration is regulated by plasma-membrane-localized stigmatic proteins along with pollen coat lipids (Dresselhaus et al. 2013). Following germination, pollen tubes penetrate the stigmatic tissues by secreting digestive enzymes and grow through the transmitting tract of style towards the ovule (Swanson et al. 2004). During pollen tube growth, the pollen tube is guided by various chemo-attractants present in the pistil extracellular matrix (Dresselhaus et al. 2013). Specifically, pollen tube guidance towards the ovule is controlled by two processes known as ovular guidance and micropylar guidance (Takeuchi et al. 2012). Ovular guidance is mediated

by signals from sporophytic cells, whereas micropylar guidance depends on the female gametophytic cells (Berger et al. 2008).

The pollen tube is guided by cysteine rich peptide LURE which are secreted by the synergid towards the ovule (Figure 1) (Dresselhaus et al. 2016). The pollen tube enters the embryo sac through the thick synergid cell wall known as filiform apparatus at the micropylar end (Figure 1) (Eckardt 2007). When the pollen tube comes in contact with one of the receptive synergid, the pollen tube ceases to grow and the receptive synergid undergoes cell death. The pollen tube discharges two sperm cells into the cytoplasm of the degenerating synergid in an event known as "pollen tube burst" (Dresselhaus et al. 2016) (Figure 1). The pollen tube burst occurs within 20 seconds after entering the female gametophyte (Drews et al. 2011). After the pollen tube bursts, the two sperm cells move to chalazal region of the degenerated receptive synergid cell within a few seconds (Figure 1). The two sperm cells remain in an immobile state in that region for approximately seven minutes (Figure 1). This is followed by the fusion of one sperm cell with the egg cell to form the embryo and the other sperm cell fuses with central cell to form the endosperm (Hamamura et al. 2012; Dresselhaus et al. 2016).

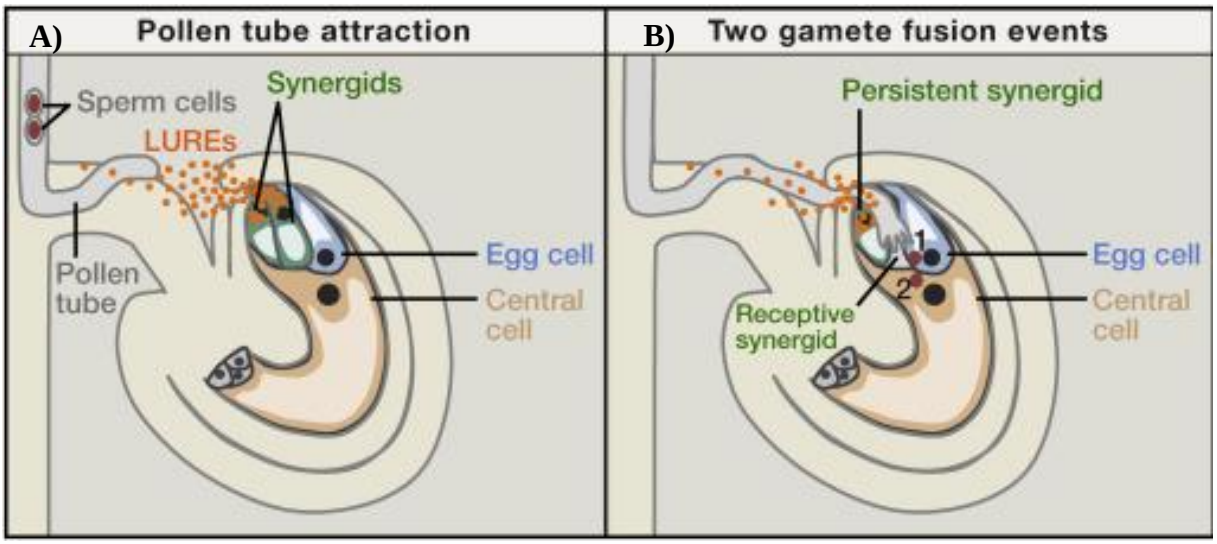

Figure 1: Double fertilization in *Arabidopsis thaliana*

(A)The pollen tube is guided by LURE peptides which is secreted by the synergids. (B) The pollen tube enters the ovule through the micropylar opening into a receptive synergid where it bursts. Two sperm cells are released and remain immobile for a few minutes after which one of them fuses with the egg cell to form an embryo, while the other sperm cell fuses with the central cell to form the endosperm.Picture modified from (Sprunck et al. 2015).

3.2 The role of cysteine-rich peptides in reproduction

Cysteine-rich peptides (CRP) is a class of small peptides that constitute around 2% of all expressed genes in some plant species (Silverstein et al. 2007). All CRPs have common features such as conserved N-terminal region, C-terminal containing 4–16 cysteine residues, and a size of less than 160 amino acid residues (Marshall et al. 2011). CRPs are categorized by their primary sequence, the position and number of cysteine residues and the location where disulfide bridges form conserved 3D structures (Silverstein et al. 2007). It has been reported that several CRPs play a vital role in pollen-pistil interactions during plant reproduction (Marshall et al. 2011).

Many species of flowering plants have developed a mechanism to prevent self-fertilization during pollen-stigma interaction, which is known as self-incompatibility (SI). Among the first CRPs where a role in reproduction was described are those involved in SI. SI determinants found in pollen and stigma are programmed as a pair in order to control self-non-self-pollen recognition (Swanson et al. 2004). An identical interaction between *S-allele* ligand–receptor activates SI downstream signalling that results in programmed cell death (PCD) (Thomas et al. 2004). SI is an important mechanism in plants which aids in maintaining genetic diversity by preventing plant species from inbreeding. In Brassicaceae, the male determinant of SI is the so-called S-locus cysteine-rich (SCR)/S-locus protein 11 (SP11), which is a CRP from those first classified as defensins. SCR is found in the pollen coat and contains eight conserved cysteine residues. Binding of SCR/SP11 to the female SI determinant, *S*-locus receptor kinase (SRK) in the stigma triggers signalling pathways that culminate into pollen rejection through blocking of pollen hydration and inhibition of pollen tube germination (Shiba 2001). In contrast, in *Papaver rhoeas*, the female SI determinant *Papaver rhoeas* stigma S-determinant (PrsS) encodes a CRP containing four conserved cysteines (Figure 2) (Wheeler et al. 2009). During the incompatible pollen grain interaction in *Papaver rhoeas*, papillae cell secretes PrsS which binds to the *Papaver rhoeas* pollen S-determinant (PrpS) and results in PCD of the pollen tube (Wheeler et al. 2010).

CRPs are also involved in pollen tube growth and guidance. In tomato, pollen-specific secreted protein LAT52 interacts with the pollen receptor LePRK2 for pollen germination (Figure 2) (Zhang et al. 2008). STIG1 a CRP from the stigma and style interacts with LePRK2 to promote pollen tube cell growth in the stigma (Figure 2) (Tang et al. 2004). In the stigma/style of lily, the stigma/style cysteine-rich adhesin (SCA) along with pectin is involved in adhesion of pollen tube and growth through transmitting tract (Figure 2).

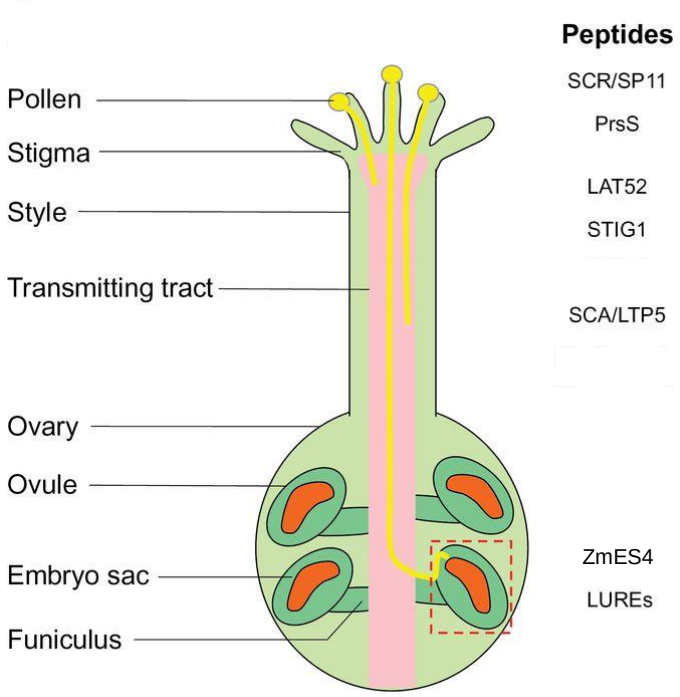

Figure 2:Schematic diagram showing CRPs involved in communication during plant reproduction

(A) Schematic representation of pollen-tube guidance in Angiosperms. (B) Schematic image representing the CRPs SP11, PrsS, SCA, LAT52 and STIG1 involved during pollen–stigma interactions leading to pollen adhesion, hydration, germination and pollen tube growth. (C) CRPs such as LUREs, ZmEA1 is involved during microphylar guidance prior to double fertilization. Picture modified from (Kanaoka et al. 2015).

LTP5s is secreted from the pollen tube tip in order to maintain the pollen tube polarity (Dresselhaus et al. 2013).CRPs have also been reported to act as short-range micropylar attractants for pollen tubes. Specifically, defensins such as LUREs are secreted by the synergid cells for pollen tube guidance towards ovule (Figure 2) (Takeuchi et al. 2012). After the pollen tube enters the micropyle, *Zea mays* defensins ZmES4 secreted by synergid ensures pollen tube growth arrest and participates in pollen tube bursting (Amien et al. 2010) (Figure 2). ZmES4 interacts with the pollen tube potassium channel KZM leading to an influx of K^+ which results in uptake of water and subsequently leads to pollen tube bursting (Amien et al. 2010).

3.3 Role of DEFLs in species -preferential manner during reproduction

Some of the female gametophyte genes that are involved in the guidance and reception of pollen tube may have species preferential interactions, and thereby contribute to establishing prezygotic reproductive isolation (Escobar-Restrepo et al. 2007; Takeuchi et al. 2012). Interspecific crosses mostly yield none or a reduced number of seeds due to the failure of

pollen tube growth arrest and failed pollen tube burst, reminiscent of the *fer (feronia)*-like phenotype (Escobar-Restrepo et al. 2007). The *fer*-like phenotypes in some interspecific crosses strongly suggest that species-preferential signal between the pollen tube and ovules mediates pollen tube growth arrest and burst. Prezygotic reproductive isolation takes place when this signal is missing in interspecific crosses.

As mentioned in the previous section, defensins and defensin-like proteins (DEFL) are one of the subgroups of CRPs. DEFLs are involved in pollen-pistil interactions in a species-preferential manner. SCR/SP11 was the first DEFL gene shown to act in species preferential manner during SI during pollen-stigma interaction (Boggs et al. 2009). DEFL peptides such as LUREs and ZmES4 are involved in pollen tube guidance, pollen tube reception and are responsible for the failure of double fertilization events by acting in a species-preferential manner during interspecific crosses (Amien et al. 2010; Takeuchi et al. 2012). The consequences of this preferentiality are that LUREs and ZmES4 peptides secreted by female gametophyte constitute a mechanism of prezygotic reproductive barrier during interspecific crosses. Overcoming this prezygotic barrier would open up possibilities to improve crop productivity. Example of overcoming prezygotic reproductive barrier has been reported in *T. fournieri*. *A. thaliana* LURE peptide was transformed in *T. fournieri and T. fournieri* ovule was able to recognize *A. thaliana* pollen (Takeuchi et al. 2012).

3.3.1 Arabidopsis species are an ideal experimental model for studying reproductive isolation

A. thaliana a selfing species and has strong prezygotic reproductive isolation mechanisms triggered when crossed with other species (Grundt et al. 2006). *Arabidopsis lyrata (A. lyrata)* and *Arabidopsis halleri (A. halleri)* are self-incompatible species that are related to *Arabidopsis thaliana* (Clauss et al. 2006).

A. lyrata diverged approximately five million years ago from *A. thaliana and* is a closely related species to *A. thaliana*. *A. lyrata* is a perennial herb with distribution in the northern hemisphere and central Europe in restricted habitats (Schmickl et al. 2010). *A. halleri* is a heavy metal accumulating species which is distributed in central Europe, eastern Asia and grows on acidic, neutral and oligotrophic soils. *A. halleri* is mostly studied for its characteristics in tolerance, accumulation of heavy metals, and is an important model of studying phytoremediation (Clauss et al. 2006). *A. halleri* and *A. lyrata are* outcrossing diploids with genomes 50% larger than the *A. thaliana* genome. They are compatible as shown by allopolyploid *Arabidopsis kamchatica*, a hybrid that originated from the

interspecific cross of *A. lyrata* and *A. halleri* (Shimizu-Inatsugi et al. 2009). *A. thaliana* along with self-incompatible *A. lyrata* and *A. halleri* are ecologically diverged, but occur in geographically overlapping region, making them an ideal plant species for studying the genetic basis of plant reproductive isolation.

In recent years, DEFLs in *Arabidopsis* species have been shown to mediate the communication between male and female gametophytes in a species preferential manner, this property makes it an ideal gene family for understanding reproductive isolation. For example, the transformation of SCR-complexes along with SRK from *S*-locus of self-incompatible *A. lyrata* to *A. thaliana* was sufficient to impart SI phenotypes in self-fertile *A. thaliana* (Boggs et al. 2009).

3.4 Role of defensins in immunity

Although plants have physical barriers to pathogen entry like the cuticle or bark, the size of stomatal pores and alteration of cell walls(Zeng et al. 2010; War et al. 2012), they fundamentally rely on an innate immune system (Dodds et al. 2010). Plant innate immune responses can be represented using a zigzag model (Figure 3).

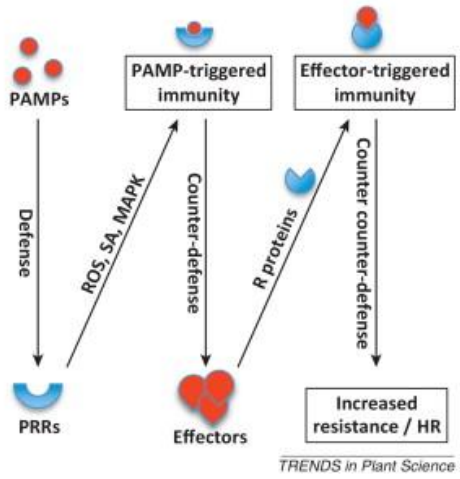

Figure 3:Zigzag model of plant innate immunity
In phase 1, plants detect PAMPs via PRRs to trigger PTI and this is followed by pathogens delivering effectors that would interfere with PTI and resulting in ETS. In phase 2, effector is recognized either directly or indirectly by an NB-LRR protein, and thereby activating ETI which often cause hypersensitive cell death (HR) and production of defence related gene. Picture was taken from (Incarbone et al. 2013)

In the first phase, pathogen-associated molecular patterns (PAMPs) such as chitin, which is a part of fungal cell wall component, are recognized by pathogen recognition receptors (PRRs), and resulting PAMP-triggered immunity (PTI) stops pathogen growth (Figure 3) (Dodds et al. 2010). In turn, pathogens deploy effectors which interfere with PTI and results in effector-triggered susceptibility (ETS) (Figure 3). In the second phase of innate immunity, effectors are recognized either directly or indirectly by NB-LRR proteins, resulting in effector-triggered

immunity (ETI) (Figure 3) (Dodds et al. 2010). The molecular events of ETI overlaps with those of PTI and specific immune responses for defence (Jones et al. 2006). The plant responds to pathogens with diverse defence strategies such as the expression of defence-related genes, oxidative bursts, increased production of hormones and programmed cell death (Wu et al. 2014; Bigeard et al. 2015). Signalling cascades such as the mitogen-activated protein kinase (MAPK) pathway, are triggered during the defence response. These cascades of protein phosphorylation respond to extracellular biotic stress by activating a wide range of cellular responses (Bigeard et al. 2015).

DEFLs are reported to participate in different biological functions, such as the previously described cell-to-cell communication during fertilization and the immune response which will be described in the following section. Plant defensins with antimicrobial activity are a vital part of the innate immune system of angiosperms (Carvalho et al. 2009)**.** Plant defensins are induced as part of defence response to a broad spectrum of fungal plant pathogens and some bacteria (Carvalho et al. 2009; Penninckx et al. 2003). Lack of antibacterial activity of most plant defensins would possibly be due to the relatively larger infection pressure exhibited by fungal pathogens in comparison to the threat posed by bacteria (Thomma et al. 2002). They also inhibit the *in vitro* growth of human pathogenic fungi *Candida albicans* and *Saccharomyces cerevisiae* (Vriens et al. 2014; Aerts et al. 2011).

Defensins and DEFLs are expressed in all plant tissues reflecting their potential role in the systemic response to fungal infection of vegetative tissues or as constitutive defence barrier, especially in seeds and reproductive organs (Hegedus et al. 2013). Plant defensins are categorized in morphogenic or non-morphogenic according to their effect on the morphology of fungal hyphae. While the inhibition of hyphal elongation by morphogenic defensins results in hyphal hyperbranching, non-morphogenic defensins inhibit hyphal growth without any distortions (Ramamoorthy et al. 2007; Thomma et al. 2002).

Defensins might also counteract the effects of wounding by herbivore insects and parasitic plants. For example, the defensin VrD1 from *Vigna radiate* seeds inhibits insect α-amylase, leading to indigestibility of plant starch in the insect gut. Defensins which have antifungal activity do not exhibit α-amylase activity and vice versa (Thomma et al. 2002; Carvalho et al. 2009). The sunflower defensin Ha-DEF1 are also involved in the defence against parasitic plant *Orobanche cumana*, which causes severe yield losses on sunflower (Hegedus et al. 2013).

Defensins have several mechanisms of action in order to carry out the defence response. One of the mechanisms is by binding to fungal ion channels (Marshall et al. 2011). Blocking of ion channels by defensins leads to inhibition of fungal hyphal tip growth and halts fungal colonization. For example, RsAFP2 defensins which were isolated from radish seeds exhibited antimicrobial activity by affecting K^+ and Ca^{2+} ion transport channels in the fungal membrane (Lacerda et al. 2014). Defensins have developed other mechanism to combat fungal invasion. For example, they have cationic characteristics and interacts with negatively charged plasma membrane components of fungi. During their interaction, defensins alter the fungal membrane by inducing the production of reactive oxygen species (ROS) (Hegedus et al. 2013). For example, NaD1 defensin isolated from *Nicotiana alata* flowers induces oxidative damage in *Candida albicans* by hyperproduction of ROS (Hayes et al. 2013).

Transgenic plants expressing defensins have an increased resistance to fungal pathogens. For example, WT1 from wasabi when overexpressed in rice, potato and orchid, resulted in increased resistance against *Magnaporthe grisea*, *Erwinia carotovora* and *Botrytis cinerea* (Kanzaki et al. 2002; Lay et al. 2005; Stotz et al. 2009). Transgenic tomato plants containing defensin Rs-AFP2 decreased the activity of phytopathogenic fungi, including *Alternaria solani*, *F. oxysporum*, *Phytophthora infestans*, and *Rhizoctonia solani* (Lacerda et al. 2014). Overexpression of Rs-AFP2 in transgenic rice (*Oryza sativa)* reduce *Magnaporthe oryzae* and *Rhizoctonia solani* infection. These two fungi are the main causative agents for rice blast and sheath blight diseases which leads to rice losses in agriculture (Jha et al. 2010). Pea defensins enhanced resistance towards blackleg diseases in *Brassica napus* which is caused by *Leptosphaeria maculans* (Wang et al. 1999).

3.5 Other functional roles of defensins

Apart from immunity and intercellular communication during fertilization, plant defensins have adopted different roles. For example, AhPDF1.1 from *A. halleri* has antifungal activity and mediates zinc tolerance (Mith et al. 2015). Plant defensins also play a role in regulating growth and development of tissue. Specifically, MsDef1, MtDef2, RsAFP2 are all capable of inhibiting the growth of plant roots *in vitro* (Hegedus et al. 2013). The tomato DEF2 is expressed during initial stages of flower development and promotes meiosis. The tomato DEF2 also influences pollen viability and is also involved in the growth of various organs (Stotz et al. 2009). In addition, plant defensins are induced in response to environmental stress. For instance, soybean defensin gene Dhn8 was induced during drought stress (Lay et al. 2005), NeThio1 and NeThio2 from *Nicotiana excelsior* are induced in response to salt

stress (Lay et al. 2005). Several defensins are also upregulated in winter wheat in response to cold induction, and potentially have a role in resistance towards freezing conditions (Gaudet et al. 2003).

3.6 Structure of Defensins

Defensins are structurally conserved in vertebrates and invertebrates including human immune cells. They exist in all plant families, including the *Brassicaceae.* In the early 1990s, defensins were initially documented to have fewer members in *Arabidopsis*, the scenario changed over the years with more in-depth studies which enabled in the identification of 324 DEFLs including 15 known defensins (Silverstein et al. 2007).

Most of the defensins genes that have been identified are composed of two exons: the first exon encodes for N-terminal signal peptide, whereas the second exon encodes for the cysteine-rich region that forms a positively charged mature peptide (Figure 4) (Silverstein et al. 2007). Defensins are categorized into two groups based on precursor proteins. In the first group, the precursor protein contains an endoplasmic reticulum (ER) signal peptide sequence and a mature defensin domain (Lay et al. 2014). The protein enters into the secretory pathway without any post-translational modification or subcellular targeting. The second group of defensins comprises of precursor protein with an additional C-terminal prodomain (Lay et al. 2014).C-terminal prodomain functions in subcellular targeting and is removed by proteolytic enzymes while entering through the secretory pathway.

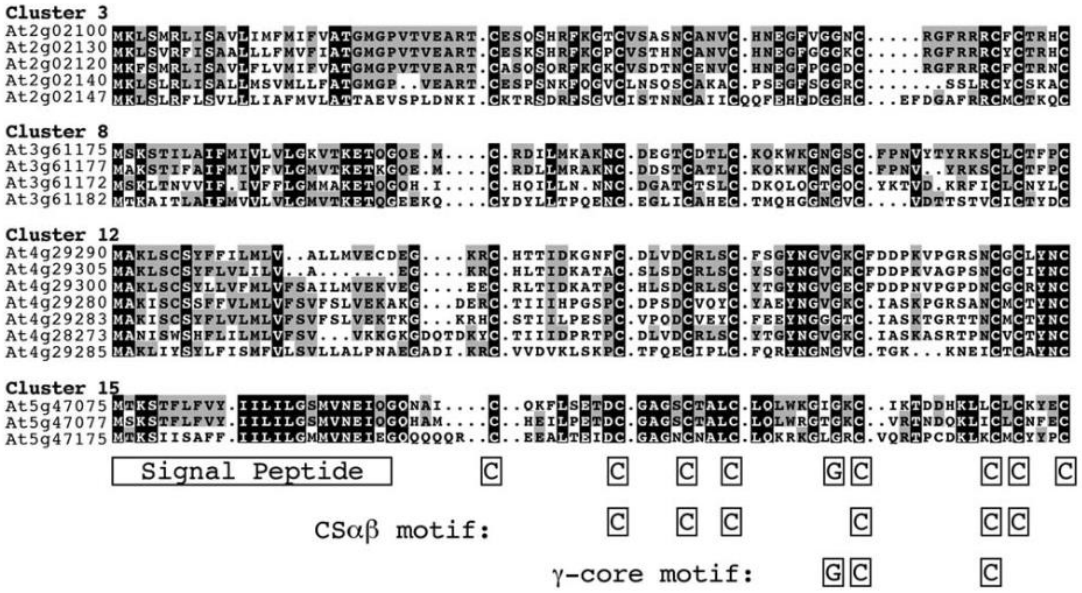

Figure 4:Alignment of different DEFL clusters from *Arabidopsis*.
Alignment represents four distinct clusters of DEFLs in Arabidopsis. Identical in clusters are shaded black, whereas grey represents similar residues. Signal peptide are box labeled below the alignment. C or G designate conserved Cys are box labelled as C and Gly residues are box labelled with G. CSα/β and γ-core are shown below the alignment. Picture taken from (Silverstein et al. 2005).

Defensin peptides are usually between 60 to120 amino acids long and have conserved six to eight cysteine residues which form intramolecular disulphide bridges (van der Weerden et al. 2013). Intramolecular disulphide bridges are responsible for the structural and thermodynamic stability of the defensins protein. The 3D structure of defensins exhibits a two motif (Figures 4 and 5). The first motif consisting of α -helix connected to triple-stranded, antiparallel β -sheet by three disulfide bonds forming cysteine-stabilized α/β motif (CSα/β) (Figures 4 and 5) (van der Weerden et al. 2013). Defensins have a conserved γ-core motif which consists of two antiparallel β-sheets with loop region. Positively-charged amino acids located at the γ-core motif are important for the antimicrobial activity of defensins (Figures 4 and 5) (Yount et al. 2004).

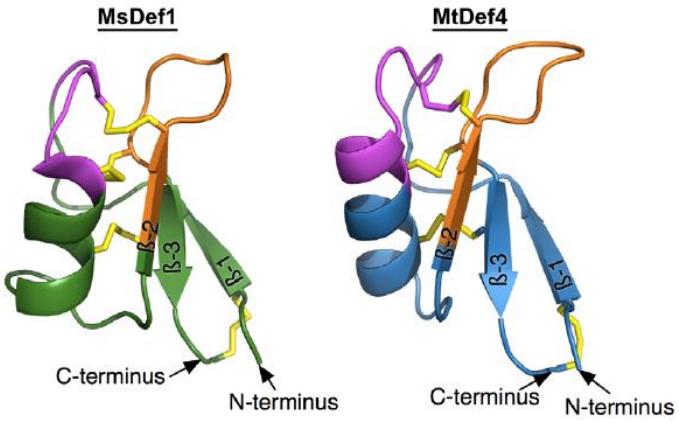

Figure 5:Three-dimensional structures of plant defensins MsDef1 and MtDef4.
MsDef1 and MtDef4 share highly conserved homology sequence. γ-core motif is represented in orange color which carries net positive charge. The CSα/β-core motif is represented in pink color and four disulfide bridges are represented in yellow color which stabilizes the defensins. Picture taken from (Sagaram et al. 2011)

3.6.1 Defensins under selection pressure

Plant defence and reproduction, are two highly conserved processes in the plants which are dependent on the various environment factor and each of the processes have biotic influence. The pathogen-host and male-female gamete interactions have strong selection pressure on the molecular evolution of genes (Takeuchi et al. 2012). Gene duplication events along with diversifying selection was an important mechanism for plants to evolve in the arms race between microbial attackers and host plants.

Defensins are predicted to exhibit diversifying selection since its primary function is to mediate innate host defence and reproduction (Tesfaye et al. 2013). Defensins have been detected with diversifying selection in ants due to selection pressure caused by microbial pathogens (Viljakainen et al. 2008). The plant defensins tend to show characteristic molecular evolution patterns and selection pressure. These interactions, in particular sexual reproduction,

exert diversifying selection in DEFLs which eventually leads to reproductive isolation from other species (Takeuchi et al. 2012).

Signal peptides of the defensin are conserved, whereas mature peptides of the defensin are possibly subjected to diversifying selection which determines the specific function aspects of these genes (Silverstein et al. 2005). DEFLs occurs both individually and in clusters throughout the *A. thaliana* genome. The gene duplication followed by successive rounds of diversifying selection might have resulted in 100 subgroups of DEFL with different activities in *A. thaliana* (Tesfaye et al. 2013; Silverstein et al. 2005).

3.7 Fusarium graminearum

Fusarium graminearum also known by teleomorph stage *Gibberella zeae* is a soil borne fungi responsible for *Fusarium* head blight (FHB), a disease from cereal crops which has a dramatic effect on productivity and food safety (Kazan et al. 2012). Between 1990 and 2002, FHB epidemics resulted in a loss of $3 billion of wheat yield and quality in the USA (Schmale et al. 2003).

F. graminearum is a haploid homothallic fungus which has a sexual and an asexual life cycle (Schmale et al. 2003). Both life cycle starts with *F. graminearum* overwintering on infected crop residues. During the asexual life cycle, *F. graminearum* produces macroconidia in chlamydospores which enable its survival during unfavorable conditions (Figure 6). Macrocondia is dispersed to plants by rain-splash, and wind dispersal allowing to resume a new cycle of infection.

During suitable temperature and humidity, the sexual (teleomorph) stage of *F. graminearum* develops on infested plant debris. They form flask-like fruiting bodies called perithecia on the surface of infested residues (Figure 6). In perithecia, the sexual spores (ascospores) are formed within sacs called asci and forcibly discharged into the air (Figure 6). Ascospores are dispersed to crops by wind and rain. Infection occurs when macroconidia or ascospores land on wheat heads and cause mycelium development in aerial parts of the plant (Paul et al. 2004; Schmale et al. 2003). Infected seeds might give rise to blighted seedlings if untreated (Figure 6). First symptoms of FHB are diseased spikelets demonstrating premature bleaching. *F. graimearum* grows through diseased spikelet and spreads within the head. *F. graminearum* is also a vascular pathogen which can spread from the rachis of infected flowers to the other parts of plants through vascular bundles of xylem and phloem (Jansen et al. 2005).

F. graminearum is hemibiotrophic pathogen meaning it has both biotrophic and a necrotrophic lifestyle (Ding et al. 2011). The biotrophic lifestyle of *F. graminearum* is characterized by intercellular hyphae growth and no intracellular hyphae during the initial stages of infection of floral tissues (Brown et al. 2010). This biotrophic phase is followed by a necrotrophic lifestyle driven by nutrients obtained by intracellular colonization and host cell death. *F. graminearum* also exhibits saprotrophic growth due to its enzymatic ability to degrade crop residues for nutrients (Leplat et al. 2013; Khonga et al. 1988). Thus, *F. graminearum* can adapt to different environment conditions.

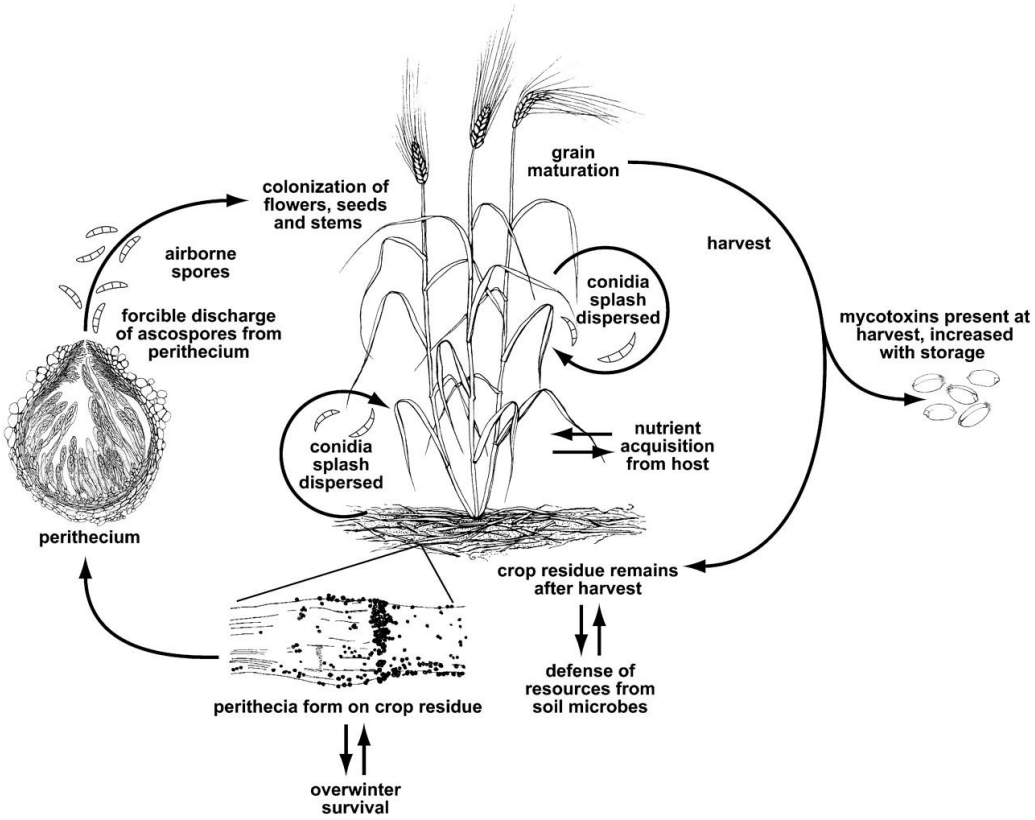

Figure 6:Disease life cycle of *F. graminearum*.
The *F. graminearum* overwinters in infested crop residues. Macroconidia are produced in asexual phase from crop residues and are dispersed by rain. During favourable conditions, perithecia are formed in crop residues in sexual phase. Ascospores are produced from perithecia and dispersed in air. Macroconidia / ascospores infect flower, seeds and stems. Mycotoxins are present in infected seeds. Illustration taken from (Trail 2009).

Analysis of the proteome from *F. graminearum* during plant colonization revealed several extracellular proteins that facilitate disease establishment and spread in the plant as well as proteins involved in acquiring nutrients (Divon et al. 2007; Paper et al. 2007; Taylor et al. 2008). Some of the proteins secreted by *F. graminearum* during pathogenesis contained putative secretion signals which might function as effectors to initiate infection (Paper et al. 2007). Along with this, numerous proteins involved in production of reactive oxygen species (ROS) which are linked to pathogenesis are secreted by *F. graminearum* (Walter et al. 2010), such as cell wall–degrading enzymes (cellulases, hemicellulases, and pectinases) which are

secreted in all the phases of diseases in order to manipulate plants physiology for its own benefit (Mary et al. 2002; Kikot et al. 2009). Proteases such as subtilisin-like and trypsin-like proteases are another important groups of virulence factors that are involved in the suppression of plant defence by degrading pathogenesis-related (PR) proteins (Olivieri et al. 2002; Pekkarinen et al. 2002).

F. graminearum produces deoxynivalenol (DON) and nivalenol (NIV) mycotoxins that are fundamentally responsible for the reduced grain quality, yield and toxicity (Rocha et al. 2005; Walter et al. 2010). Mycotoxins even at very low concentrations have adverse toxic effects on cattle and humans (Rocha et al. 2005; Sobrova et al. 2010). The DON toxin determines the aggressive nature of the *F. graminearum* to plant tissues and act as an inhibitor of biosynthesis of defence related proteins (Rocha et al. 2005; Boenisch et al. 2011).

F. graminearum is capable of infecting *A. thaliana* flowers primarily due to the abundance of choline and glycine betaine in the anthers as well as the nutrient- rich pistils and developing seeds (Strange et al. 1974) (Figure 7). In the infected *Arabidopsis* tissue, superficial aerial mycelium is observed which is influenced by the humidity levels (Urban et al. 2002). It has been reported that low concentrations of DON mycotoxin inhibit PCD in *Arabidopsis* during biotrophic phase to favor its growth (Diamond et al. 2013). Meanwhile, high concentration of DON along with proteases induces cell death in order to facilitate the necrotrophic phase (Diamond et al. 2013).

Figure 7:*F.graminearum* nfection of *Arabidopsis thaliana*
Fusarium graminearum infecting (A)*Arabidopsis thaliana* floral and (B) silique tissue. Picture modified from (Brewer et al. 2015)

Controlling of FHB in cereal crop mainly relies on biological measures which includes cultivar choice and rotation of crop. Intensive plant breeding and chemical control have reduced FHB to an extent. FHB still persists regardless of current control measures and has a drastic effect on crop production, livestock and humans. This could be overcome by investigating the molecular-genetic interaction that controls *F. graminearum* pathogenicity and plant resistance. In general, plant defence towards *F. graminearum* involves defence-response such as salicylic acid signalling (SA), jasmonic acid mediated ethylene signalling (JA/ET), ROS and production of defence related proteins.

Defensins inhibit *F. graminearum* growth, for example, MtDef4.2, *Medicago trunculata* defensin reduces its virulence by decreasing silique infection and lowering DON accumulation (Kaur et al. 2012). The role of DEFLs in response to *F. graminearum* in floral tissue has not been documented in *Arabidopsis thaliana*. Finding out which DEFL genes are behind resistance towards FHB is vital for genetically improving crop productivity.

3.8 Aims of the study

The molecular mechanism behind the fungal infection and double fertilization have similar characteristics. Fungal infection and pollen tube growth during reproduction mirror each other with germination followed by invasion of nutrient rich tissues. *Arabidopsis* pistils are thus an ideal system to investigate the molecular aspects shared by fungal hyphae colonization and pollen tube growth during pollination.

The primary objective of this project was to distinguish which defensin and defensin-like genes (DEFLs) are associated to fertilization as opposed to those involved in the immune response, based on their patterns of gene expression in the pistil,

DEFLs involved in both processes have already been characterized, however in *A. thaliana*, it has been reported that nearly 320 DEFL genes are present, yet the role of most of them is largely unknown. In this project, analysis of several pistil transcriptomes will be employed to systematically identify DEFL genes expressed in *A. thaliana* during double fertilization, particularly during pollen-tube guidance. For this aim, *A. thaliana* will be selfed, and crossed with self-incompatible species *A. lyrata* and *A. halleri*. In order to identify DEFL genes expressed during the defence response, *A. thaliana* pistils will be infected with *F. graminearum.* Additionally, DEFL genes expressed in leaves will be identified, in order to exclude those that are expressed both in pistils and in vegetative tissue from our studies.

Candidate DEFLs exclusively expressed in the pistils will be selected to carry out a detailed characterization of their expression *in planta* including pistils and roots. This information will further be employed to infer their possible roles in fertilization, infection, as well as to investigate the influence of fungal infection on fertilization.

The second objective of this project will be to gain insight into the molecular basis of *Arabidopsis-Fusarium* interaction based on the expression patterns of DEFLs. *A. thaliana* is an appropriate translational model for investigating how DEFLs counteract *F. graminearum* infection because the immune response of *A. thaliana* and its genetic basis are very well documented. The results yielded by this analysis are relevant to develop strategies to counteract *Fusarium* head blight, a major crop disease affecting yield and jeopardizing food and feed safety worldwide.

4. Material and Methods

For all reactions and experiments, only molecular grade and p.a. (*pro analysis*) chemical reagents were used. Molecular biological work was mainly based on published protocols (Green et al. 2012).

4.1 Plant materials and growth conditions

4.1.1 Surface sterilization of *Arabidopsis* seeds

The seeds of *Arabidopsis* species were taken in 2 ml Eppendorf tube and suspended in 70% ethanol for two minutes. Ethanol was discarded from the tube, and 50% volume of bleach was added and left for 5-10 minutes. The bleach was discarded and seeds were washed thoroughly with a large amount of sterile distilled water. Water is discarded and the washing step is repeated three times.

4.1.2 Growth conditions of *Arabidopsis* species

Seeds of *A. thaliana* ecotype Columbia were sown on soil and placed at 4^{o}C for three days in the dark to promote seed stratification. Seedlings were grown in long-day conditions (16h at 24^{o}C and 8h of 18^{o}C at 60% humidity) to induce flowering.

Seeds of *Arabidopsis halleri* ecotype DE-1-Heidelberg were surface sterilized and grown in Murashige & Skoog (MS) plates (10 g/L MS medium, 10 g/L Bacto agar, pH 5.8) stratified for ten days at 4^{o}C. MS plate with seeds was moved to long day conditions. Germinated plants were transferred to soil after two weeks. After two months, the plants with healthy rosettes are transferred to a vernalization chamber for ten weeks at 4^{o}C. They were removed from vernalization chamber to induce flowering under long day conditions.

Seeds of *Arabidopsis lyrata* ecotype *Lyrata* were surface sterilized. The seeds were kept in horizontally placed 15 ml falcon tube filled with sterile distilled water for three weeks at 4^{o}C. Germinated plants were transferred to soil and kept under long day conditions. After two months, the plants with healthy rosettes were transferred to vernalization chamber for ten weeks at 4^{o}C. They were removed from the vernalization chamber to induce flowering under long day conditions.

4.1.3 *Arabidopsis thaliana* root germination in MS plates

Seeds of DEFLs marker line were surface sterilized and then transferred to MS plates. To make sure that roots do not grow inside the gel, the plates were placed at a steep angle. Seeds were left to grow for 10-20 days in normal growth conditions and followed by microscopy analysis.

4.1.4 Pollen grain germination and tube growth

In vitro *Arabidopsis* pollen tube experiments were conducted as described previously by (Boavida et al. 2007) except that the pollen germination medium (PGM) was slightly modified (1 mM $CaCl_2$ $2H_2O$, 0.01% (w/v) H_3BO_3, 1 mM $CaCl_2$, 1 mM $MgSO_4$ $7H_2O$, and 18% (w/v) sucrose, 0.5 %, low melting agar pH 7.5). The *A. thaliana* flowers were removed with a pair of tweezers, and the pollen grain was rubbed on PGM in a Petri dish which was kept for 6 hours (hr) at room temperature for germination.

4.2 Pollination related work

4.2.1 Emasculation of *Arabidopsis* species flowers

The *Arabidopsis* flower was fixed gently on double sided tape on a microscope slide and placed under a 10-20 x magnification binocular. The flower bud was opened by inserting the tip of a forceps between petals and sepals. Anthers along petals were removed with the forceps from the flower bud. The emasculated pistil was marked with a piece of thread around its stem.

4.2.2 Pollination experiments

Flowers of the *Arabidopsis* species at developmental stage 12c (Smyth et al. 1990) were emasculated and left to recover for 24hr. Non-pollinated emasculated pistils of *Arabidopsis* species were collected after 24hr and quickly frozen in liquid nitrogen. Some of the emasculated pistils were pollinated with pollen grains of the respective *Arabidopsis* species.
Pistils were collected 8 hours after pollination (8HAP) and immediately frozen in liquid nitrogen. To minimize biological variation, three replicates were collected for each experiment containing 60 pistils per replicate. A few of the pollinated pistils from each experiment were collected and stained with aniline blue to visualize pollen tube growth inside the pistil.

4.2.3 Aniline blue staining of the pistils

The pistil was fixed with absolute ethanol/ glacial acetic acid (3:1) for 1-3 hours. Fixed pistil samples were washed three times with sterile distilled water for five minutes followed by bleaching with 8N NaOH overnight. Pistils were left in sterile distilled water for three hours, changing the water every hour. Pistils were stained with aniline blue (0.1% aniline blue in 100 ml K_3PO_4 O.1M) for 30-60 minutes. Stained pistils can be stored at 4^oC. Pistils were transferred to a slide and observed under a fluorescence microscope at 350-400nm.

4.3 Fusarium graminearum work

4.3.1 *Fusarium graminearum* strain

The *F. graminearum* strain SG005 was provided by Prof. Ralph Hückelhoven, Technische Universität München. This *Fusarium* strain was used in infecting *Arabidopsis* tissue for RNAseq. *F. graminearum* DsRed strain Fg8/1 was provided by Prof. Wilhelm Schaefer, University of Hamburg. This strain was used in *Arabidopsis* pistils for qPCR studies dealing with infection and pollination.

4.3.2 *F. graminearum* culturing in potato dextrose agar (PDA) plates

F. graminearum strain SG005 were grown in ¼ PDA plates (9.75 g/L of PDA) whereas *F. graminearum* DsRed strain Fg8/1 were grown in ¼ PDA plates along with geneticin antibiotic (50 μg/ml), and both strains were placed at 28^{o}C for 10-14 days.

4.3.3 Preparation of *F. graminearum* culture for infection

5 ml of sterile distilled water was poured on the surface of *F. graminearum* cultured ¼ PDA plate and scrapped with scalpel or microscope slide. The mixture was filtered through an autoclaved cotton gauze. Filtrate was added to 50 ml of wheat medium (10 g/L of wheat grass powder) or induction medium (1 g/L bacto yeast extract, 0.5 g/L magnesium sulfate heptahydrate, 15 g/L carboxyl methyl cellulose, 1 g/L ammonium nitrate, 1 g/L monopotassium phosphate, pH 6.5). The culture was incubated at 28^{o}C for 10-14 days in dark. The culture containing *F. graminearum* was filtered through sterile spandex bandage. The filtrate was centrifuged at 4^{o}C at 5000 rpm for 20 minutes. Supernatant liquid was discarded without disturbing the conidia. Conidia were suspended in sterile distilled water, diluted to the concentration ~ 8-9x10^{5} spores/ml and 1% Tween is added. Both strains of *F. graminearum* culture for infection was prepared in the same way.

4.3.4 Inoculation of *Arabidopsis* species for RNAseq

Flowers were emasculated and left to recover for 24hr before infection. The *Arabidopsis* plant was floral dipped into conidial suspension for 2-3 minutes. The plants were covered with a plastic bag sprayed with water to maintain the relative humidity. Care was taken to ensure the plant roots are not waterlogged, which greatly affects normal flower development. The plants were incubated in these conditions for 72hr for infection to develop under long day conditions. Similarly, *Arabidopsis* species were treated with sterile distilled water as a control (mock treatment). Infected leaves and pistils were collected after 72hr and immediately frozen in liquid nitrogen. Three replicates for each condition was collected. A

few infected leaves and pistils were collected and visualized by wheat germ agglutinin-tetramethylrhodamine staining (WGA-TMR) (Hoefle et al. 2011).

4.3.5 Chloral hydrate method for clearing infected tissue

The infected tissues were fixed overnight in the solution of (9:1) ethanol: acetic acid or in fixative solution (750 ml ethanol, 250 ml chloroform, 1.5 g trichloroacetic acid) for two days. The tissues were washed with 90% Ethanol for 30 – 60 minutes and followed by washing with 70% ethanol for 4hr. This was followed by washing with distilled water. Chloral hydrate solution (2.5 g of chloral hydrate is added to 1 ml of 30% glycerol) was added to washed tissue samples and left overnight. This is followed by WGA-TMR staining.

4.3.6 Wheat germ agglutinin-tetramethylrhodamine (WGA-TMR) staining of the pistil

For WGA-TMR staining, cleared tissue was washed with distilled H_2O and incubated for 20 minutes in 1x PBS buffer (8 g NaCl, 2.8 g Na_2HPO_4. $2H_2O$, 0.24 g KH_2PO_4, and 0.2 g KCl in 1L water, pH 7.4) and transferred to 5 ml of WGA-TMR staining solution (4900 µl 1x PBS, 50 µg/µl BSA, and 50 µl WGA-TMR). After vacuum infiltration of 20 minutes, leaves and pistils were left in the staining solution for at least 24h in the dark at 4^{o}C. Leaves and pistils were viewed in a confocal laser scanning microscopy (CLSM; Leica 510; Leica Microsystems). WGA TMR was excited by a 561-nm laser line and the emission was detected at 571 to 610 nm.

4.4 RNAseq related work

4.4.1 Total RNA extraction of tissue samples

Frozen tissue samples were ground with sterile steel beads. Total RNA was extracted with the RNeasy® Plant Mini Kit (Qiagen). 450 µl Buffer RLC containing guanidine hydrochloride was added to ground tissue. RNA was isolated according to the protocol of the manufacturer. In order to remove genomic DNA, the samples were treated with the 80 µl DNase set (Qiagen) for 15 minutes at room temperature. 350 µl of Buffer RW1 was added to the RNeasy spin column. RNeasy spin column was centrifuged for 15 seconds and the flow-through was discarded. 500 µl of Buffer RPE were added to the RNeasy spin column and centrifuged for 15 seconds at 13,000 rpm. The flow-through was discarded and washing step with Buffer RPE was repeated. The RNeasy spin column was placed in a new 2 ml collection tube and centrifuge at full speed for one minutes to dry the membrane, then the RNeasy spin column was placed in a new 1.5 ml collection tube and 40µl RNase-free water were added to RNeasy spin column and centrifuged for one minute at 13,000 rpm to elute the total RNA.

The concentration of total RNA was determined with the NanoDrop® ND- 1000, whereby the quality and integrity of RNA was measured on an Agilent 2100 Bioanalyzer according to the manufacturer's protocol.

4.4.2 Preparation of cDNA libraries for RNAseq and sequencing

All cDNA libraries were prepared using the TruSeq RNA sample preparation kit (Illumina) by the Kompetenzzentrum für Fluoreszente Bioanalytik (KFB) group (Biopark, University of Regensburg), starting from 500 ng of total RNA to purify poly-A containing mRNA molecules using the TruSeq RNA sample preparation kit (Illumina). The libraries were quantified using the KAPA SYBR FAST ABI Prism Library Quantification Kit (Kapa Biosystems, Inc., Woburn, MA, USA). Equimolar amounts of each library are pooled, and the pools used for cluster generation on the cBot (TruSeq PE Cluster Kit v3). The sequencing runs were performed on a HiSeq 1000 instrument using the indexed, 2x100 cycles paired end (PE) protocol and TruSeq SBS v3 Reagents. Image analysis and base calling yield in .bcl files, which are converted into fastq files with CASAVA 1.8.2 software. Libraries were multiplexed in order to obtain between 50-60millions reads with a mean quality score of 37, per biological replicate.

4.4.3 RNAseq analysis and transcriptomic analysis of differential gene expression

The quality of the reads obtained was assessed with FastQC (Babraham Institute 2011) and the results employed to trim the first and last 15 residues of every read. The trimmed reads were mapped with the CLC Genomics Workbench 7 (Qiagen) with the following parameters to the corresponding Col-0 TAIR10 version of the *A. thaliana* genome or to version 2.0 of the *A. lyrata* genome or to the version 1.1 of the *A. halleri* genome downloaded from phytozome (phytozome.jgi.doe.gov) as follows: mapping only to gene regions *A. thaliana* or to genic and inter-genic regions (*A. halleri and A. lyrata*), 10 maximum number of hits for a read, both strands, count paired reads as two, expression value as total counts, no global alignment, similarity fraction=0.8, length fraction=0.8, mismatch cost=2, insertion cost=3, deletion cost=3. Variation in the levels of expression between the biological replicates of each condition was assessed via box-plots and Principal Component Analysis. In order to maintain similar levels of variation between the biological replicates only the two most similar samples of each experimental and control conditions were further considered for the analysis of differential gene expression. Differential gene expression was investigated with the exact test for two-group comparisons incorporated in the EdgeR package (Robinson et al. 2010) implemented in the CLC Workbench. In this analysis read counts obtained from each

developmental stage in the pollination and infection treatments previously described were compared to the corresponding samples of non-pollinated, emasculated pistils of *A. thaliana.* Differentially expressed genes are those that have an FDR-corrected p-value below 0.0005 and an expression fold change ≥ 2 (upregulation) ≤ -2 (downregulation) and which are expressed with an RPKM≥ 1.

4.4 Bacterial related work

4.4.1 Preparation of chemically competent *Escherichia coli* cells

A single colony of an *Escherichia coli* (*E. coli*) strain DH5α was grown in LB medium overnight at 37°C. On the following day, the culture was diluted in 250 ml LB to about 1:100 dilutions. The culture was grown at 18°C until an OD_{600} reaches 0.6. Afterward, the cultures were cooled immediately in ice water, centrifuged at 4°C for ten minutes at 3000 rpm. The pellet was resuspended in ice-cold TB buffer (10 mM Pipes, 55 mM MnCl2, 15 mM CaCl2, 250 mM KCl) and kept on ice for ten minutes. Following an additional centrifuging, the pellet was gently resuspended in 20 ml ice-cold TB buffer. DMSO was added to a final concentration of 7% (v/v). The DH5α competent cells were aliquoted, frozen immediately in liquid nitrogen and stored at -80 °C.

LB media composition

	weight
Tryptone	10 g
Yeast Extract	5 g
NaCl	10 g

pH was adjusted to 7.0, 15 g/L Bactoagar was added in case to make LB plates and the volume was made up to 1L with distilled water.

4.4.2 *Escherichia coli* transformation of ligation reaction

E. coli DH5α competent cell was thawed on ice for a few minutes. 1-2 µl of the ligation reaction was added to the competent cells and incubated for 30 minutes on ice. Competent cells were heat shocked for 30 seconds at 42˚C and immediately transferred to ice for 3-4 minutes. 500µl of LB medium was added to the reaction and incubated in a shaker at 37˚C for 1 hour. Transformants were then plated on LB plates with the appropriate antibiotics and then incubated overnight at 37˚C.

4.4.3. Preparation of competent *Agrobacterium* cells

Agrobacterium tumefaciens strains listed below were incubated in LB media without antibiotics overnight at 30˚C. The following day, 2 ml of the culture were added to 200 ml LB media and incubated at 30°C until the OD reaches 0.7. Cells were harvested by

centrifuging at 5000 rpm for 20 min at 4°C and washed with cold TE buffer (10 mM Tris/acetate, 1 mM EDTA, pH 8.0). Subsequently, the cells were centrifuged at 5000 rpm for 20 minutes at 4°C again and finally resuspended in 20 ml cold LB medium. The cells are aliquoted, immediately frozen in liquid nitrogen and stored at -80°C.

Agrobacterium strain	Antibiotic Resistant
GV3101	Rifampicin, Gentamicin
GV3101:pSOUP	Rifampicin, Gentamicin, Tetracycline

4.4.4 *Agrobacterium tumefaciens* transformation

Agrobacterium transformation was done with *Agrobacterium tumefaciens* strains GV3101 or GV3101:pSOUP. 1 µg of the plasmid DNA was added to 200µl of *Agrobacterium* competent cells and incubated for 30 minutes on ice. *Agrobacterium* competent cells were frozen in liquid nitrogen for one minute and transferred to 37˚C water bath until the competent cells were thawed. 1 ml of YEP medium was added to competent cells and incubated in a shaker for 3 hr. at 28˚C. *Agrobacterium* cells were centrifuged for 1 minute at 5,000 rpm and the supernatant was discarded. The cell pellet was resuspended in 100µl of fresh YEP medium and transformants were plated on YEP with the appropriate antibiotics. Plates were incubated in 28˚C for three days to observe the transformed colonies.

YEP media composition

	weight
Peptone	10 g/L
Yeast Extract	10 g/L
NaCl	5 g/L

pH was adjusted to 7.0, 15 g/L Bactoagar was added in case to make YEP plates, and the volume was made up to 1L with distilled water.

4.4.5 *Agrobacterium* mediated transformation of *Arabidopsis thaliana*

Transformed *Agrobacterium tumefaciens* colony were selected and grown in 15 ml of YEP media with appropriate antibiotics overnight at 28˚C in a shaker at 200 rpm. 10 ml of miniculture was added to 200-250 ml of YEP media with the appropriate antibiotics and grown overnight at same conditions. 500 µl of the culture was made as glycerol stock (stored at -80˚C). Cells were harvested by centrifugation at 3,500 rpm for 20 minutes and the pellet was resuspended in freshly prepared 200 ml of infiltration solution (0.44 g MS including MES and vitamins, 40 µl Silwet L77, 10 g sucrose). *A. thaliana* plants were dipped into infiltration solution for three minutes and were covered with plastic bags. Plastic bags were removed the next day and transgenic plants were transferred after ten days to the greenhouse. When the seedlings develop, 200 µg/µl of BASTA was sprayed four times every four days in

order to have BASTA resistant transgenic plants. Each BASTA resistant seedlings were transferred to individual separate pots. Transgenic plants were dried for two weeks and subsequently seeds were collected. Seeds from the transgenic lines were sown in separate pots. They were vernalized for four days and then transferred later to long day conditions. The protocol was based on (Zhang et al. 2006).

4.5 Molecular biology work

4.5.1 Isolation of Genomic DNA from plants using CTAB method

Plant genomic DNA was extracted using a modified CTAB method. Approximately 2 gr of cauline leaves of *A. thaliana* were weighed and frozen in liquid nitrogen. Frozen leaf materials were ground using a mortar and pestle to a fine powder with liquid nitrogen. The 15 ml/gr of freshly prepared 2X CTAB buffer (2% CTAB (w/v), 100 mM Tris (pH 8.0), 20 mM EDTA (pH 8.0), 1.4M NaCl, 1% PVP – 10 g) were added to the freshly ground leaf materials and placed at 65˚C for 20 minutes and thereafter allowed to cool at room temperature for a few minutes. An equal volume of chloroform was added to the mixture and mixed without vortexing. The mixture was centrifuged at 5000 rpm for 10 minutes. The supernatant was transferred to a separate Eppendorf tube and one volume of 100% isopropanol was added. The mixture was allowed to precipitate for about 10 minutes at room temperature and subsequently centrifuged at 5000 rpm for 30 minutes at 4˚C. The supernatant was discarded and the pellet was resuspended in 1 ml of TE buffer. 3 µl of RNase (10mg/ml) were added and incubated for 40 minutes at 37˚C. Next ½ volume of phenol and ½ volume of chloroform were added to the mixture and mixed thoroughly without vortexing followed by centrifugation at 13,000 rpm for five minutes. The aqueous upper phase was transferred to a separate Eppendorf with one volume of chloroform and mixed well. The mixture was centrifuged at 13,000 rpm for 5 minutes, then ⅛ volume of 1M Sodium Acetate along with one volume of 100% isopropanol were added to the aqueous phase and incubated overnight at -20˚C for DNA precipitation. The overnight mixture was centrifuged for 30 minutes at 13,000 rpm at 4˚C to precipitate DNA. The pellet was collected by discarding the supernatant and washed with one volume of 70% ethanol. The sample was incubated for 15 minutes and centrifuged for 30 minutes at 13,000 rpm at 4˚C. Supernatant was discarded from the mixture and pellet was dried for 30 minutes at room temperature. Finally, the dried pellet containing genomic DNA was dissolved completely in 200 µl of sterile distilled water.

4.5.2 Primer design

All primers were designed using the Vector NTI software along with the online website, www.oligoanalyzer.com, and ordered from Biomers (Ulm, Germany). The primers used in cloning, cDNA synthesis, qPCR, genotyping are listed in the appendix section 9.1.

4.5.3 Polymerase chain reaction (PCR)

4.5.3.1 Amplification of PCR products for cloning

The PCR amplification was done with KAPA HiFi PCR Kit. Components of the PCR amplification reaction are described below.

Component	Volume [µl]
5X KAPA HiFi Buffer	0.5 µl
10 mM KAPA dNTP Mix	0.75 µl
10 µM Forward Primer	0.75 µl
10 µM Reverse Primer	0.75 µl
Genomic DNA	1 µl
KAPA HiFi	0.5 µl
PCR-grade water	Up to 25 µl

Settings used in thermocycler for gradient PCR amplification.

Step	Cycles	Temperature	Time
1	1	95°C	3 min
2	32	98°C	20 seconds
3		60-75°C	30 seconds
4		72°C	30 seconds/kb
5	1	72°C	5 min
6	Pause	4°C	∞

4.5.3.2 Colony screening from LB plates

Taq DNA Polymerase kit was used to perform screening of colonies. An individual colony from the plate was picked from transformant *E. coli* with a sterile pipette tip and re-suspended in 25 µl of the PCR master mix. Components for single screening reaction is described below:

Component	Volume
10x Tag buffer	2.5 µl
dNTP	0.5 µl
10 µM Forward Primer	1 µl
10 µM Reverse Primer	1 µl
2.5 mM MgCl2	3 µl
Sterile distilled water	16.8 µl
Tag DNA polymerase	0.2 µl

Settings used in thermocycler for screening

Step	Cycles	Temperature	Time
1	1	95°C	3 min
2	25	94°C	30 seconds
3		Tm	30 seconds
4		72°C	1 min
5	Pause	4°C	∞

4.5.3.3 Genotyping of transgenic plants

Genotyping of transgenic plants was performed with the KAPA3G™ Plant PCR Kit using *Arabidopsis* leaf samples as the template. After pipetting the KAPA3G Plant DNA Polymerase, a leaf disc of approximately 2-3 mm in diameter was cut from the plant with forceps and added to the tube. Components for a single genotyping reaction are described below:

Component	Volume
KAPA plant PCR buffer	12.5 µl
10 µM Forward GFP Primer	0.75 µl
10 µM Reverse GFP Primer	0.75 µl
Sterile water	10.8 µl
KAPA3G Plant DNA Polymerase	0.2 µl
Template plant crude sample	

Settings used in thermocycler for genotyping

Step	Cycles	Temperature	Time
1	1	95 °C	10 min
2	step 2 to 4 -40 repeats	95 °C	30 seconds
3		60 °C	30 seconds
4		72 °C	30 seconds
5		72 °C	5 min
6		4 °C	∞

4.5.4 Digestion of the plasmid

To perform single or double digestion on the plasmid, several different restriction enzymes were employed using the same basic reaction mixture. Each digestion reaction was incubated at specific temperature and time specified by the manufacturer for each enzyme. The following components were used for restriction enzyme digest reactions:

Components	Volume
DNA	up to 1µg
10X NE Buffer	2 µl
Restriction Enzymes (HF)	1 µl
Nuclease-free water	Made up to 20 µl
Total	20 µl

4.5.5 DNA ligation of digested fragments

Standard ligation protocol from New England BioLabs® was used. The amount of the insert needed in ng for the ligation reaction was calculated using the formula: ng of insert added = (kb of insert/kb of vector) x ng of vector.

The following components were used for ligation reaction:

Components	Volume
Vector	25-100 ng
Insert	1:3 molar ratio
10X T4 DNA ligase buffer	2 µl
T4 DNA ligase enzyme	1 µl
Nuclease-free water	made up to 20 µl
Total	20 µl

The ligation mixture reaction was incubated at 16˚C overnight and transformed by *E. coli* competent cells.

4.5.6 Agarose gel electrophoresis

0.7% -1.5% agarose gels were prepared based on the size of the amplicon. Agarose powder (peqGOLD universal) was melted in 1X TB buffer (10.8 g Tris-acetate,4 ml 0.5M EDTA pH 8.0,5.5 g Boric acid) and cooled down. 7 µl of Roti® safe gel stain (Roth) were added to 100 ml of agarose gel and the gel was cast. 3 µl of 6x DNA loading dye were added to 20 µl of the respective samples and loaded in gel pockets. 10 µl of the suitable DNA-ladder were applied to the pockets and the agarose gel was run for 45-60 minutes at 125V. The gel was photographed using a BioDoc Analyze Biometra Ti5 (Biometra).

4.5.7 Gel Elution

QIAquick® Gel Extraction Kit was used to extract the desired DNA fragments from agarose gels. Desired product was cut from the agarose gel using a clean scalpel and the gel slice was weighted. According to the gel weight, three volumes of buffer QG were added and vortexed at 50˚C for 10 minutes. One volume of 100% isopropanol was added to the dissolved gel sample and mixed thoroughly. The dissolved gel sample was transferred to the QIAquick spin column and centrifuged at 13,000 rpm for one minute. Flow-through was discarded from 2 ml collection tube and depending on the volume of the sample, centrifugation was repeated. 750 µl of Buffer PE was added to the spin column, allowed to stand at room temperature for two minutes and centrifuged at 13,000 rpm for one min. Centrifugation was repeated to remove the excess of buffer and to dry the column. Spin column was placed onto a sterile 1.5 ml Eppendorf tube. 25 µl of sterile distilled water was added to the spin column and was set aside for two minutes followed by centrifugation for one minute. After centrifugation, the DNA-concentration was measured with a NanoDrop® ND-1000.

4.5.8 Miniculture of bacterial colony

A fraction of the bacterial colony from the plate was taken with a pipette tip and added to 3 - 4 mL of LB-medium containing appropriate antibiotic. Minicultures were grown overnight at 37°C. Antibiotics were added to the following final concentrations:

Ampicillin	100 µg/ml
Kanamycin	50 µg/ml
Spectinomycin	50 µg/ml
Tetracycline	5 µg/ml
Gentamicin	40 µg/ml
Rifampicin	10 µg/ml

4.5.9 Isolation of plasmid DNA

Plasmid DNA was isolated using a high-speed plasmid mini kit from GENEAID. Minicultures were harvested by centrifugation at 13,000 rpm for a minute and the supernatant was discarded. 200 µl of PD1 buffer (stored at 4˚C) were added to the pellet and mixed well to completely dissolve it. 200 µl of buffer PD2 were added to the mixture and tubes were inverted ten times to mix thoroughly, without vortexing. The 1.5 ml tube containing the mixture was allowed to incubate for two minutes at room temperature. 300 µl of PD3 buffer were added to the mixture and mixed by inverting followed by centrifugation for three minutes at 13,000 rpm. The supernatant was transferred to the PD column provided in the kit and centrifuged for 30 seconds at 13,000 rpm. The flow-through was discarded. 400 µl of W1 buffer was added to the PD column and centrifuged for 30 seconds at 14,000g. The flow through was discarded and PD column containing the DNA was washed with 600µl of W2 wash buffer with the ethanol pre-added to it. PD column was centrifuged for 30 seconds at 13,000 rpm. Flow through was discarded and centrifugation was repeated to dry the column completely. DNA was eluted from the PD column by the addition of 50 µl sterile water and centrifuged for two minutes at 13,000 rpm. The PD column was left at room temperature for two minutes to have a good yield of DNA and centrifuged for two minutes at 13,000 rpm. The amount of plasmid DNA in ng/µl was measured using Nanodrop ® ND-1000.

4.5.10 Cloning strategies

4.5.10.1 pENTR/D-TOPO cloning reaction

The entry vector with the desired DNA sequence was cloned with pENTR Directional TOPO® cloning kit by Invitrogen. 50 µL PCR reaction was performed with specific primers for amplification of desired DNA sequence and this is followed by elution of DNA sequence from the gel using QIAGEN® QIAquick® gel extraction kit. The amount of DNA required

for pENTR-D/ TOPO entry vector was calculated for 1:1 molar ratio of DNA product: TOPO® vector. The required amount of DNA was added to 1µl of TOPO-vector and the volume was made to 5 µl using sterile distilled water. 1 µl of salt solution was added to the mixture and incubated at room temperature for 30 minutes. The reaction mixture was transformed on DH5α competent cells and transformants were selected on LB plates with kanamycin.

4.5.10.2 LR reaction

pENTR-D/ TOPO entry vector containing either promoter or coding sequence (CDS) is transferred to the destination vector (pB7FWG 2.0 / NLS-GW-3XGFP) to create the expression clone using LR recombination reaction. The following components were used in the LR reaction mixture:

Components	Volume
Entry clone	(50-150 ng) -1 -7µl
Destination vector	150 ng/µl -1µl
TE buffer, pH 8.0 to 8µl	

2 µl of LR clonase II enzyme were added to the mixture and incubated for 1hr at room temperature. 1 µl of proteinase K was added to the mixture for terminating the LR reaction, and the sample was incubated for 10 minutes at 37˚C. The reaction mixture was transformed in DH5α competent cells and cultured on LB plates with selective antibiotics

4.5.10.3 Cloning for subcellular localization

The CDS of the gene of interest (GOI) was amplified from cDNA pools (*Arabidopsis thaliana* fertilized with pollen from *Arabidopsis halleri)* and the putative promoter of GOI was amplified from genomic DNA information obtained from TAIR10 version of the *A. thaliana* genome in https://www.arabidopsis.org. The putative promoter was defined as the region of DNA sequence upstream of coding sequence of the gene (and does not include a neighboring gene). After the amplification of CDS from cDNA, the product was cloned into pENTR-D/TOPO (Kanamycin resistant) to create entry clones pENTR/D-TOPO-GOI-CDS. The LR reaction was performed with the entry vector pENTR/D-TOPO-GOI-CDS to destination vector pB7FWG2.0 to create an expression clone p35S::GOIg-eGFP (Spectinomycin resistant). The putative promoter of GOI was amplified from gDNA using *SacI* and *SpeI* flanked primers. The expression clone and putative promoter of the GOI flanked by *SacI* and *SpeI* sites are digested with the corresponding enzymes. The two digested fragments are ligated which results in a final vector pGOI::GOIg-eGFP. The final vector was sequenced by an external service provider (LGC genomics). The complete list of

cloned vector for subcellular localization can be seen in appendix section 9.2. The final vector pGOI::GOIg-eGFP was transformed to *Agrobacterium tumefaciens* strains GV3101 (Rifampicin and gentamicin resistant) and transformed into *A. thaliana* as previously described.

4.5.10.4 Cloning for promoter analysis.

The size of the putative promoter was between 400bp (base pair)-2kb (kilo base) depending on the GOI. All putative promoters were amplified with a forward primer containing CACC on the 5' end for directional cloning into pENTR/D-TOPO vector. The fragments including the putative promoter of each gene were cloned into pENTR/D-TOPO entry vector (kanamycin) to create pENTR/D-TOPO-GOI promoter. The resulting plasmid-pENTR/D-TOP-GOI promoter was digested to linearize the vector. The LR reaction was performed with the linearized pENTR/D-TOP-GOI promoter to destination vector GW-NLS-3XeGFP to create an expression clone in pGOI-NLS-3XeGFP (kanamycin resistant). The final vector was sequenced by external service provider (LGC genomics). The complete list of cloned vectors for promoter analysis is in Appendix section 9.2. The final plasmid pGOI-NLS-3XeGFP was transformed in *Agrobacterium tumefaciens* strain GV3101+pSOUP (including rifampicin, gentamicin and tetracycline resistance) and transformed into *A. thaliana* as previously described.

4.5.10.5 Cloning of transgenic RNAi lines

Two RNAi constructs were generated for targeting genes in two DEFL family CRP 500 and CRP 670. CRP500 consists of At3g43505 and along with highly similar DEFL paralogs At3g61182, At3g20997, At5g47075, At5g47077 and CRP500 consists of At5g38330 along with its highly similar DEFL paralogs At4g30070 and At4g30074. The specific sequences were synthesized by Thermo Scientific GeneArt AG, Germany. The selected synthesized sequences were amplified in sense orientation and antisense orientation. The resulting fragments were separated by gel electrophoresis, purified, digested with respective restriction enzymes and cloned into the corresponding sites of the pUbi-iF2 vector containing spectinomycin resistance as well as a ubiquitin maize promoter to create pUbi-RNAi-iF2 vector. This was followed by replacing the ubiquitin maize promoter with constitutive *A. thaliana* Ubiquitin 10 promoter and central cell specific promoter DD36 to create expression vector pUbi10-RNAi-iF2 vector and pDD36-RNAi-iF2 vector respectively. The expression vector was digested with *Sfi1* restriction enzyme and the fragment containing the promoter as well as sense and antisense sequences were cloned into corresponding spliced sites of binary

vector p7U to create the final vector p7U-RNAi (spectinomycin resistant). The final vector was sequenced by an external service provider (Macrogen). Complete list of cloned vector for RNAi can be seen in appendix section 9.2. This was followed by *Agrobacterium* transformation with GV3101 strains and subsequent transformation into *A. thaliana* as previously described.

4.6 qPCR related work

4.6.1 Pistil collection for qPCR analysis

4.6.1.1 Pollination study

For pollination analysis, *A. thaliana* wild-type flower was emasculated and pollinated with *A. thaliana* wild-type pollen grains. The pollinated pistils were collected 8HAP, 24HAP, 32HAP, 48HAP, 80HAP, 96HAP and additionally, non-pollinated pistil (NP) was collected**.** For each condition, 45 pistils were collected. Two biological replicates were collected for this study and total RNA was isolated as previously described in section in 4.4.1.

4.6.1.2 Pollination - infection study

In pollination - infection studies, *A. thaliana* wild type flowers were emasculated and pollinated in the same way as in pollination studies. After the specific time period (8HAP, 24HAP) pollinated plants were infected with *F. graminearum* DsRed strain Fg8/1and kept for one day after infection (DAI), and 3DAI in humid condition. Two controls were used in this studies – control and mock treatment. Control samples were emasculated, pollinated and followed by no treatment for the same time period as treated samples (32HAP, 48HAP, 80HAP and 96HAP). Mock treatment samples were similar to infected pistil except that the pollinated pistils were treated with sterile distilled water. 45 pollinated pistils were collected for each condition and two biological replicates were collected from each condition. Total RNA was isolated as previously described in section in 4.4.1.

4.6.1.3 Infection (aging) study

Infected pistils were collected after one (1DAI) or three days (3DAI) of inoculation with the *Fusarium graminearum* DsRed strain Fg8/1. Mock treatment samples consisted of flowers one day after emasculation which were treated with sterile distilled water, kept in a moisture chamber for one day (1DAT) and 3 days (3DAT). The control for the one-day treated pistils (1DAI,1DAT) were pistils two days after emasculation (2DAE), while the control for three-day treated pistils (3DAI and 3DAT) were pistils four days after emasculation (4DAE). For

each condition, three biological replicates, each containing 45 pistils were collected. Total RNA was isolated as previously described in section 4.4.1.

4.6.2 cDNA synthesis

cDNA to be used in qPCR assays was synthesized with SuperScript III RT kit starting from 1 µg of total RNA. Components for cDNA pools synthesis are:

Component	Amount	Volume
RNA template	1 µg	variable
Primer AB05	0.25 µg (50 pmol)	1 µl
dNTP Mix	10 mM each	1 µl
dd Water		add 14 µl

The mixture was incubated for five minutes at 65°C, the samples were chilled on ice and spun down. Subsequently, 6 µl of master mix (4 µl 5x Buffer, 1µl 0.1 M DTT, 1µl SuperScript III reverse transcriptase) were added to each tube. The reaction tubes were incubated for 50 minutes at 50°C. The samples were heated for 15 minutes at 70°C to stop the reaction. The cDNA samples were synthesized by three persons including me which are described in Appendix section 9.14.

4.6.3 qPCR assays

qPCR assays were performed with KAPA™ SYBR® FAST qPCR MasterMix Universal in 96- well plates. The qPCR plate layout corresponding to pollination, pollination-infection and infection assays is shown in appendix section 9.3. Each 20 µl reaction contained 10µl KAPA^{TM} SYBR$^{®}$ FAST qPCR MasterMix Universal (peqlab), 8.2 µl sterile biopak water, 0.4 µl of each forward and reverse primers (10 µM)) and 1 µl of 1:5 diluted cDNA. Negative-RT controls containing total RNA that was not reverse transcribed were added to detect genomic DNA contamination. In addition, one non-template control (NTC) as well as one positive control containing the cDNA made from mRNA that was extracted from a mix of pollinated, non-emasculated, non-treated flowers were added. Each total RNA sample was represented by one cDNA pool and each cDNA pool by three qPCR technical replicates.

Cycling program set up in the Mastercycler® ep realplex gradient S (Eppendorf).

Step	Cycles	Temperature	Time
1	1	95 °C	3 minutes
2	40	95 °C	10 seconds
		Ta*	30 seconds
		72 °C	8 seconds
3	1	95 °C	15 seconds
		55 °C	15 seconds
		55 °C - 95 °C	20 minutes
4	1	95 °C	15 seconds

* Annealing temperature for each primer is in Appendix section 9.1.

The Cq values were extracted from the Mastercycler® ep realplex software and imported into the qbase+ software. The quality control settings require the Cq values from 2 out of 3 qPCR triplicates to differ less than 0.71 cycles. Normalization factors were then calculated and applied to correct for internal variation. The resulting calibrated normalized relative quantities (CNRQs) were then exported into Excel and $\log_2$ transformed for further analysis and calculation of fold change values and statistical analysis.

4.7 Pollination studies using GFP signal quantification

The flowers of pAt3g07005 NLS-(3x)eGFP, pAt4g09153 NLS-(3x)eGFP, pAt2g42885 NLS-(3x)eGFP and pAt2g20070 NLS-(3x)eGFP marker lines were emasculated and pollinated with sperm cells labeled with RFP from marker line HTR10:RFP. The pollinated pistils were collected 8HAP, 24HAP, 48HAP and were dissected to observe GFP signal in the respective cells from the ovule. Similarly, GFP signals were observed from the ovule before pollination and were considered as non-pollinated pistil (NP). Stacked pictures of the single ovule showing GFP signal were taken at 40x magnification using an Axio Imager 2 fluorescence microscope. The exposure time chosen for each marker lines is listed here:

DEFL gene	Exposure time
At3g07005	280 ms
At4g09153	580 ms
At2g42885	600 ms
At2g20070	200 ms

GFP signals from ovules of marker lines were obtained in stacked image format and the GFP signals from the image were further quantified using ImageJ software as follows:

1) In ImageJ software, the stack image was converted to hyperstack (Figure 8A).

2) The hyperstack image was projected to an image of highest intensity by going to Image/Stacks/Z Project and in Z projection window, the settings were left as follows: Projection type: Max Intensity. Example of image with maximum intensity projection is shown in figure 8B.

3) In the maximum intensity image, elliptical or polygon selection tool circle was selected and used around every nucleus that showed GFP signal and measured as GFP measurements. After the single GFP nucleus was circled, M key was tapped in order to measure the intensity and T key was tapped in order to save the selection in ROI manager. This process was repeated depending on the number of endosperm nuclei in the image. As the background control, 10 – 20 same size circles were taken in regions next to the GFP nucleus as background measurements. An example of an image with circles around the GFP nucleus and background measurements in the maximum intensity projection image is shown in figure 8C.

4) All the values were exported to Microsoft excel sheet. The average value of the GFP measurements from the nucleus was calculated and similarly the average value of the background measurements was also calculated.

5) The average value of the background measurements was subtracted from the average value of the GFP nucleus measurements in order to acquire the signal intensity of the given condition.

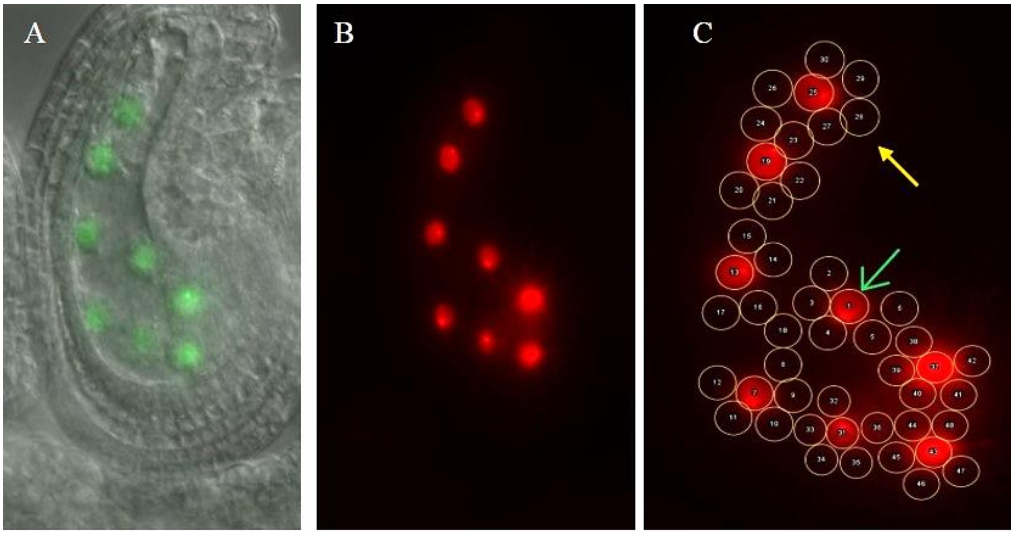

Figure 8:Measurement of GFP signal from the ovules using ImageJ software.
(A) GFP signals from ovules of marker lines were obtained in stacked image and converted to hyperstacks, (B) Hyperstack image is projected to maximum intensity projection (C) Maximum intensity projection with GFP measurements in endosperm nuclei (green arrow) and background measurements around the endosperm nuclei (yellow arrow).

4.8 Experiments on effect of fungal infection on reproduction

4.8.1 Developmental studies

Homozygous marker line of pAt1g60985:NLS-(3x)eGFP line 1 was used for developmental studies because GFP expression was observed in endosperm nuclei until 96HAP. *A. thaliana* pistils were emasculated, pollinated for each time period (8HAP and 24HAP) and followed by different treatments (infection/mock treatment) for one and two days. Control samples

were collected after 32HAP, 48HAP, 56HAP and 72HAP. Ten pistils from each condition were collected and dissected. The pictures of different stages of ovules were taken in 10x magnification with an Axio Imager 2 fluorescence microscope. The ovules from pictures were counted and categorized based on the number of developing endosperm cell nuclei. The following stages of ovules were counted for each corresponding condition: degraded, 0HAP/8HAP, 24HAP, 48HAP and 72HAP were recorded for each corresponding condition. Because non-pollinated ovules and those 8 HAP are undistinguishable, in this study they were counted as single stage.

4.8.2 Seed set experiment

4.8.2.1 Seed set data of infection followed by pollination

Emasculated pistils were inoculated with different treatments (infection/mock treatment) for one and three days. The infection was done with *F. graminearum* Ds-Red as described in section 4.3.3. The infected pistils were pollinated with wild-type *A. thaliana* pollen. The control samples were emasculation for two and four days followed by pollination without any treatment. For each experimental condition, 10- 15 pistils were taken for the study. The siliques were collected after fifteen days for seed set data analysis.

4.8.2.2 Seed set data of pollination followed by infection

Emasculated pistils were pollinated for each time period (8HAP and 24HAP) and were inoculated with different treatments (infection/mock treatment) for one, two and three days. The infection was done with *F. graminearum* Ds-Red as described in section 4.3.3. The control samples were emasculation followed by pollination without any treatment. For each experimental condition, 10- 15 pistils were taken for the study. The siliques were collected for seed set data analysis.

4.8.2.3 Seed set count

Siliques were collected twenty days after pollination and bleached in 3:1 ethanol/ acetic acid for two days. This was replaced with 70% ethanol for a few days and siliques were placed in slides with one drop of 1X PBS. Pictures of the siliques were taken with the Stereo Discovery V8 (Zeiss) microscope and the number of seeds was counted based on the pictures.

4.9 Microscopy

All microscopic studies were performed with either confocal microscopy (LSM510 or SP8) or fluorescence microscopy (Axio imager 2 from Zeiss®). The pictures were analyzed by the software LSM Imager, LAS AF lite and ZEN™, respectively. The following table shows the used excitation wavelengths, depending on the fluorescent protein.

Fluorescent protein	Excitation wavelength	Emission filter
eGFP	488 nm	500 – 550 nm
Ds Red	545 nm	570 – 640 nm

5. Results

5.1 Setting up of experimental conditions for collection of tissue

To identify DEFL genes expressed during fertilization, *A. thaliana* pistils were selfed, crossed with *A. lyrata* and *A. halleri* pollen. Similarly, in order to identify DEFL genes expressed in self-incompatible *Arabidopsis* species, *A. halleri* pistil was selfed, crossed with *A. lyrata* pollen, and *A. lyrata* pistil were selfed (Table 1). To identify DEFL gene expressed during defence, pistil and leaves of three *Arabidopsis* species were infected with *F. graminearum* (Table 1).

The major objective of these procedures was to set up the conditions for collecting tissue samples for RNAseq which would enable us to identify DEFL genes expressed (a) during pollination and (b) during the response to *Fusarium* infection.

5.1.1 Aniline blue staining of pistil

DEFL genes expressed between the pre-fertilization and fertilization events was of interest. In order to find the appropriate time point to collect pistils after pollination, pollen tube growth was followed by aniline blue staining. Visualization of the pollen tube inside the pistil is possible because aniline blue stains the callose found in the cell wall of the pollen tube. A time frame between six and eight hours after pollination (HAP) was the optimal point to observe the pollen tube advancing through the transmitting tract towards the ovules. This was also the ideal time frame to observe the pollen tube enter the ovule. For all further experiments, 8HAP was chosen as the time point for collecting the pistil samples, because most of the ovules in the pistil would have a chance of attracting the pollen tube (Figure 9). No seeds were produced in interspecific pollinations involving *A. thaliana* pistils.

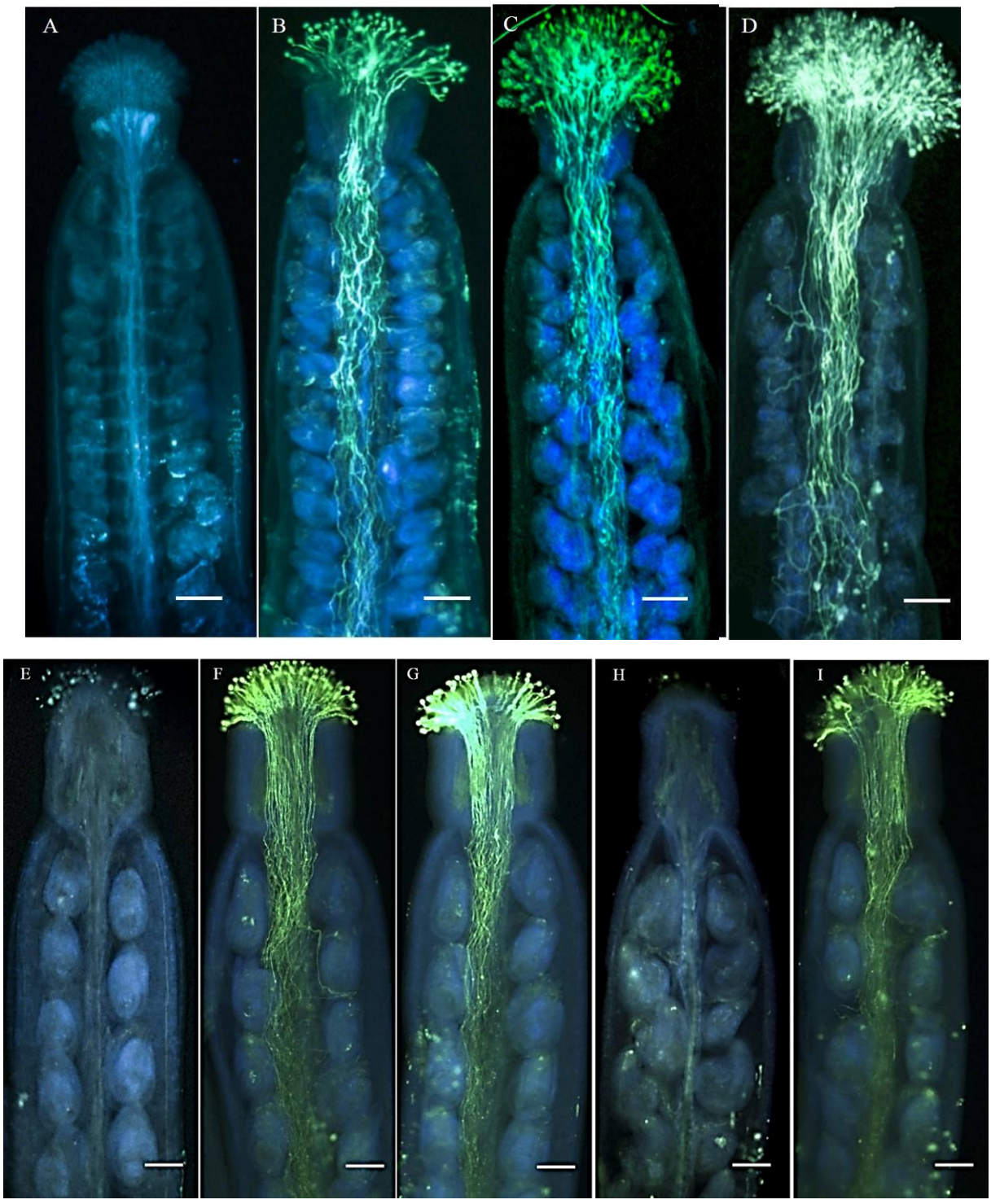

Figure 9:Aniline blue staining of *A. thaliana, A. halleri* and *A. lyrata* pistils 8 hours after pollination.

A) Image shows aniline blue staining of one-day emasculated *A. thaliana* pistil. B*) A. thaliana* pollen tubes advancing through the transmitting tract towards the ovules when *A. thaliana* is self-pollinated. C) *A. halleri* pollen tube advancing through the transmitting tract in *A. thaliana* pistil. D) *A. lyrata* pollen tube advancing through transmitting tract in *A. thaliana* pistil. E) Image shows aniline blue staining of one-day emasculated *A. halleri* pistil. F) *A. halleri* pollen tube advancing through transmitting tract towards the ovule in *A. halleri pistil*. G) *A. lyrata* pollen tube advancing through the transmitting tract of *A. halleri* pistil. H) Image shows aniline blue staining of one-day emasculated *A. lyrata* pistil. I) *A. lyrata* pollen tube advancing through transmitting tract towards the ovules in *A. lyrata* pistil. Scale bar:50µm.

5.1.2 WGA-TMR to observe fungal hyphae growth

In order to establish a plant inoculation system with *Fusarium graminearum* for three species of *Arabidopsis,* isolate Sg005 strain was provided by Dr. Ralph Hückelhoven from Technische Universität München. Pistils were emasculated one day before inoculation in order to identify the DEFL gene expressed solely due to infection and also in order to compare their expression with that of pollinated pistils. In *A. thaliana*, non-emasculated pistils had more prevalent infection in comparison to emasculated pistils and data can be seen in appendix section 9.4. Inoculation of the *A. thaliana* plant was done by dipping it in *F. graminearum* solution as described in section 4.3.4. The inoculated pistils and leaves were collected after three days. Wheat germ agglutinin-tetramethylrhodamine staining (WGA-TMR) was used to visualize fungal hyphae proliferation on the plant.

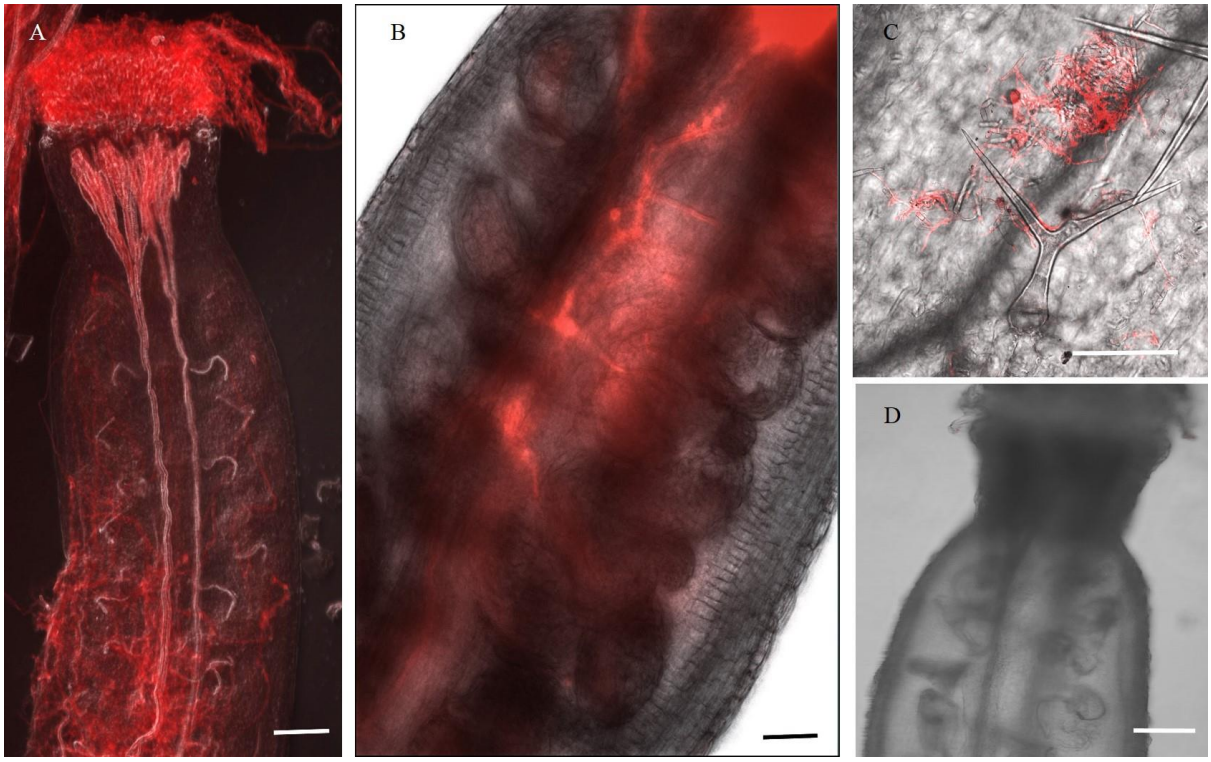

Figure 10:Proliferation of *Fusarium graminearum* after 3 days on pistils and leaves of *A. thaliana*.

A) WGA staining showing *F. graminearum* hyphae growing on the stigma of the pistil after 3 days of infection. Growth in the vasculature and between cells are observed. B) WGA staining showing *F. graminearum* hyphae growing intercellularly using transmitting tract and vasculature tissue of the pistil after 3 days of infection. C) WGA staining of *A. thaliana* leaf after 3 days of infection shows *F. graminearum* attaching to a trichome and hyphae growing on the epidermis of the leaf. D) WGA staining of mock treated pistil does not show any infection after 3 days of mock treatment. Scale bar:50µm.

Fusarium hyphae grew on the stigma of the pistils (Figure 10A) and the intercellular *Fusarium* hyphae growing through the vasculature tissue and transmitting tract of the pistil

(Figure 10A and B). Similarly, *Fusarium* conidia were found attached to the trichome of leaves (Figure 10C) and hyphae growing on the epidermis of the leaf (Figure 10C).

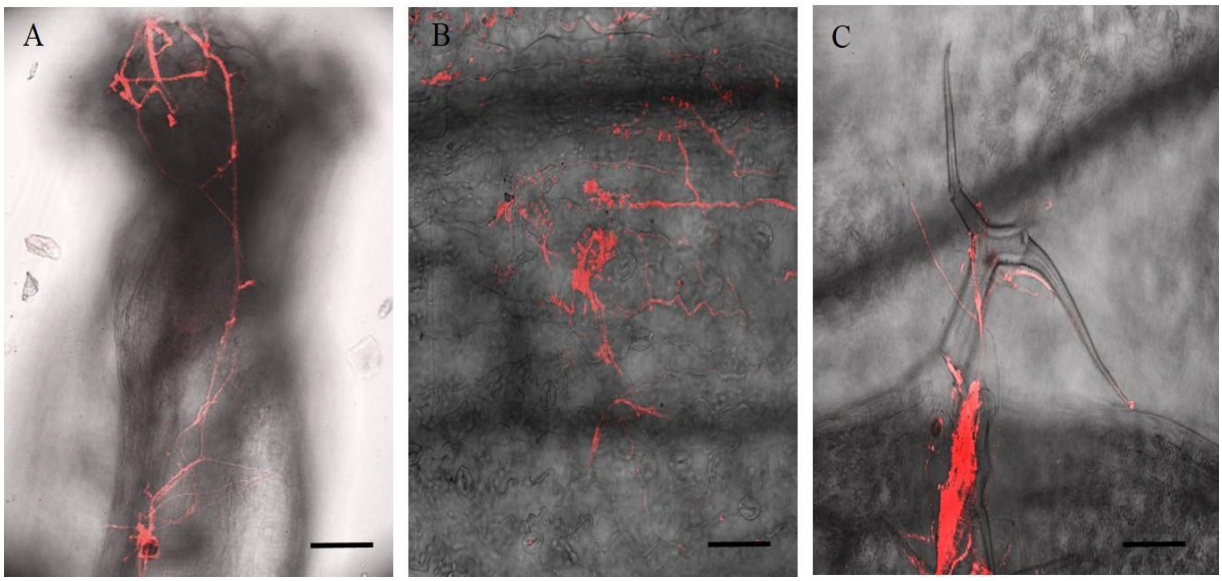

Figure 11:Proliferation of *Fusarium graminearum* after 3 days on pistils and leaves of *A. halleri*.

A) *F. graminearum* hyphae growing on the *A. halleri* 3DAI pistil stained by WGA. B) WGA staining of the 3DAI *A. halleri* infected leaf showing *F. graminearum* hyphae growing on the epidermis of the leaf. C) WGA staining of the 3DAI *A. halleri* infected leaf shows *F. graminearum* hyphae attaching to the trichome. Scale Bar:50µm.

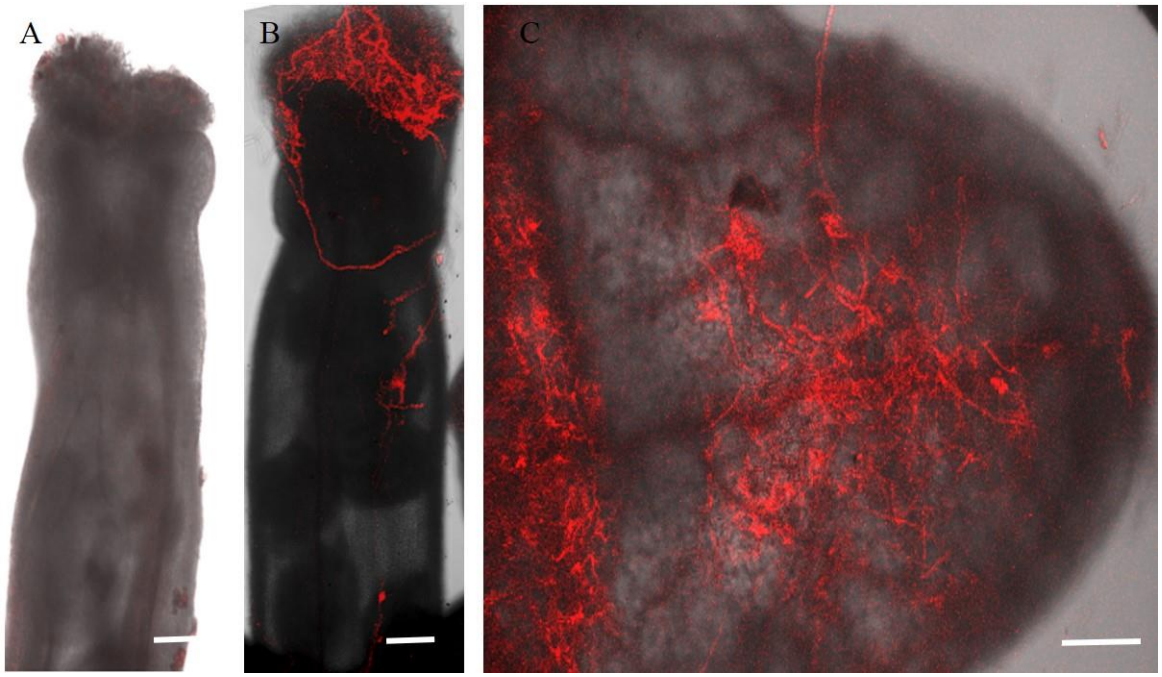

Figure 12:Proliferation *of Fusarium graminearum* after 3 days on pistils and leaves of *A. lyrata*.

A) WGA Staining of *A. lyrata* mock treated pistil showing no fungal hyphae inside the pistil. B) WGA staining of 3DAI *A. lyrata* infected pistil showing *F. graminearum* hyphae C) WGA staining of the 3DAI *A. lyrata* infected leaf showing *F. graminearum* hyphae growing on the epidermis of the leaf. Scale bar:50µm.

Using same inoculation method, *A. halleri* and *A. lyrata* pistil and leaf were infected and left for three days before the tissue sample were collected (Figures 11 and 12). Mock control samples for the *Arabidopsis* species were collected for WGA-TMR staining (Figures 10D and 12A).

The sampling of the pistil tissues for RNA sequencing (RNAseq) was performed based on the conditions identified as optimal: 8HAP for pistils during fertilization and 3 DAI for the pistils infected with *Fusarium* graminearum (Table 1). Three biological replicate samples were collected for each condition. Total RNA was purified from each sample and treated to eliminate genomic DNA contamination. Concentration and integrity of the samples were assessed with a Bioanalyzer. Samples with a RIN > 6.0 were sent for RNA sequencing to the Kompetenzzentrum für Fluoreszente Bioanalytik (KFB), Regensburg. RIN values of samples sent for RNAseq are listed in appendix section in 9.5.

Table 1:Tissue samples of three *Arabidopsis* species taken at different conditions*

Species	Condition	Tissue samples	Stages
A. thaliana	Non-Infected	Cauline leaf	-
A. lyrata	Non-Infected	Cauline leaf	-
A. halleri	Non-Infected	Cauline leaf	-
A. thaliana	Infected	Cauline leaf	3 DAI
A. lyrata	Infected	Cauline leaf	3 DAI
A. halleri	Infected	Cauline leaf	3 DAI
A. thaliana	Emasculated	Pistil	1 DAE
A. lyrata	Emasculated	Pistil	1 DAE
A. halleri	Emasculated	Pistil	1 DAE
A. thaliana	Infected	Pistil	3 DAI
A. lyrata	Infected	Pistil	3 DAI
A. halleri	Infected	Pistil	3 DAI
A. thaliana	Pollinated with *A. thaliana* pollen	Pistil	8 HAP
A. thaliana	Pollinated with *A. halleri* pollen	Pistil	8 HAP
A. thaliana	Pollinated with *A. lyrata* pollen	Pistil	8 HAP
A. halleri	Pollinated with *A. lyrata* pollen	Pistil	8 HAP
A. halleri	Pollinated with *A. halleri* pollen	Pistil	8 HAP
A. lyrata	Pollinated with *A. lyrata* pollen	Pistil	8 HAP

*Tissue samples were collected in order to identify the DEFL gene expressed in specific conditions. 1 DAE pistils denotes mature emasculated pistils after one day of recovery, 8 HAP pistil denotes emasculated pistils eight hours after hand pollination. For the purpose of identifying DEFL in response to defence, three days after infected (3 DAI) pistils and infected leaves were collected.

5.2 Transcriptome analysis and identification of DEFL candidate genes based on their patterns of expression during fungal infection and double fertilization

5.2.1 Quality of RNAseq

Raw data from RNAseq analysis was further analyzed by Dr. Mariana Mondragón Palomino, University of Regensburg on the CLC Genomics Workbench. The platform was used for mapping on the genomes of *A. thaliana, A. halleri, A.lyrata* and analysis of differential gene expression. 70% of the reads were mapped to genome of respective *Arabidopsis* species (Table 2). The RNAseq samples were of high quality with a mean score above 35 (Table 2). An average of 60% from the total genes were expressed in all the samples, when a cut-off of 1 RPKM was taken (Table 2).

Table 2:Characteristics of the transcriptomes sequenced

Conditions compared	Total reads	% of ≥ Q30 Bases	Mean Quality Score	Mapped reads	Genes expressed*
A. thaliana pistils non-pollinated	109,362,994	94.3	36.51	89,537,597	69.79
A. thaliana selfed pistils	101,942,362	94.31	36.52	96,071,451	69.06
A. thaliana pistils x *A. lyrata* pollen	100,332,498	95.34	36.84	95,899,345	68.89
A. thaliana pistils x *A. halleri* pollen	103,676,026	95.5	36.9	98,639,610	69.28
A. thaliana pistils infected	97,213,704	95	36.59	70,661,826	65.38
A. thaliana leaf	80,329,562	91.73	35.59	74,144,556	58.16
A. thaliana leaf infected	95,285,902	95.65	36.88	91,697,050	57.79
A. halleri pistils non-pollinated	106,156,558	95.5	36.88	75,012,556	73.92
A. halleri pistils selfed	93,961,972	95	36.71	67,574,404	72.59
A. halleri pistils x *A. lyrata* pollen	121,254,382	94.07	36.44	87,023,215	73.30
A. halleri pistil infected	83,771,668	94.93	36.68	56,172,094	66.81
A. halleri leaf	127,526,910	94.08	36.42	89,168,588	65.78
A. halleri leaf infected	93,279,706	95.21	36.76	66,208,233	65.35
A. lyrata pistils unpollinated	96,737,148	94.87	36.69	82,058,723	67.48
A. lyrata pistils selfed	114,829,288	94.94	36.7	97,223,266	66.11
A. lyrata pistils infected	117,134,804	94.09	36.395	89,328,582	62.78
A. lyrata leaf	123,196,130	95.34	36.805	104,112,543	58.42
A. lyrata leaf infected	92,065,932	94.89	36.645	77,815,224	58.74

*As percentage of the total genomic and mitochondrial genomes *A. thaliana* TAIR 10: 28642 genes, *A. halleri* V 1.1 25008 genes *A. lyrata* V2=29675 genes.

5.2.2 Transcriptome analysis of *A. thaliana* data

For further analysis, only the transcriptome results of the *A. thaliana* samples were considered. Differential gene expression in pistil was calculated by using the results of a non-pollinated pistil as the point of reference. Untreated leaf samples were used as a point of reference to calculate differential expression for infected leaves samples. A gene was considered as differentially expressed genes (DEG) if they had an FDR-corrected p-value below 0.0005 and an expression fold change ≥ 2 (upregulation) ≤ -2 (downregulation) and which are expressed with an RPKM≥ 1. The *A. thaliana* infected pistils had more genes differentially expressed in comparison to pollinated pistils (Table 3). About 13% of the total genes were found to be differentially expressed in the infected samples of the pistil of *A.*

thaliana (Table 3). Only 1% and 1.7% of total genes were differentially expressed in *A. thaliana* pollination during selfed condition and with foreign pollen respectively (Table 3). In all the five condition, the amount of downregulated genes was larger than the number of upregulated genes (Table 3).

Table 3: Differential expression of *A. thaliana* genes in five condition

Conditions compared	Number of genes differential expressed	Upregulated*	Downregulated*
A. thaliana pistils x *A. thaliana* pollen	341(1.1%)	81(0.2%)	260(0.9%)
A. thaliana pistils x *A. halleri* pollen	508(1.7%)	211(0.7%)	297(1.0%)
A. thaliana pistils x *A. lyrata* pollen	477(1.6%)	181(0.63%)	296(1.0%)
A. thaliana pistils infected	3935(13.7%)	1928(6.7%)	2007(7.0%)
A. thaliana leaf infected	1391(4.8%)	606 (2.1%)	785 (2.7%)

****** Non-pollinated pistils of *A. thaliana* were the point of reference for calculating differential expression for infected and pollinated pistils. Untreated leaves were the point of reference for calculating differential expression for infected leaves.

From RNAseq transcriptome data of *A. thaliana*, a total of 5088 genes were found to be differential expressed (Figure 13). 4073 genes were found to be uniquely expressed in one condition (Figure 13). *A. thaliana* infected pistils had the most genes expressed uniquely (n=3026), whereas *A. thaliana* selfed pistil had least uniquely expressed genes (n=14) (Figure 12). Nine genes were found to be commonly expressed in all five conditions (Figure 13). 41 genes were found to commonly expressed during selfed condition and cross pollination conditions. Similar 431 genes were found to commonly expressed in infected leaves and infected pistil. In general, *A. thaliana* expressed the highest DEG in infection condition compared to pollination condition (Table 3 and Figure 13)

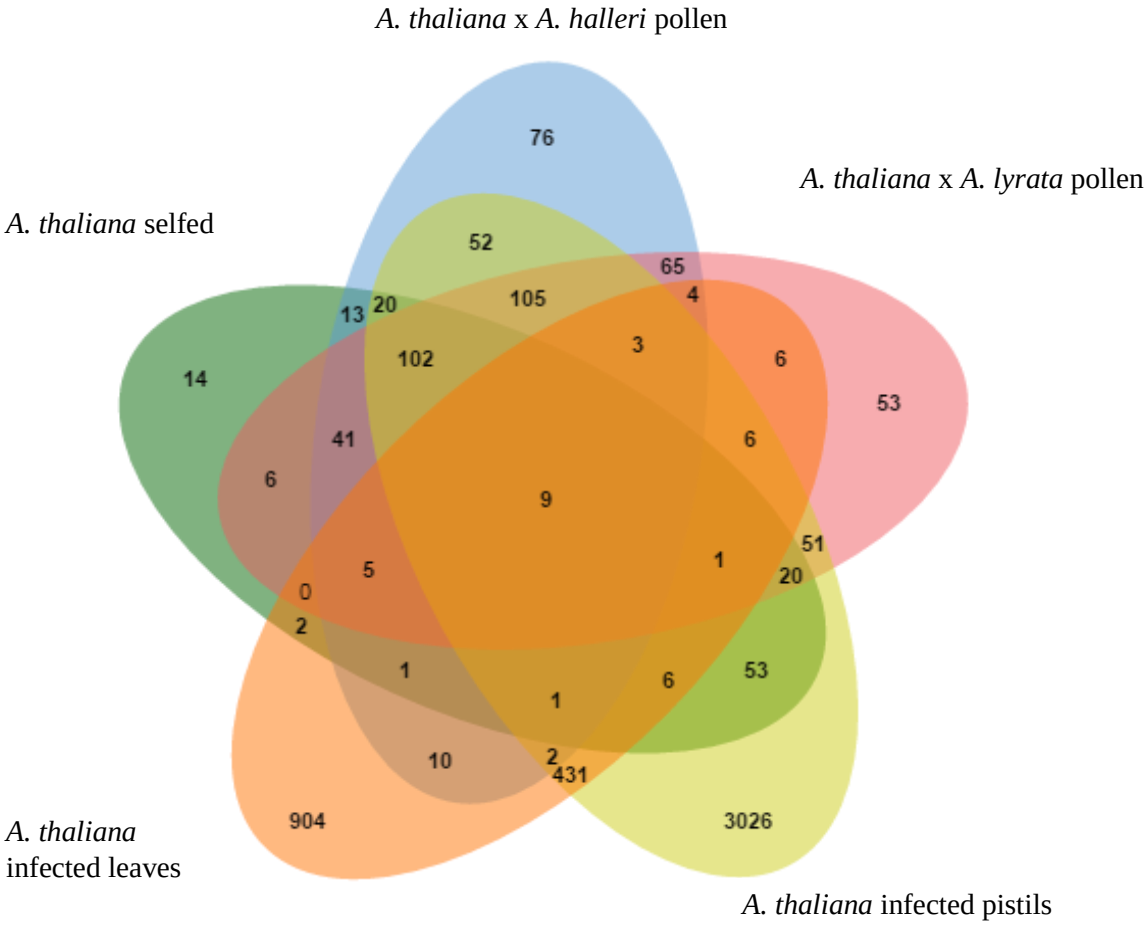

Figure 13:Distribution of the number of DEG in specific conditions.
Venn diagram illustrates the number of DEG in *A. thaliana* during selfed, cross pollination with *A. lyrata* and *A. halleri* pollen, and *F. graminearum* 3DAI of pistils and leaves. In total, 5088 genes were found to be differentially expressed in the five conditions, 4073 genes were found to be uniquely expressed in one condition, and the remaining 1015 genes were found in atleast two conditions. Nine genes were commonly expressed in all conditions. In conclusion, the *A. thaliana* infected pistil condition had the most expressed gene (n=3935), whereas *A. thaliana* selfed condition had the number of least expressed genes (n=341).

5.2.3 DEFL genes expression in transcriptome data

DEFL genes were further analysed from overall transcriptome data, 72 DEFL genes out of 324 genes were found to be differentially expressed (50 downregulated, 19 upregulated, three are upregulated in one condition and downregulated in other condition). The complete list of differential expression pattern of DEFLs can be seen in appendix section in 9.6. *A. thaliana* infected pistil had most downregulated DEFL genes (81%) and *A. thaliana* selfed pistil had no upregulated DEFL genes (Figure 14). There were nine genes found to have same pattern of downregulation in four pistil samples.

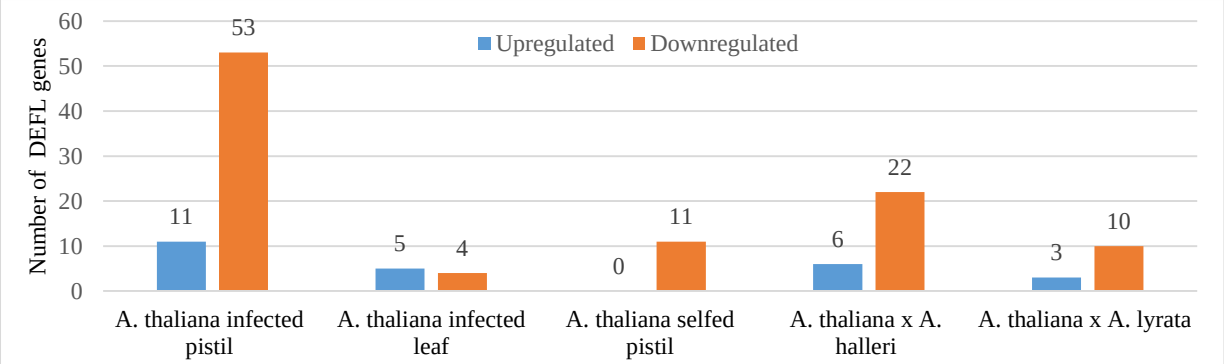

Figure 14:Differential expression pattern of DEFL genes at specific conditions.
Bar chart illustrates the upregulated (blue) and downregulated (orange) DEFL genes in the infected pistil, infected leaf, *A. thaliana* selfed pistil and *A. thaliana* pistil pollinated by *A. halleri*, *A. lyrata*. *A. thaliana* infected pistil condition had the highest number of downregulated DEFL gene (n=53), whereas the lowest number of downregulated DEFL gene was *A. thaliana* infected leaf (n=4). In the four conditions involving the pistil, the number of downregulated DEFL genes was higher in comparison to the upregulated DEFL genes. Interestingly *A. thaliana* selfed pistil had no upregulated genes. In general, DEFLs had more number of downregulated genes as response to pollination and infection.

A. thaliana infected pistils had 64 differentially expressed DEFL genes whereas infected leaves had substantially less differentially expressed DEFL genes (n=9) (Figure 14). We found 14, 11 and 28 differential expressed DEFL gene during *A. thaliana* selfed, *A. thaliana* pistil pollinated with *A. lyrata*, *A. halleri* respectively (Figure 14).

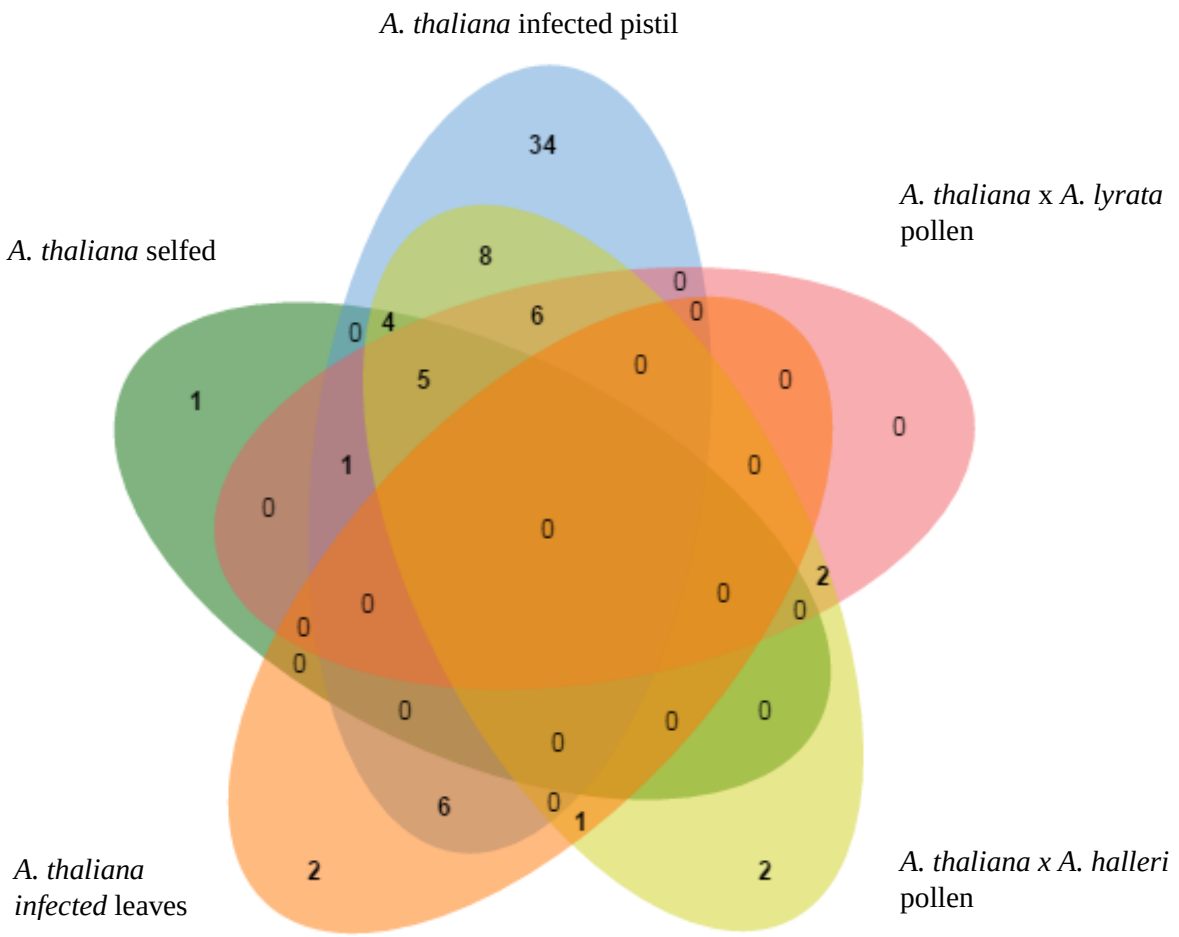

Figure 15:Distribution of differential expressed DEFL genes in *A. thaliana* during pollination and infection with *Fusarium graminearum*.
The venn diagram is used to illustrate the differentially expressed DEFL genes in *A. thaliana* during selfed, cross pollination with *A. lyrata*, *A. halleri* pollen, and *F. graminearum* infection of pistil and leaves. 72 DEFL genes were expressed in five conditions. 39 DEFLs were specifically differentially expressed in certain conditions and the remaining DEFLs were differential expressed in at least two conditions. *A. thaliana* infected pistil condition had the highest number of specifically differentially expressed DEFL genes (n=34) and the *A. thaliana* cross pollination with *A. lyrata* pollen condition had no specifically expressed DEFL genes. There was no common DEFLs differentially expressed in the five conditions. Five DEFL genes were found to be commonly expressed in all the conditions involving pistil tissue. In conclusion, *A. thaliana* infected pistil condition had the most specifically differentially expressed DEFL genes in comparison to other conditions.

Among 72 DEFL genes, 39 were specifically expressed in certain conditions whereas the rest were differential expressed in at least two conditions (Figure 15). 34 DEFL genes were specifically expressed in *A. thaliana* infected pistil (Figure 15). In the case of infected leaf, two (At2g43535, At3g05730) out of ten DEFL genes were specifically differentially expressed in leaf (Figure 15). In the case of pollinated pistils, only one out of 11 DEFL genes (At2g22941) was specifically differential expressed in *A. thaliana* selfed condition and two DEFL (At4g29285, At3g05727) out of 28 DEFL genes were specifically differential expressed during pollination with *A. halleri* pollen (Figure 15). Two DEFL genes

(At5g19315, At4g19035) were specifically expressed during both pollinations with foreign pollen (Figure 15). Six DEFL genes were found to be commonly differentially expressed during interspecific pollination with *A. lyrata* and *A. halleri* and fungal hyphae invasion. Five DEFL genes were found to be commonly expressed in all the conditions involving pistil tissue (Figure 15). There was no common DEFL gene expressed in five conditions. In conclusion, 72 of the 320 DEFL genes were represented in our transcriptome data and are differentially expressed in response to pollen tubes, fungal hyphae or both. A list of 72 DEFL gene expression in their respective conditions can be seen in the appendix section 9.6.

5.2.4 Plant defensin family (PDF) expression in transcriptome data

PDF is most notable DEFL family which contains 15 genes. It contains the following gene- At1g75830(PDF1.1), At5g44420(PDF1.2a), At2g26020(PDF1.2b), At5g44430(PDF1.2c), At2g26010(PDF1.3), At1g19610(PDF1.4), At1g55010(PDF1.5), At2g02120(PDF2.1), At2g02100(PDF2.2), At2g02130(PDF2.3), At1g61070(PDF2.4), At5g63660(PDF2.5), At2g02140(PDF2.6), At5g38330(PDF3.1) and At4g30070(PDF3.2). Eight PDF genes were found to be differential expressed in infected tissue (Table 4).

Table 4:Log_2 fold change of PDF genes

PDF	Infected pistil	Infected leaf
PDF1.2a	7.49	4.69
PDF1.2b	7.49	-
PDF1.2c	7.89	-
PDF1.3	9.78	-
PDF1.4	4.71	7.32
PDF2.2	-2.90	3.8
PDF2.6	-6.88	-8.36
PDF3.1	-2.40	-

5.2.5 Selection of DEFL genes

DEFL genes were selected for further analysis based on the previously described results of differentially expression as well as previous knowledge of expression in the female gametophyte which is described in discussion (Section 6.1.1). All the candidate DEFL genes were selected because of their expression in pistils, none of them were expressed in leaves.

Some interesting DEFL genes expressed in *A. thaliana* during fertilization events were selected as candidates. Five DEFL genes were identified to be specifically differentially expressed during pollination. Two DEFL genes, At2g29285 and At3g05727, were selected

from the five DEFL genes specifically expressed during pollination. Four DEFL genes were selected specially based on predicted expression in female gametophyte and also role in pollination events though they had not passed $\log_2$ two-fold change criteria.

Regarding the genes differentially expressed in the pistil during infection with *Fusarium*, two candidate genes were taken from the PDF family, PDF2.2 and PDF3.1 because they were downregulated during infection. LURE1(At5g43285), a known pollen tube attractant, was chosen because it was downregulated during infection. Candidate gene At4g15735 was chosen because of its upregulation during infection. Additionally, 12 DEFL genes were particularly interesting for further characterization because they were downregulated in infected pistils and which according to results from other groups, are expressed in the female gametophyte (Table 5).

Candidate DEFL genes were selected to cover various aspects of this study, including possible constitutive expression in both defence and fertilization. Under this premise, three additional DEFL genes were selected: At2g28405 and At2g28355 were downregulated during pollination with foreign pollen and during fungal infection and At4g11760 was downregulated in all pistil conditions investigated. A total of 25 DEFL candidate genes (Table 5) were taken for further analysis according to their corresponding expression pattern and their role in infection and pollination respectively.

Table 5:Log2 fold change of candidate *Arabidopsis thaliana* DEFL genes

TAIR ID	CRP family	Selfed	At pis. x Ah pol.	At pistil x Al pollen	At 3DAI *Fusarium*	TAIR10 annotation
At2g02100	CRP0000				-2.91	PDF 2.2
At5g08315	CRP0220				-3.47	DEFL Family Protein
At2g42885	CRP0300				-2.29	DEFL Family Protein
At3g06985	CRP0300				-3.70	LCR44
At3g07005	CRP0300				-2.24	LCR43
At2g20070	CRP0320				-4.84	Hypothetical protein. Similar to LCR81
At3g42473	CRP0330				-2.46	LCR47
At2g12475	CRP0360				-2.17	DEFL Family Protein
At2g40995	CRP0360				-3.57	DEFL Family Protein
At4g09153	CRP0580				-2.18	LCR36
At5g38330	CRP0670				-2.40	PDF 3.1
At5g43285	CRP0810				-3.41	LURE1.1
At1g60985	CRP0860				-2.24	SCR-like 6
At1g65352	CRP0940				-5.47	Putative membrane lipoprotein
At5g23212	CRP0960				-2.98	DEFL Family Protein
At2g28355	CRP0570		-4.58	-2.90	-5.20	LCR5
At4g11760	CRP0570	-3.30	-3.81	-3.19	-4.74	LCR17
At2g28405	CRP0570		-4.88	-6.18	-4.65	LCR32
At4g29285	CRP0580		2.17			LCR24
At3g05727	CRP0770		4.40			SLR1 binding pollen coat protein family
At4g15735	CRP0860				2.90	SCR- like 10
At5g55132	CRP0330	0.86	1.18			DEFL Family Protein
At3g43505	CRP0500	0.60	0.84			LCR30
At4g30067	CRP0660	0.54	0.76			LCR63
At4g30074	CRP0670	0.82	0.83			LCR19

Key to columns:
SLR = S locus-related glycoprotein 1, LCR = low-molecular-weight cysteine-rich protein, SCR = locus cysteine rich protein, PDF= Plant defensins family.

5.2.6 Validation of RNAseq data

This experiment was done under my supervision by Maria Pallmann for her Master Thesis. The aim of this experiment was to validate the RNAseq results through qPCR employing cDNA from the original total RNA samples employed for transcriptome sequencing. This assay measured gene expression of 14 candidate DEFLs: At4g15735, At3g43505, At4g30074, At4g30067, At3g05727, At5g55132, At4g29285, At4g11760, At2g28355, At2g28405, At2g40995, At3g07005, At4g09153, At5g38330.

Correlation analysis with log_2 fold changes detected by RNAseq and qPCR measurements showed positive correlation R^2 =0.83 (Figure 16). Log_2 fold change of DEFLs obtained in qPCR also validates the most of the expression pattern of RNAseq results. Specifically, twelve DEFL genes in qPCR had similar log_2 fold change with RNAseq data (Figure 17).

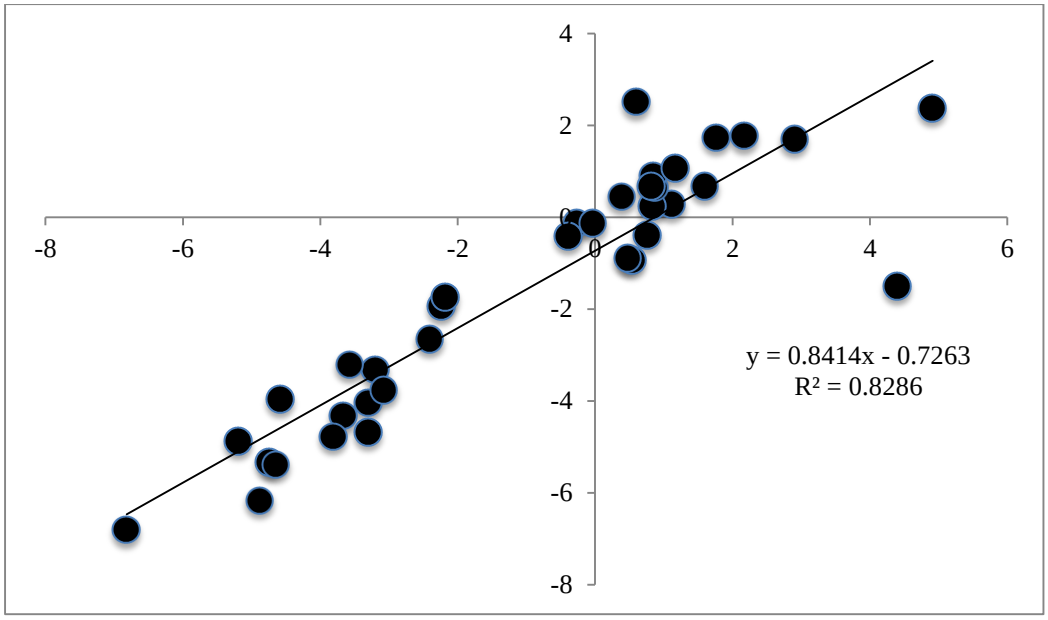

Figure 16:Positive correlation of log_2 fold change between RNAseq and qPCR measurements of 14 candidate DEFL genes.

Log_2 fold change of 14 candidate DEFL gene expression obtained in RNAseq analysis were correlated with Log_2 fold change obtained in the qPCR analysis. Correlation analysis showed positive correlation of R^2 =0.83 between Log_2 fold change measurements of qPCR and RNAseq (Figure from Mondragón-Palomino et al. Submitted).

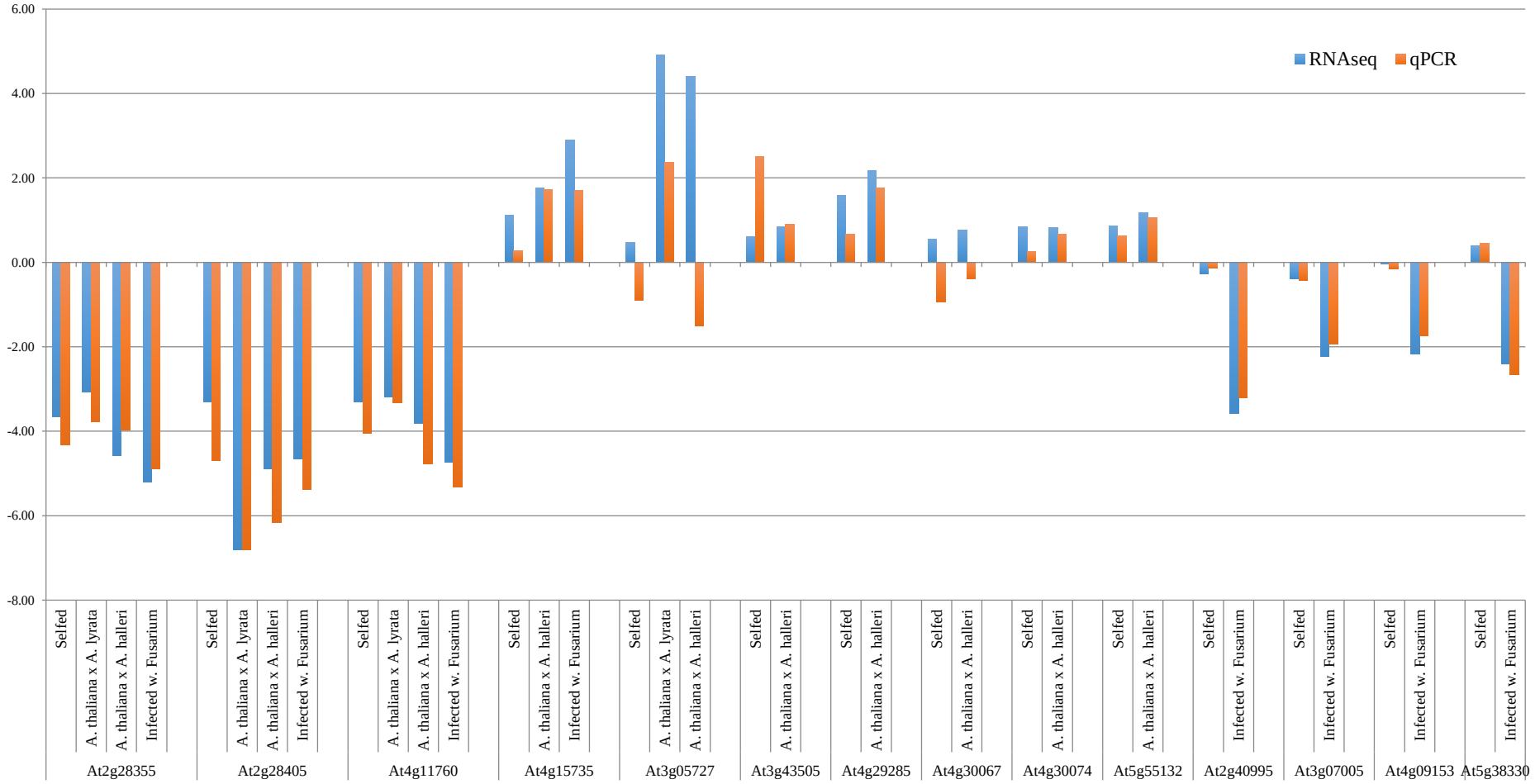

Figure 17:Comparison of log$_2$ fold change result of qPCR assay and RNAseq result of 14 candidate DEFL genes validates the RNAseq data.

The log$_2$ fold change of candidate DEFL gene expression in the qPCR analysis was obtained from total RNA samples of *A. thaliana* selfed pistils, *A. thaliana* pistil pollinated with *A. lyrata*, *A. halleri* pollen and infected pistil that were used in RNAseq. These measurements are compared with the log$_2$ fold change of candidate DEFL gene expression obtained from RNAseq analysis. Fold changes with both techniques are based on the comparison of the measurements obtained from each treatment with those of non-pollinated pistils (Figure from Mondragón-Palomino et al. in review). 12 candidate DEFL genes in qPCR had similar log$_2$ fold change to RNAseq

.

5.2.7 Defence related expression

Plant immunity is triggered by recognition of pathogen-associated molecular patterns (PAMPs) by receptors. This part of the immune response was reflected in the transcriptomes of *A. thaliana* infected pistils with the upregulation of At2g23770 and At2g33580, genes encoding lysin motif receptor kinase (LYK) known to be involved in recognition of fungal chitin (Zhang et al. 2010) (Table 6). Recognition of fungal chitin triggers several defence responses such as ROS production, MAPK signalling cascade, plant hormones and PCD.

Furthermore, the transcriptome analysis of the infected pistil showed several defence related genes including pathogenesis-related (PR) genes were upregulated. For instance, SA-responsive genes PR-1, PR-2 and PR-5, and JA/ET responsive genes PR-3 and PR-4 were upregulated in the infected pistils (Table 6). PR2 and PR3 belong to glycoside hydrolase protein family, PR1 belongs to cysteine-rich secretory protein family, PR4 belong chitin recognition protein family and PR-5 belong thaumatin family.

Similarly apoplastic peroxidases, PRX33 and PRX34, are activated during *Fusarium* infection, their products are important for ROS production which is relevant in signal transduction of molecules and oxidative burst for the defence process (Table 6) (Camejo et al. 2016). Few genes which regulate SA signalling and JA/ET signalling pathways were found to be upregulated in the transcriptome data (Table 6). These genes are vital for regulating different hormones during the defence response towards *F. graminearum* (Table 6).

PCD is part of the defence response initiated by plant in order to combat fungal hyphae. One of the initiators of PCD are α vacuolar processing enzyme (αVPE) which is upregulated in the transcriptome data of infected pistils (Table 6) (Fagundes et al. 2015). αVPE is a vacuolar enzyme which is similar to caspases and functions in initiating plant PCDs (Hatsugai et al. 2015).

These findings are important for understanding the *Arabidopsis-Fusarium* interaction and are relevant for characterizing the molecular mechanisms behind the activation of DEFL genes during the immune response towards *F. graminearum*.

Table 6:Differential expression of defence related genes in infected pistils of *A. thaliana*

Biological process	Gene name	Gene definition[1]	TAIR ID	Log_2 fold change[2]
Response to fungus	PR1	pathogenesis-related gene 1	At2g14610	5.95
	PR2	beta-1,3-glucanase 2	At3g57260	2.76
	PR5	pathogenesis-related gene 5	At1g75040	2.15
	PR4	pathogenesis-related gene 4	At3g04720	7.31
	PR3	basic chitinase	At3g12500	5.11
Reactive oxidative species metabolic process	PRX33	peroxidase CB	At3g49120	4.33
	PRX34	peroxidase CA	At3g49110	4.93
JA-mediated signalling pathway	ERF104	ethylene response factor 104	At5g61600	3.78
SA mediated signalling pathway	WKRY7	WRKY DNA-binding protein 7	At4g24240	2.36
	NPR1	regulatory protein (NPR1)	At1g64280	2.27
	LOX1	lipoxygenase 1	At1g55020	3.34
	WRKY25	WRKY DNA-binding protein 25	At2g30250	3.55
Innate Immune Response	AtLYK4	protein kinase family protein / peptidoglycan-binding LysM domain-containing protein	At2g23770	4.50
	AtLYK5	Protein kinase superfamily protein	At2g33580	2.21
	MPK3	mitogen-activated protein kinase 3	At3g45640	2.77
	MPK11	MAP kinase 11	At1g01560	4.68
	MKK7	MAP kinase kinase 7	At1g18350	2.04
	MKK9	MAP kinase kinase 9	At1g73500	2.08
Regulation in programmed cell death	AtCEP1	Cysteine proteinases superfamily protein	At5g50260	4.19
	αVPE	alpha-vacuolar processing enzyme	At2g25940	5.08
Metabolic process	DOGT1	don-glucosyltransferase 1	At2g36800	3.26

1- Definition according to database Phytozome 11 phytozome.jgi.doe.gov.
2- Log_2 fold change obtained from comparing the expression of *A. thaliana* infected pistils with that of non-pollinated pistils.

5.3 Localization of candidate DEFL genes *in planta*

This section describes the process to identify the locations and later on also the conditions under which the candidate DEFL genes are expressed. The corresponding promoters and/or coding sequences of each candidate gene were cloned into different contexts: In order to identify the tissues where the promoters of these candidates are active, they were cloned into a construct containing a nuclear localization signal (NLS) followed by three consecutive eGFP reporter genes. For investigating the subcellular localization of their corresponding proteins, the putative promoters and coding sequences of ten candidates were cloned N-terminal to eGFP (Table 7). For each construct, 10-20 independent lines were analysed under the microscope during non -pollinated condition and post-fertilization conditions starting from 8HAP until 96HAP.

Table 7:Candidate DEFLs investigated for expression localization in planta

Promoter analysis[1]	Subcellular localization analysis[2]
At4g30074	At4g30074
At5g55132	At5g55132
At3g43505	At3g43505
At2g02100	At2g28355
At5g08315	At4g11760
At2g42885	At2g28405
At3g06985	At4g29285
At3g07005	At3g05727
At2g20070	At4g15735
At3g42473	At4g30067
At2g12475	
At2g40995	
At4g09153	
At5g38330	
At5g43285	
At1g60985	
At1g65352	
At5g23212	

1- Promoter analysis: The putative promoter of each candidate gene regulates the expression of a nuclear localization signal followed by 3x eGFP.
2- Subcellular localization: Construct contains the putative promoter along with the coding sequence of the candidate gene followed by eGFP.

5.3.1 DEFL gene expression in female gametophyte

The unfertilized ovule of *A. thaliana* consists of three antipodal cells, two synergids, egg cell and central cell (Figure 18A). During *A. thaliana* self pollination, the *A. thaliana* pollen grain becomes hydrated and germinates into pollen tube. The pollen tube grows through the transmitting tract of the pistil. The pollen tube emerges from the transmitting tract and moves toward the ovule. During double fertilization, the pollen tube enters the ovule by growing through the filiform apparatus of the synergid cells. The pollen tube then comes in contact with the one of synergid cell which results in the synergid to undergo PCD. The two sperm cells are released from the pollen tube into cytoplasm of the synergid. One sperm cell fuses with the egg cell to form the embryo and other sperm cell fuses with central cell nucleus to form endosperm (Figure 18B). The embryo undergoes development to form the zygote. Fertilized central cell nucleus undergoes progressive synchronous endosperm nuclei division (Figure 18B). The three antipodal cells undergo PCD however, the time point at which they undergo PCD is still not conclusively defined.

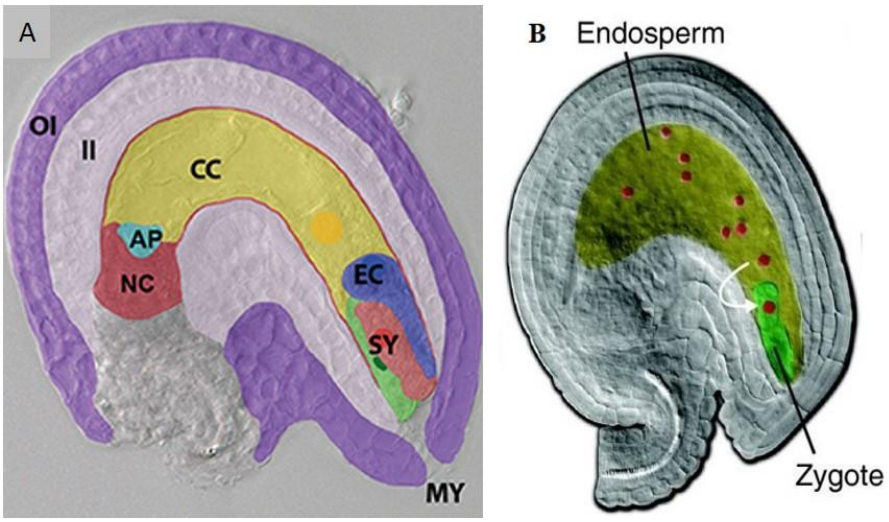

Figure 18:Schematic representation of *Arabidopsis thaliana* ovule before and after fertilization.

A) Non-pollinated ovule before fertilization consists of three antipodal cells(AP), two synergids(SY), egg cell(EC) and central cell(CC). Oi represents outer integuments and ii represents the inner integuments. Image is modified from (Bleckmann et al. 2014). B) Structure of fertilized ovule: sperm cell fuses with central cell to form endosperm (yellow) - red dots are individual nuclei in the syncytial endosperm. The second sperm cell fuses with the egg cell to form embryo(green). Embryo undergoes development to form the zygote (green). Picture taken from (Johnson et al. 2009).

The activity of the putative promoter of At5g43285, using pAt5g43285 NLS-(3x)eGFP marker line-, was observed in both synergid nuclei (Figure 19A) and after 8HAP, fluorescent GFP signal was present in the surviving synergid cell (Figure 19B).

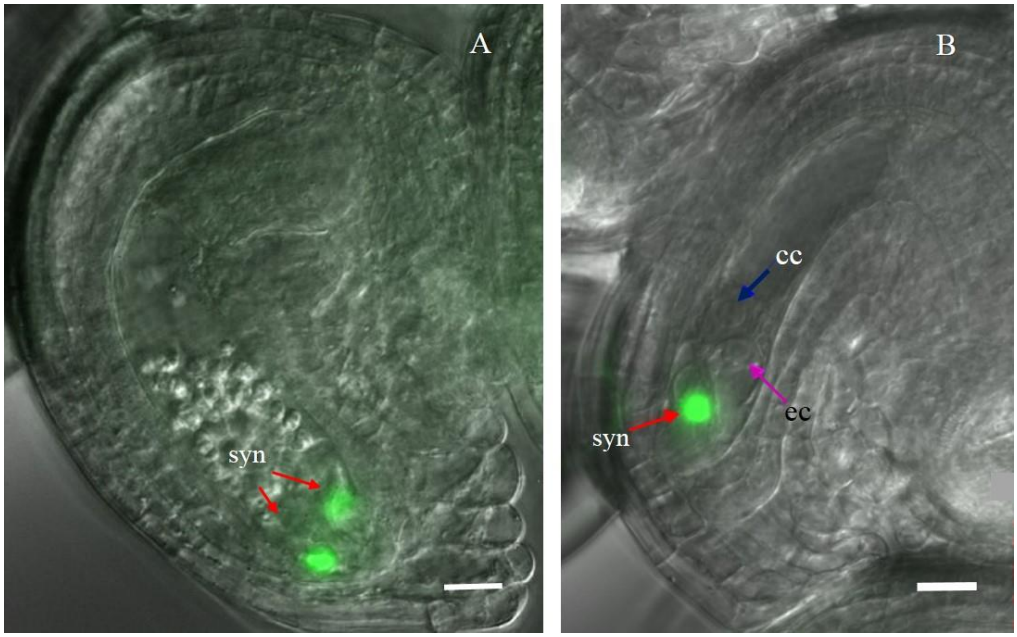

Figure 19:GFP expression under the regulation of the putative promoter of At5g43285 in the nuclei of synergids.

(A) Merged image of fluorescence light channel and DIC channel of the non-pollinated ovule showing the distinct GFP expression under the promoter activity of At5g43285 in the nuclei of both synergids. (B) Merged image of fluorescence light channel and DIC channel of the 8HAP ovule showing the GFP expression under the promoter activity of At5g43285 in the nucleus of the remaining surviving synergid cell. pAt5g43285 NLS-(3x)eGFP marker line-2 was used for this analysis. Key: syn-synergids, cc- central cell nucleus, ec-egg cell nucleus. Scale bars:50µm.

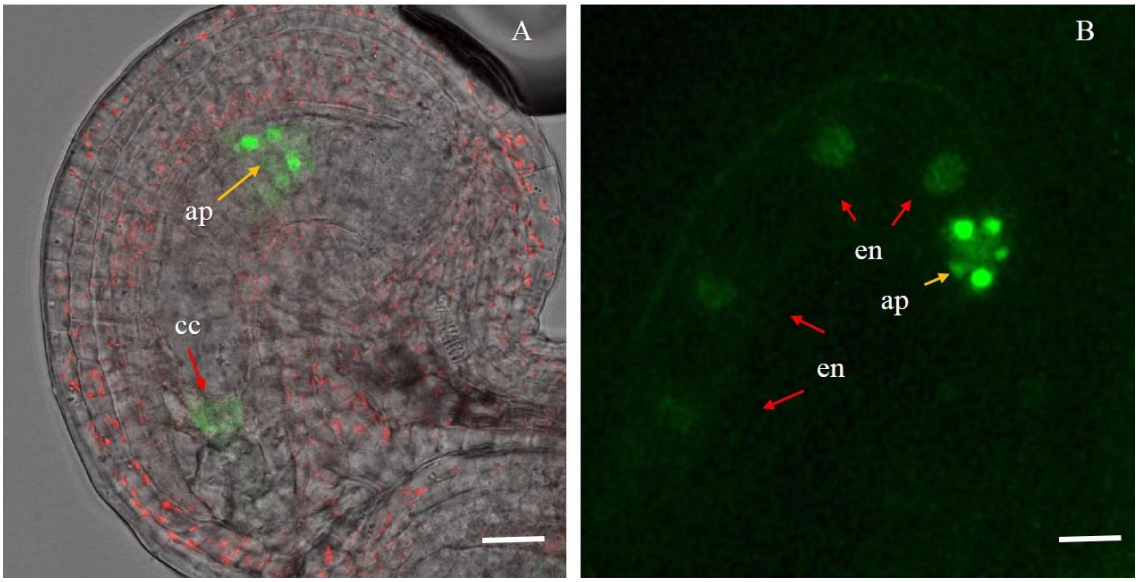

Figure 20:GFP expression under the regulation of the putative promoter of At2g20070 in the nucleus of central cell and antipodal cells.

(A) Merged image of fluorescence light channel and bright field channel of the non-pollinated ovule showing the distinct GFP expression in nucleus of antipodal (yellow arrow) and central cell (red arrow), under the promoter activity of At2g20070 gene (B) Image of fluorescence light channel of the fertilized ovule 12HAP showing the GFP expression in four-nuclei endosperm (red arrows) and antipodals nuclei (yellow arrow). Key: cc-central cell nucleus, en-endosperm nuclei, ap- antipodal cell nuclei. Scale bar:50µm. pAt2g20070:NLS-(3x)eGFP marker line -2 was used for this image.

Non-pollinated ovules of pAt2g20070:NLS-(3x)eGFP marker lines showed strong fluorescence signal on the three antipodal cell nuclei and very weak signal in the central cell nucleus (Figure 20A). In the 12HAP ovule, the GFP signal persists in the four-nuclei endosperm and in the nuclei of the three antipodal cells, which are smaller than the endosperm nuclei (Figure 20B).

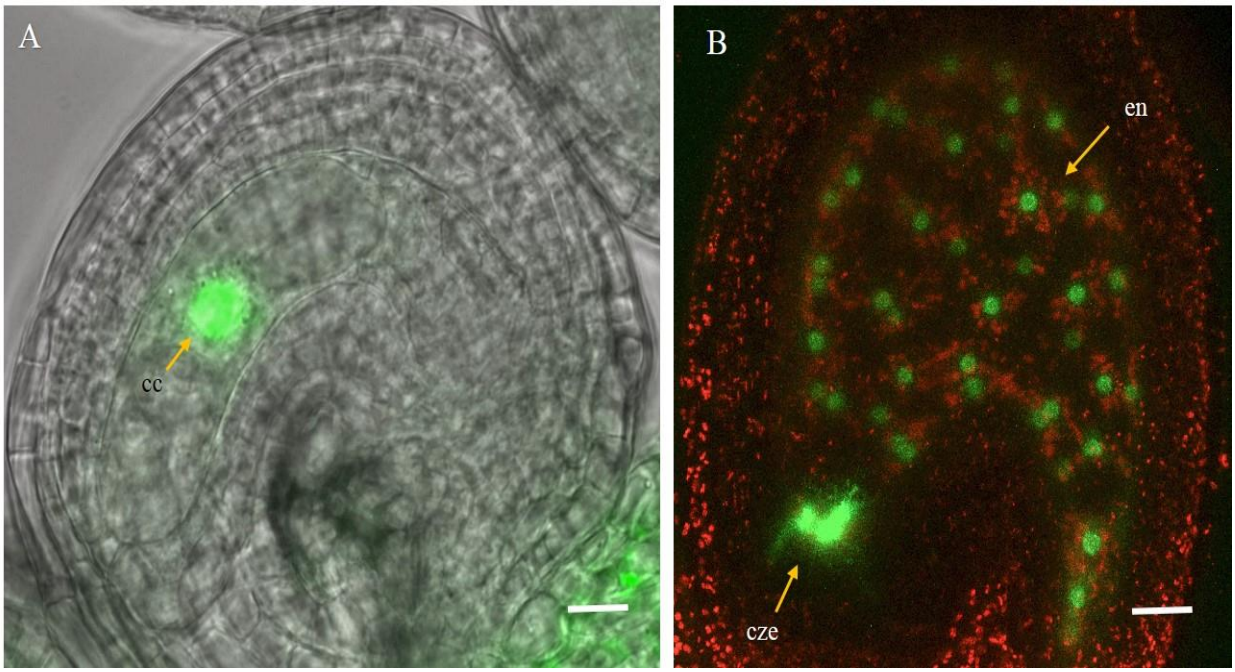

Figure 21:GFP expression under the regulation of the putative promoter of At5g55132 in central cell nucleus.
(A) Merged image of fluorescence light channel and bright field channel of the non-pollinated ovule expressing GFP under the promoter activity of At5g55132 in the nucleus of the central cell. (B) Maximum projection of merged image of fluorescence green light channel and red channel at 96HAP of pAt5g55132:NLS-(3x)eGFP showing GFP signal in the developing endosperm nuclei. pAt5g55132:NLS-(3x)eGFP- marker line -9 was used for image. Key: cc- central cell nucleus, cze-chalazal endosperm nuclei and en- endosperm nuclei. Scale bar:50µm.

In the case of pAt5g55132:NLS-(3x)eGFP and pAt3g43505:NLS-(3x)eGFP, before fertilization fluorescence was observed exclusively in the central cell nucleus of the ovule (Figures 21A and 22A). The GFP signal of pAt5g55132:NLS-(3x)eGFP and pAt3g43505:NLS-(3x)eGFP persists in the endosperm nuclei, including in the chalazal endosperm region till 96HAP (Figure 21B) and 72 HAP (Figure 22B).

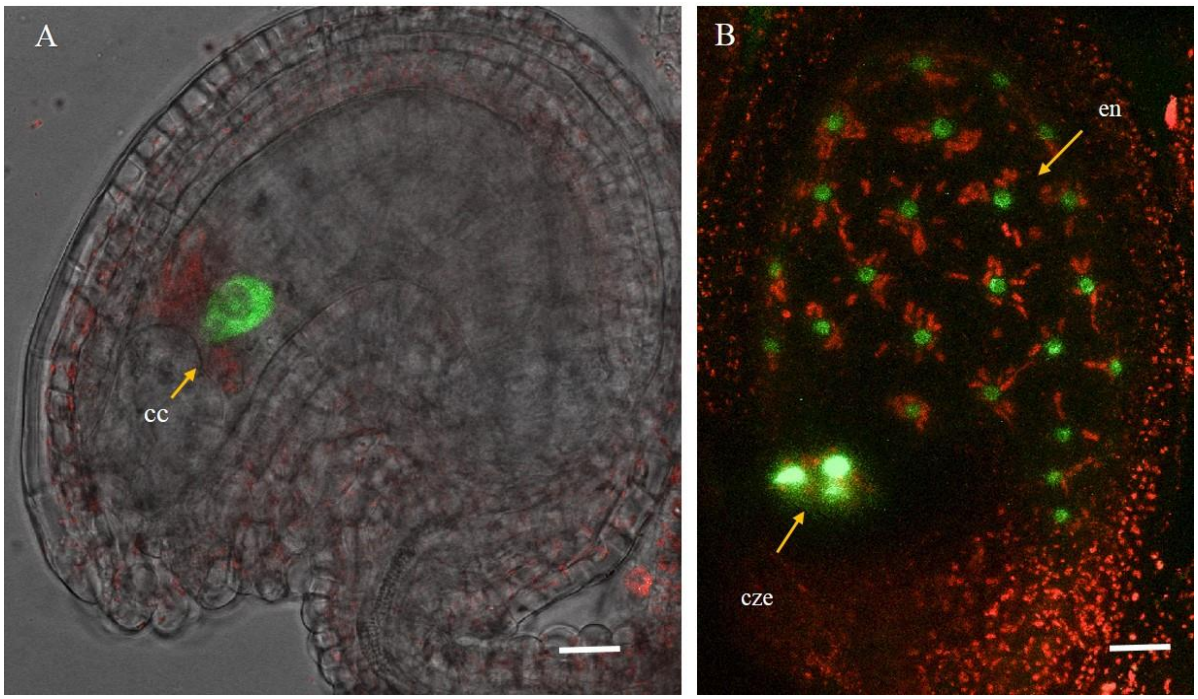

Figure 22:GFP expression under the regulation of the putative promoter of At4g43505 in central cell nucleus.

(A) Merged image of fluorescence light channel and bright field channel of the non- pollinated ovule expressing GFP under the promoter activity of At3g43505 in nucleus of central cell (B). Maximum projection of merged image of fluorescence green light channel and red channel at 72HAP of pAt3g43505:NLS-(3x)eGFP ovule showing GFP expression in the developing endosperm nuclei. pAt4g43504:NLS-(3x)eGFP- marker line-1 was used for this image. Scale bar:50 µm.

GFP expression of At4g30074 gene was localized in the nucleus of central cell (Figure 23A) in pAt4g30074:NLS-(3x)eGFP marker lines. GFP signal persists in the 16 stage endosperm nuclei until at 48HAP (Figure 23B). This localization was supported by subcellular localization marker lines pAt4g30074:At4g30074-eGFP showing At4g30074-eGFP protein being localized in the cytoplasm of the central cell and was secreted to the surrounding integument layers (Figure 23C).

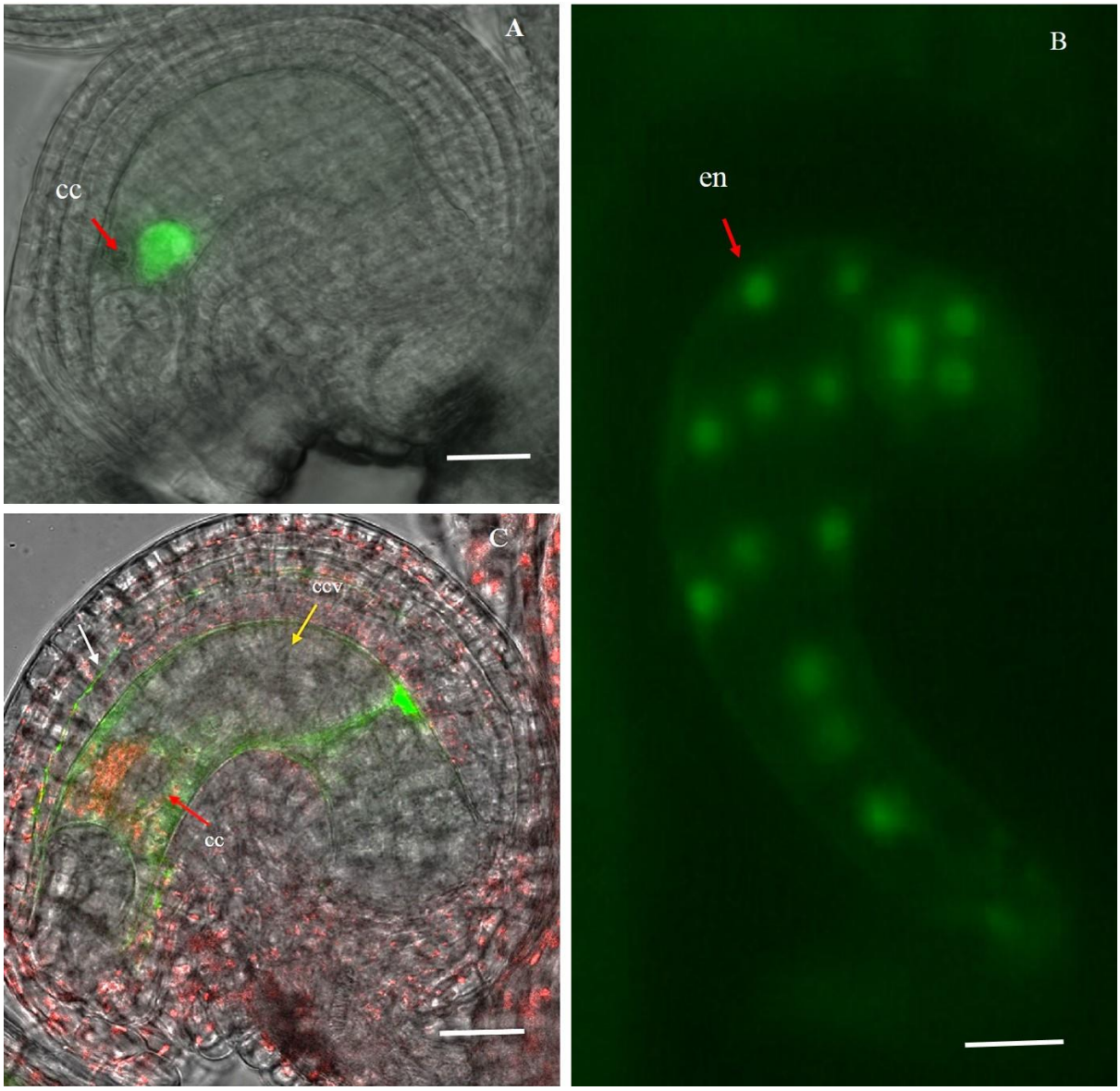

Figure 23:GFP expression of At4g30074 under regulation of putative promoter in central cell nucleus before fertilization and in endosperm nuclei after fertilization, and subcellular localization of At4g30074-eGFP protein was found in central cell.

(A) Merged image of fluorescence green light channel and bright field channel of the non-pollinated ovule expressing GFP under the promoter activity of At4g30074 in central cell nucleus (red arrow). (B) The image of fluorescence green light channel of 48HAP ovule showing GFP expression under the promoter activity of At4g30074 in endosperm nuclei. (C) Merged image of fluorescence green light channel, red light channel and bright field channel in the non-pollinated ovule expressing At4g30074-eGFP protein in the cytoplasm of central cell. The GFP signal surrounds central vacuole (yellow arrow) and central cell nucleus (red arrow). The At4g30074-eGFP protein is secreted to surrounding integument layer (white arrow). pAt4g30074:NLS-(3x)eGFP- marker line-1 was used for the image (A and B), The pAt4g30074:At4g30074-eGFP marker line -2 was used for the image (C). Key: cc- central cell nucleus, ccv -central cell vacuole, en-endosperm nuclei. Scale bar:50µm.

In the marker lines of pAt2g40995:NLS-(3x)eGFP, pAt2g42885:NLS-(3x)eGFP, pAt5g38330:NLS-(3x)eGFP, pAt3g07005:NLS-(3x)eGFP (Figures 24A to 24D respectively), localization of fluorescence signal was observed in central cell nucleus of non- pollinated

ovules. GFP signals of these marker lines are observed until 48HAP at the 16 nuclei stage (Figures 25A to 25D respectively).

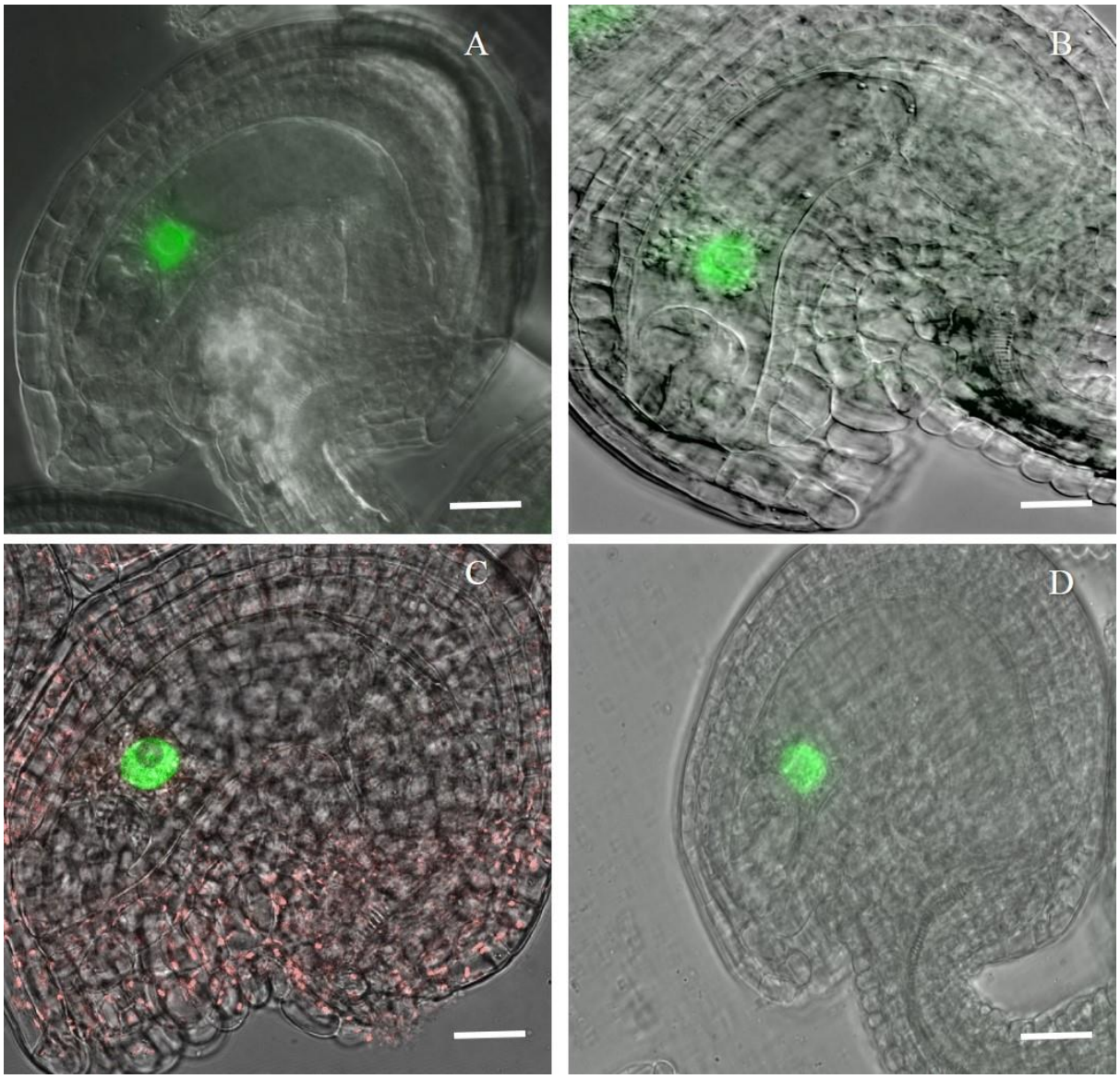

Figure 24: In non-pollinated ovules, reporter gene GFP indicates the activity in the central cell of the putative promoters of six DEFL genes:At2g40995, At2g42885, At5g38330 and At3g07005

Merged image of fluorescence light channel and DIC channel of the non-pollinated ovules expressing GFP in the nucleus of the central cell under the promoter activity in marker line of (A) pAt2g40995:NLS-(3x)eGFP-4, (B) pAt2g42885:NLS-(3x)eGFP-2. Merged image of fluorescence light channel and bright field channel of the non-pollinated ovule expressing GFP in the nucleus of the central cell under the promoter activity in marker line of (C) pAt5g38330:NLS-(3x)eGFP-4 (D)pAt3g07005:NLS-(3x)eGFP-15, in nucleus of central cell. Scale bar:50 µm.

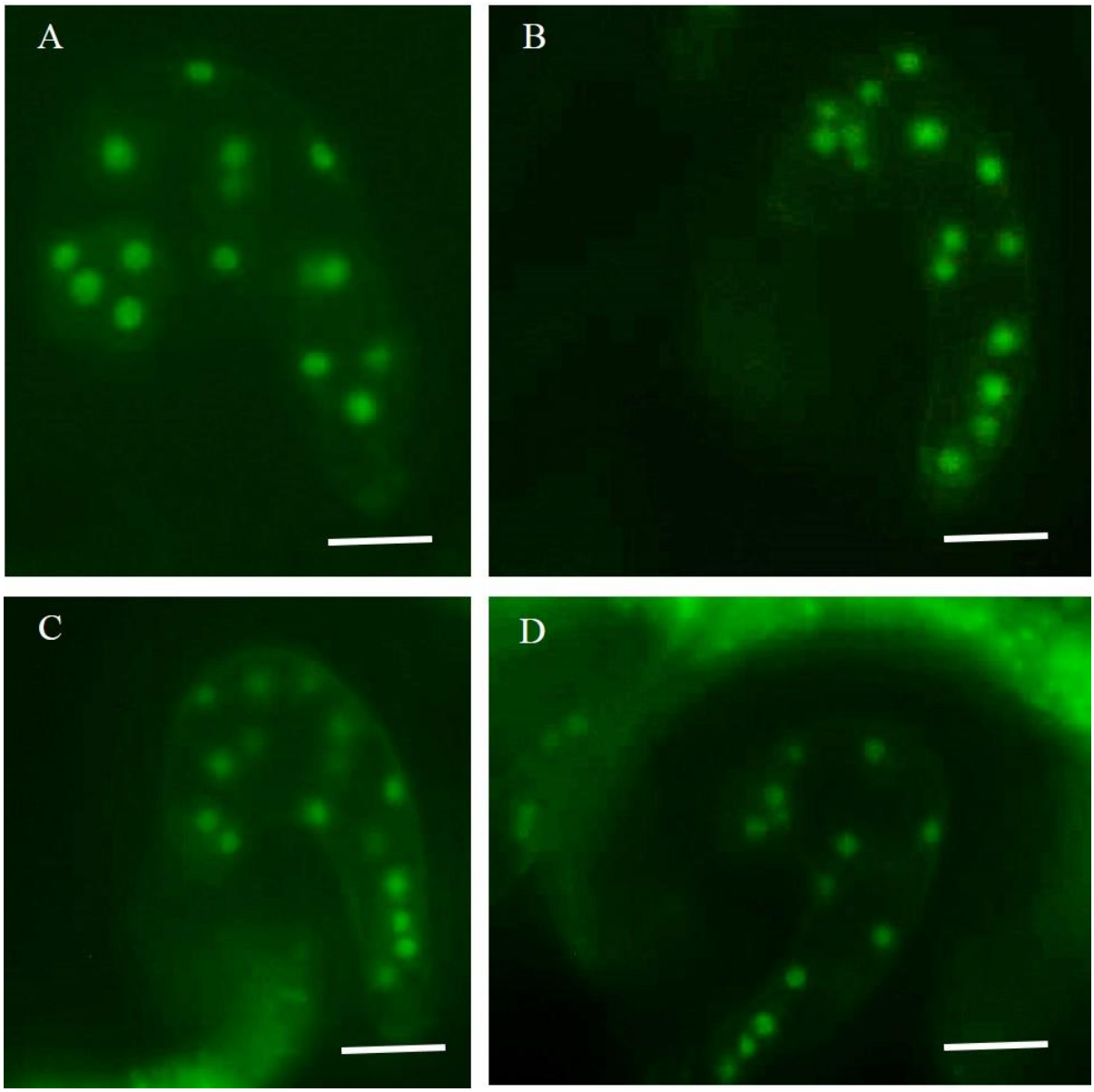

Figure 25:In 48HAP ovules, reporter gene GFP indicates the activity in the endosperm nuclei of the putative promoters of six DEFL genes: At2g40995, At2g42885, At5g38330 and At3g07005

The image of fluorescence green light channel of the 48HAP ovules showing GFP expression in the nucleus of the endosperm cell under the promoter activity in marker line of (A) pAt2g40995:NLS-(3x)eGFP-4, (B) pAt2g42885:NLS-(3x)eGFP-2, (C) pAt5g38330:NLS-(3x)eGFP-4 and (D) pAt3g07005:NLS-(3x)eGFP-15. Scale bar:50 µm.

Similarly, In the marker lines of pAt4g09153:NLS-(3x)eGFP, pAt1g60985:NLS-(3x)eGFP (Figure 26A and C), localization of fluorescence signal was observed in central cell nucleus of non- pollinated ovules. GFP signals of these marker lines are observed until 48HAP at the 16 nuclei stage (Figures 26B and D).

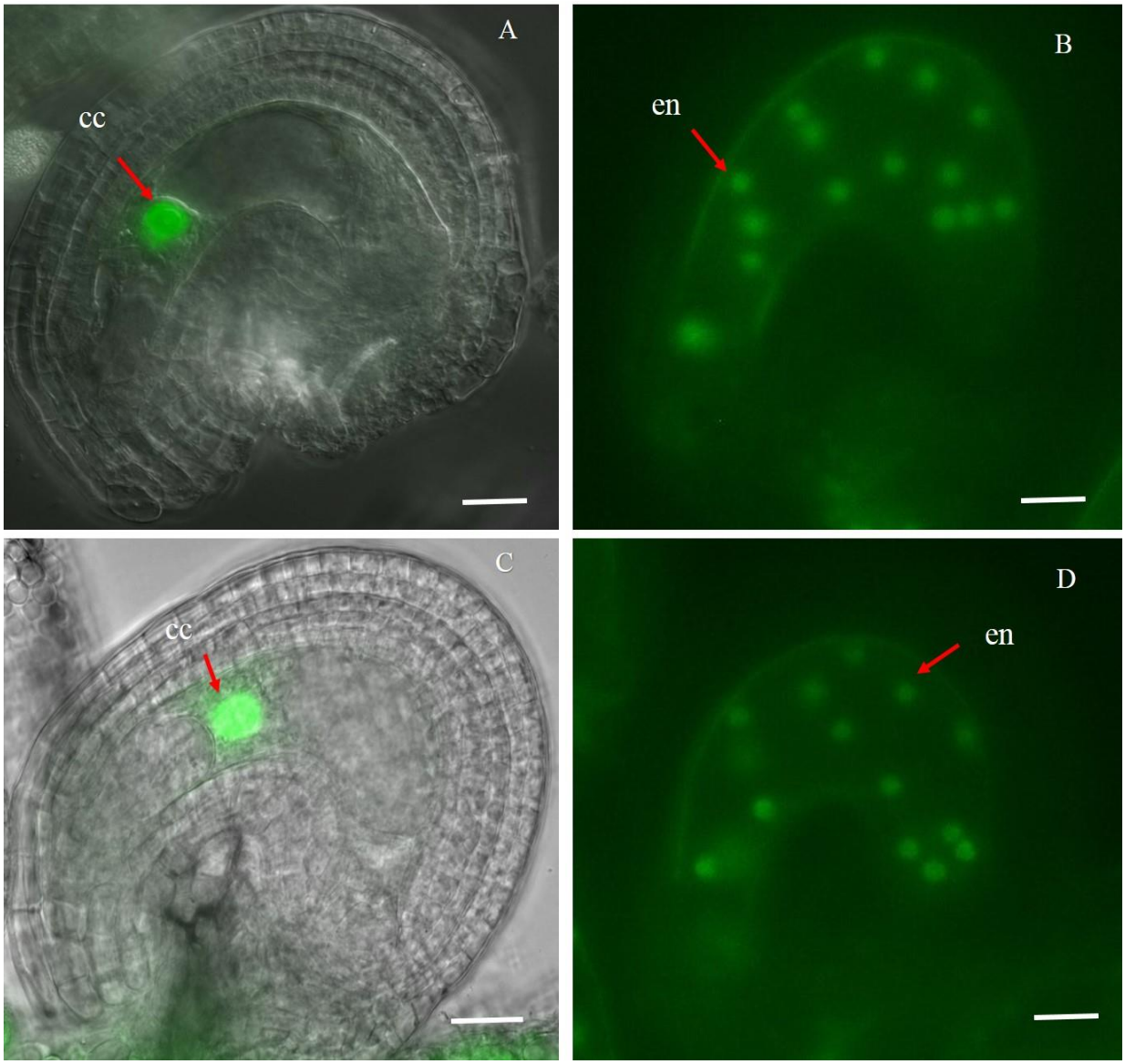

Figure 26:GFP expression under the regulation of the putative promoter of At4g09153 and At1g60985 in central cell nucleus of an unfertilized ovule and in the endosperm nuclei in 48HAP fertilized ovule.

(A) Merged image of fluorescence green light channel and bright field channel of the non-pollinated ovule expressing GFP under the promoter activity of At4g09153 in central cell nucleus (red arrow). (B) The image of fluorescence green light channel of 48HAP ovule showing GFP expression under the promoter activity of At4g09153 in endosperm nuclei (red arrow) (C) Merged image of fluorescence green light channel and bright field channel of the non-pollinated ovule expressing GFP under the promoter activity of At1g60985 in central cell nucleus (red arrow). (D) The image of fluorescence green light channel of 48HAP ovule showing GFP expression under the promoter activity of At1g60985 in endosperm nuclei (red arrow). Key: cc- central cell nucleus, en-endosperm nuclei. Scale bar:50µm.

All the marker lines with fluorescence showed a clear nuclear localization without any background or leakage of fluorescence. pAt4g30067:At4g30067-eGFP showed GFP signal in the nucleus of egg cell. This expression could not be validated because only one independent line showed this localization.

In conclusion, all candidate genes expressing GFP in ovules were clearly visible in gametophytic tissue and are not expressed in the surrounding sporophytic cells.

5.3.2 DEFL gene expression in pollen grains

The pAt4g11760:At4g11760-eGFP was found to be localized in mature pollen grains (Figure 27A) and in the cytoplasm of growing pollen tubes (Figure 27B).

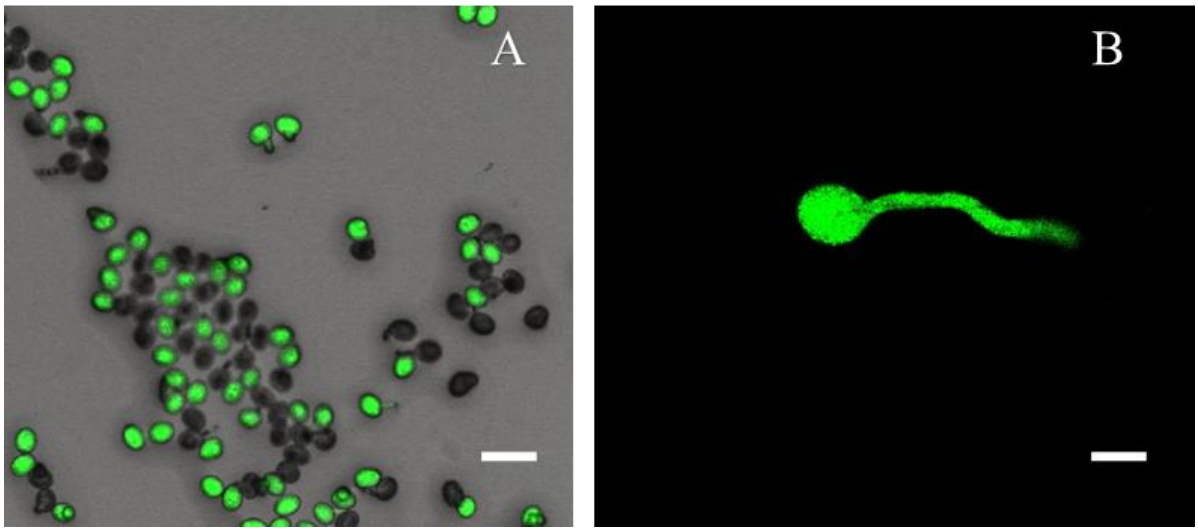

Figure 27:At4g11760 recombinant protein labelled with GFP expression in *A. thaliana* pollen grain.
T1 generation of heterozygous pollen grain in pAt4g11760:At4g11760-eGFP marker line-2 (A) showing 50% of pollen with eGFP expression and 50% are wild type (WT) pollen (B) Pollen tube of pAt4g11760: At4g11760-eGFP after 4 hours of germination. Scale bar: 50 µm.

GFP signal was specifically observed in pollen grains of the marker lines pAt3g06985:NLS-(3x)eGFP (Figure 28A), pAt3g42473:NLS-(3x)eGFP (Figure 28B) and pAt1g65352:NLS-(3x)eGFP (Figure 28C).

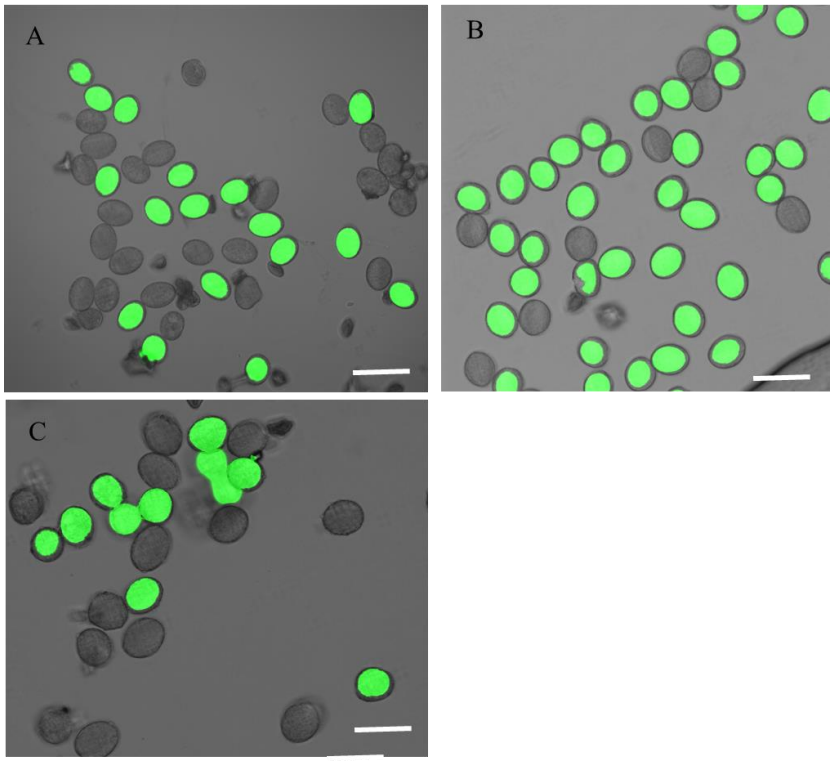

Figure 28:Localization of putative promoter activity indicated by reporter GFP in pollen grains of marker lines of At3g06985, At3g42473 andAt3g65352.
T1 generation of heterozygous pollen grain in marker line of, (A) pAt3g06985:NLS-(3x)eGFP-3, (B) pAt3g65352:NLS-(3x)eGFP-2 and (C) pAt3g42473:NLS-(3x)eGFP-4, showing 50% of pollen with GFP expression and 50% are wild type (WT). Scale bar: 50 µm.

All candidate genes which expressed GFP in pollen grains were employed to pollinate wild type *A. thaliana* pistils to assess if the fluorescent signal persisted during pollen tube growth through transmitting tract, however none of them showed any GFP signal during this process.

In summary, 15 DEFL candidate genes with either or both promoter activity assessed by reporter GFP or recombinant protein labelled with GFP were observed in the reproductive tissue of *A. thaliana*, mostly in the embryo sac. The remaining ten candidate genes At2g28355, At2g28405, At4g29285, At3g05727, At4g15735, At4g30067, At2g02100, At5g08315, At2g12475, At5g23212 were not expressed in the transmitting tract, ovule or pollen grains.

5.3.3 DEFL gene expression in roots

The roots are exposed to microorganism making them relevant to investigate DEFL expression. 15 DEFL candidate genes expressed in reproductive tissues of *A. thaliana* were selected for investigating expression in roots.

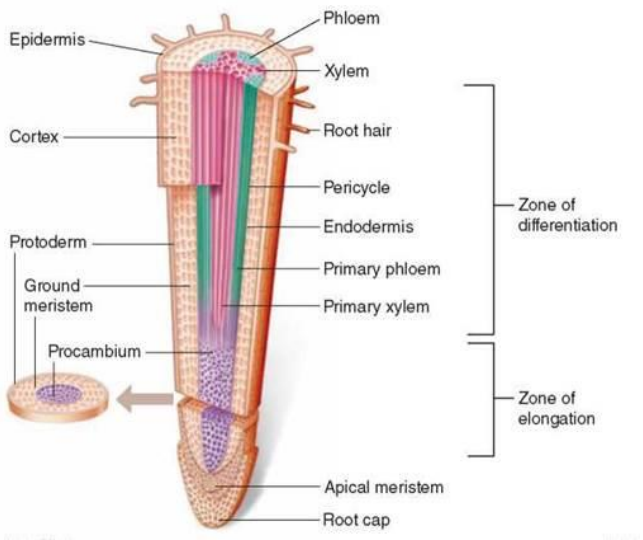

Figure 29:Representation of root structure
The diagram was taken from http://schoolbag.info/biology/living/living.files/image963.jpg

In pAt4g11760: At4g11760-eGFP, green fluorescence from protein expression was found in the root cap (Figure 30A and B). Incidentally, At4g11760 was also induced in the root epidermis when it was in contact with a pathogen (Figure 30C).

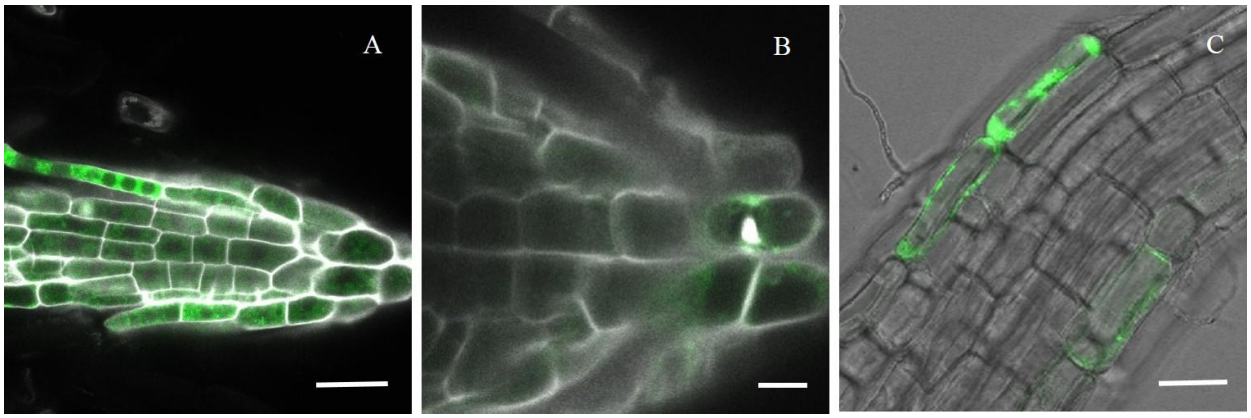

Figure 30:At4g11760 recombinant protein labelled with GFP expression in *A. thaliana* root cap and root epidermis.
T2 generation of roots of pAt4g11760:At4g11760-eGFP marker line-2 (A) roots stained with propidium iodide and eGFP expression observed in root cap (B) roots stained with propidium iodide and eGFP expression observed in tip of the root cap(C) eGFP expression in root epidermis. Scale bar:50 µm.

In pAt4g30074:At4g30074-eGFP, green fluorescence signal was observed in the epidermis of the root, they were found in root tip of lateral root hair and in the cells of root cap (Figure 31).

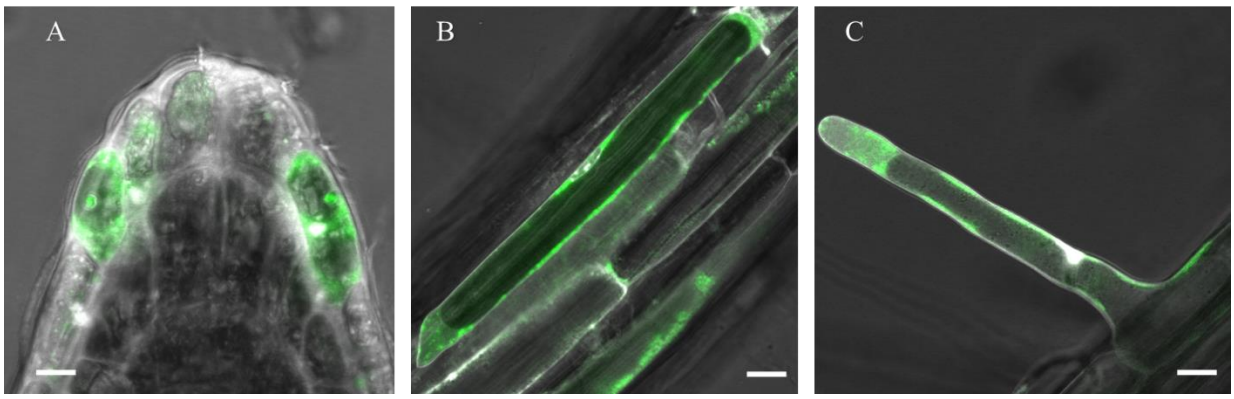

Figure 31:At4g30074 recombinant protein labelled with GFP expression in A. thaliana root cap, epidermis and root hair.
T2 generation of roots in pAt4g30074:At4g30074-eGFP (A) root cap stained with propidium iodide and eGFP expression observed in root cap (B) roots stained with propidium iodide and eGFP expression observed in epidermis of the root(C) roots stained with propidium iodide and eGFP expression observed in tip of the root hair. The pAt4g30074:At4g30074-eGFP marker line-2 was used for these images. Scale bar:50µm.

As a result of the master thesis work of Kriss Spalvins, we observed the signal of pAt5g38330:NLS-(3x)eGFP and pAt2g42885:NLS-(3x)eGFP in the nucleus of ground meristem in the root tip and can be seen in appendix section 9.7, while pAt2g40995:NLS-(3x)eGFP had fluorescent signal in the nucleus of the root apical meristem (Appendix section 9.7). Plants transformed with pAt3g07005:NLS-(3x)eGFP showed signal in the root tip (Appendix section 9.7). For marker lines pAt2g42885:NLS-(3x)eGFP and pAt3g07005:NLS-(3x)eGFP fluorescent signals were also observed in the maturation zone of root (Appendix section 9.7).

In conclusion, 15 DEFL genes were expressed in reproductive tissues and six of them were also expressed in different structures of the roots (Table 8).

Table 8:Summary of candidate DEFL genes expression in plant tissues

Defensins	Reproductive tissue	Post-fertilization GFP expression	Root GFP expression	Result obtained from
At1g65352	Pollen grain	Not tested*	No	Promoter analysis
At3g42473	Pollen grain	Not tested*	No	Promoter analysis
At3g06985	Pollen grain	Not tested*	No	Promoter analysis
At5g38330	Central cell	Endosperm	Ground meristem tissue in root tip	Promoter analysis
At5g43285	Synergids	Synergid	No	Promoter analysis
At1g60985	Central cell	Endosperm	No	Promoter analysis
At2g20070	Central cell, Antipodal cells	Endosperm, Antipodal cells	No	Promoter analysis
At2g42885	Central cell	Endosperm	Ground meristem tissue in root tip and root epidermis	Promoter analysis
At2g40995	Central cell	Endosperm	Root apical meristem.	Promoter analysis
At3g07005	Central cell	Endosperm	Root cap, lateral root	Promoter analysis
At4g09153	Central cell	Endosperm	No	Promoter analysis
At4g30074	Central cell	Endosperm	Root cap, lateral root hair, root epidermis	Promoter analysis, Subcellular localization analysis
At3g43505	Central cell	Endosperm	No	Promoter analysis
At5g55132	Central cell	Endosperm	No	Promoter analysis
At4g11760	Pollen grain and pollen tube	Not tested*	Root cap, root epidermis	Subcellular localization analysis

*-At4g11760, At1g65352, At3g42473 and At3g06985 pollen grains were pollinated on WT *A. thaliana* pistil and no GFP expression was observed during pollen tube germination in the stigma of *A. thaliana* pistil

5.4 - Testing the effect of mock treatment and pistil age on DEFL transcription during infection with *Fusarium graminearum*

The majority of the candidate defensins genes were selected based on their response to fungal infection (Table 5). These genes were downregulated more than $\log_2$ two-fold when 3DAI pistils were compared with 1DAE pistils. Two factors were initially overlooked during the sampling of the tissue for RNAseq. The first factor was possible stress caused to the plant by the procedures to infect and incubate the plant with *Fusarium graminearum* conidia where plants were taken from optimal conditions, dipped in *F. graminearum* inoculation solution and then kept for several days in a humid chamber (section 4.3.4). The second factor was the age of the pistils used for comparison in RNAseq. The flowers were emasculated, allowed to recover for one day and then inoculated and incubated in a moist chamber for three days (3DAI). The 1DAE used in RNAseq analysis was not a precise control for 3DAI pistil. Instead, an age-appropriate control would have been four days after emasculated pistil (4DAE) for 3DAI pistil. Thereby rising up the question of whether downregulation of the DEFL candidate genes was due to the age of the pistils, the procedures to infect the plants or the effect of *Fusarium* infection.

In order to assess this question qPCR assay was chosen to assess whether At5g38330, At5g43285, At1g60985, At2g20070, At2g42885, At2g40995, At3g07005 and At4g09153 genes were downregulated due to *F. graminearum* infection or if other factors such as inoculation treatment or age had an effect on the expression pattern. This was done by including two controls: emasculation without treatment for 2 and 4 days and mock treatment where plants were emasculated, let for recovery one day, dipped in water and left in a moist chamber for 1 or 3 days. According to the promoter analysis described in Table 8 these candidates were expressed in the female gametophyte of *A. thaliana*. The experiments were performed by myself and Kriss Spalvins and the qPCR experiments of all candidates was done by Dr. Mariana Mondragón Palomino and the results for candidates At5g38330, At5g43285, At1g60985 and At2g40995 included in the Master thesis of Kriss Spalvins (Appendix section 9.8). The results for these genes are included here for further analysis. Reference genes chosen for normalization in the experiment were At2g19270 and At1g10310 as previously identified and validated in the Master thesis of Maria Pallmann (2014).

Two infection points were taken for the experiment: one day after infection (1DAI) and 3DAI. The control for 1DAI was two days after emasculation (2DAE) and one day after mock treatment (1DAT). Similarly, the control for 3DAI was 4DAE and three days after mock treatment (3DAT). Three replicates of pistil samples were taken for each condition.

The values obtained as the expression of the genes from qPCR are calibrated normalized relative quantities (CNRQ).

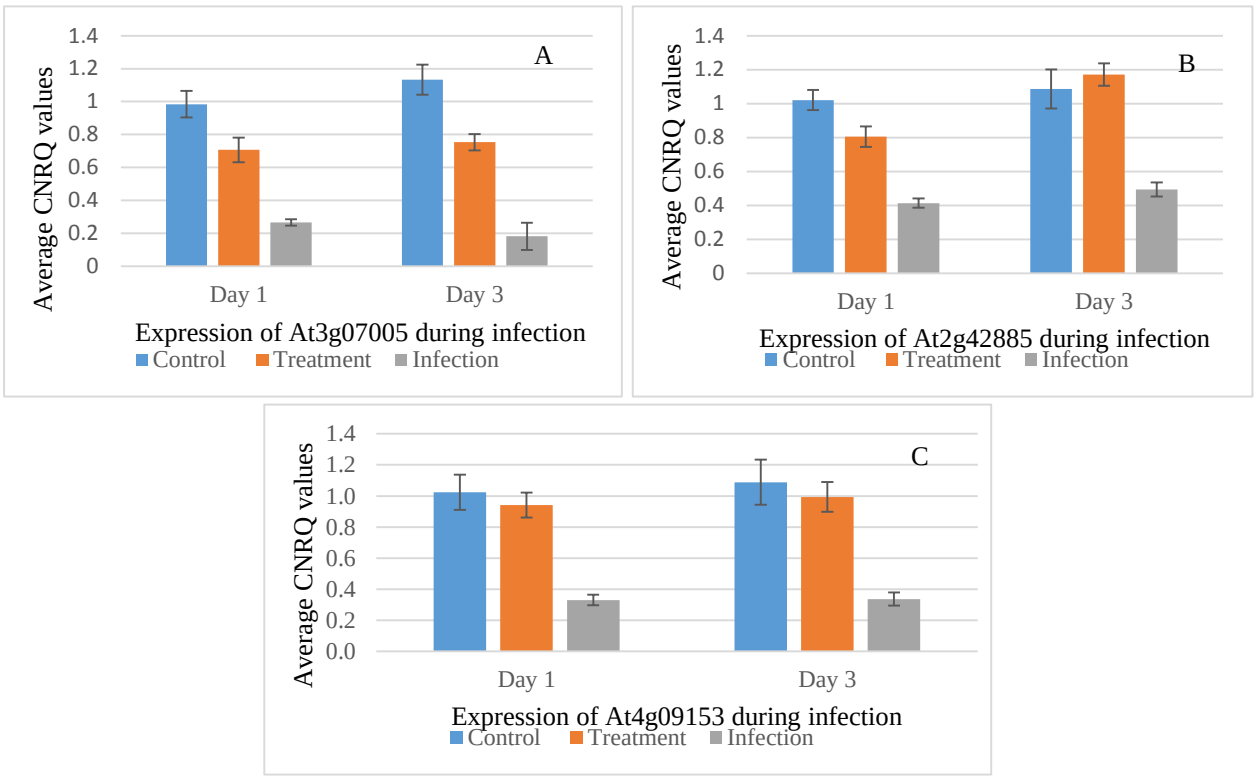

Figure 32:Down regulation of CNRQ values in infected treated samples in comparison to mock treatment and emasculated pistil of At2g42885, At3g07005 and At4g09153 at day 1 and day 3.

Average CNRQ values of control (blue column), mock treatment (orange column) and infection (grey column) for At3g07005(A), At2g42885(B), At4g09153(C) during day 1 and day 3. The infected samples of At2g42885, At3g07005 and At4g09153 at day 1 and day3 were downregulated in comparison to mock treatment and control. Error bars represent the standard error.

The average CNRQ values of At2g42885, At3g07005 and At4g09153 showed that the infected samples at 1DAI and 3DAI, are downregulated when compared with controls (Figure 32A, B and C), while the mock treatment and control were found to have similar levels of relative expression. The same pattern was observed for the rest of the candidates analysed with all three biological replicates (Mondragón-Palomino et al. in review).

All CNRQ values of the seven candidate genes were taken for further analysis. The average CNRQ values of seven candidate genes tested indicate strong downregulation between 2DAE and 3DAI (Figure 33A). The $\log_2$ fold change was calculated between the expression of 2DAE and 3DAI, while At5g38330 has the highest $\log_2$ fold change of –4.15 the smallest was observed in At2g42885 with -1.14 (Figure 33B). Three of the genes (At5g38330, At3g07005 and At2g40995) had a $\log_2$ fold change higher than -2.0, which was similar to that observed in the RNAseq analysis (Figures 33B)

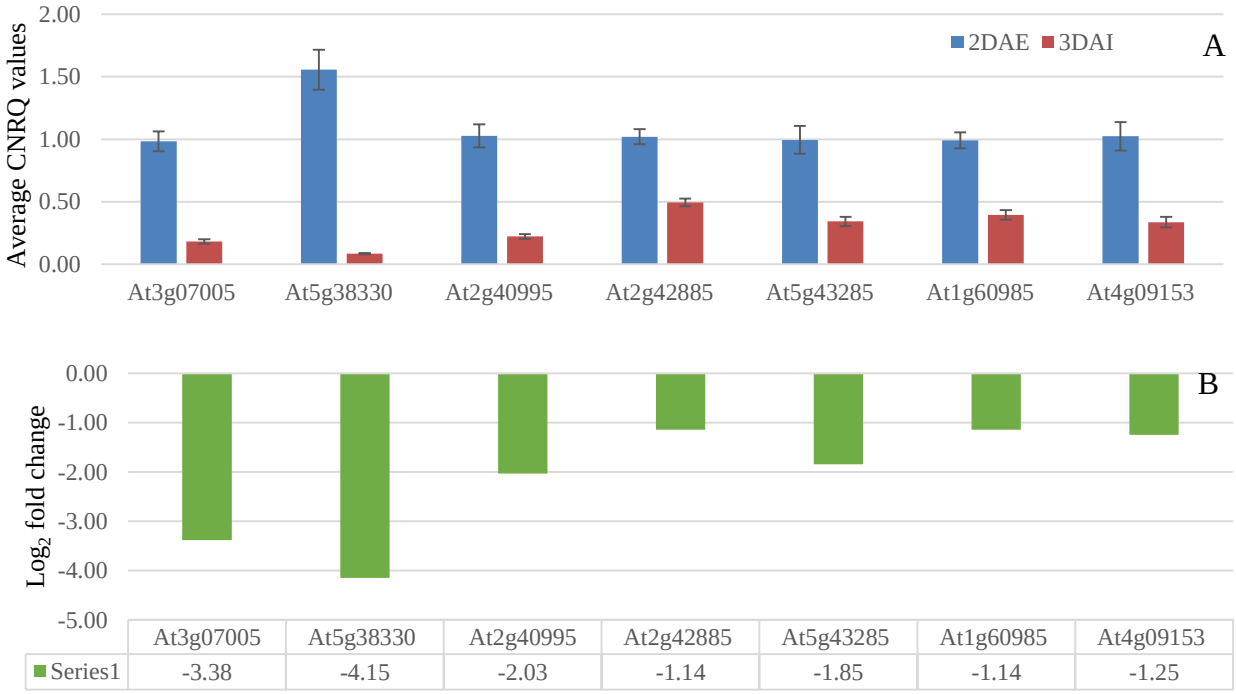

Figure 33:Data representation for seven candidate genes during 2DAE and 3DAI indicates that 3DAI has downregulation pattern of expression for the seven candidate genes in comparison to 2DAE.

A) Average CNRQ values of seven candidate genes for 2DAE was compared with 3DAI. The error bar represents standard error. The average CNRQ value of 3DAI pistil of seven candidate genes were downregulated in comparison to 2DAE. Error bars represent the standard error. B) Log_2 fold change of seven candidate genes between 2DAE and 3DAI and all the seven candidate genes had Log_2 fold change of ≤ -1.

The log_2 fold change data of DEFL candidate genes were obtained from infection with *F. graminearum* wild type (WT), which was used for RNAseq and was compared with *F. graminearum* Ds Red. The expression pattern in the candidate genes were identical and downregulated with different *F. graminearum* strains (Figure 34).

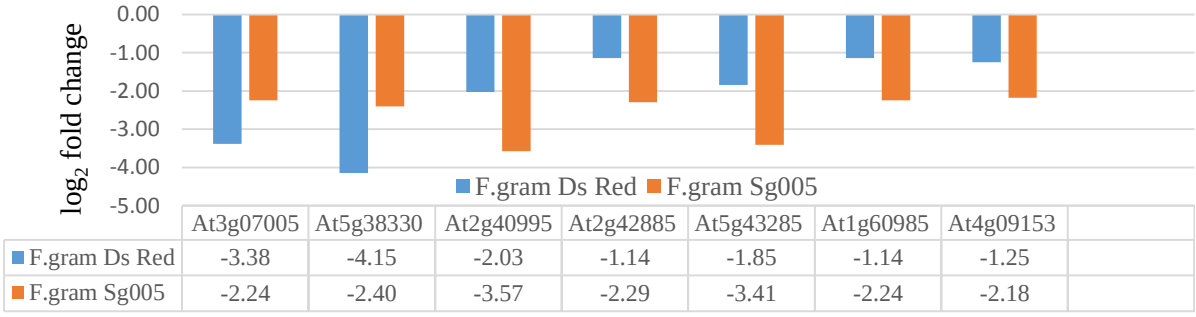

Figure 34:Similar expression patterns and log2 fold change of candidate genes were observed while comparing the two different *F. graminearum* strains used during the infection of pistil.

Log_2 fold change data of *F. graminearum Ds red which* were used in infecting pistil for qPCR analysis were compared with *F. graminearum* Sg007 which was used in infecting pistil for RNAseq. The log_2 fold change of all seven candidate genes during infection with *F. graminearum Ds red* were in similar range as in infection with *F. graminearum* Sg007.

This confirms that DEFL genes response towards different *F. graminearum* strains is alike and downregulation of these candidates is a common response towards *Fusarium* pistil infection in *A. thaliana.*

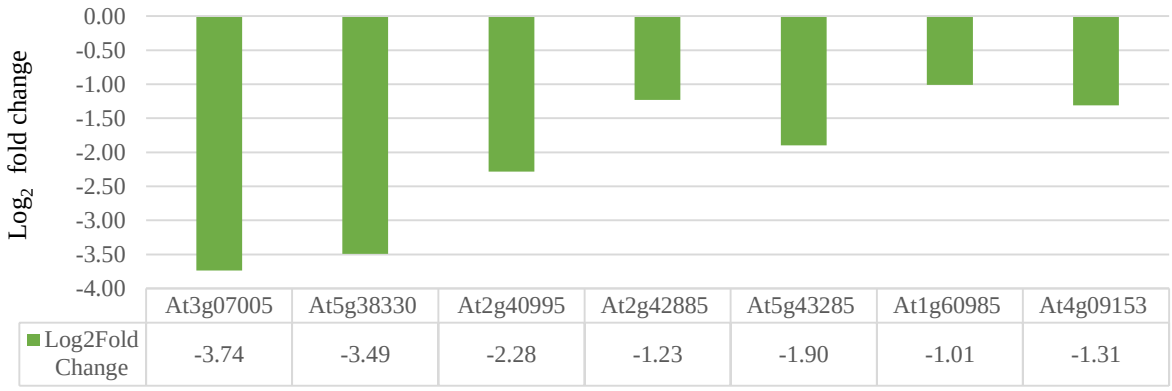

Figure 35:Log_2 fold change of candidate DEFL genes between 4DAE and 3DAI indicates that the age of the pistil has no effect on *F. gramainearum* infection.
Log_2 fold change which represent the differential expression of candidate gene during infection for the candidate gene was calculated from the average CNRQ values of 4DAE and 3DAI genes. All the seven candidate genes had Log_2 fold change of ≤ -1

Similarly, the average CNRQ values of 3DAI were compared with 4DAE in order to observe if there is an effect with the age of the emasculated pistil. The log_2 fold change was calculated between the expression of 4DAE and 3DAI. At3g07005 has the highest log_2 two-fold change of –3.74 and the least was At1g60985 with -1.14 (Figure 35). All the genes had an equivalent range of the log_2 fold change similar to 2DAE (Figure 35). Because the expression patterns of 3DAI with 4DAE are similar to 2DAE, this result endorses that the age of the emasculated pistil does not affect the expression pattern of defensins during *F. graminearum* infection. Thus, downregulation expression observed in the candidate gene is primarily due to the effect of fungal infection.

In order to assess if the treatments caused statistically significant differences in the levels of candidate gene expression the average CNRQ values of seven candidate genes were taken as single datasets for each of the six conditions divided in two datasets of pistils with the same age: the "two-day dataset" contains the data of 2DAE,1DAT,1DAI and the "four-day dataset" is comprised of the data from 4DAE, 3DAT, 3DAI. Each dataset has 21 data points comprising of seven candidate genes with three data points. This grouping of the data was preferred because the analysis of individual candidates would involve the results from three biological replicates for each condition, thus making statistical analysis unreliable. Comparison of averages shows that 1DAT and 2DAE had the same average CNRQ value of -1.09, and in the case of 4DAE and 3DAT, the average CNRQ values were almost identical,

suggesting that the mock treatment and the emasculation control are not different from each other (Figure 36).

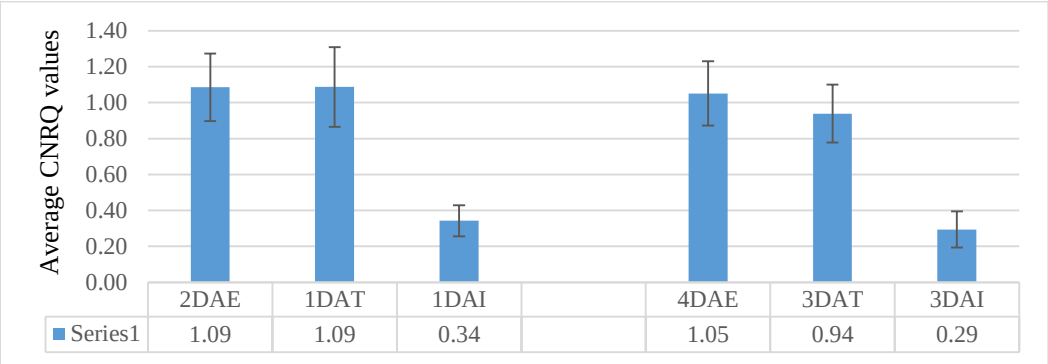

Figure 36:Comparison of the effects of emasculation, mock treatment and infection in DEFLs gene expression suggest that mock treatment do not significantly differ from the control and downregulation in DEFLs was due to infection.

Average CNRQ values of emasculation, mock treatment and infection for seven candidate genes were taken as single datasets. Infection was statistically significant in comparisons to mock treatment or the emasculation control more details in (Table 11). The error bar represents standard error.

This data is supported by statistical analysis (Table 9). One-way ANOVA was performed between the three conditions for the "two-day dataset" and the "four-day dataset" individually. The levels of expression between infection and both control treatments are statistically different (Table 9). Each individual condition was cross-checked with each other individually using t-Tests in order to see which condition was responsible for this difference (Table 9). The only statistically significant comparisons were those involving infection and mock treatment or the emasculation control. This was also verified by using the Bonferroni correction ($p < 0.0167$). This proves that the effects of the mock treatment do not significantly differ from the control and significant downregulation in gene expression pattern was primarily due to infection.

Table 9:Statistical significance of the pairwise comparisons of expression levels of DEFLs in control and infected pistils

Condition 1	Condition 2	P-value < 0.0167, t-Test	P-value < 0.05. One-way ANOVA
2DAE	1DAT	0.99593	0.002275
2DAE	1DAI	0.00023	
1DAT	1DAI	0.00439	
4DAE	3DAT	0.56514	0.00001
4DAE	3DAI	0.00006	
3DAT	3DAI	0.00004	

5.5. Expression of DEFL candidate gene during double fertilization.

Candidate defensin genes At3g07005, At4g09153, At2g42885, At2g20070, At5g38330, At5g43285, At1g60985 and At2g40995 which were found to be expressing in the embryo sac were also studied for expression pattern during pre-fertilization and post fertilization events. Two approaches were taken to analyze the expression pattern of genes during fertilization: quantification of GFP signal and qPCR analysis. At5g38330, At5g43285, At1g60985 and At2g40995 were investigated by Kriss Spalvins for his Master thesis under my supervision and the results will be discussed. The quantification of GFP signal was done using the previously described marker lines containing the putative promoter of the candidate cloned next to a nuclear localization signal and consecutive triplicate GFP genes.

5.5.1 Quantification of GFP signal

The GFP signal under the control of the promoters for At3g07005, At4g09153, At2g42885 and At2g20070 genes were outlined in Table 8. For the quantification of GFP signal of each candidate, pictures of individual ovules were taken in two independent marker lines. The time points that were taken for the analysis were non-pollinated and 8, 24 and 48 hours after pollination (HAP). The quantified GFP signals of these time points were compared with the values measured in non-pollinated ovules.

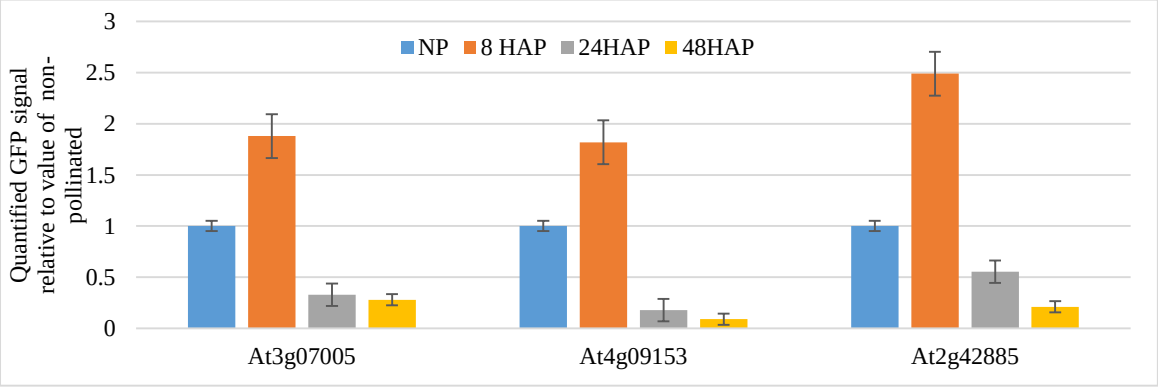

Figure 37:Quantification of GFP signal in the central cell of candidate genes At3g07005, At4g09153 and At2g42885 at different time points after pollination suggests the candidate genes may have a role during fertilization.

GFP signal of the central cell nucleus of marker lines with NLS-3xeGFP under the control of the putative promoters of At3g07005, At4g09153 and At2g42885 was quantified at different time points after pollination. The three candidate genes had an increase of GFP signal at 8HAP followed by decrease of GFP signal in subsequent time points. Columns represent the mean of the measured signal in ten ovules, error bars represent the standard error of the data set. NP=Non-pollinated, HAP=Hours after pollination.

Promoter analysis in Table 10 showed that candidate genes At3g07005, At4g09153 and At2g42885 were expressed in the central cell nucleus of the ovule. For all of them, there is a visible increase of the GFP signal 8 HAP (Figure 37), suggesting these genes might be involved in fertilization related events in the ovule. The central cell undergoes synchronous

nuclear division after fertilization, during this period the GFP signal decreases relative to the values measured at 8HAP and continues until it reaches its minimum at 48HAP (Figure 37) when endosperm nuclei divides to 16 endosperm nuclei.

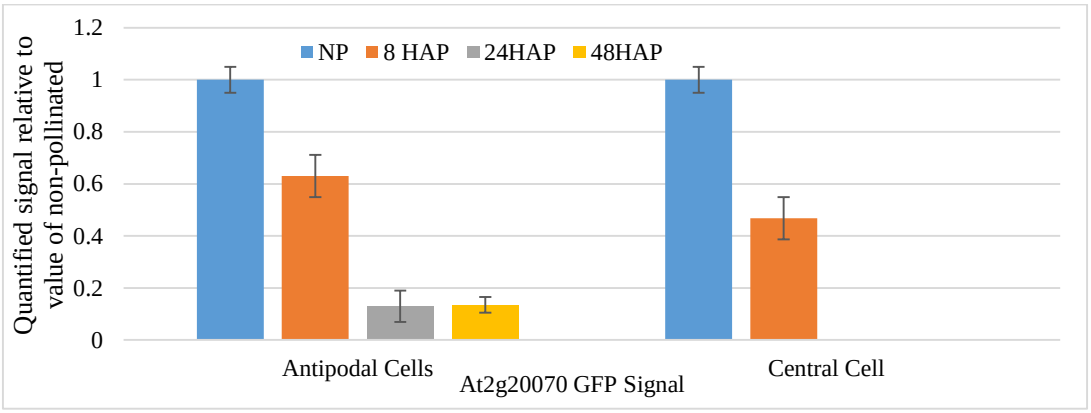

Figure 38:Quantification of GFP signal in antipodal cells and central cell of At2g20070 at different time points after pollination suggests the At2g20070 may have a role in pre-fertilization events.
GFP signal in the antipodal cells and central cell of marker lines with NLS-3xeGFP under the control of the putative promoters of At2g20070 was quantified at different time points after pollination. Antipodal cell and central cell of At2g20070 had decrease of GFP signal from NP timepoint. Columns represent the mean of the measured signal in ten ovules, error bars represent the standard error of the data set. NP=Non-pollinated, HAP=Hours after pollination.

The promoter analysis of At2g20070 indicates it was expressed in the antipodal cells and in the central cell of the ovule (Table 8). The analysis of GFP signal indicates a decreasing trend observed at 8HAP in both kinds of cells (Figure 38). The downregulation of GFP signal continues in antipodal cells during later stages of endosperm development. In the case of the central cell, At2g20070 is not expressed during endosperm development at 24HAP and 48HAP (Figure 38). This data suggests At2g20070 may have a role in pre-fertilization events. The decreasing signal in the antipodal cells is possibly due to the fact after fertilization they undergo cell death.

This study relies on the expression of gene promoter not the gene itself. This might not be very descriptive of the characteristics of the actual genes in question, but is a good starting point for investigating its pattern of expression before, during and after fertilization.

5.5.2 qPCR assay for pollination

qPCR assays were the second method used for checking the expression of candidate genes in pistils at different time points after pollination. The use of a second technical approach aims to determine if the data from GFP signal quantification corresponds with the data acquired from qPCR. The time points that were taken for this analysis were non-pollinated, 8, 24, 48, 80, 96 hours after pollination. Two biological replicates were used in these qPCR assays. The

At2g42885 and At4g09153 genes were excluded from this study due to non-specificity of the primers employed.

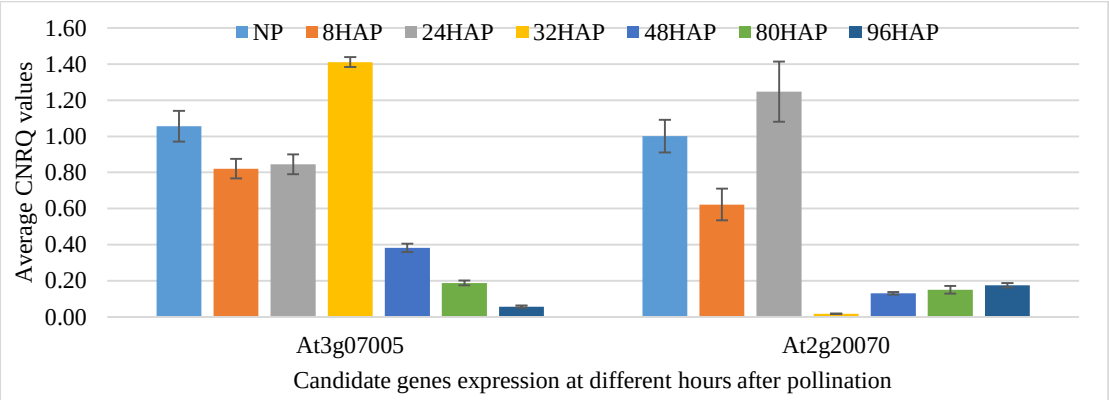

Figure 39:Average CNRQ values of candidate genes At3g07005 and At2g20070 during different time points after pollination indicates that At3g07005 and At2g20070 genes have role in early endosperm development.

Data obtained from qPCR analysis of At3g07005 and At2g20070 genes at different time points after pollination. At3g07005 had highest peak expression at32HAP and followed by downregulation, whereas, At2g20070 had highest peak expression in 24HAP and followed by downregulation. Each column represents average CNRQs values of three technical replicates for each of two biological replicates at different time points after pollination. Error bars represent the standard error.

Average CNRQ values of At3g07005 gene follow a decreasing pattern of expression from non-pollinated to 24HAP and increase at 32HAP (Figure 39). After the peak expression at 32HAP, only to decrease again during the course of remaining time points (Figure 39). In the case of At2g20070, average CNRQ values decrease from non-pollinated to 8HAP and followed by highest expression at 24HAP (Figure 39). After peaking at 24HAP, the value is almost zero at 32HAP (Figure 39) and continues being downregulated over the course of the remaining time points relative to the value measured in non-pollinated pistils.

5.5.3 Comparison of biological replicates used for qPCR

The variation of CNRQ values between the two biological replicates of At3g07005 was measured. In general, replicate A had a higher expression value of CNRQ compared with replicate B (Figure 40). The expression pattern of replicate A had a linear downward pattern of expression from non-pollinated to 96HAP whereas the replicate B had a bell-curved expression pattern with the peak at 32HAP (Figure 40).

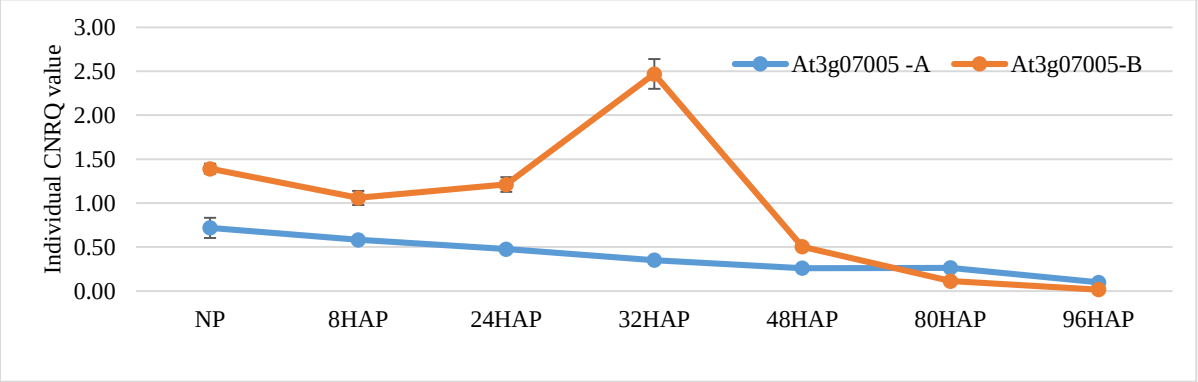

Figure 40:Different trends of CNRQ expression were observed while comparing two biological replicates for At3g07005 at different time points after pollination.

CNRQ values of individual replicates (each based on two technical replicates) were compared with each other using different time points after pollination for At3g07005 gene. Blue line represents At3g07005 replicate A and orange line represents At3g07005 replicate B. Both replicates had opposite trends with each other at certain timepoints. Error bars represent the standard error of two technical replicates.

In the case of gene At2g20070, there was not much variation of CNRQ values between the two biological replicates. The expression pattern and expression values of At2g20070 replicate A and At2g20070 replicate B were similar to each other (Figure 41). From the above data, it was clear that the variation between replicates was specific for each gene.

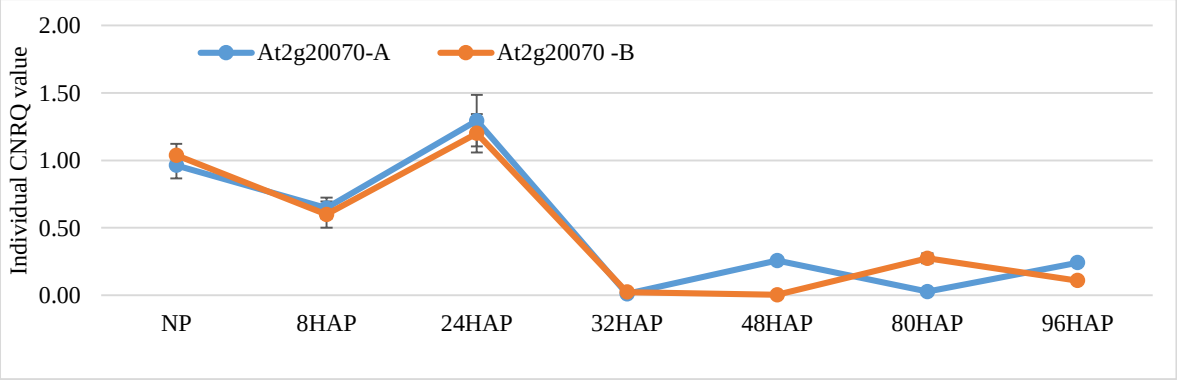

Figure 41:Similar expression trend of CNRQ values were observed while comparing the two replicates for At2g20070 at different time points after pollination.

CNRQ values of individual replicates were compared with each other using different time points after pollination for At2g20070 gene. Blue line represents At2g20070 replicate A and orange line represents At2g20070 replicate B. Both replicates had similar trend during different time points. Error bars represent the standard error of two technical replicates.

When comparing the result of qPCR with GFP signal quantification of At3g07005 and At2g20070 genes we can observe variations in their patterns of expression. These variations are possibly due to the fact that the whole pistils rather than the dissected ovules were employed in qPCR studies. The ovules within the pistils are not at one specific developmental stage thus affecting the homogeneity of the samples used for the assays.

5.6 Examining the effect of *Fusarium graminearum* in double fertilization

In the previous two chapters, we observed the expression of candidate genes during infection and during fertilization events. Next we investigated the candidate DEFL gene expression during pollination followed by fungal infection in order to observe how this process affects fertilization as ultimately reflected on gene expression of the candidates and seed set. A qPCR approach was used to evaluate the expression of candidate DEFL gene during pollination followed by infection. Time points 8HAP and 24HAP were chosen to follow up pollination events, which were followed by inoculation with *F. graminearum* and incubation on a moist chamber for one or three days. Two controls were employed: a mock treatment where pollinated pistils inoculated with water were incubated in a moist chamber, while the second control are pistils that are only pollinated and left untreated for the same amount of time the experimental samples were incubated with *Fusarium*. Six candidate genes: At3g07005, At2g42885, At5g38330, At5g43285, At1g60985 and At2g40995 were selected for this study. At5g38330, At5g43285, At1g60985 and At2g40995 were investigated by Kriss Spalvins for his Master thesis under my supervision.

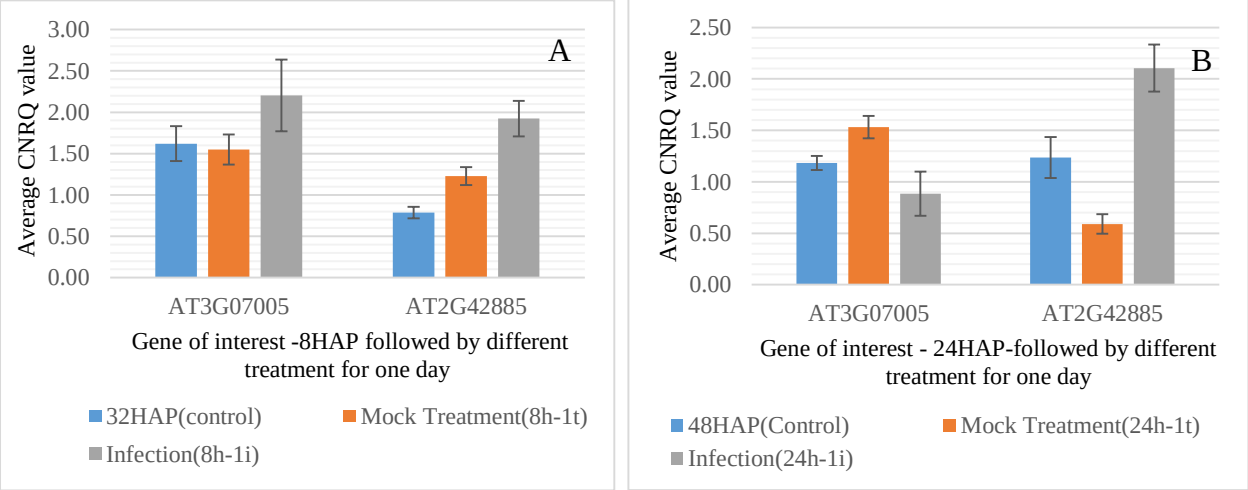

Figure 42:Average CNRQ values of candidates At3g07005 and At2gs42885 at either 8HAP or 24 HAP followed by infection or control treatments lasting one day suggests no common trend of expression between candidate genes.

Average CNRQ values of control (blue column), mock treatment (orange column) and infection (grey column) for At3g07005, At2g42885 (A) 8HAP followed by one day of different treatment or during (B) 24 HAP followed by one day of treatment. The 8h-1t sample denotes 8 hours after pollination followed by mock treatment for one day, 8h-1i sample denotes 8hours after pollination followed by inoculation with *F. graminearum* for one day. There was no common trend between At3g07005 and At2g42885 in pollination followed by different treatment for one day. Error bars represent the standard error of two biological replicates, each represented by three technical replicates.

At 8HAP followed by one day of treatment, the average CNRQ values for At3g07005 and At2g42885 of infected pistils were upregulated when compared with the 32HAP control and the mock treatment, (Figure 42A and B). In the case of 24HAP followed by one day of

treatment, At3g07005 was not different from the controls and At2g42885 was still expressed at a higher level (Figure 42A and B).

The results of At5g38330, At5g43285, At1g60985 and At2g40995 obtained by Kriss Spalvins for his Masters Thesis were included again here for further analysis together with those of At3g07005 and At2g42885.

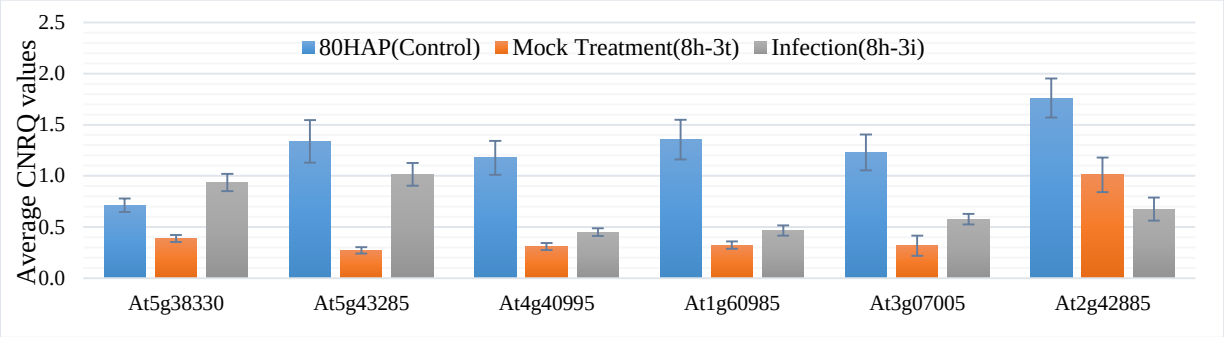

Figure 43:Average CNRQ values of candidate DEFLs 8 HAP followed by infection or control treatments lasting three days indicates that candidate genes are downregulated in mock treatmed and infection treated samples in comparison to control.

Average CNRQ values of control (blue column), mock treatment (orange column) and infection (grey column) for At5g38330, At5g43285, At4g40095, At1g60985, At3g07005 and At2g42885 during 24HAP followed by three days of different treatment. 80HAP sample denotes 80 hours after pollination, 8h-3t sample denotes 8 hours after pollination followed by mock treatment for three days, 8h-3i sample denotes 8 hours after pollination followed by incubation with *F. graminearum* for three days. Expression of mock treatment and infection of six candidate genes were downregulated in comparison to 80HAP control. Error bars represent the standard error of two biological replicates, each represented by three technical replicates.

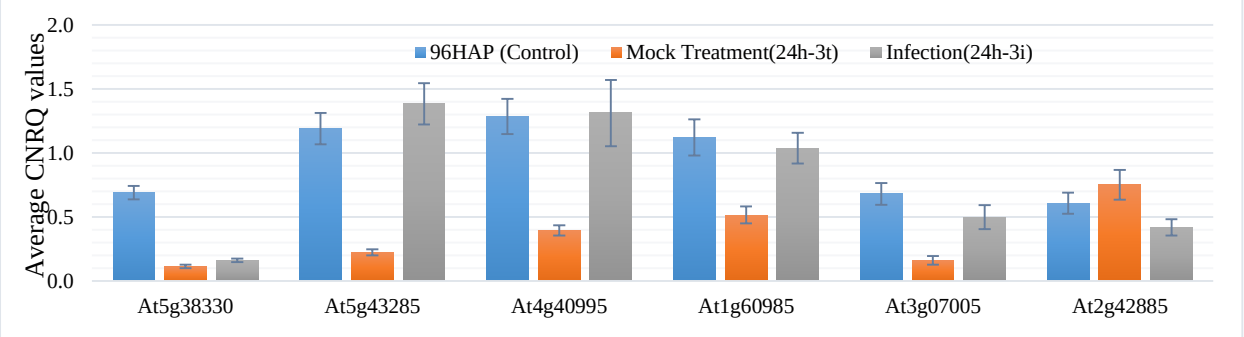

Figure 44:Average CNRQ values of candidate DEFLs 24 HAP followed by infection or control treatments lasting three days suggests that candidate genes have no common pattern of expression in the mock treatment and infection in comparison to control.

Average CNRQ values of control (blue column), mock treatment (orange column) and infection (grey column) for At5g38330, At5g43285, At4g40095, At1g60985, At3g07005 and At2g42885 during 24HAP followed by three days of different treatments. 96HAP sample denotes 96 hours after pollination, 24h-3t sample denotes 24 hours after pollination followed by mock treatment for three days, 24h-3i sample denotes of 24hours after pollination followed by inoculation with *F. graminearum*. Expression of mock treatment and infection of six candidate genes were downregulated in comparison to 96HAP control. Error bars represent the standard error of two biological replicates, each represented by three technical replicates

When the infection or mock treatments were prolonged for three days all 6 gene of interest (GOIs) are downregulated in the mock treatment compared to the control at 80HAP (Figure 43). A similar pattern of expression was found in mock treatment when compared to the

96HAP control in all genes except in At2g42885 (Figure 44). The downregulation of the mock treatment at 8HAP and 24HAP followed by three days of incubation in a moist chamber, indicates that treatment might have some effect in endosperm developmental stages. Three days of incubation with *Fusarium* upregulated expression at different levels when compared with mock treatment at 8HAP and 24HAP in five GOIs except in At2g42885 (in both 8HAP and 24 HAP) and At5g38330 in 24HAP (Figures 43 and 44). Infection has no specific trend of expression pattern when compared with the 80HAP control and 96HAP control. These patterns of expression indicate that the effect of pollination and infection on expression of the candidate genes cannot be generalized with a specific trend as it was done in infection studies.

5.6.1 *F. graminearum* effect on development of seeds

Seed set data was gathered in order to find out how double fertilization is affected by infection. It also helps to understand the overall effects of various treatments on double fertilization.

5.6.1.1 Seed set development during pollination followed by infection

The aims of these experiments were to test if different days of incubation with *F. graminearum* have an effect on seed set development and if the time point of inoculation has an effect on seed set development. To this aim, incubation with *F. graminearum* for one, two and three days was performed after 8HAP and 24HAP.

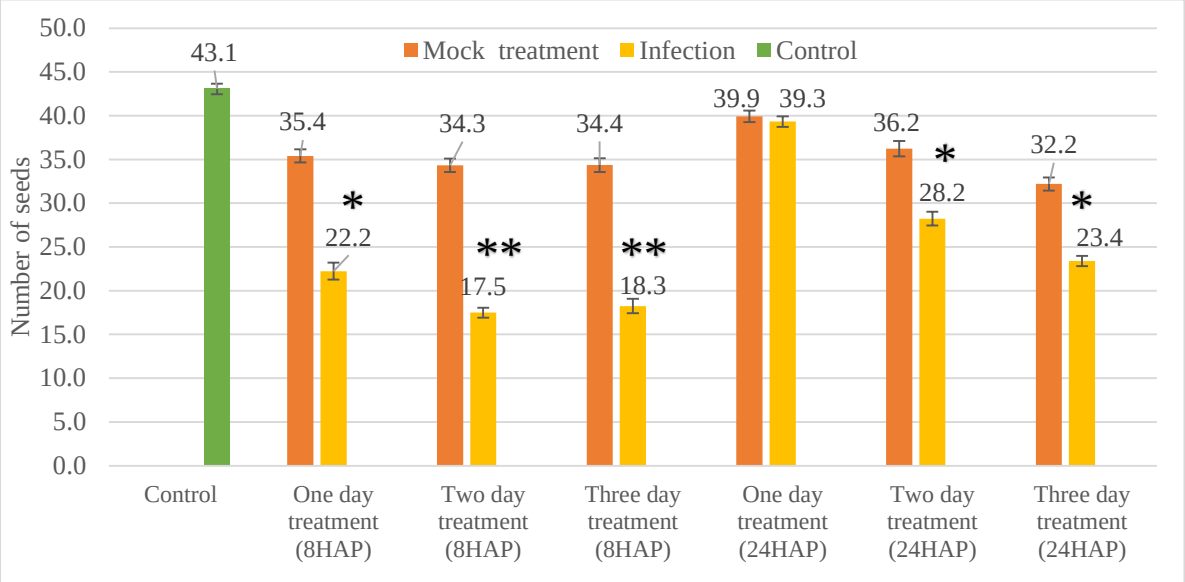

Figure 45:Comparison of seed set data for pollination followed by different treatments indicate that *F. graminearum* infection has severe effect on 8HAP pistil in comparison to 24HAP.

Blue columns represent the mean seed count obtained from pollinated pistil without any treatment. Orange columns represent mean seed count obtained from pollinated pistil for certain time points (8HAP or 24HAP) followed by mock treatment for different days. Grey columns represent mean seed count obtained from pollinated pistil for certain time points (8HAP or 24HAP) followed by *F. graminearum* infection for different days. Error bars represent the standard error. ***-** statistically significant reduction on seed set caused by infection when compared with control and mock treatment. (p value < 0.001, t-test), ****** -statistically significant of infection when compared with control and mock treatment. (p value < 0.001, t-test). 15 siliques for each condition was taken.

Seed set control for pollination-infection experiments was one day after emasculation (1DAE), while the mock treatment had the aim of investigating its effect in seed set. 8HAP and 24HAP pistils were inoculated with *F. graminearum* for one, two and three days. The number of seed developed after mock treatment were not much different than the control in all condition (Figure 45). This indicates that mock treatment and control are not statistically different from each other (p value < 0.001). This was also verified by using the Bonferroni correction ($p < 0.0003$). In the case of 8HAP followed by one, two or three days of mock treatment or incubation with *Fusarium*, the average seed set of infected pistils was statistically significantly lower when compared with the controls (Figure 45). In the case of 24HAP followed by one day of mock treatment or incubation with *Fusarium*, the average seed set of infection (n= 39) and of mock treatment (n=40) was not statistically different from the control (n=43) (Figure 45). In general, infected siliques had a decrease in seed count when compared to the siliques of the control and mock treatment. As the days of inoculation increased from one day to three days, the seed set number decreased irrespective of time of inoculation. Specifically, the seed set obtained after two or three days of infection is significantly lower to that of the controls regardless of whether infection took place 8HAP or

24HAP (Figure 45). Significant differences of 20%- 50% in seed set showed that the chances for an ovule to be fertilized and proceed to seed development are higher if infection takes place 24HAP than if plants are infected 8HAP (Figure 45).

Examples of siliques containing seed set of different pollination time points followed by three days of treatment is shown in Figure 46. The silique of different pollination time points followed by one and two days of treatment is found in appendix section 9.9.1. The previous results also indicate that infection with *F. graminearum* affects development of seed set while the mock treatment has no effect on seed set.

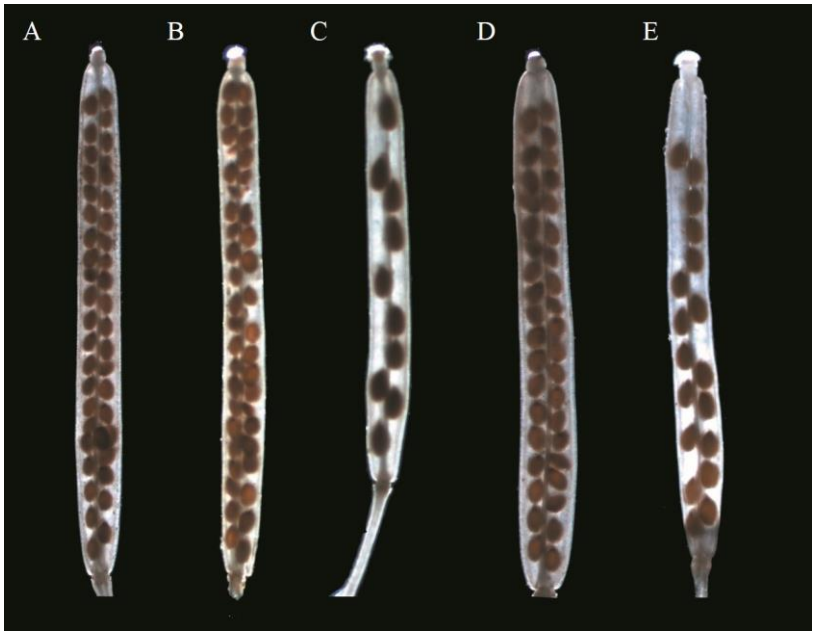

Figure 46:Comparison of seed set data for pollination followed by different treatments indicate that F. graminearum infection has severe effect on 8HAP pistil in comparison to 24HAP.

A) Control: silique resulting from one day of emasculation and followed by pollination B) 8HAP-3DAT: silique resulting from 8HAP followed by three days of mock treatment C) 8HAP-3DAI: silique resulting from 8HAP followed by three days of *F. graminearum* infection. D) 24HAP-3DAT: silique resulting from 24HAP followed by three days of mock treatment E) 24HAP-3DAI: silique resulting from 24HAP followed by three days of *F. graminearum* infection.

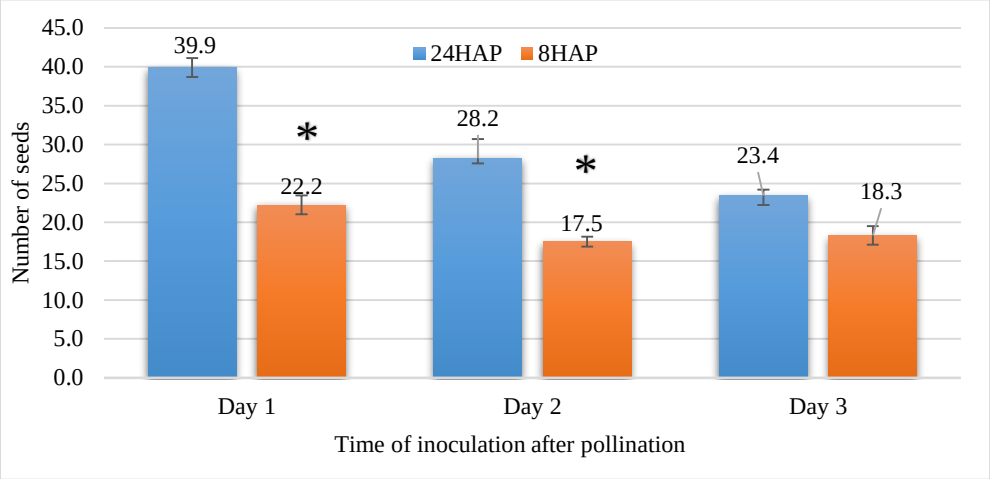

Figure 47:Comparison of infected seed set data at different pollination time points in one days, two days and three days indicates that three days of infection has severe effect in seed set formation irrespective of pollination time point.
Blue columns represent the mean seed count for 24HAP followed by infection. Orange columns represent the mean seed count for 24HAP followed by infection. Error bars represent the standard error. ***-** statistically significant of 8HAP infection when compared with 24HAP (p value < 0.001, t-test). For the sake of comparison this figure re-arranges the data already presented in Figure 45.

The data in Figure 45 was rearranged to compare the infected seed set data based on different pollination time points (Figure 47). Inoculated siliques of 24HAP have more seeds than 8HAP regardless of the length of incubation with *Fusarium* (Figure 47). After one day and two days of infection, seed number of 8HAP was statistically significant when compared with 24HAP (Figure 47). After three days of inoculation, the average number of seeds of 8HAP are not statistically different from 24HAP (Figure 47). This indicates that inoculation with *F. graminearum* for three days is more virulent and reduces the number of seed developed. In general, this data also indicates that inoculation after 24HAP resulted in a higher seed set than 8HAP (Figure 47). This could be explained because there is more chance for the ovule to be fertilized and proceed in seed development before fungal inoculation.

5.6.1.2 Seed set development during infection followed by pollination

To see the effect of inoculation before pollination in silique development, pistils were emasculated and incubated with *F. graminearum* for one and three days. This was followed by pollination.

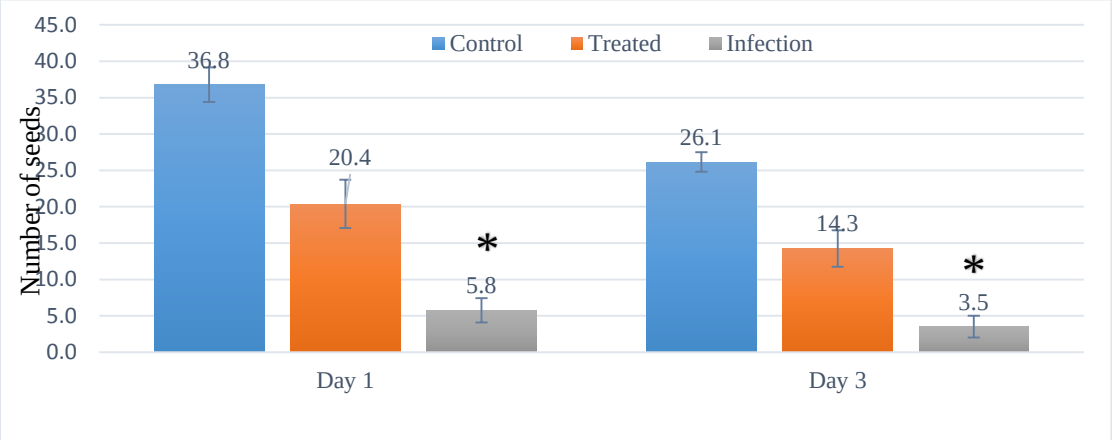

Figure 48:Comparison of seed set data for different treatment before pollination for one day and three days signifies that infection has drastic effect on seed development.
Blue columns represent the mean seed count obtained emasculated pistil followed by pollination. Orange columns represent the mean seed count obtained from different days (1 day or 3 day) of mock treatment followed by pollination. Grey columns represent the mean seed count obtained from different days (1 Day or 3 Day) of *F. graminearum* infection followed by pollination. Infected treated samples had less number of seeds developed in comparison to control and mock treatment.15 siliques for each condition was taken. Error bar represent the standard error. ***-** statistically significant of infection when compared with control. ($p < 0.001$, t-test)

In this study, both mock and infection treatments show decrease in average seed count (Figure 48). The control for one-day treatment were pistils pollinated two days after emasculation, similarly pistils pollinated four days after emasculation were employed as controls for the three days treated pistils. In both infection treatments, the seed count obtained from infected pistils is significantly lower than the control (Figure 48). At both days of inoculation, seed set in infected samples was significantly lower when compared with the control. Mock treatment also has decreased seed set (Figure 48), This indicates that the mock treatment causes severe stress to the pistils and this is reflected on lower seed set development.

Example of silique during 3DAI infected pistil followed by pollination compared with two controls is reported in Figure 49. Image of silique during 1DAI infected pistil followed by pollination compared with two controls is found in appendix section 9.9.2.

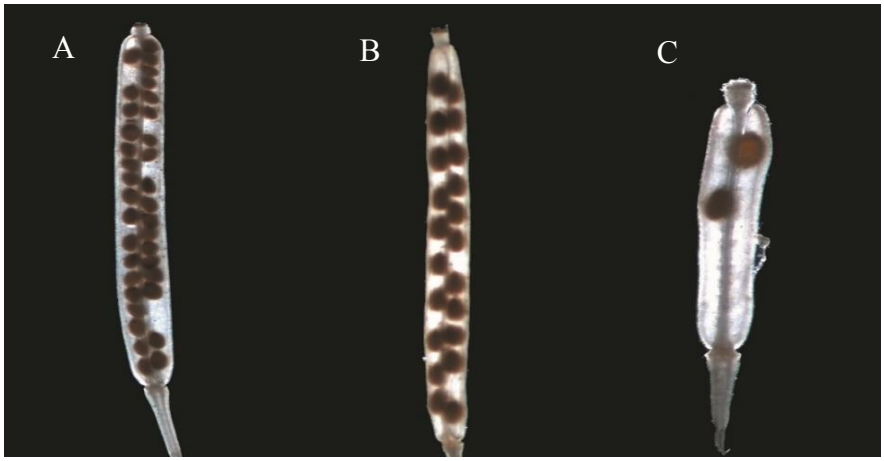

Figure 49:Comparison of silique of 3 DAI followed by pollination with two controls.
A) Control -Silique resulting four days after emasculation followed by pollinated B) Mock treated control - Silique resulting from three day of mock treatment with water followed by pollination after. C) Silique resulting from 3DAI followed by pollination.

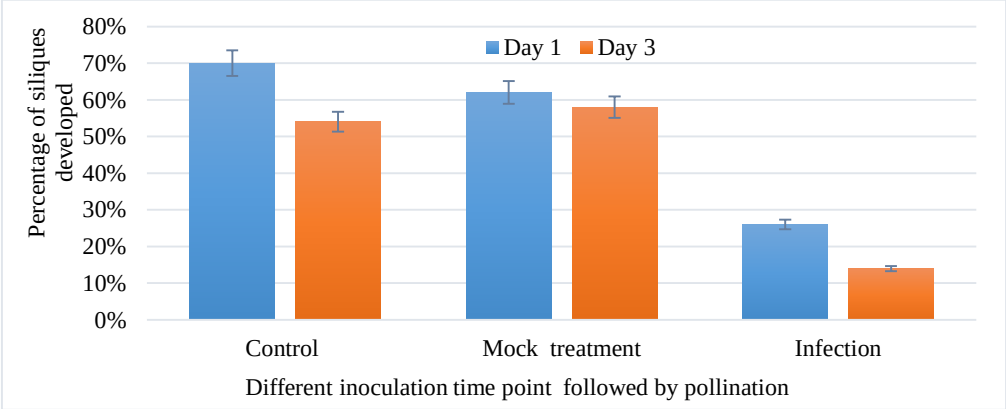

Figure 50:Percentage of silique developed during different treatments followed by pollination indicate that the infected pistils followed by pollination had fewer chance in developing into silique.
Columns represent the percentage of siliques developed from treatment followed by pollination from ca 15 pistils. Blue column represents day 1 after inoculation followed by inoculation, orange column denotes three days after inoculation followed by pollination. The percentage of silique developed after infection was lesser in comparison to control and mock treatment. Error bars represent the standard error.

Only 25% of siliques developed seed after one day of incubation with *F. graminearum*, while 10% of siliques developed seed after three days of infection (Figure 50). In control and mock treatment nearly 50% to 70% of siliques developed (Figure 50), which is a difference from 40-50% measured in infected plants. Specifically, the siliques surviving infection have less seeds after one day of treatment (n=6) and even lesser (n=3) after three days of incubation with the *F. graminearum* (Figure 48). This suggests that in the event of infection before pollination, seed number is drastically reduced when compared with pollination followed by infection (Table 10). This is also suggesting that the process of double fertilization is sensitive to fungal attack since the amount of seed set developed in infection followed by

pollination was less than other treatments investigated. This data suggests that in the event of infection followed by pollination, pollen tube growth could be severely affected by fungal hyphae growing on the stigma of the pistil.

Table 10:Average seed set in two experimental conditions

Average seed set during pollination followed by infection	Average seed set during infection followed by pollination
26	5

5.7 Correlation between patterns of expression of individual candidates

A correlation analysis of the patterns of expression measured by qPCR was performed in order to test if particular genes have similar responses to the different treatments employed. The results from this analysis would suggest that genes could be co-regulated with each other in the tissues and conditions where they are co-expressed (e.g. in the ovule). Correlation coefficients were calculated using the average CNRQ values obtained from characterizing the patterns of expression after pollination, infection and during infection after pollination (Example given in Figure 51). When comparing the patterns of expression between multiple genes, correlation coefficients with ≥ 0.80 were considered noteworthy. Data of At4g09153 and At2g20070 were not considered for the analysis of pollination followed by infection due to technical variations. Similarly, data of At4g09153 gene and At2g42885 gene were not included in pollination analysis.

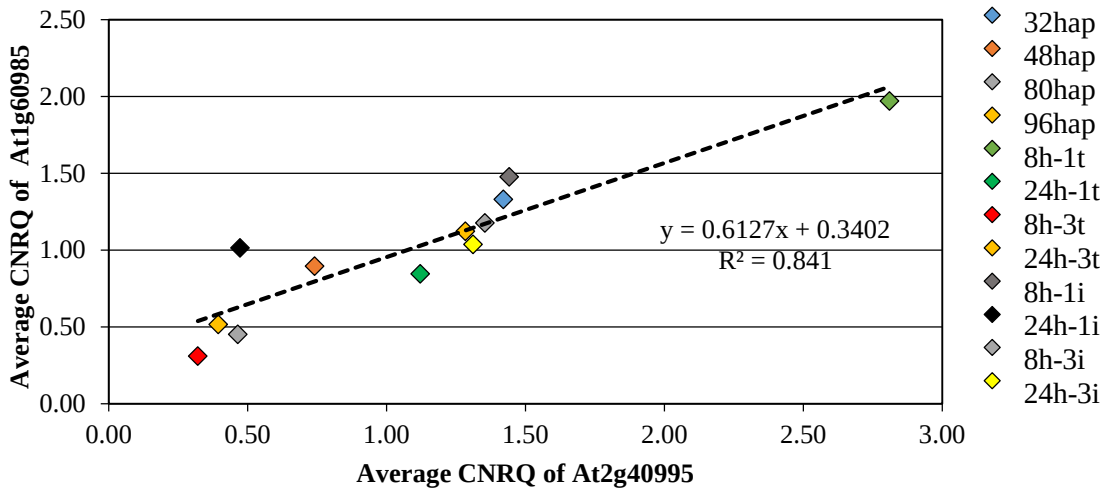

Figure 51:Positive correlation coefficient between the levels of relative expression of At2g40995-At1g60985 during pollination followed by infection

Average CNRQ values of control, mock treatment and infection for At1g60985 gene were compared with average CNRQ values of At2g40995 gene during pollination followed by infection for correlation coefficient. The pearson correlation coefficient of At2g40995-At1g60985 during pollination followed by infection was 0.841.

Table 11 represents all the gene pairs that have correlational coefficient of > 0.80, the remaining gene pairs are found in appendix section 9.10. At2g40995-At3g07005, At3g07005-At5g38330 and At2g40995-At5g43285 were found to have correlation coefficient ≥ 0.80 in all the three conditions (Table 13). Gene comparison pairs of At2g40995-At1g60985, At2g40995-At5g38330 and At3g07005-At5g43285 were found to have a correlation coefficient of ≥ 0.80 in two out of three conditions and in other conditions

they were found to have a correlation coefficient close to the range. The comparison of genes pairs At5g38330-At1g60985, At5g38330-At5g43285, At5g43285-At2g20070 and At3g07005-At2g20070 were specifically found to have a correlation coefficient of ≥ 0.80 in the pollination dataset while At2g40995-At2g42885, At3g07005-At2g42885, At2g40995-At4g09153, At1g60985-At4g09153, At2G42885-At4g09153 gene pairs are correlated in the infection dataset (Table 11). All but one gene pair had at least one gene expressed in central cell.

Table 11:Pairwise correlation coefficient of relative gene expression using the average CNRQ values during different conditions.

Genes grouped according to correlation > 0.8	Comparison	Expression in planta*	Pollination-infection	Pollination	Infection
Correlated in all datasets tested	At2g40995-At3g07005	Central cell – Central cell	0.83	0.93	0.86
	At3g07005-At5g38330	Central cell – Central cell	0.82	0.81	0.88
	At2g40995-At5g43285	Central cell – synergids	0.80	0.91	0.93
Correlated at least in two datasets	At2g40995-At1g60985	Central cell – Central cell	0.92	0.70	0.83
	At2g40995-At5g38330	Central cell – Central cell	0.74	0.89	0.83
	At3g07005-At5g43285	Central cell – synergids	0.80	0.91	0.74
Correlated only in the pollination dataset	At5g38330-At1g60985	Central cell – Central cell	0.73	0.93	0.60
	At5g38330-At5g43285	Central cell – Central cell	0.76	0.88	0.67
	At5g43285-At2g20070	Synergids – Antipodal cells	N. A	0.91	-0.26
	At3g07005-At2g20070	Central cell – Central cell	N. A	0.86	-0.13
Correlated only in the infection dataset	At2g40995-At2g42885	Central cell – Central cell	0.45	N. A.	0.81
	At3g07005-At2g42885	Central cell – Central cell	0.31	N. A.	0.86
	At2g40995-At4g09153	Central cell – Central cell	N. A.	N. A.	0.81
	At1g60985-At4g09153	Central cell – Central cell	N. A.	N. A.	0.94
	At2g42885-At4g09153	Central cell – Central cell	N. A.	N. A.	0.82

*according to the results of the marker line analyses described in table 10.

The 15 gene pairs with correlation coefficients ≥ 0.80 from table 13 were further cross checked with 10 RPKM values for each obtained from RNAseq. Specifically, two RPKM values corresponding to two biological replicates of each expression in *A. thaliana* non-pollinated pistils, *A. thaliana* selfed pistils, *A. thaliana* pollinated with *A. lyrata*, *A. thaliana*

pollinated with *A. halleri* and *A. thaliana* infected pistils for each gene were selected for correlation analysis. Majority of the gene pairs (n=11) were identified to have correlation coefficients ≥ 0.80 using RPKM values (Table 12), and were similar in comparison to correlation coefficients obtained using the average CNRQ values (Table 11). These correlation coefficients obtained from independently obtained RPKM values further validates that the DEFL genes may co-regulate with each other during the pollination or infection process in the ovule.

Table 12:Pairwise correlation coefficient of relative gene expression using the RPKM values

Comparison	Correlation coefficients
At2g40995-At3g07005	0.90
At3g07005-At5g38330	0.73
At2g40995-At5g43285	0.82
At2g40995-At1g60985	0.88
At2g40995-At5g38330	0.82
At3g07005-At5g43285	0.96
At5g38330-At1g60985	0.95
At5g38330-At5g43285	0.67
At5g43285-At2g20070	0.87
At3g07005-At2g20070	0.77
At2g40995-At2g42885	0.81
At3g07005-At2g42885	0.74
At2g40995-At4g09153	0.94
At1g60985-At4g09153	0.84
At2g42885-At4g09153	0.84

5.8 Effect of *Fusarium graminearum* infection during early stages of seed development

This experiment was done under my supervision by Kriss Spalvins for his Master Thesis. The aim of the study was to understand the effects of infection on early seed development. This study was motivated by the observation of severe tissue degradation, possibly PCD, in ovules infected with *F. graminearum*. The experiment was done with the central cell marker line pAt1g60985:NLS-(3x)eGFP-18 which has GFP expression until 96HAP (Figure 52). 8HAP and 24HAP followed by one and two days of infection or mock treatment, were compared with their respective controls 32HAP, 56HAP, 48HAP and 72HAP. Specifically, the following stages of central cell/endosperm nuclei in the dissected pistil were classified according to the appearance these structures normally have in healthy pistils at different points before and after pollination, the occurrence of these different stages in a given treatment was documented as counts: degraded, 0/8HAP, 24HAP, 48HAP, 72HAP (Figure 52). Ovules that did not undergo any degradation were counted as developed. Ovules are classified as degraded if the morphology of the ovule are either smaller in size along with collapse of embryo sac tissue or disintegration of outer and inner integuments and lack of GFP signal (Figure 52).

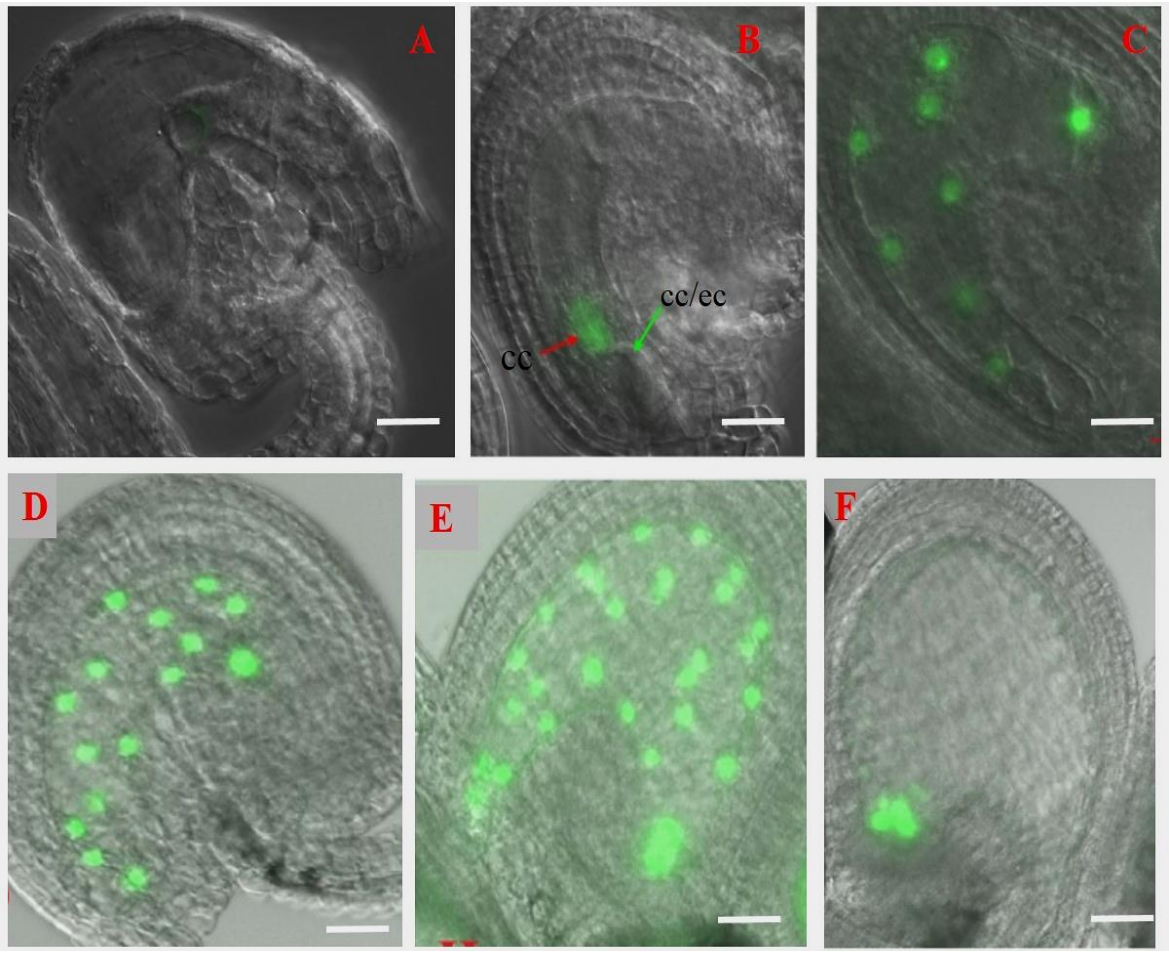

Figure 52:Classification of different ovule stages for endosperm developmental studies using the marker line A. thaliana pAt1g60985:NLS-(3x)eGFP-18.
(A) An example of degraded ovule. (B) 0h/8h ovule is denoted with single central cell nucleus (red arrow) and egg cell/central cell boundary (green arrow). (C) A 24HAP ovule is classified as such if it shows 8 endosperm nuclei. (D) A 48HAP ovule is classified as such by showing 16 endosperm nuclei. (E) A 72HAP ovule is characterized by 24 endosperm nuclei (F) A 96HAP ovule showing GFP signal at chalazal endosperm nuclei. Scale bar:50µm.

In the following section, the morphological characterization of endosperm development at different points after pollination in combination with infection and mock treatments is further analysed.

5.8.1 Endosperm developmental studies during infection

The main aim of the present analysis was to assess the extent of cell death in the developing endosperm and if the development rate of the endosperm, reflected by the expected number of nuclei in normally developing seeds, is affected by infection with *F. graminearum*. Control samples of 32HAP, 56HAP, 48HAP and 72HAP showed that more than 80% of the ovules developed and less than 20% of ovules degraded (Figures 53A and 53B). The small percentage of degraded ovules in the controls could have been a result of the stress caused by flower emasculation. Both infection and mock treatment had effects on the developing ovules. Pistils 8HAP followed by one or two days of inoculation with *Fusarium* had a higher

percentage of ovule degradation 37% and 51% (8h-1i and 8h-2i in figure 53A) respectively, whereas the mock treatment samples had a noticeable percentage of degradation at 28% and 47% at 24HAP (24h-1t and 24h-2t in figure 53B) regardless of the length of the treatment. This suggests that both infection with *Fusarium* and the mock treatment aggravate cell death of developing seeds.

By arranging the data according to the days of treatment after pollination (Figure 54A and B), we observed that degradation increased over subsequent time in almost all the conditions compared. A comparison of the control and treatment samples show that the percentage of the degraded ovules has an increasing trend over time in all conditions, while the percentage of developing ovules decreases over time in most of the conditions (Figure 54A and B), except in control (48HAP and 72HAP in figure 54B).

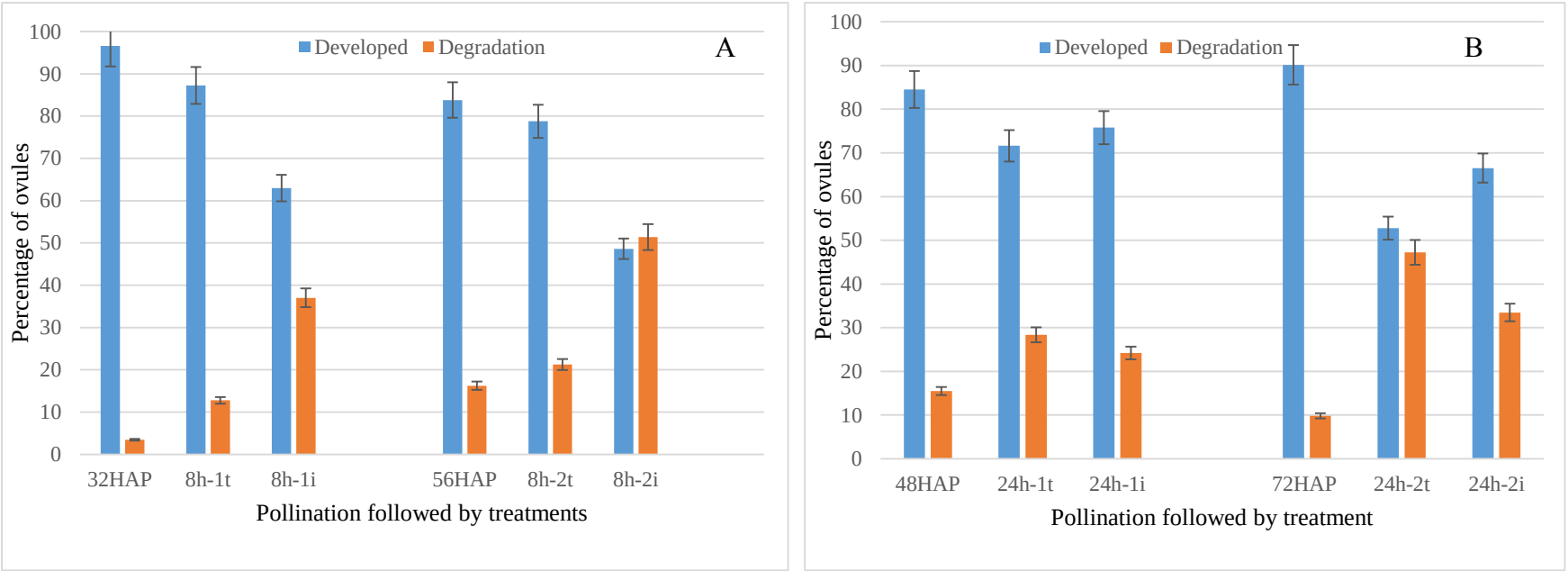

Figure 53:Comparison of the endosperm development status of different treatments in different time point indicates that infection and mock treatment cause the cell death of ovules.

The status of endosperm development during mock treatment and infection was compared with that of untreated pistils at different time points after pollination: 32HAP, 56HAP (A) and 48HAP, 72HAP (B)respectively. The blue column represents the ovules that developed normally and the orange column represents the ovules that are degraded. Error bars represent standard deviation of ovules observed in 10 pistils. 8h denotes 8HAP, 24h denotes 24HAP, 1t denotes one day of mock treatment, 2t denotes two days of mock treatment, 1i denotes one day of infection, 2i denotes two days of infection. For example, 24h-2t means 24HAP followed by two days of mock treatment, 8h-1i means 8HAP followed by one day of infection. Error bars represent standard deviation of ovules observed in 10 pistils.

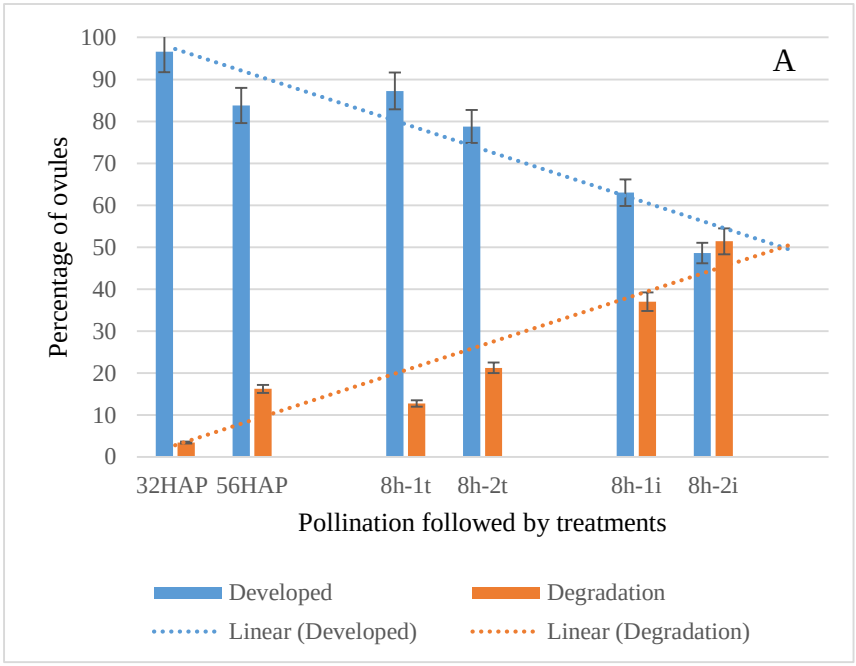

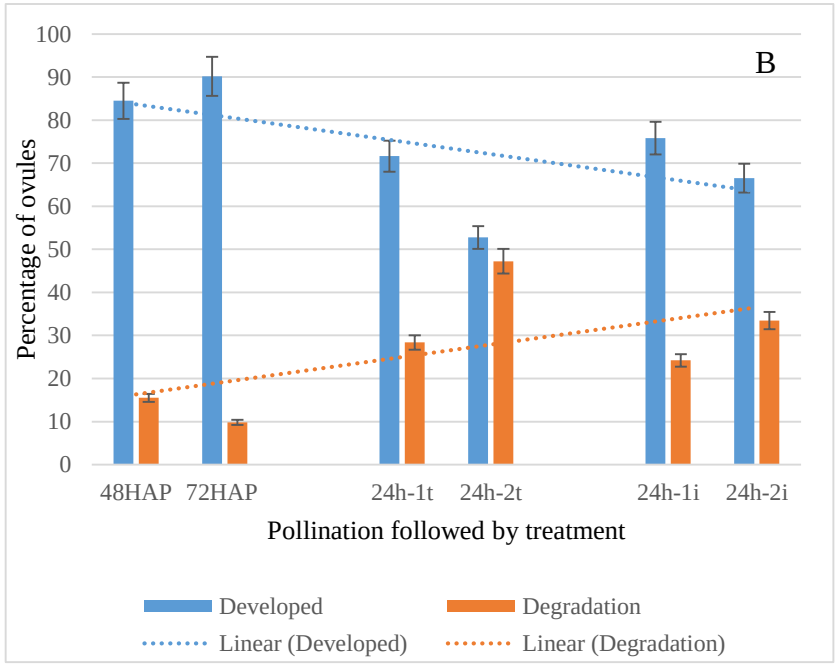

Figure 54:Comparison of the endosperm development status based on day of different treatments indicates mock treatment and infection treated samples had an increase of ovules in degradation stage from one day to two days.

The data in 52(A) and (B) is rearranged to compare the status of endosperm development based on the day of mock treatment, infection and untreated pistil following 8HAP (A) and 24HAP(B). The blue column represents the ovules that developed normally and the orange column represents the ovules that are degraded. Error bars represent standard deviation of ovules observed in 10 pistils. 8h denotes 8HAP, 24h denotes 24HAP, 1t denotes one day of mock treatment, 2t denotes two days of mock treatment, 1i denotes one day of infection, 2i denotes two days of infection. For example, 24h-2t means 24HAP followed by two days of mock treatment, 8h-1i means 8HAP followed by one day of infection. The percentage of ovules in control, mock treatment and infection in degradation stage increased from one day to two days.

5.8.1.1 Effect of infection on rate of endosperm development

In order to see if the infection and mock treatment had an effect on the rate of endosperm development, data of developmental studies was further analysed. The developing seed was further classified into different stages according to the number of endosperm nuclei. They were divided into expected development, slow development and 0h/8h ovule. 0 or 8HAP ovule in this study was counted as a single data point because it was impossible to tell them apart at the 10x magnification. 0h/8h had one nucleus in central cell at this stage. Expected development ovules are the ovules which have corresponding numbers of dividing endosperm nuclei to hours after pollination: the stage 24HAP has eight endosperm nuclei, stage 32HAP has 12 endosperm nuclei, the stage 48HAP has 16 endosperm nuclei, the stage 56HAP has 20 endosperm nuclei. In this context if the developing ovule has less endosperm nuclei than expected following certain time after pollination, it was considered as slow development. Data of 8HAP followed by one and two days of infection or mock treatment, along with the corresponding control was selected for further analysis.

In pistils 8HAP followed by one day of different treatment, the ovules of control, mock treatment and infection treatment samples had a lower percentage of ovules in the expected development stages and slow development stages (< 20%), whereas the highest percentage of ovules (50-75%) was at 0h/8h stages (Figure 55A). This would signify that most ovules in control, mock treatment and infection treatment samples are either yet to be fertilized or are in the early stages of successful fertilization. Thus, ovules at 0h/8h are assumed that most of ovules are non-pollinated for further analysis.

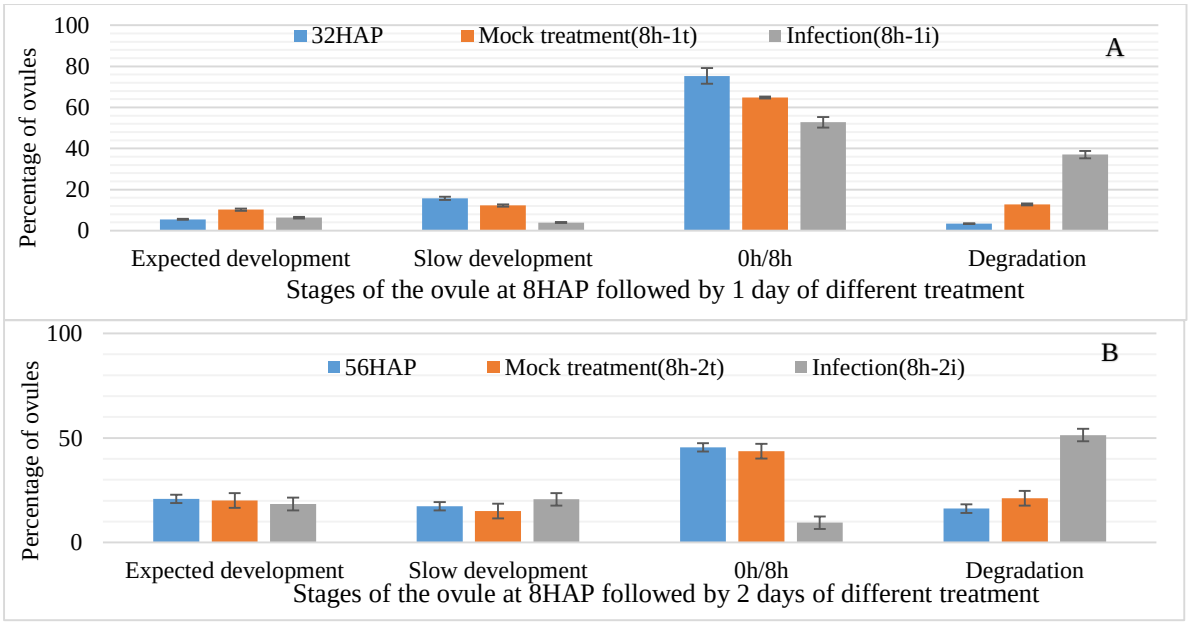

Figure 55:Comparison of the development stages of ovules during 8HAP after different treatment for one and two days indicates that rate of endosperm development is not effected by *F. graminearum* infection.

A) Effect on ovule development during 8HAP followed by one day of mock treatment or infection. B) Effect on the ovule development during 8HAP followed by two days of mock treatment or infection. The blue column represents the percentage of control ovules 56HAP. The orange column represents the percentage of mock treated ovules. The grey column represents the percentage of infection treated ovules. In the 8HAP followed by 2 days of different treatment, the percentage of ovules in control, mock treatment and infection at the 0h/8h stage has decreased in comparison to 1 day of different treatment. Similarly, in the 8HAP followed by 2 days of different treatment, the percentage of ovules in control, mock treatment and infection at the degradation stage has increased in comparison to 1 day of different treatment. The percentage of ovules in the expected development stage and slow development stage in infection treated samples is similar to the mock treatment and control. The error bars represent the standard deviation.

In pistils 8HAP followed by one day of different treatment, the ovules of the infected treatment sample had the highest percentage of degraded ovules (37%) in comparison to those counted in the mock treatment (13%) and control (3%). In contrast pistils 8HAP followed by two days of different treatment, show an increase in the percentage of degraded ovules in infected pistils (51%) in the, mock treatment (21%) and in the control (16%) (Figure 55A and B). Meanwhile, in 8HAP followed by two days of different treatment we can see a gradual decrease in the percentage of ovules at 0h/8h stage in control (46%), mock treatment (44%) and infection treatment (10%) samples (Figure 55B). In the infected samples, a decrease in the percentage of 0h/8h ovule could also be attributed to *F. graminearum* infection which results in degradation of the ovule. This can be observed in 8HAP followed by two days of infection, where the ovule of the infection treated samples had the highest percentage (51%) in degradation stage (Figure 55B).

In 8HAP followed by two day of different treatment, ovules of infection samples have similar percentage of development as in mock treatment and control in the expected development

stages and slow development stages (Figure 55A and B). This indicates that *F. graminearum* infection has no effect in the development rate of fertilized ovule to early endosperm stages. In general, we can conclude that the developmental rate of endosperm is not drastically affected by *Fusarium graminearum.* Although at a lower level, mock treatment also caused ovule degradation, which suggests that the treatment also causes stress to the ovule.

5.8.1.2 Ovules at 0h/8h stage are susceptible to *F. graminearum* infection

As described in previous section, ovules in 0h/8h stages were assumed to be susceptible to *Fusarium* infection. In order to further support this finding, data of 0h/8h and degradation in 8HAP followed by one or two days of different treatments were further analysed.

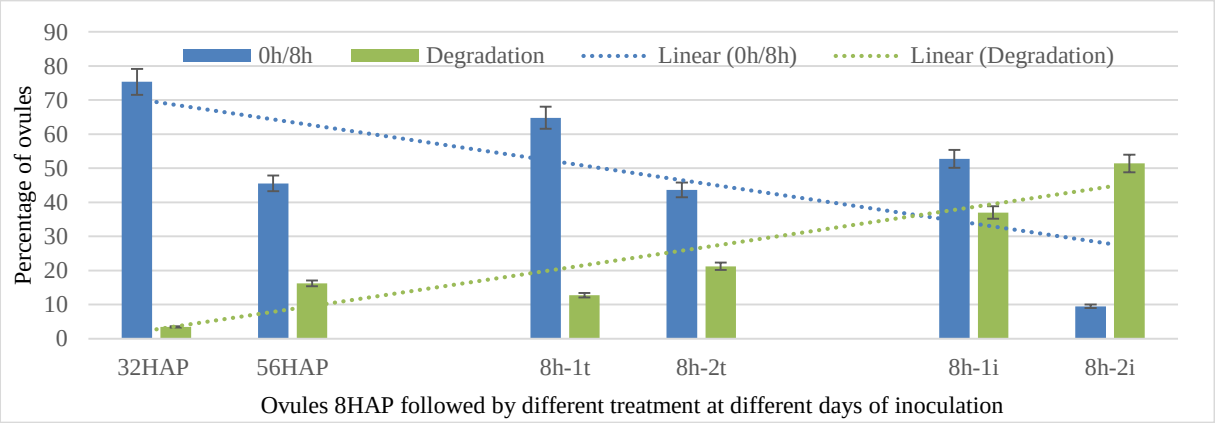

Figure 56:Comparison of the percentages of ovule in 0h/8h stage to degradation stage in 8HAP followed by one and two days of different treatment indicates that non-pollinated ovules are more prone to *F. graminearum* infection.
The green column represents ovules, which are in 0h/8h, and the blue column represents the ovules which are degraded. There was increasing trend of ovules in degradation stage in subsequent day, whereas there was decreasing trend of ovule in 0h/8h stage. 8h-denotes 8HAP, 24h denotes 24HAP, 1t denotes 1 day of mock treatment, 2t denotes 2 days of mock treatment, 1i denotes 1 day of infection. 2i denotes 2 days of infection. Example of legends 8h-1t denotes 8HAP followed by 1 day of mock treatment,24h-2i denotes 24 HAP followed by 2 day of infection. The error bar represents standard deviation.

The percentage of ovules at 0h/8h stage and degradation stage is arranged based on the day of mock treatment, infection and untreated pistil following 8HAP (Figure 56). In pistil 8HAP followed mock treatment along with control, there is gradual decrease of ovule in 0h/8h stage with gradual increase with degradation in subsequent days in control and mock treatment (Figure 56). Irrespective of increase in degradation in subsequent days, the highest percentage of ovules in mock treatment (44%) and control (46%) were at 0h/8h stage in comparison to degradation in mock treatment (16%) and control (21%) (Figure 56).

Interestingly, the highest percentage of ovules in pistil 8HAP followed by one day after infection was at 0h/8h stage (53%) in comparison to degradation (37%) whereas ovule in

8HAP followed by two days after infection shows an opposite trend with higher percentage of degraded ovules (51%) in comparison to 0h/8h stage (9%) (Figure 56). This signify that ovule in 0h/8h are more susceptible to *F. graminearum* infection. This is further supported by correlation study using data of 0h/8h and degraded ovule (Figure 57).

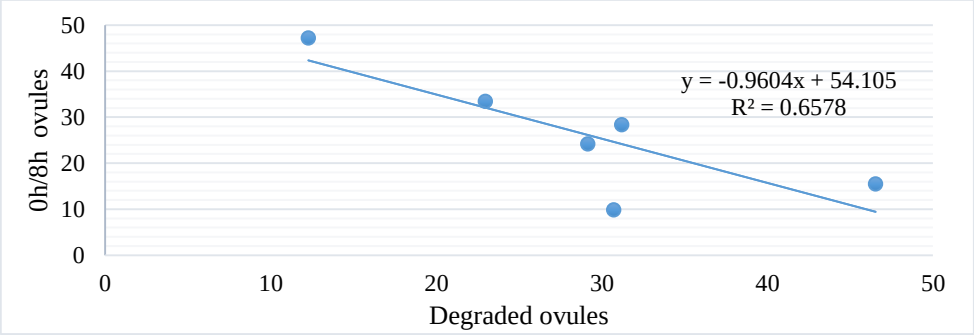

Figure 57:Negative correlation between the percentages of ovules at the 0h/8h stage and degradation stage in 8HAP followed by one and two days of different treatments.
In pistil 8HAP followed by one or two days of different treatments: percentage of ovules in control, mock treatment and infection at 0h/8h stage were correlated with percentage of ovules in control, mock treatment and infection at degradation stage. There was negative correlation of R^2 = -0.65 between ovules in 0h/8h stage and ovules in degraded stage.

Correlation studies were done with the six data points of ovule at 0h/8h stage and degradation stage in the 8HAP followed by one and two days with mock treatment, infection along with controls. There was strong negative pearson correlation R^2 = -0.65 (Figure 57) between the percentage of degraded ovules and those at stage 0h/8h.

This whole analysis indicates that the non-pollinated ovule or just fertilized ovule are prone to degradation during *F. graminearum* infection. This is supported by the seed set data in Table 12 in section 5.6.2.2, in which the seed set number is drastically affected in the case of infection followed by pollination of the pistil in comparison to pollination followed by infection.

5.8.2 Programmed Cell Death induced in the *F. graminearum* infected ovule

To check if PCD occurs in infected ovule, PCD marker line AtCEP1-eGFP was obtained from a published study by members of our group (Zhou et al. 2016). In normal conditions, AtCEP1-eGFP is expressed in nucellus cells surrounding the chalazal pole of the central cell vacuole (Figure 58A). AtCEP1-eGFP flowers were emasculated and infected with *F. graminearum* for three days following the protocol described in 5.1.2. Two controls were taken for this condition: AtCEP1-eGFP flowers was emasculated and left untreated for four days, while the second control were emasculated AtCEP1-GFP flowers followed by mock treatment with water and left for three days in a moist chamber, as the infected plants.

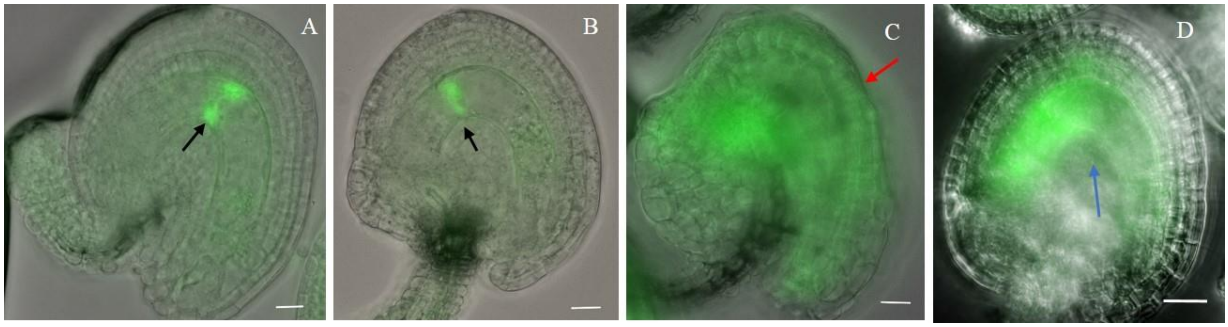

Figure 58:Comparison of AtCEP1-GFP ovules during *F. graminearum* infection along with control indicates that PCD occurs in the infected ovule.

AtCEP1-GFP plants were infected with *F. graminearum* for 3DAI along with mock treatment and 4DAE controls. A) 4DAE control AtCEP1-GFP ovule has intact GFP in nucellus cells (black arrow) B) 3DAT Mock treatment control - AtCEP1-GFP ovule has intact GFP in nucellus cells (black arrow) C) In 3DAI AtCEP1-GFP ovule GFP signal is not observed and autofluorescence is observed with outer integument damaged (red arrow) D) In 3DAI WT ovule, autofluorescence was observed in embryo sac region(blue arrow). Scale bar:50µm.

The infected AtCEP1-eGFP ovule had no GFP signal in nucellus signal and there was severe damage to the outer integuments, whereas the mock treatment and the untreated control ovules had intact GFP signal in nucellus cells and intact integuments (Figure 58A and B). Protease AtCEP1 is involved in PCD by contributing to the general collapse of the cell and tissue breakdown. AtCEP1was found to be upregulated in our transcriptome data of the 3DAI pistil (Table 6 in section 5.2.7). This signifies that AtCEP1-eGFP ovule undergo PCD which is characterised by collapse of ovule and disintegration of outer ovule integuments. The widespread fluorescence signal observed in disintegrated infected AtCEP1-eGFP ovule would be attributed to embryo sac collapse filled with cellular autofluorescent material. Similar autofluorescence signal was visible in WT *A. thaliana* ovule when infected with *F. graminearum* (Figure 58D). Thus in conclusion, the ovules undergo PCD during infection with *F. graminearum* either as part of the defence response by the host or induced by *Fusarium* to benefit its own growth.

6. Discussion

6.1 Transcriptome analysis of DEFL genes

72 DEFL genes were found to have differential expression ≥ 2 $\log_2$ fold change or ≤ 2 $\log_2$ fold change in the transcriptome analysis of differential gene expression (Appendix section 9.6). 25 DEFL genes were selected from the 72 DEFL gene list for further analysis in order to understand DEFL expression in the female gametophyte during infection and reproduction events (Table 5 in section 5.2.5). The criteria for selection of the candidate gene was based on DEFL expression in certain experimental conditions and its prediction to be expressed in female gametophyte obtained from the literature. The following section explains how our results fit in the context of previous transcriptomic analyses of the *Arabidopsis thaliana* gametophytes.

6.1.1 Comparison to published transcriptome analyses

It is important to consider the RNAseq analysis of the pistil during pollination and infection with *Fusarium graminearum*is among the first to provide this kind of data on *A. thaliana*. The major hurdle to follow and understand the expression of DEFLs using transcriptomics is their underrepresentation in ATH1, the most complete commercially available array design for *Arabidopsis* which has probe sets for 36 of the 324 DEFLs. For this reason, it is important to keep in mind that if previous transcriptomics studies detect only a fraction of our candidates it is because several of them are not represented in ATH1 microarray.

In *dif1* mutant, gametogenesis does not take place and this leads to the lack of embryo sac in *A. thaliana* ovules (Jones-Rhoades et al. 2007). The microarray data containing *dif1* mutant ovules compared to wild type ovules was cross referenced and found out 15 of our candidate DEFL genes are downregulated in *dif1* mutants, thus suggesting they are expressed in the embryo sac. Similarly microarray data containing male sterility1 (*ms1*) ovules compared to *dif1* ovules was cross referenced, four candidate DEFL At1g60985, At5g38330, At2g20070 and At4g29285 genes were found to be highly expressed in siliques between one to two days after pollination as well, but no signal was detected in other plant tissues like anthers, leaves, roots, stems (Steffen et al. 2007).

Transcriptomes data was also compared with microarray data of specific female gametophyte cell-synergids, egg cell and central cell (Wuest et al. 2010). Five DEFL genes At2g02100, At1g60985, At5g38330, At2g20070 and At4g29285 were found to be highly enriched in the female gametophytes. They were predominantly expressed in the microarray data of central

cell and thus exhibiting tissue specific functions (Wuest et al. 2010). In the analysis of promoter activity, the expression of At1g60985, At5g38330 and At2g20070 were localized in central cell and antipodal cells, respectively (Table 8).

The expression data here obtained for DEFL genes was also compared with other RNAseq-based studies. Specifically, 18 of the 72 DEFL genes were expressed in embryo sac enriched samples of *A. thaliana* (Huang et al. *2015*), and few more DEFL genes which were enriched in ovule samples were found to be expressed in central cell via RNAseq data of central cell (Schmid et al. 2012).

The 72 DEFL genes which were found in the transcriptome data were further explored in literature documenting pollen-specific DEFL genes. From microarray data of pollen grain (PG) and pollen tube germination (PTG), 5 DEFL genes were identified to be pollen-specific (Wang et al. 2008; Boavida et al. 2011; Wuest et al. 2010). As most DEFL genes are underrepresented in microarray gene chips, RNAseq data of pollen grains indicates there are 27 additional pollen-specific DEFL genes among the 72 differentially expressed DEFLs (Loraine et al. 2013; Huang et al. 2015).

In conclusion, from various literature data mentioned in this section, 72 DEFL genes were categorized to tissue specific expressions (Appendix section 9.11) as follows: 33 DEFL genes were expressed in the female gametophyte, 32 DEFL genes are specificaly expressed in pollen and the remaining seven DEFL genes (At2g26010, At2g26020, At5g44430, At1g56233, At4g22235, At5g42223, At3g05727) were only differentially expressed in our data.

6.1.2 Localization of DEFL gene in reproductive tissue

To further analyse, 25 candidate genes were expressed along with GFP to visualize their expression *in planta*. In total, the localization of 15 candidate DEFL genes were reported in specific tissue and cell-types (Table 8 in section 5.3). The remaining ten candidate DEFL candidate genes could not be localized via eGFP signal which could be attributed to several reasons, such as low promoter activity, improper integration of Transfer-DNA (T-DNA), and DNA sequence taken for cloning.

Of the 15 candidate DEFL genes reported by GFP localization studies, only four DEFL genes - At5g43285, At5g38330, At2g20070 and At1g60985 have been previously identified to be expressed in female gametophyte (Steffen et al. 2007; Takeuchi et al. 2012; Li et al. 2015). Seven candidate DEFL genes (At2g42885, At2g40995, At3g07005, At4g09153, At4g30074, At3g43505, At5g55132) and one DEFL gene (At4g11760) in pollen grain were identified for the first time, thus providing expression evidence for these eight DEFL genes. The eGFP

localization of newly identified seven candidate genes in the central cell were in line with the predicted RNAseq data of central cell (Schmid et al. 2012).

Candidates At1g65352, At3g42473 and At3g06985 showed eGFP signal in mature pollen grains (Figure 28 in section 5.3.2). The putative promoter of these genes were cloned to NLS fused to eGFP however the localization of eGFP in these marker lines did not represent a signal from the nucleus. Many independent lines for each marker were checked and each had the same pattern of expression. The probable cause of improper cloning for three genes can be ruled out since sequencing confirmed that promoter sequences was cloned in frame with NLS without any deletion, substitution, or mutation. There was no observed signal peptide in the selected promoter sequences, thereby also ruling out the possibility of unidentified signal peptides in overriding the NLS signal. This unexpected fluorescent signal could possibly be attributed to T-DNA not being integrated to nucleus completely or integration of T-DNA not being stable (Nam 1999; Janssen et al. 1990). This expression pattern in pollen grain is not supported by other transcriptome data. The localization of these genes suggests they are expressed in the central cell of the ovule (Huang et al. 2015; Schmid et al. 2012). To confirm the localization, gene and promoter of these genes were cloned along with GFP to observe sub-cellular localization. Due to the lack of time, further experiments to identify the sub-cellular localization of these proteins were not continued.

In conclusion, ten candidate DEFL genes were found to be localized in central cell and these genes were selected as candidate because they belong to an evolutionary conserved group downregulated during infection (Mondragón-Palomino et al. in review). This finding is quite interesting in the aspect that the DEFL protein might be secreted from central cell as a defence response in the female gametophyte towards fungi. Pathogen toxins possibly downregulate these group of DEFLs in order to facilitate *Fusarium* growth in the developing seed.

6.1.3 DEFLs expression in roots

Using marker lines, Expression of six DEFL genes were identified in roots (Table 8 in section 5.3). These six DEFL genes were found in root and reproductive tissue, thus possibly leading to dual roles for plant development and defence. Expression of two DEFL gene (At4g11760, At5g38330) in root is supported by expression data from Genevestigator (Hruz et al. 2008)(Appendix section 9.12). Along with these two genes, 16 of the 72 DEFL genes were also found to be expressed in root according to published data obtained from database

Genevestigator (Hruz et al. 2008)(Appendix section 9.12). Expression of DEFL genes in Genevestigator were found in different experiments of roots that involved stress-related, growth development and microbial studies (Hruz et al. 2008). DEFL gene (At5g60553) was downregulated in the transcriptome data of the infected pistil (Appendix section 9.6); this has been reported to be expressed in the root (Tesfaye et al. 2013). PDF2.2 (At2g02100) which was downregulated in the transcriptome data of infected pistil (Table 4 in section 5.2.4) and has been reported to be constitutively expressed throughout the plant with strongest expression in roots and siliques (Siddique et al. 2011; Hruz et al. 2008). GFP expression of At4g40995, At4g42885 and At3g07005 in roots has not been reported in the literature, thus making it a novel finding that can be explored for further analysis. According to published data, from 72 differentially expressed DEFLs, 23 are also expressed in roots, thus suggesting our finding of candidate DEFL expressed in root and reproductive organs is just the tip of the iceberg (Appendix section 9.12).

6.1.4 Upregulation of CRP in *A. thaliana* pistil during interspecific crosses

There was no seed set observed in *A. thaliana* during interspecific cross with *A. halleri* and *A. lyrata* pollen. This can be due to several genes which would have been responsible for mediating the reproductive barrier. The transcriptome data of *A. thaliana* pistils pollinated with *A. lyrata* or *A. halleri* pollen was further analysed. CRPs including six DEFLs (At5g19315, At5g39365, At4g19035, At4g29285, At1g13609 and At3g05727) along with few thionins and RALFs like peptide were found to be upregulated to in transcriptome data of *A. thaliana* pistils pollinated with *A. lyrata* or *A. halleri* pollen (Appendix section 9.6 and 9.15). Among six DEFL genes, only At2g29285 gene has been reported to localized in the central cell (Li et al. 2015) and rest is largely unknown, this opens the possibility of At2g29285 to be involved in some sort of prezygotic reproductive barrier (Mondragón-Palomino et al. in review). Thionins represents the largest group of CRPs whose transcript levels were upregulated during interspecific pollination. Thionin like defensins are toxic to pathogens and can be induced by phytopathogenic fungi (Vignutelli et al. 1998). Thionin have been reported to be expressed in ovules and individual female gametophyte in *A. thaliana* (Jones-Rhoades et al. 2007; Wuest et al. 2010; Huang et al. 2015), yet their role in reproduction is not known. This upregulation pattern of thionin hints at a possible role in reproductive barrier during interspecific crosses. RALF-like peptides are involved in the acidification of the extracellular environment and inhibit cell expansion during development (Murphy et al. 2014). Thus RALF like peptide might contribute to pollen tube rejection by

inhibiting pollen tube growth, which has been previously observed in vitro for AtRALF4 and SlPRALF from Solanum lycopersicum (Covey et al. 2010; Morato do Canto et al. 2014). In conclusion, these CRP might mediate some sort of reproductive barrier, further functional analysis would help us to understand their role in recognition of foreign pollen.

6.1.5 Importance of DEFL in female gametophyte

The developing embryo and endosperm are an attractive niche for pathogens because they are rich in nutrients that requires defence mechanisms against pathogens invading the also nutrient-rich tissues of the pistils. This hypothesis is supported by finding that several DEFL genes are present in female gametophyte which was proved through GFP localization studies. The gene expression of DEFL continues during early seed development, which has been shown through quantification of GFP (Figure 37, 38 in section 5.5.1). This data corresponds well with similar time points analyzed by RNAseq (Huang et al. 2015). However, this pattern of expression could also mean that DEFLs may be involved in pollen tube guidance and pollen tube reception during double fertilization and in early seed development. Thus, DEFL candidates have a distinct involvement in defence and reproduction which has been observed in tomato defensin DEF2 (Stotz et al. 2009).

6.2 Coordination of DEFL genes in female gametophyte during double fertilization.

The correlation of expression data from DEFL gene–pairs obtained from different conditions using independent measurements via RNAseq and qPCR (Table 11 and 12 in section 5.7.) suggests the genes compared are co-regulated in the female gametophyte. Of the seven DEFL genes that were chosen for correlational studies, five of them (At2g40995, At3g07005, At5g38330, At4g09153 and At5g60985) were localized in central cell, one DEFL gene (At2g20070) in antipodal cells and one DEFL gene (At5g43285) in synergids (Table 8 in section 5.3). All the noteworthy correlated result except one (Table 11 in section 5.7) had at least one central cell expressed DEFL gene in the gene pairs. The proposed co-regulation of these genes is plausible in view of published evidences the central cell and the synergids coordinate their activities in pollen tube guidance, prevent polytubey and are involved in antipodal cell degeneration (Maruyama et al. 2015; Li et al. 2015).

6.2.1 Central cell role in antipodal degradation

Antipodal cells have been previously predicted to have undergone PCD before fertilization. Using antipodal DEFL marker gene At2g20070, eGFP was reported to exhibit expression until 12HAP (Figure 20 in section 5.3.1). This signifies that antipodal cells survive after double fertilization and degenerate at early developing endosperm stages. This is supported by a similar finding by (Song et al. 2014). In several grasses, such as maize and wheat, antipodal cells proliferate, forming up to several hundred cells, which persist during endosperm development, where they appear to serve a nutritive function (Wittich et al. 1998). Thus, a similar phenomenon maybe predicted in antipodal cell which might function in transferring nutrients from the maternal sporophyte to the early developing endosperm stages in *Arabidopsis.* The second possible interaction between central cell and antipodal cells is in PCD events. There is a strong evidence for PCD in antipodal cells that it requires antipodal factors and signalling cues which are provided by the central cell. For example, mutation of the central cell protein FIONA has been shown to prolong the lifespan of antipodal cells (Kagi et al. 2010). It has also been reported that *Zea mays* EAL1, secreted by egg cell, prevents antipodal cell in adapting central cell fate (Krohn et al. 2012). The examples described above indicates the relationship between antipodal cells and other cells in the embryo sac.

Antipodal cell specific DEFL gene At2g20070, may co-regulate with central cell DEFL genes such as, At3g07005, in determining the PCD event of antipodal cells or may be

involved in nutritive transfer during the early stages of developing endosperm. This is supported by correlation data, which shows At2g20070 has a high positive correlation with At3g07005 only during pollination events. The interaction between DEFL peptides of central cell and antipodal cells is highly possible since the central cell is adjacent to the antipodal cells. For further future analysis, using At2g20070 mutant lines would be starting point for identifying the precise function of this candidate during double fertilization.

6.2.2 Central cell interaction with synergid

Synergid expressed At5g43285 DEFL gene had a high correlation coefficient with some of central cell genes -At2g40995, At3g07005, At5g38330, during pollination or infection and when both processes took place. The central cell is known to coordinate its activity with that of synergids in two events a) for preventing polytubey b) for attracting pollen tube.

First coordination event between central cell and synergid is after sperm cells fuses with female gametes. A fertilized central cell (endosperm) fuses with a persistent synergid to form synergid endosperm fusion (SE fusion), which prevents polytubey (Maruyama et al. 2015). During SE fusion, pollen tube attractants such as At5g43285 (LURE1.1) and other unique transcripts from synergid cell are diluted into developing endosperm. Thus At5g43285 gene would be expressed even after fertilization via SE fusion which was observed in pollination studies or qPCR data (Appendix section 9.13). The initiation of SE fusion is caused by successful fertilization of the central cell, independent of egg cell fertilization (Maruyama et al. 2015).

The second coordination event between central cell and synergids takes place before the fertilization events. Specifically, the central cell has been observed to have an effect on pollen tube guidance. For example, *magatama 3*, an *Arabidopsis* mutant defective in size and fusion of polar nuclei in central cell, also exhibited defect in pollen tube attraction (Shimizu et al. 2008). Furthermore, one of the prominent evidences of central cell involved in pollen tube guidance is CENTRAL CELL GUIDANCE (CCG) gene. In the *ccg* mutant, development of embryo sac is normal, but pollen tube guidance was found to be disrupted (Chen et al. 2007). Furthermore, they reported the expression profiling of *ccg* ovules driven by CBP1 revealed downregulation of several DEFL genes including LURE1.1 (Li et al. 2015). Few of the DEFL genes expressed in the transcriptome data of infected pistil were found to overlap with their transcriptome data (Li et al. 2015). Specifically, At5g38330 and At1g60985 which were specifically expressed in the central cells were observed to be severely affected in *ccg* mutant (Li et al. 2015). At5g43285 (LURE1.1) which is regulated by synergid-specific transcription

factor MYB98 was also impaired in *ccg* mutant (Li et al. 2015). This would suggest that several DEFL genes may be secreted in central cell and would have intercellular interactions with synergids for attraction of pollen tube. Thus it is possible that central cell DEFL peptides may co-regulate with LURE1 peptides in pollen tube attraction. The other possible interaction is LURE1.1 and central cell DEFL peptides may be part of a complex mixture of signalling peptides which are involved in attracting the pollen tube. It has been observed that the cell wall is absent, and the plasma membrane is in direct contact between egg cell, central cell, and synergid (Li et al. 2015). It is possible then that central cell DEFL peptides (size of ~5 kDa) could diffuse to the synergid and from there be secreted in order to attract the pollen tube (Han et al. 2000).

These two evidences signify that the central cell interacts with synergids in two processes during the different events of double fertilization: They interact in an indirect manner for pollen tube guidance before fertilization and in a direct manner for polytubey block after double fertilization of gametes. Thus, we can conclude that central cell plays a key role in double fertilization and during seed development regulation by correlating with the accessory cell (synergids, antipodal cells). This should be further investigated in order to characterize the joint activities of central cells with synergids and antipodal cells within the embryo sac. This would enable us with deeper knowledge of central cell since it seems to be a key player in the process of double fertilization.

6.3 Effects of hemibiotrophic lifestyle of *Fusarium graminearum* in *Arabidopsis pistil*

At present, the mechanisms underlying *A. thaliana* resistance in pistil tissue towards hemibiotrophic lifestyle *of F. graminearum* is still not analyzed in detail. This offers the potential to use the transcriptomic data of the infected pistil to analyze different defence responses including DEFLs (PDF 1.2a-c) towards the different phases of *F. graminearum* infection. By understanding these processes, we would be able to improve the plant responses to the different phases of FHB.

6.3.1 PDF1.2a-c and PR1 are regulated as defence response towards hemibiotrophic phases of *Fusarium graminearum*

In *A. thaliana*, defence in the biotrophic phase is initiated by salicylic acid (SA) signalling pathway, whereas in the necrotrophic phase the defence response is based on the synergistic action of jasmonic acid (JA) and the ethylene (ET) signalling pathway (Glazebrook 2005). In the transcriptome data of infected pistils, JA/ET-associated genes such as PDF1.2a, PDF1.2b, PDF1.2c and PDF1.3 were upregulated (Table 6 in section 5.2.4) (Makandar et al. 2010). Additionally, the genes encoding PR1 and PR2, which are considered as markers for SA-mediated defences (Makandar et al. 2010), were found to be upregulated during fungal infection of *A. thaliana* pistils (Table 6 in section 5.2.7). Thus from this data, we can confirm that SA and JA/ET mediated defence was activated as defence response towards the hemibiotrophic lifestyle of *F. graminearum.*

The gene encoding DON Glucosyltransferase 1 (DOGT1), was found to be upregulated in the infected pistil (Table 6 in section 5.2.7), which is involved in the degradation of mycotoxin DON (Poppenberger et al. 2003). This indirectly confirms that in the pistils 3DAI, DON mycotoxin was secreted by *F. graminearum.* DON induces host plant genes such as LOX1, WRKY25, WKRY7 to act as negative regulator of SA signalling pathway and therby suppress SA mediated defence response (Figure 59) (Kim et al. 2006; Zheng et al. 2007; Nalam et al. 2015). LOX1, WRKY25, WKRY7 were found to be upregulated in infected pistil (Table 6 in section 5.2.7). Thus the DON mycotoxin produced during necrotrophic phase targets and manipulates some of the regulatory genes of SA defence signalling pathway in order to make the *A. thaliana* susceptible for further fungal infection.

NON-EXPRESSOR OF PR1 (NPR1) is a major player which is involved in activation of PR1, PR2 and downregulation of PDF1.2a (Figure 59). NPR1 was found to be upregulated in the transcriptome data of infected pistils (Table 6 in section 5.2.7). This data suggests

regulators of SA suppress JA/ET signalling, whereas SA is in turn suppressed by DON mycotoxin. Thus JA/ET and SA defence signalling pathways generally interact in antagonistically manner with each other which benefits the hemibiotrophic lifestyle *F. graminearum* (Makandar et al. 2010). The upregulation of PR4, PR3 and PDF1.2a genes(JA/ET) in comparison with the PR1(SA) in the pistil transcriptome 3DAI (Table 6 in section 5.2.7) suggest the necrotrophic phase takes place at this time point.

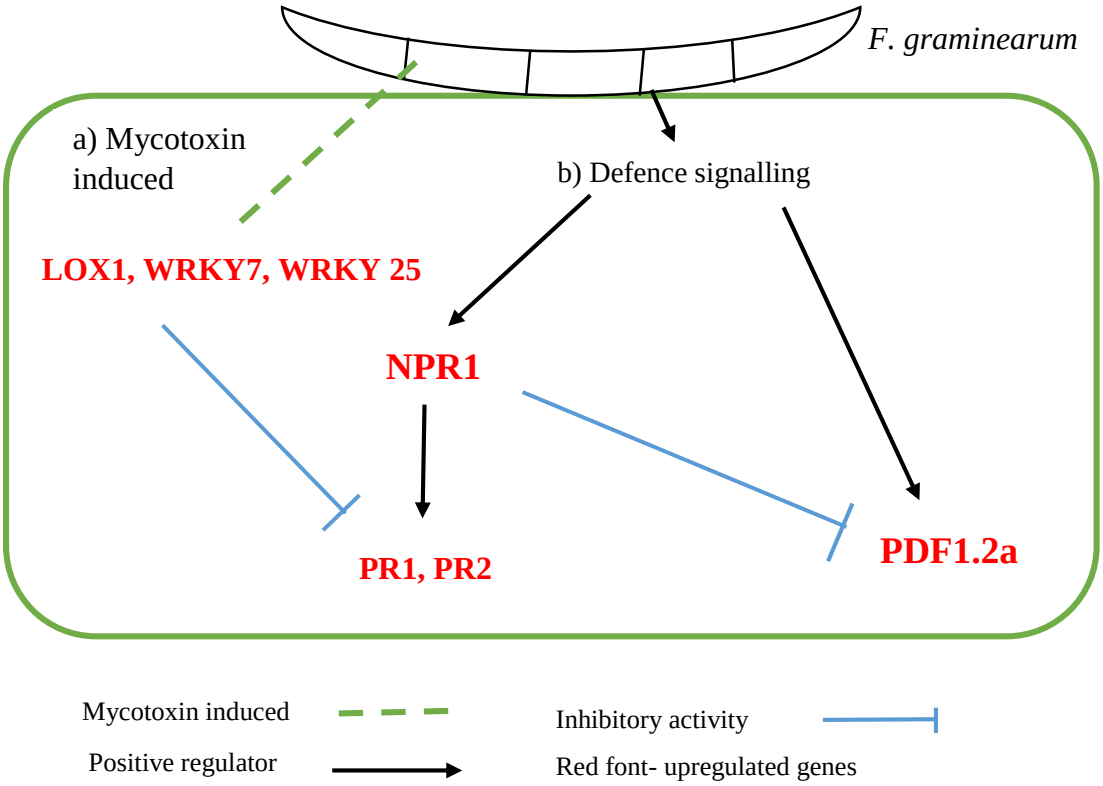

Figure 59:Crosstalk between regulatory genes of SA and JA/ET signalling pathway for defence response along with mycotoxin induced genes in F. graminearum infected pistil which is inferred from infected pistil transcriptome data and the literature.
a) Mycotoxin of *F. graminearum* induces the upregulation of WRKY7, WRKY25 and LOX1 to inhibit the SA mediated defence. b) NPR1 activates the expression of PR1, PR2 for SA mediated defence pathway, meanwhile NPR1 activates GRX480/TGA1 complex to inhibit PDF1.2(JA/ET). PDF1.2 is regulated as JA/ET mediated defence pathway during the necrotrophic phase of *F. graminearum*. Red font denotes the upregulated gene in the infected pistil of the transcriptome data.

In conclusion, having insight to defence response towards hemibiotroph lifestyle of *F. graminearum* is vital for halting its invasion. For example, it has been reported that *Medicago spp* defensins MsDef1 and MtDef4 inhibit *F. graminearum* biotrophic (extracellular) and necrotrophic (intracellular) phase respectively (Ramamoorthy et al. 2007). Thus by understanding the molecular players behind hemibiotroph life style we would be able target the two different phase of *F. graminearum* in order to improve crop productivity against FHB.

6.3.2 – Nectrophic phase of *F. graminearum* influences the seed development

The reduction in seed set documented during *F. graminearum* infection (section 5.6.2) is indicative of the major effect of infection in seed development. Specifically, assuming one-day infection of *F. graminearum* corresponds to the biotrophic phase and three days' infection corresponds to transitional phase of biotrophic- necrotrophic phase.

As the virulence of *F. graminearum* proceed to change from biotrophic to necrotrophic phase, siliques develop a lower number of seeds, irrespective of pollination time. This suggests that cell-death caused during necrotrophic phase is the first major factor interfering with seed development as has been shown in cereals infected with FHB (Schmale et al. 2003). The time point for infection with respect to pollination is the second factor of *Fusarium* infection which according to our results most importantly affects seed development. This was observed by comparing the seed set data between the experiments involving pollination followed by infection (Infected seed set data = 26, control =43) and infection followed by pollination (Infected seed set data = 5, control=32) (Table 10 in section 5.6.2). The experiment of infection followed by pollination indicates that fungal infection targets the unfertilized ovule in a more virulent manner, in comparison to the fertilized ovules from the experiment where pollination was followed by infection. In the case of infection followed by pollination, it is therefore obvious that necrotrophic phase of infection is an obstacle for double fertilization. Specifically, double fertilization machinery in plants might be sidelined by the transcriptional reprogramming needed to combat growing fungal hyphae and cell death in the unfertilized ovule, interferes pollen tube growth and reception. The other factors which was evident from pollination followed by infection seed set data is that the fertilized ovule has more chances to survive and develop into seeds despite of fungal growth on the pistil because defensins are being expressed in the developing seed and act in defence function. Thus, in general, the necrotrophic phase of *F. graminearum* is a major influence in infection of the seed development. There are no preceding findings in the literature regarding the influence of *F. graminearum* on the ovule susceptibility and seed development. Thus, making this study a first of its kind to see the hemibiotrophic lifestyle influence of *F. graminearum* on seed development.

6.3.3 *F. graminearum* initiates programmed cell death in the infected ovule

The occurrence of PCD in the unfertilized ovules during *Fusarium* infection was validated by infecting marker carrying PCD marker AtCEP1-eGFP. It was observed that AtCEP1-eGFP ovule had undergone PCD with collapse of outer integuments with no eGFP signal in

nucellus. Autofluorescence signal was observed in the collapsed embryo sac whereas the control samples had intact GFP signal in nucellus cells (Figure 58 in section 5.8.2). This was supported by upregulation of AtCEP1 in transcriptome data of the infected pistil (Table 6 in section 5.2.7). The cysteine endopeptidase AtCEP1 is involved cell collapse and breakdown of the tissue by digesting of cell wall extensins in last stage of PCD. Like AtCEP1, the gene encoding α vacuolar processing enzyme (αVPE) was also upregulated in the transcriptome data of infected pistil (Table 6 in section 5.2.7).The literature suggests that PCD process can be initiated by a VPE which is similar to caspases (Hara-Nishimura et al. 2005). The plant vacuole contains many hydrolytic enzymes for digestive processes and is important for providing structural support to the cell. (Marty 1999). Vacuole-mediated cell death is associated with the vacuolar membrane collapse and release of vacuolar hydrolytic enzymes into the cytoplasm (Qiang et al. 2012). This is followed by degradation of the remaining cellular components and a complete collapse of the cell. The morphology observed in AtCEP1-eGFP infected ovules (Figure 58C) may be due to the vacuole mediated cell death mechanism initiated by αVPE in response to *F. graminearum* infection. It is reported in literature that that fungal toxins manipulate VPEs to induce PCD of the host in order to acquire nutrients (Kuroyanagi et al. 2005). This supports an scenario where necrotrophic *F. graminearum* toxins cause unfertilized ovule PCD to obtain nutrients.

6.4 –DEFLs are involved in PTI triggered by *Fusarium graminearum* infection

DEFL genes which were selected for qPCR studies in infection (Figure 32 in section 5.4) gave us valuable insight, such as the treatment and the age of the emasculate pistil, which has no effect on infection. This information validates that the downregulation of DEFL genes in the transcriptome data of infection pistil was primarily due to *F. graminearum* infection. This leads us to further investigate the molecular mechanism of the DEFLs in defence towards invading fungal infection. The primary focus was on the role of the DEFL during PTI, which is based on a multilayer host defence response towards *F. graminearum* (Dodds et al. 2010).

Fungal pathogen-associated molecular patterns (PAMPs) chitin is identified by lysin motif receptor kinases (LYK) bound to the plasma membrane (Zhang et al. 2010). AtLYK5, a primary receptor for chitin, along with AtLYK4 were upregulated in the transcriptome data of infected pistil (Table 6 in section 5.2.7). The AtLYK5-AtLYK4 are known to induce PTI in recognition of chitin and are thereby involved in downstream defence mechanisms such as MAPKs activation of reactive oxygen species (ROS)(Zhang et al. 2010), production of defence related genes and PCD at the site of infection to limit pathogen progression (Bigeard et al. 2015; Zhang et al. 2010).

6.4.1 PDF 1.2a activated by mitogen activated protein kinase signalling cascades

Each specific MAPK cascade contributes towards the establishment of disease resistance in the plants. Several of the kinase components which includes MAPKKKs, MKKs and MPKs were upregulated in infected pistils (Table 6 in section 5.2.7, Appendix section 9.17).

MPK3 plays critical roles in plant disease resistance by regulating multiple defence responses, as well as ovule development (Guan et al. 2014). MKK7 and MKK9 are reported to be downstream of MPK3, and thereby activating defence response (Kannan et al. 2012). Also ERF104 was upregulated in the transcriptome data of infected pistil (Table 6 in section 5.2.7). It has been documented that phosphorylation of ERF104 by MPK3 is able to constitutively activate PDF1.2a (Meng et al. 2013; Bethke et al. 2009) and induce resistance to the necrotrophic fungal pathogen (Meng et al. 2013) (Figure 60).

MPK11 may regulate JA/ET mediated defence pathway and regulate the expression of PDF1.2a in response to *F. graminearum*. This is possible since MPK11 is a paralog of MPK4 which is relevant for embryo development and found to be overlapping with MPK4 in regulating cell division (Bethke et al. 2012). Thus, MPK11 can be predicted to have a similar

role as MPK4 in regulating PDF1.2a (Figure 60). Thus MPK3 and MPK11 constitutively express PDF1.2a as the defence response for the necrotrophic phase of *F. graminearum*.

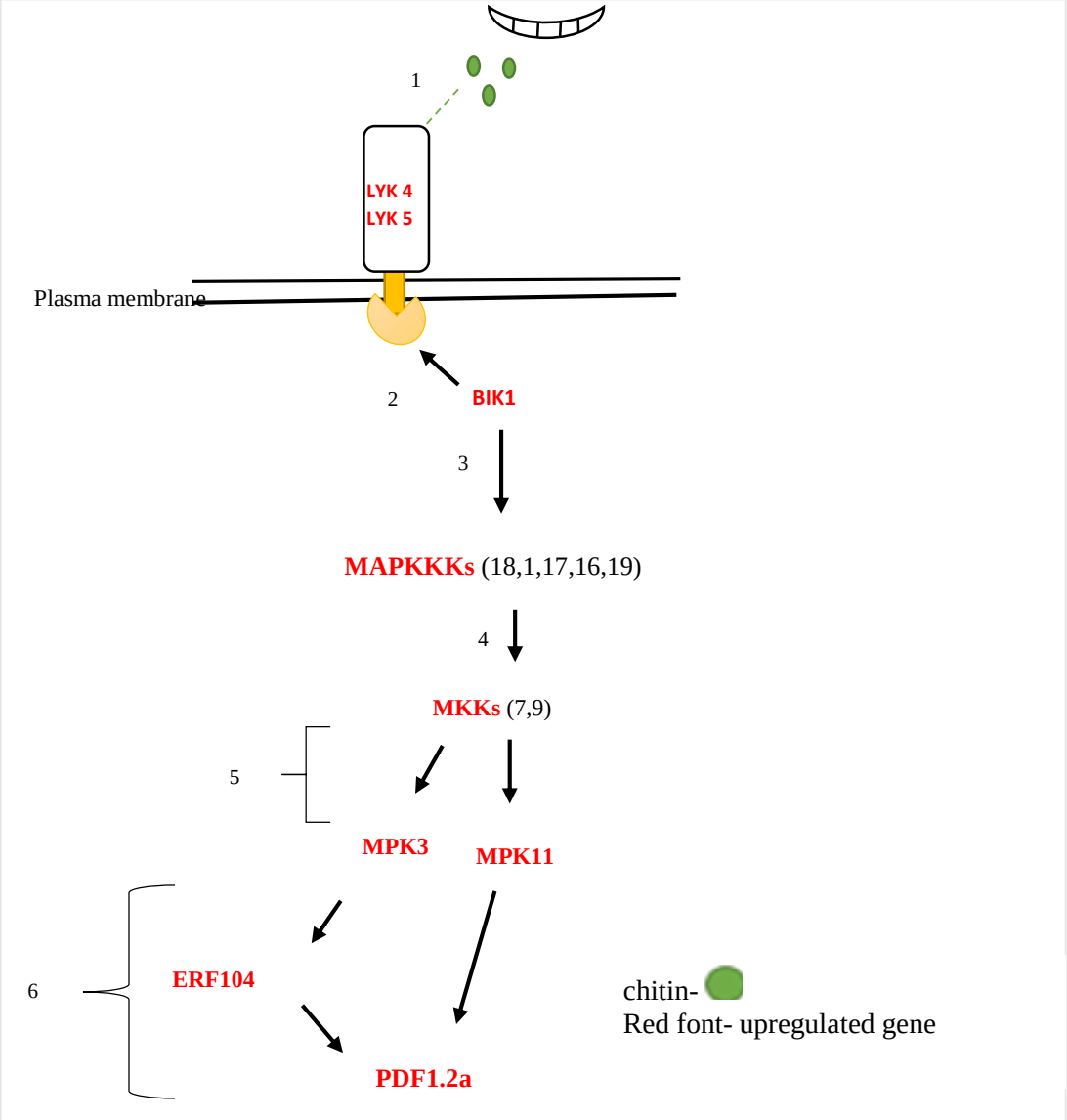

Figure 60:Schematic representation of activation of PDF1.2a by MAPK signalling pathway during PTI in Fusarium infected pistils as inferred from the transcriptome and literature.

(1) Chitin is recognized by LYK4/LYK5 receptor (2) BIK1 associates with LYK4/5 complex (3) to activate MAPK signal pathway (4). MAPKKK phosphorylate MKKs (5) and MKKs in turn phosphorylate MPK (6). MPK3 phosphorylate ERF104(6) which regulate PDF1.2 defence related gene, MPK11 is predicted to regulate PDF1.2 (6a).

6.4.2 PDF 2.2a is activated by apoplastic peroxidase

In the transcriptome data of the infected pistil, peroxidase encoding genes PRX33 and PRX34 responsible for ROS production were found to be upregulated (Table 6 in section 5.2.7). PRXs are important enzymes responsible for PTI via apoplastic peroxidase-dependent oxidative burst (Camejo et al. 2016). ROS are generated by apoplastic peroxidases in

recognition of PAMPs by pathogen recognition receptors (PRRs) (Camejo et al. 2016). ROS generated by peroxidase are involved in cell wall defence such as lignification, callose deposition and cell wall crosslinking (Camejo et al. 2016)(Figure 61). There is evidence that knockdown lines of the PRX33/PRX34 leads to the decreased expression of PDF2.2 and reduced levels of ROS (O'Brien et al. 2012; Camejo et al. 2016). This signifies that the PRX are involved in ROS production which acts as second messengers for the expression of PDF2.2(Figure 61).

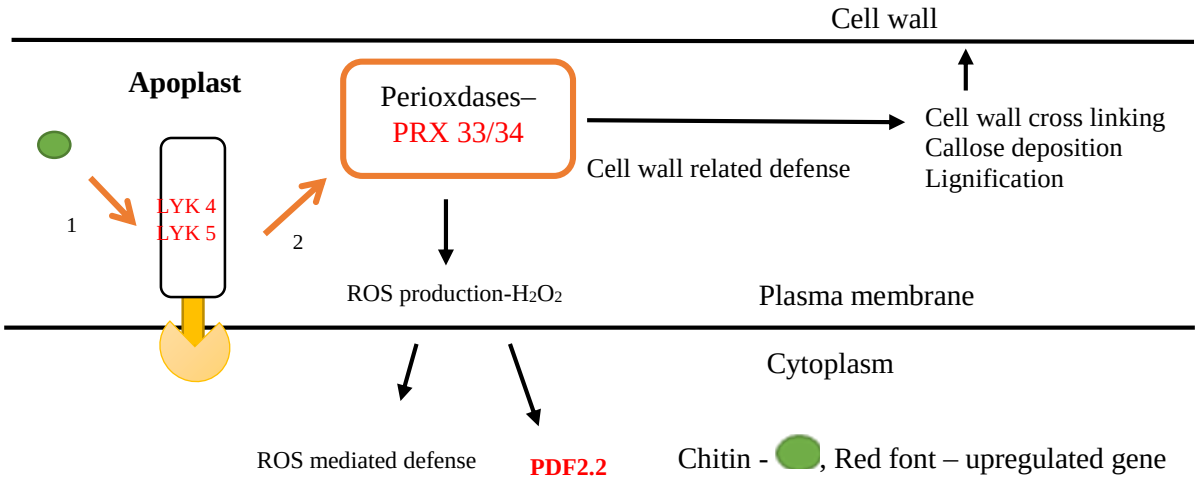

Figure 61:Schematic representation of activation of PDF2.2a and other defence mechanism by PRX 33/ 34 during PTI in *Fusarium* infected pistils as inferred from the transcriptome and literature.
(1) Chitin recognition by LYK4/5 complex (2) initiates PRX 33 and PRX34) in apoplastic as a defence response. ROS is produced by PRX which is involved in ROS mediated defence in cytoplasm and acts in regulation of PDF2.2. Perioxdases are also involved in cell wall related defence mechanism. Red font denotes the upregulated gene in infected pistil of our transcriptome data.

6.4.3 Eight DEFL genes are involved as defence response in PTI

In the infected pistil transcriptome, we identified eight DEFL genes that have been previously documented during PTI. For example, in a recent study, PDF1.2a, PDF1.2b, PDF1.2c, PDF1.4, PDF1.3, and LURE1.1 gene were found to differential expressed after inoculation with bacterial strain PtoDC3000hrcC (Tesfaye et al. 2013). These six genes were found to be differentially expressed in the transcriptome data of infected pistil (Table 6,7 in section 5.2). Five DEFL genes (PDF1.2a-c, PDF1.4, PDF1.3), that are confirmed to be involved in PTI, function downstream of the JA/ET defence signalling pathway. In addition, DEFL gene At2g43510 was found to be upregulated in our transcriptome data of the infected pistil (Appendix section 9.6). This gene has been previously reported to have co-regulating expression patterns with FRK1, PAMPs-inducible gene (Tesfaye et al. 2013). Similarly, PAMPs-inducible gene, PDF2.2 was observed to be downregulated in the transcriptome data

of infected pistil (Tables 6 and 7 in section 5.2). By using these data from the literature, a total number of eight DEFL genes including LURE1.1 found in our transcriptome data of the infected pistil can be confirmed to be involved in PTI defence in response against *F. graminearum.*

6.4.4 Possible role of DEFLs in proanthocyanidin mediated defence

Three DEFL genes that were upregulated in the transcriptomes of *A. thaliana* selfed and infected pistils (At4g15735, At1g13605, At3g43505) were found to be upregulated in seedstick (*stk*) mutant (Mizzotti et al. 2014). The expression of At3g43505 was found in central cell and had expression until 72HAP (Figure 22 in section 5.3.1). STK is a major regulator in the production of proanthocyanidins (PA) and in the accumulation of epicatechin monomer (Routaboul et al. 2006). PA are important for the pigmentation of the seeds and also have antimicrobial properties (Bais et al. 2003). The three upregulated DEFL genes are believed to be involved in biosynthesis flavonol the precursor of PA (Mizzotti et al. 2014). Epicatechin, part of the flavonol family, was found to confer resistance to fungus at higher concentrations (Ardi et al. 1998). Thus DEFL genes could be involved in PA-mediated defence and overexpression of these DEFLs gene could possibly result in resistance to fungal through PA mediated defence to seeds. Presence of DEFLs in seeds is vital because they come in direct contact with diverse soil-borne pathogens.

In conclusion, these findings signify the importance of DEFLs in plant immunity in the *Arabidopsis-Fusarium* interaction. The results obtained regarding DEFL expression in this *Arabidopsis-Fusarium* interaction, can be transferred to crops to generate new strategies for disease control. There are already precedents of successful transference of resistance to fungus conferred by recombinant defensins. For example, transgenic cotton plants constitutively expressing the NaD1 were found to have more resistance against the fungus *Verticillium dahlia* and *F. oxysporium* in field trials (Gaspar et al. 2014).

6.5 – Bifunctional role of At5g43285 in defence and reproduction

At5g43285 which encodes, LURE 1.1 was observed to be downregulated during infection with *F. graminearum* (Table 5 in section 6.2). LURE peptides are secreted by synergids to attract pollen tubes in a species-preferential manner to reach the female gametophyte (Takeuchi et al. 2012). At5g43285 gene was discussed in the previous chapter as being involved in PTI. This finding makes At5g43285 an interesting gene to be followed in the future due to the possibility of its bifunctional role in pollen tube attraction and plant defence. This hypothesis is supported by the similarity in the molecular mechanisms behind the fungal hyphae infection of plant tissue and the pollen tube growth during double fertilization. Similar to pollen tube growth, directional growth of fungal is controlled by a cytosolic Ca^{2+} gradient generated by Ca^{2+} channels localized in hyphal tip (Dauphin et al. 2007).

There have been evidence of genes having overlapping functions in the pollen tube reception and fungal invasion (Dresselhaus et al. 2009). Receptor-like kinase FERONIA (FER) was observed to be involved in pollen tube reception in synergids (Escobar-Restrepo et al. 2007), in addition it was found to mediate compatible interaction between plant cells and powdery mildew (PM) hyphae. The *fer* homozygous mutants exhibited resistance to biotrophic *Erysiphe orontii* and also pollen tube reception was affected (Kessler et al. 2010). Additionally, in synergids, FER initiates NORTIA (NTA), a mildew-resistant locus O (MLO) protein for pollen tube growth arrest and burst (Kessler et al. 2010). NTA was initially recognized in mediating PM susceptibility via Ca^{2+-} dependent CaM to suppress defence in cereal (Kim et al. 2002). These two genes point to the interesting connection between PT reception and fungal invasion.

In addition, FER appears to control the production of ROS in the female gametophyte during pollen tube rupture and sperm release (Duan et al. 2010; van der Weerden. et al. 2010). Signalling molecules secreted by the synergids modulates signalling cascades of pollen tubes to generate an excess of ROS leading to simultaneously pollen tube burst and synergid cell death. Since pollen tube and fungal invasion have similar molecular mechanisms, we can hypothesize that ROS induced cell death could be a possible mechanism for LURE peptides against fungi. Such phenomenon has been observed by defensin NaD1 for triggering ROS induced cell death in *Candida albicans* (van der Weerden. et al. 2010). Ca^{2+} signalling is the second important molecular player occurring both in reproductive and defensive signalling mechanisms. The arrival of pollen tube triggers an oscillation of cytoplasmic Ca^{2+} in synergids which is similar to cytoplasmic increase of Ca^{2+} during early signalling for cell

death (Levy et al. 2004; Iwano et al. 2012). Ca^{2+} signalling has been reported to play an important role during pollen tube contact and rupture of its content into female gametophyte (Iwano et al. 2012; Denninger et al. 2014; Duan et al. 2010). The Ca^{2+} influx plays an important role in the promotion of ROS burst. There are examples of several defensins in other plant species such as Rs-AFP2 and Dm-AMP1 inhibiting the growth of *Neurospora crassa* via gradient change by influx of Ca^{2+} (Vriens et al. 2014). Therefore, these data demonstrate the importance of ROS and Ca^{2+}, signalling it is vital for pollen tube interaction and fungal reception. Thus we can hypothesis that LURE 1.1 peptides could either have ROS and Ca^{2+} signalling mechanism as part of their antifungal activity**.**

There has been evidences of bifunctional role in defensins such as tomato defensin DEF2 which regulates pollen grain development and is involved in resistance to *Botrytis cinerea* (Stotz et al. 2009). Overexpression of ZmES4 peptides, which are involved in pollen tube burst, were also found to exhibit antifungal properties against *Peronospora* parasitica (Amien et al. 2010). This data supports the proposal LURE1.1 has bifunctional roles in microphylar guidance of pollen tube towards ovule and its induced as part of the immune response to a fungal pathogen.

6.6 Perspectives

The candidate DEFLs investigated in this dissertation are predominantly expressed in the embryo sac, which suggests they encode peptides involved in protecting the ovule and developing seeds from pathogens and might participate in the cell-to-cell communication during fertilization. Additionally, the importance of DEFLs in reproduction was shown through by their patterns of expression obtained from eGFP quantification studies and qPCR analysis of pistils during pollination. Further studies of the candidate DEFL genes are necessary to determine their specific role in reproduction and defence. This can be addressed by using knock down RNAi lines or CRISPR/Cas9-gRNA complex for genome editing.

At5g38330 (PDF3.1) and At1g60985 can be considered as top candidates for further studies. Both of them were found to be downregulated in the transcriptome data of infected pistil and were found to be specifically localized in the central cell of the ovule and also expressed during early endosperm development events (Table 8 in section 5.2). The main argument for choosing them is their possible role in central cell mediated guidance of the pollen tube as suggested by their downregulation in in *ccg* mutants. RNAi lines were created for PDF3.1 along with its most similar paralogs, including At4g30074 and At4g30070 in order to understand their role in infection and reproduction. Further analysis of this RNAi line was not continued due to the lack of time, so this would be a good starting point for further analysis.

Another interesting hypothesis derived from the analysis of transcriptomic data and marker lines is the possible involvement of LURE1.1 in both reproduction and defence response. An initial approach to test this possibility would be to synthesize LURE1.1 and determine whether it inhibits fungal growth and if this effect is associated to triggering the release of reactive oxygen species.

Most candidate DEFL genes were found to be expressed in the central cell and were predicted to be co-regulated with those expressed along in the synergids, suggesting they might participate in pollen tube guidance and preventing the entry of second pollen tube after fertilization. In order to test this scenario live cell imaging analysis of a central-cell-specific DEFL marker genes would enable us to shed more insight into their actual role in cell-cell communication during fertilization.

Expression of six DEFLs, including At5g38330, was identified in roots using eGFP marker lines. These lines are a valuable resource to further investigate the role of these candidates in root development as well as their possible involvement in pathogen resistance.

Using the transcriptome data of the infected pistil, several new insights were obtained regarding *Arabidopsis -Fusarium* interaction, such as the negative effect of nectrophic *Fusarium* on seed set and the mycotoxin-mediated manipulation of the plant immune response. In this subject, the most important finding was the identification of eight DEFL genes as part of the defence response in PTI. These candidates should be further explored in functional analysis to test their role in plant immunity.

By understanding the molecular players behind DEFL gene function in the plant immune response to *F. graminearum* infection, it will be possible to develop strategies to improve cereal crop productivity and ensure that fungal mycotoxins do not threaten food and feed safety.

Altogether, the results obtained in this work indicate the importance of DEFLs in two highly conserved process, reproduction and defence and by understanding the participation of DEFLs in both processes it will be possible to improve crop productivity for food, fibre and biofuels production.

7. Publication

Parts of this work have been submitted for publication in the following manuscript:

Mondragón-Palomino, M; John-Arputharaj, A; Pallmann, M; Spalvins, K; Dresselhaus, T (in review): Similarities between reproductive and immune processes in the pistil of *Arabidopsis* species.

8. Bibliography

Aerts, A; Bammens, L; Govaert, G; Carmona-Gutierrez, D; Madeo, F; Cammue, B; Thevissen, K (2011): The Antifungal Plant Defensin HsAFP1 from Heuchera sanguinea Induces Apoptosis in Candida albicans. In *Frontiers in microbiology* 2, p. 47. DOI: 10.3389/fmicb.2011.00047.

Amien, S; Kliwer, I; Marton, M; Debener, T; Geiger, D; Becker, D; Dresselhaus, T (2010): Defensin-like ZmES4 mediates pollen tube burst in maize via opening of the potassium channel KZM1. In *PLoS biology* 8 (6), e1000388. DOI: 10.1371/journal.pbio.1000388.

Ardi, R; Kobiler, I; Jacoby, B; Keen, N; Prusky, D (1998): Involvement of epicatechin biosynthesis in the activation of the mechanism of resistance of avocado fruits toColletotrichum gloeosporioides. In *Physiological and Molecular Plant Pathology* 53 (5-6), pp. 269–285. DOI: 10.1006/pmpp.1998.0181.

Bais, H; Vepachedu, R; Gilroy, S; Callaway, R; Vivanco, J (2003): Allelopathy and exotic plant invasion: from molecules and genes to species interactions. In *Science (New York, N.Y.)* 301 (5638), pp. 1377–1380. DOI: 10.1126/science.1083245.

Berger, F; Hamamura, Y; Ingouff, M; Higashiyama, T (2008): Double fertilization - caught in the act. In *Trends in plant science* 13 (8), pp. 437–443. DOI: 10.1016/j.tplants.2008.05.011.

Bethke, G; Pecher, P; Eschen-Lippold, L; Tsuda, K; Katagiri, F; Glazebrook, J; Scheel, D; Lee, J (2012): Activation of the Arabidopsis thaliana mitogen-activated protein kinase MPK11 by the flagellin-derived elicitor peptide, flg22. In *Molecular plant-microbe interactions : MPMI* 25 (4), pp. 471–480. DOI: 10.1094/MPMI-11-11-0281.

Bethke, G; Scheel, D; Lee, J (2009): Sometimes new results raise new questions: the question marks between mitogen-activated protein kinase and ethylene signaling. In *Plant Signaling & Behavior* 4 (7), pp. 672–674. DOI: 10.1073/pnas.0810206106.

Bigeard, J; Colcombet, J; Hirt, H (2015): Signaling mechanisms in pattern-triggered immunity (PTI). In *Molecular plant* 8 (4), pp. 521–539. DOI: 10.1016/j.molp.2014.12.022.

Bleckmann, A; Alter, S; Dresselhaus, T (2014): The beginning of a seed: regulatory mechanisms of double fertilization. In *Frontiers in plant science* 5, p. 452. DOI: 10.3389/fpls.2014.00452.

Boavida, L; Borges, F; Becker, J; Feijo, J (2011): Whole genome analysis of gene expression reveals coordinated activation of signaling and metabolic pathways during pollen-pistil interactions in Arabidopsis. In *Plant physiology* 155 (4), pp. 2066–2080. DOI: 10.1104/pp.110.169813.

Boavida, L; McCormick, S (2007): Temperature as a determinant factor for increased and reproducible in vitro pollen germination in Arabidopsis thaliana. In *The Plant journal : for cell and molecular biology* 52 (3), pp. 570–582. DOI: 10.1111/j.1365-313X.2007.03248.x.

Boenisch, M; Schafer, W (2011): Fusarium graminearum forms mycotoxin producing infection structures on wheat. In *BMC plant biology* 11, p. 110. DOI: 10.1186/1471-2229-11-110.

Boggs, N; Nasrallah, J; Nasrallah, M (2009): Independent S-locus mutations caused self-fertility in Arabidopsis thaliana. In *PLoS genetics* 5 (3), e1000426. DOI: 10.1371/journal.pgen.1000426.

Brewer, H; Hammond-Kosack, K (2015): Host to a Stranger: Arabidopsis and Fusarium Ear Blight. In *Trends in plant science* 20 (10), pp. 651–663. DOI: 10.1016/j.tplants.2015.06.011.

Brown, N; Urban, M; van de Meene, A; Hammond-Kosack, K (2010): The infection biology of Fusarium graminearum: defining the pathways of spikelet to spikelet colonisation in wheat ears. In *Fungal biology* 114 (7), pp. 555–571. DOI: 10.1016/j.funbio.2010.04.006.

Camejo, D; Guzman-Cedeno, A; Moreno, A (2016): Reactive oxygen species, essential molecules, during plant-pathogen interactions. In *Plant physiology and biochemistry : PPB / Societe francaise de physiologie vegetale* 103, pp. 10–23. DOI: 10.1016/j.plaphy.2016.02.035.

Carvalho, A; Gomes, V (2009): Plant defensins--prospects for the biological functions and biotechnological properties. In *Peptides* 30 (5), pp. 1007–1020. DOI: 10.1016/j.peptides.2009.01.018.

Chen, Y-H; Li, H-J; Shi, D-Q; Yuan, L; Liu, J; Sreenivasan, R; Baskar, R; Grossniklaus, U; Yang, W-C (2007): The central cell plays a critical role in pollen tube guidance in Arabidopsis. In *The Plant cell* 19 (11), pp. 3563–3577. DOI: 10.1105/tpc.107.053967.

Clauss, M; Koch, M (2006): Poorly known relatives of Arabidopsis thaliana. In *Trends in plant science* 11 (9), pp. 449–459. DOI: 10.1016/j.tplants.2006.07.005.

Covey, P; Subbaiah, C; Parsons, R; Pearce, G; Lay, F; Anderson, M; Ryan, C; Bedinger, P (2010): A pollen-specific RALF from tomato that regulates pollen tube elongation. In *Plant physiology* 153 (2), pp. 703–715. DOI: 10.1104/pp.110.155457.

Dauphin, A; Gerard, J; Lapeyrie, F; Legue, V (2007): Fungal hypaphorine reduces growth and induces cytosolic calcium increase in root hairs of Eucalyptus globulus. In *Protoplasma* 231 (1-2), pp. 83–88. DOI: 10.1007/s00709-006-0240-9.

Denninger, P; Bleckmann, A; Lausser, A; Vogler, F; Ott, T; Ehrhardt, D; Frommer, W; Sprunck, S; Dresselhaus, T; Grossmann, G (2014): Male-female communication triggers calcium signatures during fertilization in Arabidopsis. In *Nature communications* 5, p. 4645. DOI: 10.1038/ncomms5645.

Diamond, M; Reape, T; Rocha, O; Doyle, S; Kacprzyk, J; Doohan, F; McCabe, P (2013): The fusarium mycotoxin deoxynivalenol can inhibit plant apoptosis-like programmed cell death. In *PloS one* 8 (7), e69542. DOI: 10.1371/journal.pone.0069542.

Ding, L; Xu, H; Yi, H; Yang, L; Kong, Z; Zhang, L; Xue, S; Jia, H; Ma, Z (2011): Resistance to hemi-biotrophic F. graminearum infection is associated with coordinated and ordered expression of diverse defense signaling pathways. In *PloS one* 6 (4), e19008. DOI: 10.1371/journal.pone.0019008.

Divon, H; Fluhr, R (2007): Nutrition acquisition strategies during fungal infection of plants. In *FEMS microbiology letters* 266 (1), pp. 65–74. DOI: 10.1111/j.1574-6968.2006.00504.x.

Dodds, P; Rathjen, J (2010): Plant immunity: towards an integrated view of plant-pathogen interactions. In *Nature reviews. Genetics* 11 (8), pp. 539–548. DOI: 10.1038/nrg2812.

Dresselhaus, T; Franklin-Tong, N (2013): Male-female crosstalk during pollen germination, tube growth and guidance, and double fertilization. In *Molecular plant* 6 (4), pp. 1018–1036. DOI: 10.1093/mp/sst061.

Dresselhaus, T; Marton, M (2009): Micropylar pollen tube guidance and burst: adapted from defense mechanisms? In *Current opinion in plant biology* 12 (6), pp. 773–780. DOI: 10.1016/j.pbi.2009.09.015.

Dresselhaus, T; Sprunck, S; Wessel, G (2016): Fertilization Mechanisms in Flowering Plants. In *Current biology : CB* 26 (3), R125-39. DOI: 10.1016/j.cub.2015.12.032.

Drews, G; Koltunow, A (2011): The female gametophyte. In *The Arabidopsis book* 9, e0155. DOI: 10.1199/tab.0155.

Duan, Q; Kita, D; Li, C; Cheung, A; Wu, H-M (2010): FERONIA receptor-like kinase regulates RHO GTPase signaling of root hair development. In *Proceedings of the National Academy of Sciences of the United States of America* 107 (41), pp. 17821–17826. DOI: 10.1073/pnas.1005366107.

Eckardt, N (2007): Elucidating the Function of Synergid Cells. A Regulatory Role for MYB98. In *THE PLANT CELL ONLINE* 19 (8), pp. 2320–2321. DOI: 10.1105/tpc.107.055640.

Escobar-Restrepo, J-M; Huck, N; Kessler, S; Gagliardini, V; Gheyselinck, J; Yang, W-C; Grossniklaus, U (2007): The FERONIA receptor-like kinase mediates male-female interactions during

pollen tube reception. In *Science (New York, N.Y.)* 317 (5838), pp. 656–660. DOI: 10.1126/science.1143562.

Fagundes, D; Bohn, B; Cabreira, C; Leipelt, F; Dias, N; Bodanese-Zanettini, M; Cagliari, A (2015): Caspases in plants: metacaspase gene family in plant stress responses. In *Functional & integrative genomics* 15 (6), pp. 639–649. DOI: 10.1007/s10142-015-0459-7.

Gaspar, Y; McKenna, J; McGinness, B; Hinch, J; Poon, S; Connelly, A; Anderson, M; Heath, R (2014): Field resistance to Fusarium oxysporum and Verticillium dahliae in transgenic cotton expressing the plant defensin NaD1. In *Journal of experimental botany* 65 (6), pp. 1541–1550. DOI: 10.1093/jxb/eru021.

Gaudet, D; Laroche, A; Frick, M; Huel, R; Puchalski, B (2003): Cold induced expression of plant defensin and lipid transfer protein transcripts in winter wheat. In *Physiol Plant* 117 (2), pp. 195–205. DOI: 10.1034/j.1399-3054.2003.00041.x.

Glazebrook, J (2005): Contrasting mechanisms of defense against biotrophic and necrotrophic pathogens. In *Annual review of phytopathology* 43, pp. 205–227. DOI: 10.1146/annurev.phyto.43.040204.135923.

Green, M; Sambrook, J (2012): Molecular cloning. A laboratory manual. 4th ed. / Michael R. Green, Joseph Sambrook. Cold Spring Harbor, N.Y.: Cold Spring Harbor Laboratory Press.

Grundt, H; Kjolner, S; Borgen, L; Rieseberg, L; Brochmann, C (2006): High biological species diversity in the arctic flora. In *Proceedings of the National Academy of Sciences of the United States of America* 103 (4), pp. 972–975. DOI: 10.1073/pnas.0510270103.

Guan, Y; Lu, J; Xu, J; McClure, B; Zhang, S (2014): Two Mitogen-Activated Protein Kinases, MPK3 and MPK6, Are Required for Funicular Guidance of Pollen Tubes in Arabidopsis. In *Plant physiology* 165 (2), pp. 528–533. DOI: 10.1104/pp.113.231274.

Hamamura, Y; Nagahara, S; Higashiyama, T (2012): Double fertilization on the move. In *Current opinion in plant biology* 15 (1), pp. 70–77. DOI: 10.1016/j.pbi.2011.11.001.

Han, Y; Huang, B; Zee, S; Yuan, M (2000): Symplastic communication between the central cell and the egg apparatus cells in the embryo sac of Torenia fournieri Lind. before and during fertilization. In *Planta* 211 (1), pp. 158–162. DOI: 10.1007/s004250000289.

Hara-Nishimura, I; Hatsugai, N; Nakaune, S; Kuroyanagi, M; Nishimura, M (2005): Vacuolar processing enzyme: an executor of plant cell death. In *Current opinion in plant biology* 8 (4), pp. 404–408. DOI: 10.1016/j.pbi.2005.05.016.

Hatsugai, N; Yamada, K; Goto-Yamada, S; Hara-Nishimura, I (2015): Vacuolar processing enzyme in plant programmed cell death. In *Frontiers in plant science* 6, p. 234. DOI: 10.3389/fpls.2015.00234.

Hayes, B; Bleackley, M; Wiltshire, J; Anderson, M; Traven, A; van der Weerden, Nicole L. (2013): Identification and mechanism of action of the plant defensin NaD1 as a new member of the antifungal drug arsenal against Candida albicans. In *Antimicrobial agents and chemotherapy* 57 (8), pp. 3667–3675. DOI: 10.1128/AAC.00365-13.

Hegedus, N; Marx, F (2013): Antifungal proteins: More than antimicrobials? In *Fungal Biology Reviews* 26 (4), pp. 132–145. DOI: 10.1016/j.fbr.2012.07.002.

Hoefle, C; Huesmann, C; Schultheiss, H; Bornke, F; Hensel, G; Kumlehn, J; Huckelhoven, R (2011): A barley ROP GTPase ACTIVATING PROTEIN associates with microtubules and regulates entry of the barley powdery mildew fungus into leaf epidermal cells. In *The Plant cell* 23 (6), pp. 2422–2439. DOI: 10.1105/tpc.110.082131.

Hruz, T; Laule, O; Szabo, G; Wessendorp, F; Bleuler, S; Oertle, L; Widmayer, P; Gruissem, W; Zimmermann, P (2008): Genevestigator v3: a reference expression database for the meta-analysis of transcriptomes. In *Advances in bioinformatics* 2008, p. 420747. DOI: 10.1155/2008/420747.

Huang, Q; Dresselhaus, T; Gu, H; Qu, L-J (2015): Active role of small peptides in Arabidopsis reproduction: Expression evidence. In *Journal of integrative plant biology* 57 (6), pp. 518–521. DOI: 10.1111/jipb.12356.

Incarbone, M; Dunoyer, P (2013): RNA silencing and its suppression: novel insights from in planta analyses. In *Trends in plant science* 18 (7), pp. 382–392. DOI: 10.1016/j.tplants.2013.04.001.

Iwano, M; Ngo, Q; Entani, T; Shiba, H; Nagai, T; Miyawaki, A; Isogai, A; Grossniklaus, U; Takayama, S (2012): Cytoplasmic Ca2+ changes dynamically during the interaction of the pollen tube with synergid cells. In *Development (Cambridge, England)* 139 (22), pp. 4202–4209. DOI: 10.1242/dev.081208.

Jansen, C; Wettstein, D von; Schafer, W; Kogel, K-H; Felk, A; Maier, F (2005): Infection patterns in barley and wheat spikes inoculated with wild-type and trichodiene synthase gene disrupted Fusarium graminearum. In *Proceedings of the National Academy of Sciences of the United States of America* 102 (46), pp. 16892–16897. DOI: 10.1073/pnas.0508467102.

Janssen, B-J; Gardner, R (1990): Localized transient expression of GUS in leaf discs following cocultivation with Agrobacterium. In *Plant Mol Biol* 14 (1), pp. 61–72. DOI: 10.1007/BF00015655.

Jha, S; Chattoo, B (2010): Expression of a plant defensin in rice confers resistance to fungal phytopathogens. In *Transgenic research* 19 (3), pp. 373–384. DOI: 10.1007/s11248-009-9315-7.

Johnson, M; Bender, J (2009): Reprogramming the epigenome during germline and seed development. In *Genome biology* 10 (8), p. 232. DOI: 10.1186/gb-2009-10-8-232.

Jones, J; Dangl, J (2006): The plant immune system. In *Nature* 444 (7117), pp. 323–329. DOI: 10.1038/nature05286.

Jones-Rhoades, M; Borevitz, J; Preuss, D (2007): Genome-wide expression profiling of the Arabidopsis female gametophyte identifies families of small, secreted proteins. In *PLoS genetics* 3 (10), pp. 1848–1861. DOI: 10.1371/journal.pgen.0030171.

Kagi, C; Baumann, N; Nielsen, N; Stierhof, Y-D; Gross-Hardt, R (2010): The gametic central cell of Arabidopsis determines the lifespan of adjacent accessory cells. In *Proceedings of the National Academy of Sciences of the United States of America* 107 (51), pp. 22350–22355. DOI: 10.1073/pnas.1012795108.

Kanaoka, M; Higashiyama, T (2015): Peptide signaling in pollen tube guidance. In *Current opinion in plant biology* 28, pp. 127–136. DOI: 10.1016/j.pbi.2015.10.006.

Kannan, P; Pandey, D; Gupta, A; Punetha, H; Taj, G; Kumar, A (2012): Expression analysis of MAP2K9 and MAPK6 during pathogenesis of Alternaria blight in Arabidopsis thaliana ecotype Columbia. In *Molecular biology reports* 39 (4), pp. 4439–4444. DOI: 10.1007/s11033-011-1232-1.

Kanzaki, H; Nirasawa, S; Saitoh, H; Ito, M; Nishihara, M; Terauchi, R; Nakamura, I (2002): Overexpression of the wasabi defensin gene confers enhanced resistance to blast fungus (Magnaporthe grisea) in transgenic rice. In *TAG. Theoretical and applied genetics. Theoretische und angewandte Genetik* 105 (6-7), pp. 809–814. DOI: 10.1007/s00122-001-0817-9.

Kaur, J; Thokala, M; Robert-Seilaniantz, A; Zhao, P; Peyret, H; Berg, H; Pandey, S; Jones, J; Shah, D (2012): Subcellular targeting of an evolutionarily conserved plant defensin MtDef4.2 determines the outcome of plant-pathogen interaction in transgenic Arabidopsis. In *Molecular plant pathology* 13 (9), pp. 1032–1046. DOI: 10.1111/j.1364-3703.2012.00813.x.

Kazan, K; Gardiner, D; Manners, J (2012): On the trail of a cereal killer: recent advances in Fusarium graminearum pathogenomics and host resistance. In *Molecular plant pathology* 13 (4), pp. 399–413. DOI: 10.1111/j.1364-3703.2011.00762.x.

Kessler, S; Shimosato-Asano, H; Keinath, N; Wuest, S; Ingram, G; Panstruga, R; Grossniklaus, U (2010): Conserved molecular components for pollen tube reception and fungal invasion. In *Science (New York, N.Y.)* 330 (6006), pp. 968–971. DOI: 10.1126/science.1195211.

Khonga, E; Sutton, J (1988): Inoculum production and survival of Gibberella zeae in maize and wheat residues. In *Canadian Journal of Plant Pathology* 10 (3), pp. 232–239. DOI: 10.1080/07060668809501730.

Kikot, G; Hours, R; Alconada, T (2009): Contribution of cell wall degrading enzymes to pathogenesis of Fusarium graminearum: a review. In *Journal of basic microbiology* 49 (3), pp. 231–241. DOI: 10.1002/jobm.200800231.

Kim, K-C; Fan, B; Chen, Z (2006): Pathogen-induced Arabidopsis WRKY7 is a transcriptional repressor and enhances plant susceptibility to Pseudomonas syringae. In *Plant physiology* 142 (3), pp. 1180–1192. DOI: 10.1104/pp.106.082487.

Kim, M; Panstruga, R; Elliott, C; Muller, J; Devoto, A; Yoon, H; Park, H; Cho, M; Schulze-Lefert, P (2002): Calmodulin interacts with MLO protein to regulate defence against mildew in barley. In *Nature* 416 (6879), pp. 447–451. DOI: 10.1038/416447a.

Krohn, N; Lausser, A; Juranic, M; Dresselhaus, T (2012): Egg cell signaling by the secreted peptide ZmEAL1 controls antipodal cell fate. In *Developmental cell* 23 (1), pp. 219–225. DOI: 10.1016/j.devcel.2012.05.018.

Lacerda, A; Vasconcelos, E; Pelegrini, P; Grossi de Sa, M (2014): Antifungal defensins and their role in plant defense. In *Frontiers in microbiology* 5, p. 116. DOI: 10.3389/fmicb.2014.00116.

Lay, F; Anderson, M (2005): Defensins - Components of the Innate Immune System in Plants. In *CPPS* 6 (1), pp. 85–101. DOI: 10.2174/1389203053027575.

Lay, F; Poon, S; McKenna, J; Connelly, A; Barbeta, B; McGinness, B; Fox, J; Daly, N; Craik, D; Heath, R; Anderson, M (2014): The C-terminal propeptide of a plant defensin confers cytoprotective and subcellular targeting functions. In *BMC plant biology* 14, p. 41. DOI: 10.1186/1471-2229-14-41.

Leplat, J; Friberg, H; Abid, M; Steinberg, C (2013): Survival of Fusarium graminearum, the causal agent of Fusarium head blight. A review. In *Agron. Sustain. Dev.* 33 (1), pp. 97–111. DOI: 10.1007/s13593-012-0098-5.

Levy, J; Bres, C; Geurts, R; Chalhoub, B; Kulikova, O; Duc, G; Journet, E-P; Ane, J-M; Lauber, E; Bisseling, T et al. (2004): A putative Ca2+ and calmodulin-dependent protein kinase required for bacterial and fungal symbioses. In *Science (New York, N.Y.)* 303 (5662), pp. 1361–1364. DOI: 10.1126/science.1093038.

Li, H-J; Zhu, S-S; Zhang, M-X; Wang, T; Liang, L; Xue, Y; Shi, D-Q; Liu, J; Yang, W-C (2015): Arabidopsis CBP1 Is a Novel Regulator of Transcription Initiation in Central Cell-Mediated Pollen Tube Guidance. In *The Plant cell* 27 (10), pp. 2880–2893. DOI: 10.1105/tpc.15.00370.

Loraine, A; McCormick, S; Estrada, A; Patel, K; Qin, P (2013): RNA-seq of Arabidopsis pollen uncovers novel transcription and alternative splicing. In *Plant physiology* 162 (2), pp. 1092–1109. DOI: 10.1104/pp.112.211441.

Makandar, R; Nalam, V; Chaturvedi, R; Jeannotte, R; Sparks, A; Shah, J (2010): Involvement of salicylate and jasmonate signaling pathways in Arabidopsis interaction with Fusarium graminearum. In *Molecular plant-microbe interactions : MPMI* 23 (7), pp. 861–870. DOI: 10.1094/MPMI-23-7-0861.

Marshall, E; Costa, L; Gutierrez-Marcos, J (2011): Cysteine-rich peptides (CRPs) mediate diverse aspects of cell-cell communication in plant reproduction and development. In *Journal of experimental botany* 62 (5), pp. 1677–1686. DOI: 10.1093/jxb/err002.

Marty, F (1999): Plant Vacuoles. In *The Plant cell* 11 (4), p. 587. DOI: 10.2307/3870886.

Maruyama, D; Volz, R; Takeuchi, H; Mori, T; Igawa, T; Kurihara, D; Kawashima, T; Ueda, M; Ito, M; Umeda, M et al. (2015): Rapid Elimination of the Persistent Synergid through a Cell Fusion Mechanism. In *Cell* 161 (4), pp. 907–918. DOI: 10.1016/j.cell.2015.03.018.

Mary, W; Zhensheng, K; Buchenauer, H (2002). In *European Journal of Plant Pathology* 108 (8), pp. 803–810. DOI: 10.1023/A:1020847216155.

Meng, X; Xu, J; He, Y; Yang, K-Y; Mordorski, B; Liu, Y; Zhang, S (2013): Phosphorylation of an ERF transcription factor by Arabidopsis MPK3/MPK6 regulates plant defense gene induction and fungal resistance. In *The Plant cell* 25 (3), pp. 1126–1142. DOI: 10.1105/tpc.112.109074.

Mith, O; Benhamdi, A; Castillo, T; Berge, M; MacDiarmid, C; Steffen, J; Eide, D; Perrier, V; Subileau, M; Gosti, F et al. (2015): The antifungal plant defensin AhPDF1.1b is a beneficial factor involved in adaptive response to zinc overload when it is expressed in yeast cells. In *MicrobiologyOpen* 4 (3), pp. 409–422. DOI: 10.1002/mbo3.248.

Mizzotti, C; Ezquer, I; Paolo, D; Rueda-Romero, P; Guerra, R; Battaglia, R; Rogachev, I; Aharoni, A; Kater, M; Caporali, E; Colombo, L (2014): SEEDSTICK is a master regulator of development and metabolism in the Arabidopsis seed coat. In *PLoS genetics* 10 (12), e1004856. DOI: 10.1371/journal.pgen.1004856.

Mondragón-Palomino, M; John-Arputharaj, A; Pallmann, M; Spalvins, K; Dresselhaus, T (in review): Similarities between reproductive and immune processes in the pistil of Arabidopsis species.

Morato do Canto, A; Ceciliato, P; Ribeiro, B; Ortiz Morea, F; Franco Garcia, A; Silva-Filho, M; Moura, D (2014): Biological activity of nine recombinant AtRALF peptides: implications for their perception and function in Arabidopsis. In *Plant physiology and biochemistry : PPB* 75, pp. 45–54. DOI: 10.1016/j.plaphy.2013.12.005.

Murphy, E; Smet, I de (2014): Understanding the RALF family: a tale of many species. In *Trends in plant science* 19 (10), pp. 664–671. DOI: 10.1016/j.tplants.2014.06.005.

Nalam, V; Alam, S; Keereetaweep, J; Venables, B; Burdan, D; Lee, H; Trick, H; Sarowar, S; Makandar, R; Shah, J (2015): Facilitation of Fusarium graminearum Infection by 9-Lipoxygenases in Arabidopsis and Wheat. In *Molecular plant-microbe interactions : MPMI* 28 (10), pp. 1142–1152. DOI: 10.1094/MPMI-04-15-0096-R.

Nam, J (1999): Identification of T-DNA tagged Arabidopsis mutants that are resistant to transformation by Agrobacterium. In *Molecular and General Genetics MGG* 261 (3), pp. 429–438. DOI: 10.1007/s004380050985.

Nawaschin (1898): Resultate einer Revision der Befruchtungsvorgänge bei Lilium martagon und Fritillaria tenella. In *Bulletin de l'Académie Impériale des Sciences* 9 (4), pp. 377–382.

O'Brien, J; Daudi, A; Finch, P; Butt, V; Whitelegge, J; Souda, P; Ausubel, F; Bolwell, G (2012): A peroxidase-dependent apoplastic oxidative burst in cultured Arabidopsis cells functions in MAMP-elicited defense. In *Plant physiology* 158 (4), pp. 2013–2027. DOI: 10.1104/pp.111.190140.

Olivieri, F; Eugenia Zanetti, M; Oliva, C; Covarrubias, A; Casalongué, C (2002). In *European Journal of Plant Pathology* 108 (1), pp. 63–72. DOI: 10.1023/A:1013920929965.

Paper, J; Scott-Craig, J; Adhikari, N; Cuomo, C; Walton, J (2007): Comparative proteomics of extracellular proteins in vitro and in planta from the pathogenic fungus Fusarium graminearum. In *Proteomics* 7 (17), pp. 3171–3183. DOI: 10.1002/pmic.200700184.

Paul, P; El-Allaf, S; Lipps, P; Madden, L (2004): Rain Splash Dispersal of Gibberella zeae Within Wheat Canopies in Ohio. In *Phytopathology* 94 (12), pp. 1342–1349. DOI: 10.1094/PHYTO.2004.94.12.1342.

Pekkarinen, A; Jones, B (2002): Trypsin-Like Proteinase Produced by Fusarium culmorum Grown on Grain Proteins. In *J. Agric. Food Chem.* 50 (13), pp. 3849–3855. DOI: 10.1021/jf020027x.

Penninckx, I; Eggermont, K; Schenk, P; van den Ackerveken, G; Cammue, B; Thomma, B (2003): The Arabidopsis mutant iop1 exhibits induced over-expression of the plant defensin gene PDF1.2 and enhanced pathogen resistance. In *Molecular plant pathology* 4 (6), pp. 479–486. DOI: 10.1046/j.1364-3703.2003.00193.x.

Poppenberger, B; Berthiller, F; Lucyshyn, D; Sieberer, T; Schuhmacher, R; Krska, R; Kuchler, K; Glossl, J; Luschnig, C; Adam, G (2003): Detoxification of the Fusarium mycotoxin deoxynivalenol by a UDP-glucosyltransferase from Arabidopsis thaliana. In *The Journal of biological chemistry* 278 (48), pp. 47905–47914. DOI: 10.1074/jbc.M307552200.

Qiang, X; Zechmann, B; Reitz, M; Kogel, K-H; Schafer, P (2012): The mutualistic fungus Piriformospora indica colonizes Arabidopsis roots by inducing an endoplasmic reticulum stress-triggered caspase-dependent cell death. In *The Plant cell* 24 (2), pp. 794–809. DOI: 10.1105/tpc.111.093260.

Ramamoorthy, V; Zhao, X; Snyder, A; Xu, J-R; Shah, D (2007): Two mitogen-activated protein kinase signalling cascades mediate basal resistance to antifungal plant defensins in Fusarium graminearum. In *Cellular microbiology* 9 (6), pp. 1491–1506. DOI: 10.1111/j.1462-5822.2006.00887.x.

Robinson, M; McCarthy, D; Smyth, G (2010): edgeR: a Bioconductor package for differential expression analysis of digital gene expression data. In *Bioinformatics (Oxford, England)* 26 (1), pp. 139–140. DOI: 10.1093/bioinformatics/btp616.

Rocha, O; Ansari, K; Doohan, F (2005): Effects of trichothecene mycotoxins on eukaryotic cells: a review. In *Food additives and contaminants* 22 (4), pp. 369–378. DOI: 10.1080/02652030500058403.

Routaboul, J-M; Kerhoas, L; Debeaujon, I; Pourcel, L; Caboche, M; Einhorn, J; Lepiniec, L (2006): Flavonoid diversity and biosynthesis in seed of Arabidopsis thaliana. In *Planta* 224 (1), pp. 96–107. DOI: 10.1007/s00425-005-0197-5.

Sagaram, U; Pandurangi, R; Kaur, J; Smith, T; Shah, D (2011): Structure-activity determinants in antifungal plant defensins MsDef1 and MtDef4 with different modes of action against Fusarium graminearum. In *PloS one* 6 (4), e18550. DOI: 10.1371/journal.pone.0018550.

Schmale, D; Bergstrom, G (2003): Fusarium head blight (FHB) or scab. In *APS Feat. DOI:* 10.1094/PHI-I-2003-0612-01.

Schmale, D.G,and Bergstrom, G. C (2003): Fusarium head blight. In *The Plant Health Instructor*.

Schmickl, R; Jorgensen, M; Brysting, A; Koch, M (2010): The evolutionary history of the Arabidopsis lyrata complex: a hybrid in the amphi-Beringian area closes a large distribution gap and builds up a genetic barrier. In *BMC evolutionary biology* 10, p. 98. DOI: 10.1186/1471-2148-10-98.

Schmid, M; Schmidt, A; Klostermeier, U; Barann, M; Rosenstiel, P; Grossniklaus, U (2012): A powerful method for transcriptional profiling of specific cell types in eukaryotes: laser-assisted microdissection and RNA sequencing. In *PloS one* 7 (1), e29685. DOI: 10.1371/journal.pone.0029685.

Shiba, H (2001): A Pollen Coat Protein, SP11/SCR, Determines the Pollen S-Specificity in the Self-Incompatibility of Brassica Species. In *Plant physiology* 125 (4), pp. 2095–2103. DOI: 10.1104/pp.125.4.2095.

Shimizu, K; Ito, T; Ishiguro, S; Okada, K (2008): MAA3 (MAGATAMA3) helicase gene is required for female gametophyte development and pollen tube guidance in Arabidopsis thaliana. In *Plant & cell physiology* 49 (10), pp. 1478–1483. DOI: 10.1093/pcp/pcn130.

Shimizu-Inatsugi, R; Lihova, J; Iwanaga, H; Kudoh, H; Marhold, K; Savolainen, O; Watanabe, K; Yakubov, V; Shimizu, K (2009): The allopolyploid Arabidopsis kamchatica originated from multiple individuals of Arabidopsis lyrata and Arabidopsis halleri. In *Molecular ecology* 18 (19), pp. 4024–4048. DOI: 10.1111/j.1365-294X.2009.04329.x.

Siddique, S; Wieczorek, K; Szakasits, D; Kreil, D; Bohlmann, H (2011): The promoter of a plant defensin gene directs specific expression in nematode-induced syncytia in Arabidopsis roots. In *Plant physiology and biochemistry : PPB / Societe francaise de physiologie vegetale* 49 (10), pp. 1100–1107. DOI: 10.1016/j.plaphy.2011.07.005.

Silverstein, K; Graham, M; Paape, T; VandenBosch, K (2005): Genome organization of more than 300 defensin-like genes in Arabidopsis. In *Plant physiology* 138 (2), pp. 600–610. DOI: 10.1104/pp.105.060079.

Silverstein, K; Moskal, W, JR; Wu, H; Underwood, B; Graham, M; Town, C; VandenBosch, K (2007): Small cysteine-rich peptides resembling antimicrobial peptides have been under-predicted in plants. In *The Plant journal : for cell and molecular biology* 51 (2), pp. 262–280. DOI: 10.1111/j.1365-313X.2007.03136.x.

Smyth, D; Bowman, J; Meyerowitz, E (1990): Early flower development in Arabidopsis. In *The Plant cell* 2 (8), pp. 755–767. DOI: 10.1105/tpc.2.8.755.

Sobrova, P; Adam, V; Vasatkova, A; Beklova, M; Zeman, L; Kizek, R (2010): Deoxynivalenol and its toxicity. In *Interdisciplinary toxicology* 3 (3), pp. 94–99. DOI: 10.2478/v10102-010-0019-x.

Song, X; Yuan, L; Sundaresan, V (2014): Antipodal cells persist through fertilization in the female gametophyte of Arabidopsis. In *Plant reproduction* 27 (4), pp. 197–203. DOI: 10.1007/s00497-014-0251-1.

Sprunck, S; Dresselhaus, T (2015): Three Cell Fusions during Double Fertilization. In *Cell* 161 (4), pp. 708–709. DOI: 10.1016/j.cell.2015.04.032.

Steffen, J; Kang, I-H; Macfarlane, J; Drews, G (2007): Identification of genes expressed in the Arabidopsis female gametophyte. In *The Plant journal : for cell and molecular biology* 51 (2), pp. 281–292. DOI: 10.1111/j.1365-313X.2007.03137.x.

Stotz, H; Spence, B; Wang, Y (2009): A defensin from tomato with dual function in defense and development. In *Plant molecular biology* 71 (1-2), pp. 131–143. DOI: 10.1007/s11103-009-9512-z.

Strange, R; Majer, J; Smith, H (1974): The isolation and identification of choline and betaine as the two major components in anthers and wheat germ that stimulate Fusarium graminearum in vitro. In *Physiological Plant Pathology* 4 (2), pp. 277–290. DOI: 10.1016/0048-4059(74)90015-0.

Sundaresan, V; Alandete-Saez, M (2010): Pattern formation in miniature: the female gametophyte of flowering plants. In *Development (Cambridge, England)* 137 (2), pp. 179–189. DOI: 10.1242/dev.030346.

Swanson, R; Edlund, A; Preuss, D (2004): Species specificity in pollen-pistil interactions. In *Annual review of genetics* 38, pp. 793–818. DOI: 10.1146/annurev.genet.38.072902.092356.

Takeuchi, H; Higashiyama, T (2012): A species-specific cluster of defensin-like genes encodes diffusible pollen tube attractants in Arabidopsis. In *PLoS biology* 10 (12), e1001449. DOI: 10.1371/journal.pbio.1001449.

Tang, W; Kelley, D; Ezcurra, I; Cotter, R; McCormick, S (2004): LeSTIG1, an extracellular binding partner for the pollen receptor kinases LePRK1 and LePRK2, promotes pollen tube growth in vitro. In

The Plant journal : for cell and molecular biology 39 (3), pp. 343–353. DOI: 10.1111/j.1365-313X.2004.02139.x.

Taylor, R; Saparno, A; Blackwell, B; Anoop, V; Gleddie, S; Tinker, N; Harris, L (2008): Proteomic analyses of Fusarium graminearum grown under mycotoxin-inducing conditions. In *Proteomics* 8 (11), pp. 2256–2265. DOI: 10.1002/pmic.200700610.

Tesfaye, M; Silverstein, K; Nallu, S; Wang, L; Botanga, C; Gomez, S; Costa, L; Harrison, M; Samac, D; Glazebrook, J et al. (2013): Spatio-temporal expression patterns of Arabidopsis thaliana and Medicago truncatula defensin-like genes. In *PloS one* 8 (3), e58992. DOI: 10.1371/journal.pone.0058992.

Thomas, S; Franklin-Tong, V (2004): Self-incompatibility triggers programmed cell death in Papaver pollen. In *Nature* 429 (6989), pp. 305–309. DOI: 10.1038/nature02540.

Thomma, B; Cammue, B; Thevissen, K (2002): Plant defensins. In *Planta* 216 (2), pp. 193–202. DOI: 10.1007/s00425-002-0902-6.

Trail, F (2009): For blighted waves of grain: Fusarium graminearum in the postgenomics era. In *Plant physiology* 149 (1), pp. 103–110. DOI: 10.1104/pp.108.129684.

Urban, M; Daniels, S; Mott, E; Hammond-Kosack, K (2002): Arabidopsis is susceptible to the cereal ear blight fungal pathogens Fusarium graminearum and Fusarium culmorum. In *Plant J* 32 (6), pp. 961–973. DOI: 10.1046/j.1365-313X.2002.01480.x.

van der Weerden; Anderson, M (2013): Plant defensins. Common fold, multiple functions. In *Fungal Biology Reviews* 26 (4), pp. 121–131. DOI: 10.1016/j.fbr.2012.08.004.

van der Weerden.; Hancock, R; Anderson, M (2010): Permeabilization of fungal hyphae by the plant defensin NaD1 occurs through a cell wall-dependent process. In *The Journal of biological chemistry* 285 (48), pp. 37513–37520. DOI: 10.1074/jbc.M110.134882.

Vignutelli, A; Wasternack, C; Apel, K; Bohlmann, H (1998): Systemic and local induction of an Arabidopsis thionin gene by wounding and pathogens. In *Plant J* 14 (3), pp. 285–295. DOI: 10.1046/j.1365-313X.1998.00117.x.

Viljakainen, L; Pamilo, P (2008): Selection on an antimicrobial peptide defensin in ants. In *Journal of molecular evolution* 67 (6), pp. 643–652. DOI: 10.1007/s00239-008-9173-6.

Vriens, K; Cammue, B; Thevissen, K (2014): Antifungal plant defensins: mechanisms of action and production. In *Molecules (Basel, Switzerland)* 19 (8), pp. 12280–12303. DOI: 10.3390/molecules190812280.

Walter, S; Nicholson, P; Doohan, F (2010): Action and reaction of host and pathogen during Fusarium head blight disease. In *New Phytologist* 185 (1), pp. 54–66. DOI: 10.1111/j.1469-8137.2009.03041.x.

Wang, Y; Nowak, G; Culley, D; Hadwiger, L; Fristensky, B (1999): Constitutive Expression of Pea Defense Gene DRR206 Confers Resistance to Blackleg (Leptosphaeria maculans) Disease in Transgenic Canola (Brassica napus). In *MPMI* 12 (5), pp. 410–418. DOI: 10.1094/MPMI.1999.12.5.410.

Wang, Y; Zhang, W-Z; Song, L-F; Zou, J-J; Su, Z; Wu, W-H (2008): Transcriptome analyses show changes in gene expression to accompany pollen germination and tube growth in Arabidopsis. In *Plant physiology* 148 (3), pp. 1201–1211. DOI: 10.1104/pp.108.126375.

War, A; Paulraj, M; Ahmad, T; Buhroo, A; Hussain, B; Ignacimuthu, S; Sharma, H (2012): Mechanisms of plant defense against insect herbivores. In *Plant Signaling & Behavior* 7 (10), pp. 1306–1320. DOI: 10.4161/psb.21663.

Wheeler, M; Graaf, B de; Hadjiosif, N; Perry, R; Poulter, N; Osman, K; Vatovec, S; Harper, A; Franklin, F; Franklin-Tong, V (2009): Identification of the pollen self-incompatibility determinant in Papaver rhoeas. In *Nature* 459 (7249), pp. 992–995. DOI: 10.1038/nature08027.

Wheeler, M; Vatovec, S; Franklin-Tong, V (2010): The pollen S-determinant in Papaver: comparisons with known plant receptors and protein ligand partners. In *Journal of experimental botany* 61 (7), pp. 2015–2025. DOI: 10.1093/jxb/erp383.

Wittich, P; Vreugdenhil, D (1998): Localization of sucrose synthase activity in developing maize kernels by in situ enzyme histochemistry. In *Journal of experimental botany* 49 (324), pp. 1163–1171. DOI: 10.1093/jxb/49.324.1163.

Wu, L; Chen, H; Curtis, C; Fu, Z (2014): Go in for the kill: How plants deploy effector-triggered immunity to combat pathogens. Corrected. In *Virulence* 5 (7), pp. 710–721. DOI: 10.4161/viru.29755.

Wuest, S; Vijverberg, K; Schmidt, A; Weiss, M; Gheyselinck, J; Lohr, M; Wellmer, F; Rahnenfuhrer, J; Mering, C von; Grossniklaus, U (2010): Arabidopsis female gametophyte gene expression map reveals similarities between plant and animal gametes. In *Current biology : CB* 20 (6), pp. 506–512. DOI: 10.1016/j.cub.2010.01.051.

Yount, N; Yeaman, M (2004): Multidimensional signatures in antimicrobial peptides. In *Proceedings of the National Academy of Sciences of the United States of America* 101 (19), pp. 7363–7368. DOI: 10.1073/pnas.0401567101.

Zeng, W; Melotto, M; He, S (2010): Plant stomata: a checkpoint of host immunity and pathogen virulence. In *Current opinion in biotechnology* 21 (5), pp. 599–603. DOI: 10.1016/j.copbio.2010.05.006.

Zhang, D; Wengier, D; Shuai, B; Gui, C-P; Muschietti, J; McCormick, S; Tang, W-H (2008): The pollen receptor kinase LePRK2 mediates growth-promoting signals and positively regulates pollen germination and tube growth. In *Plant physiology* 148 (3), pp. 1368–1379. DOI: 10.1104/pp.108.124420.

Zhang, J; Li, W; Xiang, T; Liu, Z; Laluk, K; Ding, X; Zou, Y; Gao, M; Zhang, X; Chen, S et al. (2010): Receptor-like cytoplasmic kinases integrate signaling from multiple plant immune receptors and are targeted by a Pseudomonas syringae effector. In *Cell host & microbe* 7 (4), pp. 290–301. DOI: 10.1016/j.chom.2010.03.007.

Zhang, X; Henriques, R; Lin, S-S; Niu, Q-W; Chua, N-H (2006): Agrobacterium-mediated transformation of Arabidopsis thaliana using the floral dip method. In *Nature protocols* 1 (2), pp. 641–646. DOI: 10.1038/nprot.2006.97.

Zheng, Z; Mosher, S; Fan, B; Klessig, D; Chen, Z (2007): Functional analysis of Arabidopsis WRKY25 transcription factor in plant defense against Pseudomonas syringae. In *BMC plant biology* 7, p. 2. DOI: 10.1186/1471-2229-7-2.

Zhou, L-Z; Howing, T; Muller, B; Hammes, U; Gietl, C; Dresselhaus, T (2016): Expression analysis of KDEL-CysEPs programmed cell death markers during reproduction in Arabidopsis. In *Plant reproduction* 29 (3), pp. 265–272. DOI: 10.1007/s00497-016-0288-4.

9. Appendix

9.1 List of Primers

Primer name	Primer sequence	T_m °C	Amplicon(bp)
Primer for promoter analysis (GW:NLS-3GFP)			
At4g30074_prom_forward	CACCATACCCAAAATATAATACCAATCTCGAG	64.3	1014
At4g30074_prom_reverse	ATTTTCTAAGTTTTTCTTTTTTCTTTCTGAAAATTGG		
At5g55132_prom_forward	CACCTTGATCTCTTATTCTATATGTACTC	60.5	2095
At5g55132_prom_reverse	TTTGTTGTTATTTGTTATTCTTTCAAGA		
At3g043505_prom_forward	CACCTAGTAAATGTGTAAATATGTTGAAT	60	1092
At3g043505_prom_reverse	ATAACGGTGGTTTTAGACATCTTTG		
At2g02100_prom_forward	CACCTCAAATTCATGATTATATTATTGCG	60.5	1000
At2g02100_prom_reverse	TGCAAGAGAGATAAAGAGAGAGTTC		
At5g38330_prom_forward	CACCACTTTCATTAGCGTTTTCG	60.1	996
At5g38330_prom_reverse	ACTTTCACGTTTTCTTTTAAACTTTTCTC		
At2g40995_prom_forward	CACCTTTGTCGTGATACACATATCC	59	976
At2g40995_prom_reverse	TTTCATAATAATCTCTTACTTCTTTCTTTTTTTTG		
At2g20070_prom_forward	CACCTGATTTGCCTCAAAAACTT	61.0	552
At2g20070_prom_reverse	TTTAGTTGTTATAAAAAAAATTGTGTTGTGC		
At3g07005_prom_forward	CACCTCTTCTTTTATCTTTATCCCC	60.0	759
At3g07005_prom_reverse	TTTCGTTGTATTATCAAAATATATCACTTTG		
At3g06985_prom_forward	CACCAATTGATGCCCCAAATC	60.9	562
At3g06985_prom_reverse	TTTCGTTGTAGCTAATCTATTCGTTTT		
At3g42473_prom_forward	CACCTGGTTCCTAATTTACAAGGATTC	63.0	992
At3g42473_prom_reverse	TGCCTGTGTTTCCAAATGGTAAAAC		
At4g09153_prom_forward	CACCTTTGTTGTATTTAATGATTTTTTTTTGG	62	994
At4g09153_prom_reverse	GATCAATGTATATCACAACAAAAGAAAGC		
At5g43285_prom_forward	CACCAGAAATATTTAATATGTTTGATATTGC	60.5	983
At5g43285_prom_reverse	TTCTTCATAGAAATTAACCAATACCACA		
At5g23212_prom_forward	CACCTTCTCTTTGTATTAATGTTCAATC	60.2	995
At5g23212_prom_reverse	CTTTCGATCTATATAATATTGATATAAGATCCTTT		
At2g12475_prom_forward	CACCTCGTTTGGACGTTTCATAC	62.8	766
At2g12475_prom_reverse	TTTGTTTCTATGATTTTTTGCTTCTATTTTTATTTTG		
At2g42885_prom_forward	CACCTGTAAACTAAATTGATCCATAGTG	61.0	980
At2g42885_prom_reverse	AGGTTCTATTATCTTTTAGGTTTTCGTG		
At5g08315_prom_forward	CACCAGAAGAAGTTAGGCCTC	60.5	994
At5g08315_prom_reverse	TGTTAATAGTTTTTTTTTTTTTTATAAGTGTTTATAG		
At1g60985_prom_forward	CACCAGCCAAAAGGATAGAGTTAA	61.5	999
At1g60985_prom_reverse	ATTGTTTTGCAAGTTTCTTCTCTCTTT		
At1g65352_prom_forward	CACCACGAAGACGCAACACAAG	62.0	947
At1g65352_prom_reverse	TCCTGATAGTATTGATTATCATTATACAAACGTGT		
At4g11760_prom_forward	CACCTCATCATTAGCCAAAATCCC	62.5	775
At4g11760_prom_reverse	CTTGTATGCTATAATAAATAAATTGCTGATGTTTT		

Primer for subcellular localization analysis (pGOI::GOIg-eGFP**)**			
Primer name	Primer sequence	T_m °C	Amplicon (bp)
At4g30074_cds_for	CACCATGGAGAAGGCACTTTCACTTGTG	68	382
At4g30074_cds_rev	GCAATTATATTGGCATTTACACAAAGAAGTATTGCCAA		
At4g30074_Prom_for_sac	ATTAGAGCTCTCTCTTTTTTTTTCTATACCCAAAATA	65	1029
At4g30074_Prom_for_spe	TATTACTAGTATTTTCTAAGTTTTTCTTTTTTCTTTCTGAA		
At5g55132_cds_for	CACCATGGTTGCATCTCATCGATTACTTACG	68	244
At5g55132_cds_rev	ATTGATGACCGGACTGGAGATGGGAGA		
At5g55132_Prom_for_sac	ATTAGAGCTCTTGATCTCTTATTCTATATGTACTCT	64	2095
At5g55132_Prom_rev_spe	TATTACTAGTTTTGGTTGTTATTTGTTATTCTTTCAA		
At3g43505_cds_for	CACCATGTCTAAAACCACCGTTATTGCTA	66.8	232
At3g43505_cds_rev	AGCGTTGCAACTATAAGTGCAGACG		
At3g43505_Prom_for_sac	AGAGCTCTAGTAAATGTGTAAATATGTTG	60	1092
At3g43505_Prom_rev_spe	AACTAGTATAACGGTGGTTTTAGACA		
At4g11760_cds_for	CACCATGAAGAAACCCAGTCAACT	63.8	291
At4g11760_cds_rev	CTTGTAGGGGGTTCCATCTGATTTAC		
At4g11760_Prom_for_sac	AAGAGCTCTCATCATTAGCCAAAATCCC	61	775
At4g11760_Prom_rev_spe	AAACTAGTCTTGTATGCTATAATAAATAAATTGCTGATGT		
At2g28355_cds_for	CACCATGATGAAGAAACTCATTCA	60	237
At2g28355_cds_rev	TTAAGGGCAATGATAATAGCAGTAAC		
At2g28355_Prom_for_sac	TCATGAGCTCGAAATTGAAGAAAAAAG	62.5	1469
At2g28355_Prom_for_spe	TATTACTAGTAGATGATATAAATGAATTGACTGTT		
At2g28405_cds_for	CACCATGATGGGCAAACATATTC	62	252
At2g28405_cds_rev	TTAACAATGATAAATGCATCTACACCG		
At2g28405_Prom_for_sac	ATTAGAGCTCTGTGAAATAAAGTGGTT	62	2000
At2g28405_Prom_rev_spe	TATTACTAGTAGATGATATACATGATTTGTTTTTTTT		
At4g15735_cds_for	CACCATGAAGGTTGTGGCAATCTTTTTG	62.5	325
At4g15735_cds_rev	ATTTTTTACACAACAATCGGTGCAAATAACTGA		
At4g15735_Prom_for_sac	AGAGCTCGTTATTCTTTCGATTCC	61.5	965
At4g15735_Prom_rev_spe	AACTAGTATTTTGTTCTCTTGACTATTCTTT		
At4g29285_Prom_ for_sac	AGAGCTCGATCAATATATCACAACAAAAG	62	1012
At4g29285_Prom_ rev_spe	AACTAGTGAATTGCTGAAAATGAAGAGG		
At4g29285_cds_for	CACCATGGCTAAACTAATATATTCGTATCTATTCATCTC	66	232
At4g29285_cds_rev	ACAATTGTAGGCGCAAGTGCAAATTTC		
At3g05727_ cds_for	CACCATGGCAAAGACCTTCA	65	241
At3g05727_ cds_rev	GTGATAATCACCGTAGCAGTGG		
At3g05727_Prom_for_sac	TGAGCTCGTCTCTCTATCTCTACTCT	59	475
At3g05727_Prom_ rev_spe	TACTAGTTCGTAGTTTTTTTTTTTTCTTAAGCT		
At4g30067_cds_for	CACCATGGCCAAGGCACCTTCTCC	69	238
At4g30067_cds_rev	ATATGTATTTCCTTAGTCTGACAGGGGTAAGTACAAATAC		
At4g30067_Prom_for_sac	AAGAGCTCTATATACATGCAGTAGTGTAA	61.5	1430
At4g30067_Prom_rev_spe	TACTAGTATTTTTAGTTGACCGACCTGA		

Primers used for DNA sequencing			
Primer name	Primer sequence	T_m °C	Amplicon (bp)
M13_Forward	GTAAAACGACGGCCAG	55	300+

M13_Reverse	CAGGAAACAGCTATGAC		
GwNls_forward	TATCAACATTAACGTTTACAATTTCGCGC		
GwNls_Reverse	GACCTTTCTCTTCTTCTTTGGAGCC		
pB7_Rev	TGAACAGCTCCTCGCCCTTGCTCACCA		
RNAi_Prom_forward	CAAGCTCGAAATTAACCCTCACTAAAG		
RNAi_Prom_reverse	CTACTGGAAAGAAATAAGAATCA		
RNAi _Sense_forward	GCATGCTCTGTTTTTTAGAATTAATG		
RNAi_Sense_reverse	ATTAGAATGAACCGAAACCGGCGG		
Lig_prom_forward	TATCCTGTCAAACACTGATAGTTTAAACT	62.1	100+
Lig_prom_reverse	GCGGAGCCTGCTTTTTTGTA		

Primers used in qPCR			
Primer name	Primer sequence	T_m °C	Amplicon (bp)
At2g42885_qPCR_fwd	TGGTGCTTGCCTTTTTCTATGT	59.8	120
At2g42885_qPCR_rev	CAACAACAGCGTGGAGGATT		
At3g07005_qPCR_fwd	GGTTCCAGATAAAGTAGAAGCG	57.1	172
At3g07005_qPCR_rev	TTTCCTAATCCCGACGCAAG		
At4g09153_qPCR_fwd	AGGCTAAGGGAGATAAGCGTTG	57.3	148
At4g09153_qPCR_rev	TCTCCATCTCCATTGCGCTC		
At2g20070_qPCR_fwd	TGGCAAACAATATGGTCGCATC	54	86
At2g20070_qPCR_rev	CCATTCGATCTTGCTTCTGAACC		
At2g19270_qPCR_for	CTTCCGCATCTCACGATTCATCAGTAAG	62	350
At2g19270_qPCR_rev	CACCACCATTCCAAGTATTACCTCCATAG		
At1g10310_qPCR_fwd	TTCCTCTTCGACCAATCATCTCCTCCTC	62	391
At1g10310_qPCR_rev	ACTACTGCCATTCCTTCAACTACTTCCTT		

Efficiency of primers used in the qPCR assays.

Gene	Amplicon (bp)	Efficiency
At2g42885	120	2.2
At3g07005	172	2.18
At5g09153	148	2.04
At1g20070	86	1.81
At2g19270	351	1.86
At1g10310	390	1.86

cDNA synthesis primer

Primer name	Sequence
AB05	5’-GACTCGAGTCGACATCTGTTTTTTTTTTTTT -3’

Mariana Mondragon-Palomino (University of Regensburg, Regensburg, Germany) provided the cDNA primers:

Primers for genotyping			
Primer name	Primer sequence	T_m °C	Amplicon (bp)
Basta_new_forward	TATTGCGCGTTCAAAAGTCG	60.1	721
Basta_new_reverse	CGATCTGCTTGACTCTAGGG		
GFP_forward	CATCCTGGTCGAGCTGGACGGC	66	450
GFP_reverse	TCGATGTTGTGGCGGATCTTGAAGTT		

Primer for RNAi vectors			
Primer name	Primer sequence	T_m °C	Amplicon (bp)
Ubiq10Prom_Nco1_Forward	ATACCATGGCGACGAGTCAGTAATAAAC	65.1	634
Ubiq10Prom_Bam1_Reverse	ATTTGGATCCCTGTTAATCAGAAAAACTCAG		
DD36Prom_Nco1_Forward	AACCATGGCTTGATACTAACGAGGAAAT	62.6	990
DD36Prom_Bam1_Reverse	ATTGGATCCTGAAAGTTTGCTATGTATTCG		
CRP670_Pst1_forward	AACTGCAGAAATGCGACGGTG	64.5	670
CRP670_Mlu1_reverse	AATTACGCGTTTTATTGATTTTTGCTTATTCTAG		
CRP670_Ecor1_forward	ATGAATTCAAATGCGACGGTGGG	64.6	670
CRP670_BamH1_reverse	ATGGATCCTTTATTGATTTTTGCTTATTCTAGAAAC		
CRP500_Pst1_forward	AAGAATTCGAGAAGAAAAACAGTGTTATGAT	63.5	816
CRP500_Mlu1_reverse	AAGGATCCTCAAGCGTTGCAAC		
CRP500_Ecor1_forward	AACTGCAGGAGAAGAAAAACAGTGTTATGATT	64.1	816
CRP500_BamH1_reverse	ATACGCGTTCAAGCGTTGCAAC		

9.2 Plasmid for cloning

Due to the great number of cloned plasmids, only important vectors are depicted below

9.2.1 Promoter analysis

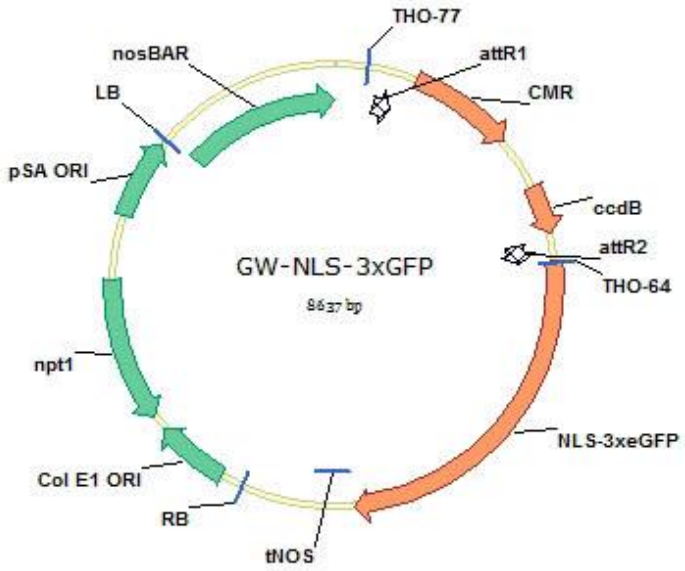

Vector	Insert	Name of plasmid
GW-NLS-3XeGFP	At4g30074 promoter	pAt4g30074 NLS-(3x)eGFP
GW-NLS-3XeGFP	At5g55132 promoter	pAt5g55132 NLS-(3x)eGFP
GW-NLS-3XeGFP	At3g43505 promoter	pAt3g43505 NLS-(3x)eGFP
GW-NLS-3XeGFP	At2g02100 promoter	pAt2g02100 NLS-(3x)eGFP
GW-NLS-3XeGFP	At5g08315 promoter	pAt5g08315 NLS-(3x)eGFP
GW-NLS-3XeGFP	At2g42885 promoter	pAt2g42885 NLS-(3x)eGFP
GW-NLS-3XeGFP	At3g06985 promoter	pAt3g06985 NLS-(3x)eGFP
GW-NLS-3XeGFP	At3g07005 promoter	pAt3g07005 NLS-(3x)eGFP

GW-NLS-3XeGFP	At2g20070 promoter	pAt2g20070 NLS-(3x)eGFP
GW-NLS-3XeGFP	At3g42473 promoter	pAt3g42473 NLS-(3x)eGFP
GW-NLS-3XeGFP	At2g12475 promoter	pAt2g12475 NLS-(3x)eGFP
GW-NLS-3XeGFP	At2g40995 promoter	pAt2g40995 NLS-(3x)eGFP
GW-NLS-3XeGFP	At4g09153 promoter	pAt4g09153 NLS-(3x)eGFP
GW-NLS-3XeGFP	At5g38330 promoter	pAt5g38330NLS-(3x)eGFP
GW-NLS-3XeGFP	At5g43285 promoter	pAt5g43285 NLS-(3x)eGFP
GW-NLS-3XeGFP	At1g60985 promoter	pAt1g60985 NLS-(3x)eGFP
GW-NLS-3XeGFP	At1g65352 promoter	pAt1g65352 NLS-(3x)eGFP
GW-NLS-3XeGFP	At5g23212 promoter	pAt5g23212 NLS-(3x)eGFP

9.2.2 Subcellular localization analysis

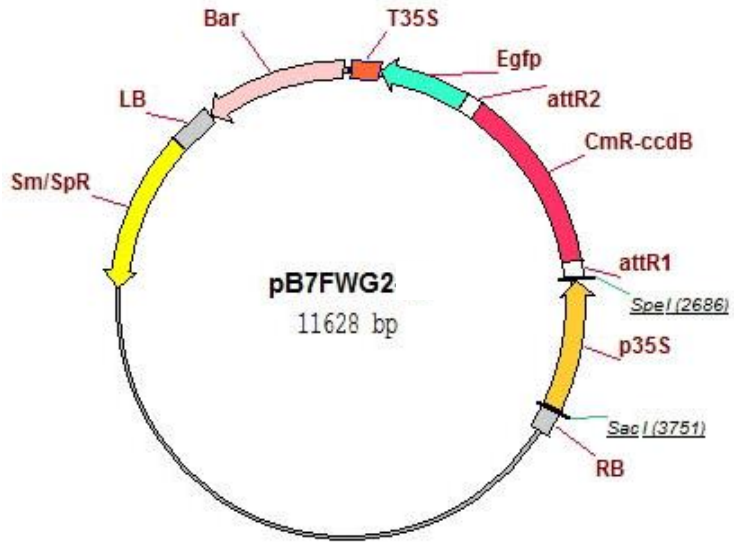

Vector	Insert	Name of plasmid
pB7FWG2.0	At4g30074 promoter and cds	pAt4g30074:At4g30074-eGFP
pB7FWG2.0	At4g11760 promoter and cds	pAt4g11760:At4g11760-eGFP
pB7FWG2.0	At4g15735 promoter and cds	pAt4g15735:At4g15735-eGFP
pB7FWG2.0	At5g55132 promoter and cds	pAt5g55132:At5g55132-eGFP
pB7FWG2.0	At3g43505 promoter and cds	pAt3g43505:At3g43505-eGFP
pB7FWG2.0	At2g28355 promoter and cds	pAt2g28355:At2g28355-eGFP
pB7FWG2.0	At4g30067 promoter and cds	pAt4g30067:At4g30067-eGFP
pB7FWG2.0	At2g28405 promoter and cds	pAt2g28405:At2g28405-eGFP
pB7FWG2.0	At4g29285 promoter and cds	pAt4t29285:At4g29285-eGFP
pB7FWG2.0	At3g05727 promoter and cds	pAt3g05727:At3g05727-eGFP

9.2.3 RNAi Vector

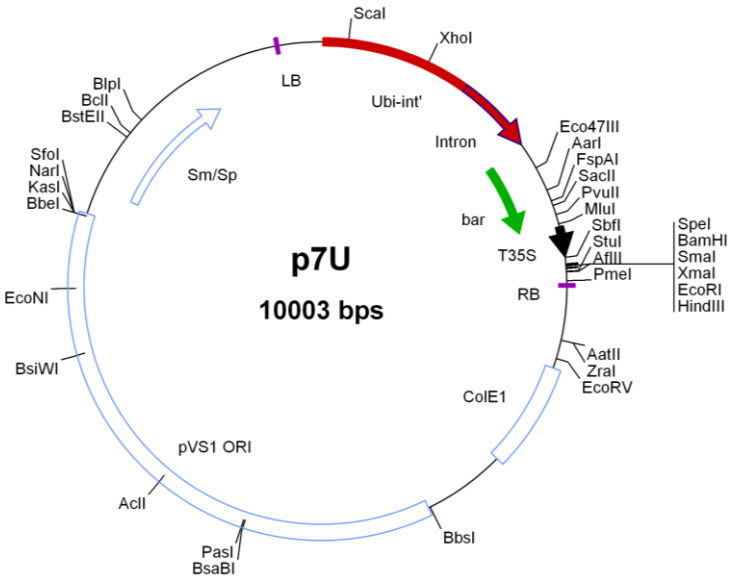

Vector	Insert	Name of plasmid
P7U	CRP0500 RNAi sequence and Ubi 10 promoter	P7U- Ubi 10-CRP500
P7U	CRP670 RNAi sequence and Ubi 10 promoter	P7U-Ubi 10-CRP670
P7U	CRP670 RNAi sequence and DD 36 promoter	P7U-DD36-CRP670

9.3 qPCR plate layout

Three same coloring circles represent three technical replicates of each sample. A, B - biological replicates. NTC - negative control, s13_cDNA - positive control (cDNA of full flowers), RT inf. - infection treatment mRNA samples, RT mt. - mock treatment mRNA samples, RT cont. - control treatment mRNA samples. RT control was used for checking if there are any DNA remains in initial mRNA samples. Plate layout for pollination-infection qPCR assay of gene of interest (GOI). HAP -hours after pollination, DAT-Days after treatment, DAI-Days after infection, DAE- Days after emasculation.

9.3.1 qPCR plate layout for pollination

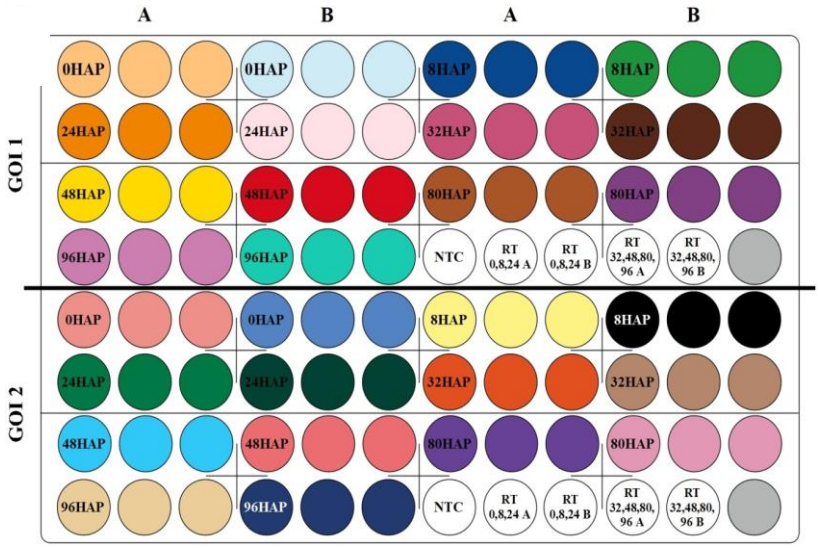

9.3.2 qPCR plate layout of gene of interest (GOI) during infection

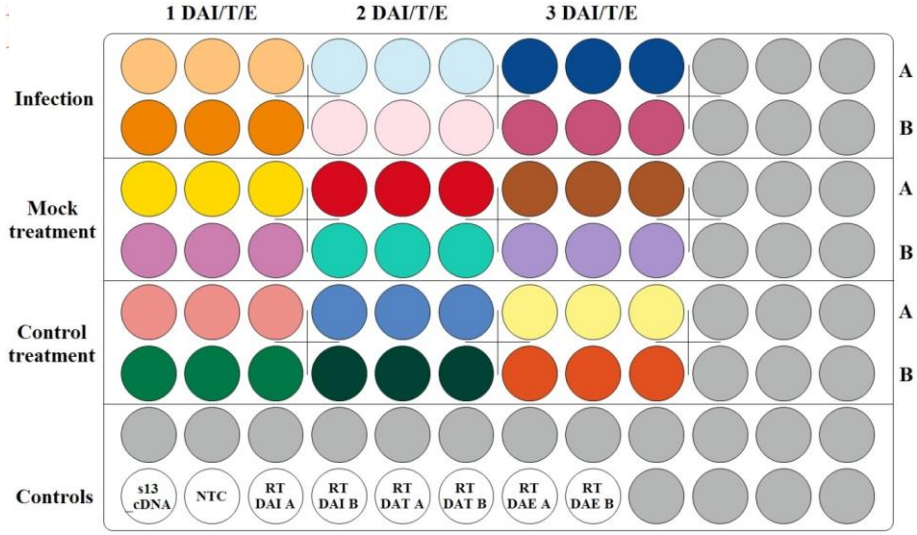

9.3.3 qPCR plate layout for gene of interest (GOI) during pollination-infection

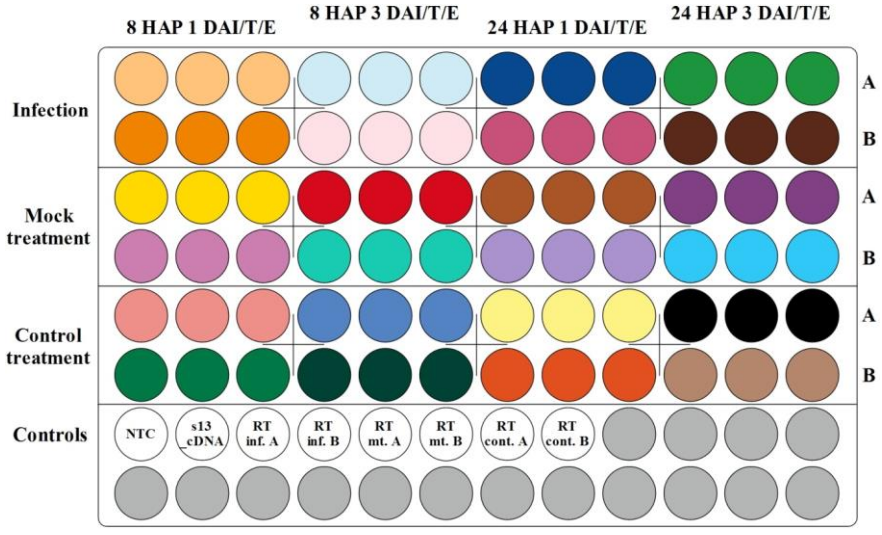

9.4 Comparison of *A. thaliana* emasculated pistil with non-emasculated pistil during *F. graminearum* infection

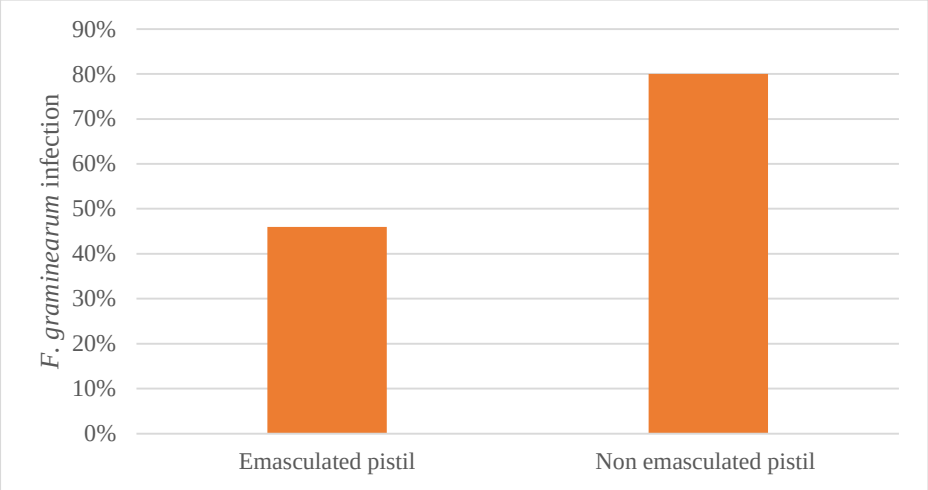

Figure S1:Comparison of emasculated pistil and non-emasculated pistil during *F. graminearum* infection.

15 non-emasculated pistils along with 15 pistils of *A. thaliana* was emasculated and was infected with *F. graminearum* Sg007 strain. The pistils were collected and looked for infection using WGA-TMR staining. We observed that non-emasculated pistil had the highest infection(n=12) in comparison to infection in emasculated pistil (n=7).

9.5 List of concentration, sample purity (260/230,260/280 ratio) and RIN values for tissue samples used for RNAseq

Tissue Sample	260/280	260/230	ng/ul	RIN
A. thaliana leaf -1	2.16	2.02	180.7	n/a
A. thaliana leaf -2	2.09	2.39	133.5	n/a
A. thaliana leaf -3	2.13	2.13	412.1	n/a
A. thaliana infected leaf -1	2.15	2.46	219.7	n/a
A. thaliana infected leaf -2	2.12	2.48	230.0	n/a
A. thaliana infected leaf -3	2.11	2.36	117.3	n/a
A. halleri leaf -1	2.16	1.9	467.6	n/a
A. halleri leaf -2	2.14	2.35	638.3	n/a
A. halleri leaf -3	2.15	2.46	600.7	n/a
A. halleri infected leaf -1	2.14	2.37	448.0	n/a
A. halleri infected leaf -2	2.13	2.45	568.9	n/a
A. halleri infected leaf -3	2.19	3.00	503.3	n/a
A. lyrata leaf-1	2.17	2.32	368.1	n/a
A. lyrata leaf-2	2.13	2.43	219.9	n/a
A. lyrata leaf-3	2.13	2.24	248.5	n/a
A. lyrata Infected leaf-1	2.16	2.42	790	n/a
A. lyrata Infected leaf-2	2.12	2.36	653.3	n/a
A. lyrata Infected leaf-3	2.18	2.48	459.3	n/a
A. thaliana nonpollinated pistils(S13)-1	2.14	2.5	787.7	7.90

A. thaliana nonpollinated pistils(S13)-2	2.16	2.42	481.5	8.30
A. thaliana nonpollinated pistils(S13)-3	2.15	2.34	362	7.60
A. halleri nonpollinated pistils- 1	2.09	2.45	535.1	8.10
A. halleri nonpollinated pistils -2	2.12	2.30	523.0	5.90
A. halleri nonpollinated pistils- 3	2.14	2.30	385.4	8.20
A. lyrata nonpollinated pistils- 1	2.15	2.41	464.1	8.60
A. lyrata nonpollinated pistils- 2	2.15	2.41	484.8	9.00
A. lyrata nonpollinated pistils- 3	2.04	1.65	308.0	9.00
A. thaliana infected pistil-1	2.13	2.51	250.4	6.00
A. thaliana infected pistil-2	2.13	2.45	237.9	7.10
A. thaliana infected pistil-3	2.11	2.45	365.1	7.30
A. halleri infected pistils- 1	2.12	2.24	103.4	8.30
A. halleri infected pistils-2	2.14	2.28	383.3	8.20
A. halleri infected pistils-3	2.14	2.40	350.4	8.60
A. lyrata infected pistils-1	2.18	1.92	205.8	6.50
A. lyrata infected pistil-2	2.14	2.37	226.5	8.40
A. lyrata infected pistils-3	2.14	2.42	399.9	9.20
A. thaliana selfed pistils -1	2.16	2.38	631.3	9.10
A. thaliana selfed pistils -2	2.14	2.40	716.4	8.20
A. thaliana selfed pistils -3	2.12	2.62	642.1	8.50
A. thaliana pistil X *A. halleri* pollen -1	2.14	2.47	714.8	6.40
A. thaliana pistil X *A. halleri* pollen -2	2.14	2.52	546.8	7.30
A. thaliana pistil X *A. halleri* pollen -3	2.19	2.49	534.7	7.50
A. thaliana pistil X *A. lyrata* pollen- *1*	2.15	2.57	453.2	8.70
A. thaliana pistil X *A. lyrata* pollen- 2	2.13	2.46	534.9	9.90
A. thaliana pistil X *A. lyrata* pollen -3	2.12	2.43	362.3	9.90
A. halleri pistil X *A. halleri* pollen -1	2.18	2.50	213.2	9.60
A. halleri pistil X *A. halleri* pollen -2	2.12	2.37	439.7	9.30
A. halleri pistil X *A. halleri* pollen -3	2.13	2.48	304.5	8.40
A. halleri pistil X *A. lyrata* pollen-1	2.14	2.43	468.0	9.40
A. halleri pistil X *A. lyrata* pollen-2	2.15	2.48	636.9	9.00
A. halleri pistil X *A. lyrata* pollen- 3	2.14	2.32	307.1	8.60
A. lyrata pistil X *A. lyrata* pollen-1	2.14	2.50	600.0	9.20
A. lyrata pistil X *A. lyrata* pollen-2	2.16	2.43	653.3	9.10
A. lyrata pistil X *A. lyrata* pollen-3	2.12	2.48	459.3	8.60

9.6 List of differential expression pattern of 72 DEFL genes in the five conditions of our transcriptome data

Defensin	AtS14 vs At S13	At 3dai vs AtS13	At x Ah pol vs At S13	At x Aly pol vs At S13	At 3dai leaf vs At leaf
At2g02100		-2.91			3.87
At2g02140		-6.89			-8.37
At2g26010		9.78			
At2g26020		7.49			
At5g44420		7.50			4.69
At5g44430		7.89			
At1g19610		4.71			7.33
At5g08315		-3.47			
At5g19315			4.34	4.56	
At2g24615		-8.10	-8.10		

At5g39365		-6.52	2.51	5.83	
At2g42885		-2.29			
At3g06985		-3.70			
At3g07005		-2.24			
At5g54225		3.06			
At2g20070		-4.84			
At1g56233		4.86			
At3g42473		-2.46			
At4g22235		-3.00			
At2g12465		-3.76			
At2g12475		-2.17			
At2g40995		-3.57			
At5g42223		7.13			
At5g40155		-3.17			
At3g43083	-4.02	-10.54	-5.17	-5.97	
At4g19035			4.30	4.44	
At4g19038		-6.32			
At1g28335	-2.48	-12.33	-2.51	-2.97	
At2g15535		-10.40	-4.69	-4.99	
At2g28355		-5.20	-4.58		
At2g28405		-4.65	-4.88	-6.82	
At3g25265	-3.58	-7.14	-4.81	-5.49	
At4g09984		-5.47	-5.19	-6.31	
At4g10595	-4.39	-8.35		-4.02	
At4g11485	-2.33	-7.03	-3.28	-2.47	
At4g11760	-3.30	-4.74	-3.81	-3.20	
At5g48543		-4.03	-4.81	-6.11	
At4g09153		-2.18			
At4g29285			2.17		
At4g29300		-4.42			
At4g10603		-5.72	-6.58	-9.64	
At5g38330		-2.40			
At2g43510		4.37			6.58
At2g43535					4.42
At2g22805		-11.07	-3.25		
At2g22807		-7.25	-3.80		
At2g22941	-4.34				
At3g05727			4.40		
At3g05730					-9.09
At5g43285		-3.41			
At1g08695		-7.50			
At1g65113		-7.29	-3.15		
At2g06983		-6.40			
At2g14282		-10.08			
At3g27503	-3.04	-6.53	-4.15		
At4g10115	-3.94	-10.51	-4.36		
At4g14785	-4.16	-5.02	-4.36		
At4g22115		2.96			
At4g32714		-5.32	-6.51		
At4g32717	-3.25	-5.63	-4.14		
At4g33465		-5.14	-5.12		
At1g60985		-2.24			
At3g23727		-9.58	-4.50		
At4g15735		2.90			

At1g13605		2.16			
At1g65352		-5.47			
At1g35435		-3.32			
At5g23212		-2.98			
At5g60553		-2.73			
At5g60615		-6.14			-6.06
At1g13609			2.57		-9.93
At4g17713		-3.16			

Yellow labelled- downregulated DEFL gene, Green labelled – upregulated DEFL gene, Blue labelled- downregulated in one condition and upregulated in other condition

All values are the $\log_2$ fold change of comparing the mapping results from following conditions with those obtained from *A.thaliana* unpollinated, S13 pistils: AtS14 = *A.thaliana* self-pollinated pistils S14, At x Aly pol = *A.thaliana* pistils pollinated with *A.lyrata* pollen, At x Ah pol = *A.thaliana* pistils pollinated with *A.halleri* pollen,At 3dai = 3dai infected pistils. Values of $\log_2$ fold change was obtained by comparing *A. thaliana* 3DAI leaf with *A. thaliana* uninfected leaves.

9.7 GFP expression of At5g38330, At2g42885, At2g40995 and At3g07005 in the *A. thaliana* roots

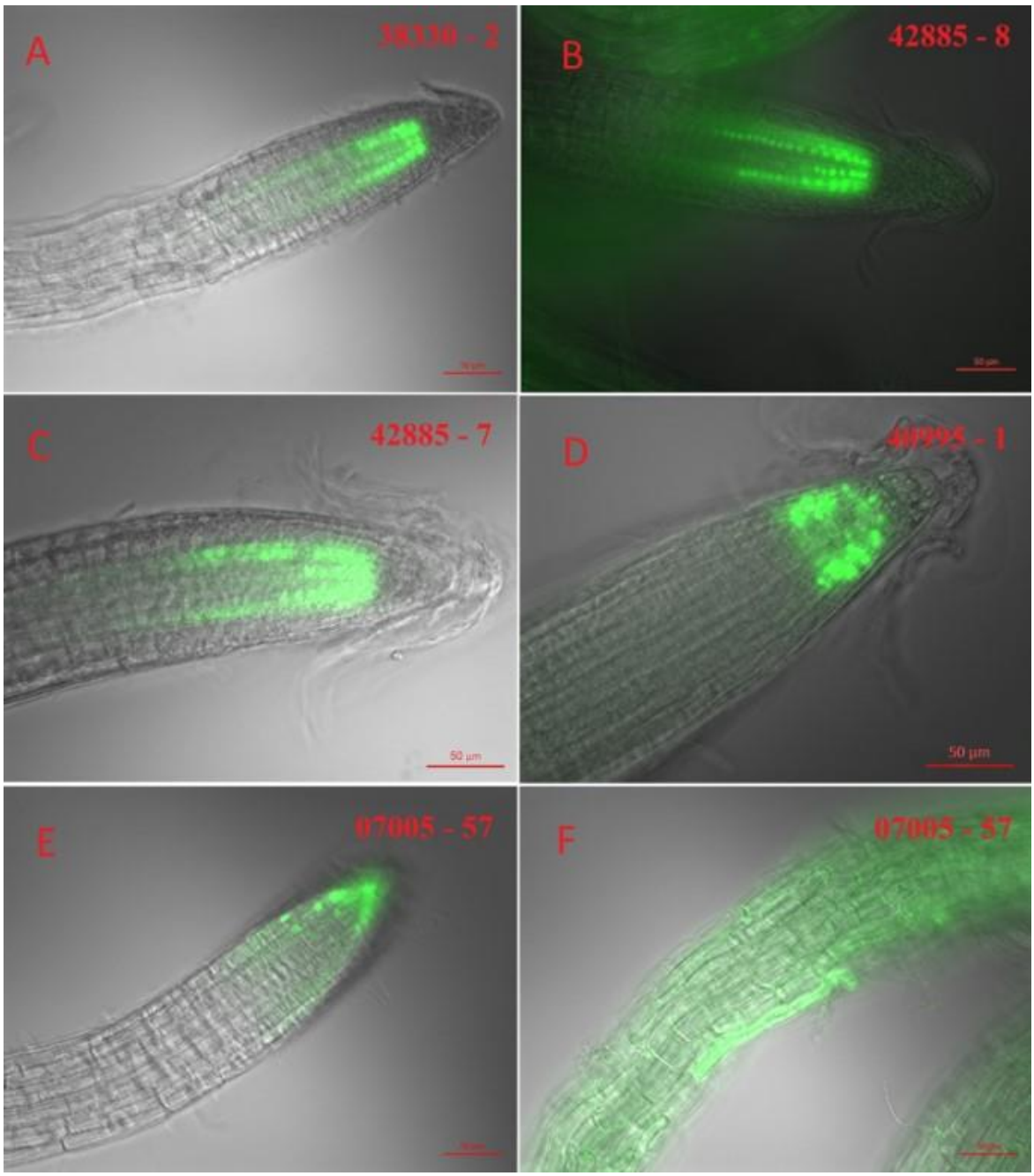

Figure S2:eGFP expression of At5g38330, At5g42885, At2g40995 and At3g07005 in roots.

Merged image of fluorescence green light channel and bright field channel of the *A. thaliana* root-(A) The marker line pAt5g38330:NLS-(3x)eGFP-2 showing GFP expression in nucleus of ground meristem of root tip, (B and C) The marker line pAt5g42885:NLS-(3x)eGFP-7 and 8 showing GFP expression in nucleus ground meristem of root tip, (D) The marker line showing pAt2g40995:NLS-(3x)eGFP-1 showing GFP expression in nucleus of apical meristem in the root tip, (E) The marker line showing pAt3g07005:NLS-(3x)eGFP -57 showing GFP expression in nucleus of apical meristem in the root tip, (F) The marker line showing pAt3g07005:NLS-(3x)eGFP -57 showing autoflurorescene in epidermis of maturation zone of the root. This information was obtained from Masters Thesis of Kriss spalvins

9.8 qPCR analysis of At5g38330, At2g40995, At5g43285 and At1g60985 to test the effect of age, mock treatment and *F. graminearum* infection

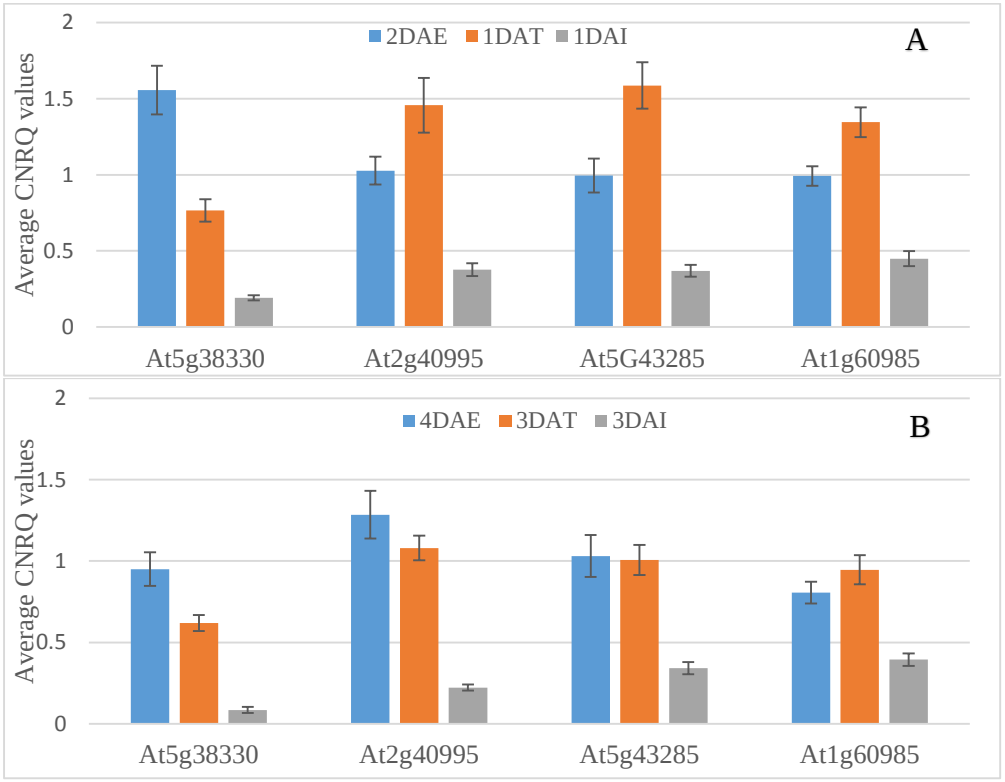

Figure S3:CNRQ values of At5g38330, At2g40995, At5g43285 and At1g60985 during infection along with mock treatment and control at day 1 and day 3.
Average CNRQ values of control (blue column), mock treatment (orange column) and infection (grey column) for At5g38330, At2g40995, At5g43285 and At1g60985 during day 1(A) and day 3(B). The infected samples of At5g38330, At2g40995, At5g43285 and At1g60985 at day 1 and day3 were downregulated in comparison to mock treatment and control. Error bars represent the standard error. This information was obtained from Masters Thesis of Kriss spalvins.

9.9 Seed set image

9.9.1 Seed set image of pollination followed by infection.

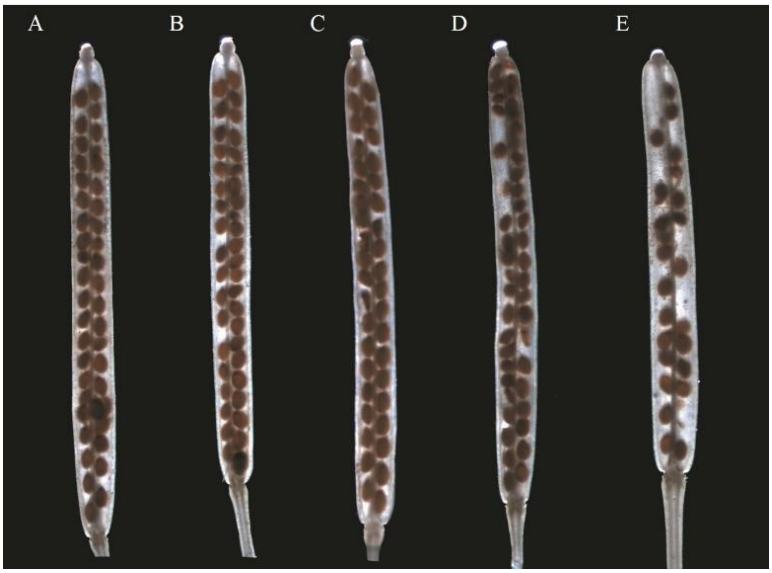

Figure S4:Silique comparison of different pollination time point followed by one day of infection or mock treatment.
A) Control: silique resulting from one day of emasculation and followed by pollination B) 24HAP-1DAT: silique resulting from 24HAP followed by one day of mock treatment C) 24HAP-1DAI: silique resulting from 24HAP followed by one day of *F. graminearum* infection. D) 8HAP-1DAT: silique resulting from 8HAP followed by one day of mock treatment E) 8HAP-1DAI: silique resulting from 8HAP followed by one day of *F. graminearum* infection.

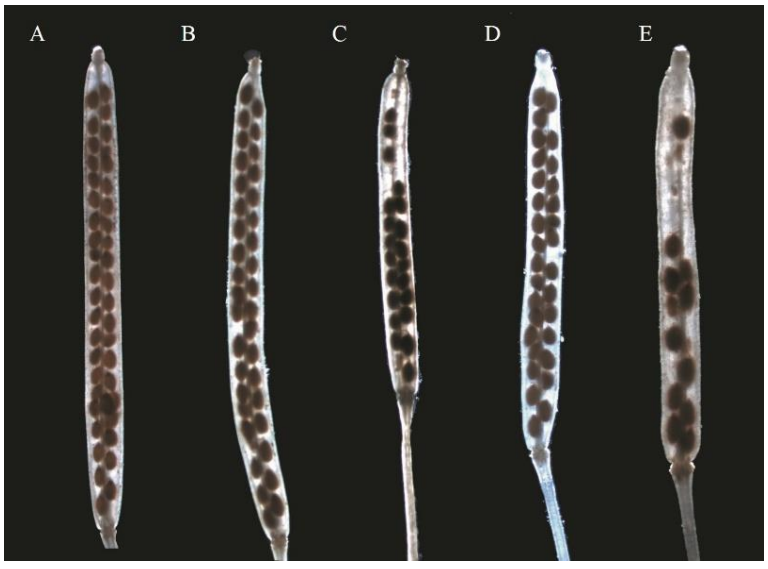

Figure S5:Silique comparison of different pollination time point followed by two days of infection or mock treatment.
A) Control: silique resulting from one day of emasculation and followed by pollination B) 24HAP-2DAT: silique resulting from 24HAP followed by two days of mock treatment C) 24HAP-1DAI: silique resulting from 24HAP followed by two days of *F. graminearum* infection. D) 8HAP-1DAT: silique resulting from 8HAP followed by two days of mock treatment E) 8HAP-1DAI: silique resulting from 8HAP followed by two days of *F. graminearum* infection.

9.9.2 Seed set image of infection followed by pollination.

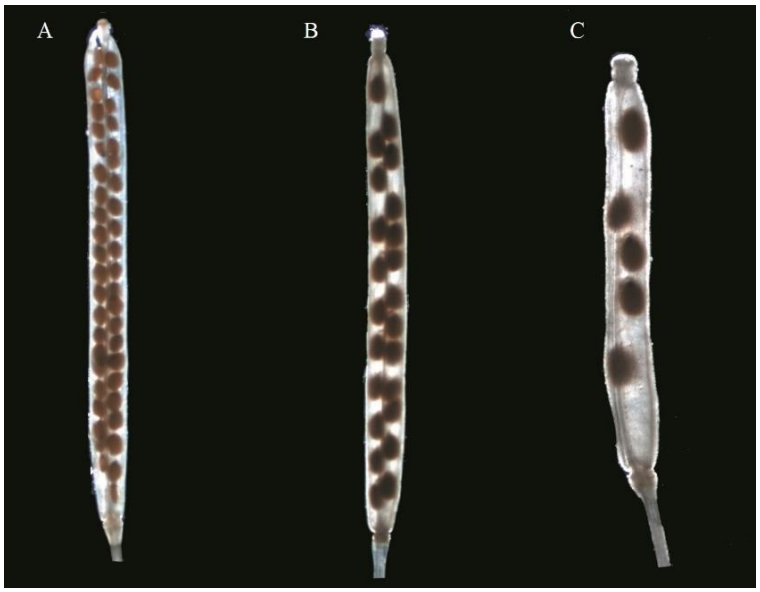

Figure S6:Comparison of silique of 1DAI followed by pollination with two controls.
A) Control -Silique resulting from two days after emasculation followed by pollinated B) Mock treated control - Silique resulting from one day of mock treatment with water followed by pollination after. C) Silique resulting from 1DAI followed by pollination.

9.10 List of pairwise correlation coefficient of relative gene expression using the average CNRQ values during different conditions

Gene comparison	Pollination-infection	Pollination	Infection
At5g43285-At1g60985	0.74	0.77	0.76
At2g42885-At5g43285	0.34	N. A	0.67
At3g07005-At1g60985	0.72	0.67	0.67
At5g43285-At4g09153	0.20	N. A	0.66
At2g42885-At1g60985	0.19	N. A	0.69
At3g07005-At4g09153	N. A	N. A	0.77
At5g38330-At4g09153	N. A	N. A	0.62
At2g42885-At2g20070	N. A	N. A	0.07
At2g42885-At5g38330	-0.08	N. A	0.67
At1g60985-At2g20070	N. A	0.46	0.17
At4g09153-At2g20070	N. A	-0.44	0.24
At2g40995-At2g20070	N. A	0.79	-0.15
At5g38330-At2g20070	N. A	0.63	-0.22

9.11 Prediction of DEFL gene expression based on literature

(A)- Loraine et al. 2013 , (B)- Huang et al. 2015 , (C) - Wang et al. 2008 , (D)- Qin et al. 2009, (E)- Boavida et al. 2011, (F) - Wuest et al. 2010, (G) - Schmid et al. 2012, (H) - Steffen et al. 2007, (I) - Jones-Rhoades et al. 2007, (J) - Yu et al. 2005.

A) DEFL genes predicted to be expressed in female gametophyte

33 DEFL genes were found to be predicted to be expressed in female gametophyte

Female gametophyte	Reference for female gametophyte
At2g02100	(B), (E), (F), (G)
At5g44420	(E)
At1g19610	(B), (E)
At5g08315	(B), (G), (I)
At5g54225	(G)
At2g42885	(B), (G)
At3g06985	(B), (G)
At3g07005	(B), (G), (I)
At2g20070	(B), (F), (G), (H), (I), (J)
At3g42473	(B), (I)
At2g12465	(B), (G), (I)
At2g12475	(B), (G), (I)
At2g40995	(B), (G), (I)
At4g19035	(B), (G)
At4g09153	(B), (G), (I)
At4g29285	(B), (E), (F), (G), (H), (J)
At4g29300	(G)
At5g38330	(B), (E), (F), (G), (H), (I), (J)
At2g43510	(E), (F)
At2g43535	(B), (E), (G)
At3g05730	(E)
At5g43285	(B), (G)
At4g22115	(B), (G)
At1g60985	(B), (E), (F), (G), (H), (I), (J)
At4g15735	(B), (G)
At1g13605	(B), (G)
At1g65352	(B), (G)
At1g35435	(B), (G)
At5g23212	(B), (G), (I)
At5g60553	(B), (G), (I)
At1g13609	(B), (G)
At4g17713	(B), (G), (I)
At2g24615	(H)

B) DEFL gene predicted to be expressed in pollen grains

32 DEFL genes were found to be predicted to be expressed in pollen grains

Pollen grain	References
At2g02140	(A), (B), (E), (F)
At5g19315	(B)
At5g39365	(A), (B)
At5g40155	(A), (B), (C), (D), (E), (F)
At3g43083	(A), (B)
At4g19038	(A), (B)
At1g28335	(A), (B)
At2g15535	(A), (B), (C), (D), (E), (F)
At2g28355	(A), (B), (C), (D), (E), (F)
At2g28405	(A), (B)
At3g25265	(A), (B)
At4g09984	(A), (B)
At4g10595	(A), (B)
At4g11485	(A), (B)
At4g11760	(A), (B), (C), (D), (E), (F)
At5g48543	(A), (B)
At4g10603	(B)
At2g22805	(A), (B)
At2g22807	(A), (B)
At2g22941	(A), (B)
At1g08695	(A), (B)
At1g65113	(A), (B)
At2g06983	(A), (B)
At2g14282	(A), (B)
At3g27503	(A), (B)
At4g10115	(A), (B)
At4g14785	(A), (B)
At4g32714	(A), (B)
At4g32717	(A), (B)
At4g33465	(A), (B)
At3g23727	(A), (B)
At5g60615	(A), (B)

C) 7 DEFL genes were found with no proper evidence in female gametophyte or pollen grain in any of the references.

At3g05727, At2g26010, At2g26020, At5g44430, At1g56233, At5g42223 and At4g22235

9.12 Prediction of DEFLs in root expression based on literature along with the results

Defensin	Result from GFP localization study	Genevestigator data base - Microarray	Genevestigator data base - RNAseq	References (Tesfaye et al. 2013)
At2g02100		x		x
At2g02140		x		
At2g26020		x		
At5g44420		x		
At1g19610		x		
At2g20070		x		
At4g22235			x	
At5g40155		x		
At2g15535		x		
At3g07005	x			
At2g28355		x		
At4g11760	x	x		
At4g29285		x		
At5g38330	x	x		
At2g43510		x		
At2g43535		x		
At3g05730		x		
At2g40995	x			
At1g60985		x		
At2g42885	x			
At1g13609			x	
At4g30074	x			x
At5g60553				x

x- found in that study.

9.13 At5g43285 expression during pollination events

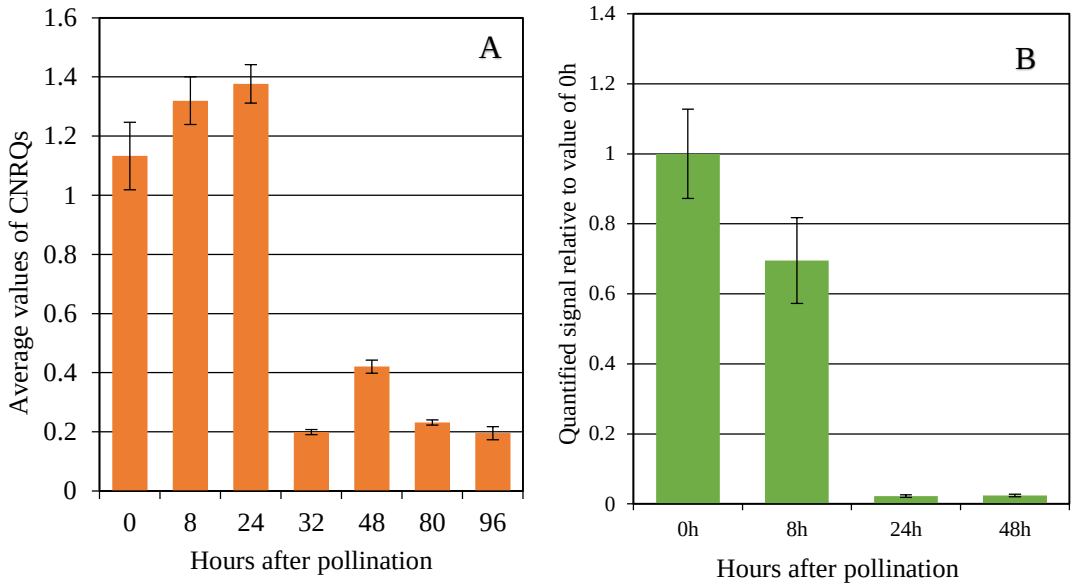

Figure S7:Expression pattern of At5g43285 gene during different hours after pollination in different studies (A) qPCR study (B) quantification of eGFP signal.

(A) qPCR assays were used for checking the expression of candidate genes in pistils at different time points after pollination. The time points that were taken for this analysis were non-pollinated, 8, 24, 48, 80, 96 hours after pollination. At5g43285 was upregulated until 24HAP and then followed by downregulated in subsequent time points.

(B) The GFP signal under the control of the promoters for At5g43285 were taken for GFP quantification studies. The time points that were taken for the analysis were non-pollinated and 8, 24 and 48 hours after pollination (HAP). At5g43285 had decrease of GFP signal in subsequent days.

9.14: List of synthesized cDNA pools for different qPCR analysis.

Pollination studies		Infection (ageing) studies			Pollination - Infection studies	
0 HAP A *	0 HAP B *	2 DAE A †	2 DAE B †	2 DAE C †	32 HAP A *	32 HAP B ‡
8 HAP A *	8 HAP B *	4 DAE A †	4 DAE B †	4 DAE C †	48 HAP A *	48 HAP B ‡
24 HAP A *	24 HAP B *				80 HAP A *	80 HAP B ‡
32 HAP A *	32 HAP B ‡	1 DAT A †	1 DAT B †	1 DAT C †	96 HAP A *	96 HAP B ‡
48 HAP A *	48 HAP B ‡	3 DAT A †	3 DAT B †	3 DAT C †	8 HAP- 1 DAT A *	8 HAP- 1 DAT B ‡
80 HAP A *	80 HAP B ‡				24 HAP- 1 DAT A *	24 HAP- 1 DAT B ‡
96 HAP A *	96 HAP B ‡	1 DAI A †	1 DAI B †	1 DAI C †	8 HAP- 3 DAT A *	8 HAP- 3 DAT B ‡
		3 DAI A †	3 DAI B †	3 DAI C †	24 HAP- 3 DAT A *	24 HAP- 3 DAT B ‡
					8 HAP- 1 DAI A *	8 HAP- 1 DAI B ‡
					24 HAP- 1 DAI A *	24 HAP- 1 DAI B ‡
* Synthesized by Ajay John Arputharaj (University of Regensburg, Regensburg, Germany).					8 HAP- 3 DAI A *	8 HAP- 3 DAI B ‡
† Synthesized by Dr. Mariana Mondragon-Palomino (University of Regensburg, Regensburg, Germany). ‡ Synthesized by the Kriss Splavins (Master thesis, 2016).					24 HAP -3 DAI A *	24 HAP- 3 DAI B ‡
HAP-Hours after pollination, DAE -Days after emasculation, DAT- Days after treatment, DAI -Days after infection, A- first biological replicate sample, B- second biological replicate sample, C - third biological replicate sample						

9.15 List of differential expression of some genes related to plant immunity

Gene name	Gene definition[1]	TAIR ID	Log_2 fold change[2]
MAPKKK1	MAP Kinase kinase Kinase 1	At1g09000	-2.14
MAPKKK16	MAP Kinase kinase Kinase 16	At4g26890	2.19
MAPKKK17	MAP Kinase kinase Kinase 17	At2g32510	2.88
MAPKKK18	MAP Kinase kinase Kinase 18	At1g05100	2.35
MAPKKK19	MAP Kinase kinase Kinase 19	At5g67080	4.867316844

9.16 List of stuff in CD appendix

9.16.1 Log_2 fold change of all genes expressed transcriptome data of A. thaliana selfed condition,A. thaliana pistil pollinated with A. halleri, A. thaliana pistil pollinated with A. halleri, A. thaliana pistil infected with *F.graminearum* and A. thaliana leaf infected with *F.graminearum*

9.16.2 Word document containing nucleotide sequence of candidate gene used for cloning

9.16.3 Folder containing excel sheet containing the grey value of quantification of eGFP signal from candidate gene

9.16.4 Excel sheet containing CNRQ values of candidate genes during qPCR study of pollination

9.16.5 Excel sheet CNRQ values of candidate genes during qPCR study of infection (aging studies)

9.16.6 Excel sheet CNRQ values of candidate genes during qPCR study of Pollination followed by Infection in qPCR study

9.16.7 Excel sheet containing seed set data of pollination followed by different treatment experiment

9.16.8 Excel sheet containing seed set data of infection follwed by pollination experiment

9.16.9 Excel sheet containing effect of fungal infection on the rate of endosperm development

9.17 Log_2 fold change of thionins and RALF like peptides in transcriptome data of *A. thaliana* pistil during foreign pollen

Gene Number	Gene Definition	A. thaliana x A. lyrata pollen	A. thaliana x A. halleri pollen
At1g21864	Plant thionin family protein	5.71	7.41
At1g21866	Plant thionin family protein	5.84	7.96
At1g21925	Plant thionin family protein	4.63	5.53
At1g21928	Plant thionin family protein	3.48	3.19
At1g30974	Plant thionin family protein		2.59
At1g58245	Plant thionin family protein	3.52	3.21
At3g24465	Plant thionin family protein	3.86	
At5g36720	Plant thionin family protein	7.17	
At5g36805	Plant thionin family protein	7.22	
At5g38378	Plant thionin family protein	4.34	3.81
At2g19045	Protein RALF-like 13	2.76	2.24
At1g60625	Protein RALF-like 6		6.84

10. Acknowledgement

First and foremost, I am deeply grateful to Professor Thomas Dresselhaus for giving me the opportunity to work on this interesting project for scientific discussion, as well as for his open door policy concerning any issues, and last but not least for funding me during my work.

Furthermore, I would also like to take this opportunity to thank my supervisor and friend, Dr. Mariana Mondragón-Palomino for sharing her knowledge, for scientific discussion, guidance in my work, and for being a constant support in all the tough situations. Moreover, I appreciate the time taken for discussing the dissertation with me, as well as for editing the dissertation.

I would like to thank Prof. Ralph Hückelhoven (TUM) for providing us the fusarium strain, as well as for being a part of my examination committee as my second PhD assessor. I would also like to thank PD Dr. Joachim Griesenbeck for being a part of the examination committee. I would also like to thank Prof. Wilhelm Schaefer (University of Hamburg) for providing a different Fusarium strain and Kompetenzzentrum für Fluoreszente Bioanalytik (KFB) group (Biopark, University of Regensburg) for their work regarding RNAseq.

I would like to thank, Veronika Mrosek for her assistance in administrative related work, and would also like to thank Ursula Wittmann, Günther Peissig and Armin Hildebrand for taking care of my plants. I would like to thank all my colleagues in the department of Cell Biology and Plant Biochemistry for their advice regarding the research. I would like to especially thank all my current and former members of the maize lab for providing an excellent fun working atmosphere.

I further want to thank all the student that I was allowed to supervise during my time and for their supportive work: Maximilian, Alexander, Niveditha, Maria, Johanna, Micaela, Fabian, Anna, Kriss, and Mathias.

I would also like to thank my friends and church group in India and Regensburg, for their support. A special thanks to Velavan for teaching me the details regarding Microsoft office.

I want to thank my parents John and Vasanthi, who provide me with love and support throughout these years. I am also grateful to my two brothers, Vijay and Charles, for their support and care that has helped me get through all situations.

Last but not least, I would like to thank the person who helped me the most of all – my wife Nivetha. I thank her for her continuous support, sacrifice, constant love, for keeping me grounded, and for the taking care of our son, Jayden. Finally, I would like to thank my saviour Jesus Christ for giving me peace, his grace and mercy in my life.